Institute of Cell
and
Molecular Biology

The Hebrew University
of Jerusalem
Faculty of Agricultural
Food and Environmental
Quality Sciences

Quantitative Measurement of the Ca^{2+}-Signature in Living Hyphae of *Neurospora crassa*, and a Genomic Analysis of Ca^{2+}-Signalling Machinery in Filamentous Fungi

Alexander Zelter

Doctor of Philosophy
University of Edinburgh
20 March 2004

Declaration

This thesis has been composed by myself, and the work of which it is a record has been carried out by myself. All sources of information have been specifically acknowledged by means of reference.

Acknowledgments

The experimental work for this thesis was performed in the University of Edinburgh, Institute of Cell and Molecular Biology, Edinburgh, Scotland and the Hebrew University of Jerusalem, Faculty of Agricultural, Food and Environmental Quality Sciences, Rehovot, Israel during the years 1999 to 2003.

This peculiar and interesting combination of locations was made possible by my two supervisors, Nick Read and Oded Yarden, to whom I would like to give my warmest thanks for their constant support, encouragement and expert guidance, along with their thorough revision of all my work.

My work was funded by several grants, and I would like to thank the following organisations for funding. DEFR funded two years of work in Scotland (grant no. is AE9221). The Wellcome Trust (grant no. 066392/Z/01/Z) provided some support for traveling and living in Israel. The remainder of the work done in Israel was supported by the Israel Science Foundation.

During my research I have used a vast amount of software provided free, as a result of the good will of other people. This thesis was written using the LaTeX document processing package (http://www.latex-project.org) on computers running the Linux operating system (http://www.linux.org) and using open source software (http://www.gnu.org). Other free software is acknowledged in proceeding sections of this thesis.

Thanks to all the people in both the Rehovot and the Edinburgh labs in which I have been working and especially to Michal Efrat, Arik Harel, Zipi Resheat-Eini and Carmit Ziv for there help in experiments and for interesting conversations.

A big thank you to Pat Hickey for teaching me which end of the microscope to look down and for all his support during my PhD. I am very grateful to Mojca Bencina, with whom I have collaborated, for all her work and ideas and to my second supervisor, Tony Trewavas, for answering all of my many questions.

Finally thanks to my family for their support and encouragement and for putting up with my long absences. Thanks to Magi for his friendship and for loads of help with mathematics and computers. Last but definitely not least I want to thank Nina for her constant love, patience and support during these four years.

Contents

List of Tables

List of Figures

Abstract

Growing evidence indicates the involvement of Ca^{2+}-signalling in the control of numerous processes in filamentous fungi. Despite the obvious importance of Ca^{2+}-signalling, and in contrast to the situation in budding yeast, plants and animals, very little is currently known about the mechanisms of Ca^{2+}-signalling in filamentous fungi. Only a handful of filamentous fungal Ca^{2+}-signalling genes have been cloned and characterised to date, and it is only recently that methods have been developed to enable the routine, easy and reliable measurement of Ca^{2+} within living fungal hyphae. Thus much of the evidence supporting the importance of Ca^{2+}-signalling in filamentous fungi has been indirect.

The aims of this research were to develop and an aequorin-based approach for measuring cytosolic Ca^{2+} ($[Ca^{2+}]_c$) in living hyphae of *Neurospora crassa* and to use this method to investigate the contribution of individual proteins to the generation of the specific Ca^{2+}-signatures associated with $[Ca^{2+}]_c$ transients. Molecular and genomic methods were also used to identify Ca^{2+}-signalling proteins in *Neurospora crassa*, *Aspergillus fumigatus* and *Magnaporthe grisea*.

Results confirmed that a reliable method for the quantitative measurement of $[Ca^{2+}]_c$ in living *N. crassa* hyphae had been developed with the aequorin reporter system. This method was used to characterise Ca^{2+}-signatures in *N. crassa* in response to (a) mechanical perturbation, (b) hypo-osmotic shock and (c) high external Ca^{2+} under different environmental conditions. Ca^{2+}-signatures in response to these stimuli were shown to have a unique set of characteristics

in response to each stimulus. These characteristics were apparent under all the conditions tested.

Ca^{2+}-signatures in response to the three stimuli were measured in wild-type *N. crassa* treated with Ca^{2+} antagonists and agonists and in untreated mutant strains of *N. crassa* compromised in Ca^{2+}-signalling. In each case, differences in Ca^{2+}-signatures could be quantitatively measured.

Cloning of the *cot-4* gene in the *cot-4* morphological mutant of *N. crassa* showed it to encode the catalytic subunit of calcineurin, a Ca^{2+}/calmodulin-dependent protein phosphatase.

An analysis of the genomes of *N. crassa*, *A. fumigatus* and *M. grisea* identified many of the key Ca^{2+}-signalling proteins present in filamentous fungi. An inventory of Ca^{2+}-signalling proteins in filamentous fungi is an important starting point for reverse genetic and physiological approaches aiming at elucidating the biological significance of these proteins. The construction of mutant strains, impaired in the function of specific Ca^{2+}-signalling proteins, and the quantification of Ca^{2+}-signatures in these strains are therefore important directions for future experimental work.

Abbreviations

A_x	=	absorbance at x nm
A_{tot}	=	total area
amdS	=	acetamidase-encoding gene of *Aspergillus nidulans*
amp	=	amplitude
2-APB	=	2-aminoethoxy-biphenylborate
BLM	=	bilayer lipid membrane (Silverman-Gavrila and Lew, 2002)
BSA	=	bovine serum albumin
Ca^{2+}	=	calcium ion
$[Ca^{2+}]_c$	=	cytosolic free calcium
cADPR	=	cyclic ADP-Ribose
calcineurin	=	phosphoprotein phosphatase type 2B (PP2B)
CaM	=	calmodulin
cAMP	=	cyclic 3',5'-adenosine monophosphate
CaMPK	=	Ca^{2+}/CaM-kinase
CAX	=	Ca^{2+} exchanger
cGMP	=	cyclic GMP
CICR	=	Ca^{2+}-induced Ca^{2+} release
CIP	=	calf intestinal alkaline phosphatase
CNS	=	central nervous system
CPA	=	cyclopiazonic acid
CPC	=	Ca^{2+}-permeable channel
CsA	=	cyclosporin A
cot-1	=	colonial temperature-sensitive 1

cpc-1	=	cross pathway control 1
CTAB	=	cetyltrimethylammonium bromide
CTC	=	chlortetracycline
DAG	=	diacylglycerol
dH_2O	=	distilled water
DME	=	dimethylethanolamine
DMSO	=	dimethyl sulfoxide
DNA	=	deoxyribose nucleic acid
EDTA	=	ethylenediaminetetraacetic acid
ER	=	endoplasmic reticulum
EST	=	expressed sequence tag
EtBr	=	ethidium bromide
g	=	gram
gnaeqD	=	codon optimised aequorin gene
FGSC	=	Fungal Genetics Stock Centre
fr	=	*frost*
FRET	=	fluorescence resonance energy transfer
FWHM	=	full width half maximum
h	=	hour
HACS	=	high-affinity Ca^{2+} influx system
hph	=	hygromycin phosphotransferase gene
hyg	=	hygromycin B
$InsP_3$	=	inositol 1,4,5-trisphosphate
$InsP_3R$	=	inositol 1,4,5-trisphosphate receptor
kb	=	kilobase pairs
l	=	litre
LACS	=	low-affinity Ca2+ influx system
LB	=	Luria-Bertani
LT	=	lag time
M	=	molar

min	=	minute
Mbp	=	mega base pairs
MME	=	monomethylethanolamine
NCBI	=	National Center for Biotechnology Information
NO	=	nitric oxide
ORF	=	open reading frame
PC	=	personal computer
PCD	=	programmed cell death
PCR	=	polymerase chain reaction
PDL	=	perl data language
PEG 4000	=	polyethylene glycol 4000
PKC	=	protein kinase C
PLC	=	phospholipase C
PMCA	=	plasma membrane Ca^{2+}
pph-1	=	gene encoding PP2Ac
PP1	=	protein phosphatase type 1
PP2A	=	protein phosphatase type 2A
PP2B	=	calcineurin, or phosphoprotein phosphatase type 2B
psi	=	pounds per square inch
pvn1	=	*pvn1-121A*
pvn2	=	*pvn2-53-19A*
RIP	=	repeat-induced point mutation
RLU	=	relative light units
rpm	=	revolutions per minute
RT	=	rise time
RYR	=	ryanodine receptors
s	=	second
SA	=	stretch activated
SDS	=	sodium dodecyl sulphate
SERCA	=	sarcoplasmic reticulum Ca^{2+}

sp	=	*spray*
Spk	=	Spitzenkörper
SR	=	sarcoplasmic reticulum
S1P	=	sphingosine 1-phosphate
TM	=	transmembrane
TRP	=	transient receptor potential
UV	=	ultraviolet
VSC	=	vesicle supply centre
VgS	=	Vogel's media
W	=	Watt

Chapter 1

Introduction

To survive, organisms must sense their environment and react accordingly. This is achieved through a network of signalling pathways, which ultimately influence the behaviour of individual cells (Equation 1.1).

$$\begin{array}{lcllcllcl} \text{External} & & \text{Surface Receptors} & & \text{Internal Signal} & & \text{Effector} & \\ \text{Signal} & \longrightarrow & \text{(cell membrane)} & \longrightarrow & \text{Pathway} & \longrightarrow & \text{Activation} & (1.1) \end{array}$$

Calcium (Ca^{2+}) is a ubiquitous signalling molecule, employed in all organisms, from prokaryotes to higher animals (Michiels et al., 2002; Gadd, 1994; Berridge et al., 2000; Carafoli, 2002; Sanders et al., 2002). The reasons that Ca^{2+} is used so globally as a signalling molecule are not known. However, it is clear that cells had to develop a Ca^{2+} transport mechanism to remove Ca^{2+} from the cytoplasm very early on in evolution. This is because at elevated concentrations, Ca^{2+} forms an insoluble precipitate with inorganic phosphate that inhibits phosphate based energy metabolism (Hepler and Wayne, 1985). As the concentration of Ca^{2+} in seawater is in the millimolar (mM) range, cells must have been able to regulate their internal Ca^{2+} concentration to survive. A low and precisely controlled concentration is an important characteristic of any second messenger, thus part of the cell signalling apparatus had already been developed with respect to Ca^{2+}-signalling. Furthermore, calcium ions are well suited for use as signalling

molecules because they can coordinate 6 to 8 uncharged oxygen atoms enabling protein conformations in which remote domains can participate in Ca^{2+}-binding. Such changes can invoke a wide variety of downstream responses (Sanders et al., 1999).

1.1 Ca^{2+}-Signalling - an Overview

Intracellular Ca^{2+}-signalling is characterised by a transient increase in cytosolic free Ca^{2+} ($[Ca^{2+}]_c$), which precedes the cellular response to the primary stimulus. The progress of a $[Ca^{2+}]_c$ transient through the cytoplasm can be described as a wave (Malhó et al., 1998). The duration, propagation and amplitude of Ca^{2+} waves is dependent on the type and intensity of the stimuli (Berridge and Dupont, 1994). Both active (Ca^{2+}-pumps and transporters) and passive (Ca^{2+}-binding proteins) systems exist (Berridge and Dupont, 1994), which typically maintain resting $[Ca^{2+}]_c$ concentrations between 50 and 200 nM (Malhó et al., 1998; Miller et al., 1990; Bush, 1995; Ohya et al., 1991b). In contrast, the Ca^{2+} concentration in the endoplasmic reticulum (ER), cell wall, vacuole, and extracellular environment varies from 0.1 to 100 mM (Trewavas and Malhó, 1997; Levina et al., 1995; Sanders et al., 1999). During signalling the $[Ca^{2+}]_c$ concentration typically increases 3 to 100 fold over the basal level. In eukaryotes, intracellular Ca^{2+}-signalling relies upon Ca^{2+} entry across the plasma membrane and into the cell, or on the release of Ca^{2+} from intracellular stores, or both. Ca^{2+}-permeable channel (CPC) closure, buffering of Ca^{2+} by Ca^{2+}-binding proteins and active removal of $[Ca^{2+}]_c$ by Ca^{2+}-pumps and transporters reduces the diffusion rate of $[Ca^{2+}]_c$ to the extent that Ca^{2+} waves cannot rely solely on diffusion for propagation through the cytosol. After initiation, waves must therefore be propagated by Ca^{2+}-induced Ca^{2+} release (CICR) from intracellular stores (Berridge, 1995). $[Ca^{2+}]_c$ transients diffuse outwards to excite neighbouring stores, which respond by releasing their own Ca^{2+} that in turn diffuses outwards

repeating the process. Upon release, $[Ca^{2+}]_c$ is rapidly pumped back into the intracellular stores returning the cytosol to its resting state. Intracellular Ca^{2+}-signalling thus relies upon the initiation and the propagation of Ca^{2+} transients.

Current thinking suggests several factors provide the necessary specificity for a particular stimulus to illicit a defined response. These factors include: (a) input from other signalling systems; (b) spatial location of the Ca^{2+} signal within the cell; (c) presence of specific response elements; and (d) information encoded in the Ca^{2+}-signature (Sanders et al., 2002). In both plants and animals the unique Ca^{2+}-signatures associated with $[Ca^{2+}]_c$ transients have been shown to encode information and there is growing evidence that these signatures can be decoded by the signal transduction machinery of the cell in order to induce specific cellular responses (Malhó et al., 1998; Berridge et al., 1998, 2000; Bootman et al., 2001; Sanders et al., 2002). $[Ca^{2+}]_c$ transients can be induced by many factors. These factors may be endogenous or exogenous (with respect to the cell or to the organism) and some examples are: gravity, light, mechanical signals (e.g. wind and touch), cold shock, heat shock, oxidative anaerobic, hypo-osmotic and hyper-osmotic stresses, salination, drought, and hormones (Allen et al., 1995; Trewavas and Malhó, 1997; Malhó et al., 1998; Shaw et al., 2001; Greene et al., 2002; Kozlova-Zwinderman, 2002; Nelson et al., 2003).

Stimuli may activate stretch activated (SA), ligand-gated or voltage-gated CPCs (Sanders et al., 2002; Berridge et al., 2000), including non-selective cation channels, which serve to elevate $[Ca^{2+}]_c$ concentrations by allowing the passive flux of Ca^{2+} down an electrochemical gradient (Gadd, 1994; Pietrobon et al., 1990) across a membrane and into the cytoplasm. A transmembrane electrochemical gradient for Ca^{2+} is therefore a crucial prerequisite for signal transduction, and $[Ca^{2+}]_c$ concentrations must be maintained at a low level in the resting state (Miller et al., 1990). Such gradients are sustained principally by transport systems that catalyse efflux of Ca^{2+} from the cytosol. CPCs are membranous proteins and have been found in the plasma membrane, the endoplasmic and sarcoplasmic

reticulum, and the vacuole (Berridge et al., 2000; Gustin et al., 1988; Zhou et al., 1991; Garrill et al., 1992; Zhou et al., 1992; Levina et al., 1995; Gadd, 1994; Palmer et al., 2001; Maruoka et al., 2002; Locke et al., 2000; Paidhungat and Garrett, 1997). Mechanisms for Ca^{2+} release from other internal organelles such as Golgi and mitochondria (which have both been shown to sequester Ca^{2+} under some circumstances (Bootman et al., 2001; Pitt and Barnes, 1993; Antebi and Fink, 1992; Park et al., 2001)) may also exist. CPC activation may be achieved directly, for example via membrane hyperpolarisation or depolarisation or as a result of mechanical stimulation or the binding of a ligand, such as a hormone, to a plasma membrane receptor. Alternatively, upon reaching the surface of the target cell, external signals may activate G-protein linked receptors or tyrosine kinases (Berridge, 1993; Sailsbury and Ross, 1992) resulting in the formation of second messengers such as inositol 1,4,5-trisphosphate ($InsP_3$), diacylglycerol (DAG) and cyclic nucleotides (e.g. cyclic ADP-Ribose [cADPR]) (Equation 1.2).

$$\begin{array}{c} \text{G}-\text{protein linked receptors} \\ \text{and / or} \\ \text{Tyrosine kinases} \end{array} \longrightarrow \begin{array}{c} \text{Activation of} \\ \text{Phospholipase C} \\ \text{(PLC)} \end{array} \qquad (1.2)$$

$$\begin{array}{c} \text{Phosphatidylinositol} \\ 4,5-\text{bisphosphate} \end{array} \xrightarrow[\text{(hydrolysis)}]{\text{PLC}} InsP_3 \text{ \& DAG}$$

DAG stays in the cell membrane where it activates protein kinase C (PKC). PKC uses ATP to phosphorylate enzymes that regulate metabolism thereby affecting the growth and behaviour of the cell (Sailsbury and Ross, 1992). $InsP_3$ and cADPR diffuse through the cytosol to activate $InsP_3$ and cADPR receptors situated on the surface of intracellular Ca^{2+} stores. These receptors are known as $InsP_3R$ and ryanodine receptors (RYR) respectively, and their activation by second messengers is also thought to be dependent on the concentration of $[Ca^{2+}]_c$

(Berridge and Dupont, 1994). If all the conditions are met, they open and a $[Ca^{2+}]_c$ transient is produced by release of Ca^{2+} from their respective intracellular stores. Ca^{2+} itself can also activate CPCs, for example during CICR or in the case of store-operated CPCs that operate in response to depletion of the intracellular store that they gate (Bootman et al., 2001; Sanders et al., 2002).

$[Ca^{2+}]_c$ waves are often accompanied by nuclear Ca^{2+} waves. However, gene expression can be differentially controlled by cytosolic and nuclear Ca^{2+} (Hardingham et al., 1997). The specific mechanisms through which Ca^{2+} affects cell behaviour are still largely unknown. Ca^{2+} may act directly to trigger a variety of biochemical events involved in cell differentiation and proliferation (Gadd, 1994). However, the cellular action of Ca^{2+} more commonly involves the site-specific binding of Ca^{2+} to specialised Ca^{2+}-binding proteins.

Most Ca^{2+}-binding proteins bind Ca^{2+} through 6 or 7 oxygen atoms provided by glutamate or aspartate residues. Another common component of Ca^{2+}-binding proteins is the 'EF hand'. The EF hand consists of a series of α-helices and its name was derived from the fact that α-helices E and F are positioned such that they point like the forefinger and thumb of a right hand. A loop containing active Ca^{2+}-binding glutamate and aspartate residues lies between these α-helices, and it is this that allows Ca^{2+}-binding. Many Ca^{2+}-binding proteins undergo a major conformational change when they bind to Ca^{2+}. This change exposes active sites on the protein allowing the signal to be effected (Hancock, 1997). Ca^{2+}-bound proteins can act on the cell directly, or through the modulation of other proteins (Gilchrist et al., 1994).

Calmodulin (CaM) is the most common Ca^{2+}-binding protein. It is involved in an immense number of regulatory pathways. Examples include the regulation of metabolic activity and gene expression along with the regulation of other signalling pathways such as nitric oxide (NO) generation, the control of cyclic 3',5'-adenosine monophosphate (cAMP) production via adenylyl cyclase and cAMP destruction by Ca^{2+}/CaM-dependent phosphodiesterase. CaM can also

regulate plasma membrane and ER Ca^{2+}-pumps, which remove Ca^{2+} from the cytosol (Hancock, 1997). The CaM gene has been shown to be essential in *S. cerevisiae*, *S. pombe* and *A. nidulans* (Davis, 1992).

Calcineurin, a Ca^{2+}/CaM dependent protein phosphatase (PP2B), is another important transducer of Ca^{2+} signals. It has recently been found to regulate gene expression, in *S. cerevisiae*, through the regulation of the Crz1p/Tcn1p transcription factor (Matheos et al., 1997). The dephosphorylation of Crz1p by calcineurin results in its translocation of Crz1p to the nucleus (Stathopoulos-Gerontides et al., 1999). DNA microarray analysis of calcineurin/Crz1p-dependent gene expression following Ca^{2+} addition revealed 125 genes that showed Ca^{2+}-induced calcineurin-dependent expression (Yoshimoto et al., 2002).

1.2 Ca^{2+}-Signalling in Fungi

When compared to mammalian and plant systems, information on Ca^{2+}-signalling in fungi is relatively sparse. This is particularly true for filamentous species (Gadd, 1994). However, the use of both budding and fission yeast as eukaryotic cell models is rapidly alleviating the situation, and recent filamentous fungal genome sequencing efforts also promise to shed new light on this important area.

1.2.1 Yeasts

Yeasts express many of the same signalling molecules used by animal cells. Some of the discoveries made regarding Ca^{2+}-signalling in yeasts are described below.

1.2.1.1 Ca^{2+} influx, efflux and homeostasis

Ca^{2+} homeostasis in yeast cells is achieved by complex feedback mechanisms involving Ca^{2+}-permeable channels, Ca^{2+}-pumps (Ca^{2+}-ATPases) and -transporters (Ca^{2+}-exchangers). In *Saccharomyces cerevisiae* three Ca^{2+}-permeable channel proteins have been identified. These are Cch1p (Fischer et al., 1997), Mid1p

(Maruoka et al., 2002) and Yvc1p (Denis and Cyert, 2002). The Ca^{2+}-ATPases Pmc1p (Degand et al., 1999), Pmr1p (Park et al., 2001), Spf1p (Cronin et al., 2000; Suzuki, 2001) and Neo1p (Prezant et al., 1996), the Ca^{2+}-transporter Vcx1p (del Pozo et al., 1999), calmodulin (CaM), calcineurin and probably several other Ca^{2+}/CaM regulated proteins are all part of the Ca^{2+} homeostatic network. Plc1p (Andoh et al., 1995), the yeast phospholipase C (PLC) protein, may also be an important part of the yeast Ca^{2+}-signalling network as this gene is essential for glucose-induced Ca^{2+} influx in *S. cerevisiae* (Tisi et al., 2002) and PLC is known to be important in plant and animal Ca^{2+}-signalling networks.

The vacuole is a major Ca^{2+} sink in yeast (Cunningham and Fink, 1994a) and Ca^{2+} uptake into purified vacuoles and vacuolar membranes is totally dependant on the transmembrane pH gradient that is normally produced by the vacuolar H^+-ATPase (Dunn et al., 1994). *vma1* mutants of *S. cerevisiae* (and other mutants deficient in the vacuolar H^+-ATPase necessary for H^+/Ca^{2+}-exchange activity) are therefore extremely sensitive to added Ca^{2+} (Antebi and Fink, 1992) and exhibit a 6-fold elevation in $[Ca^{2+}]_c$. It is thought that inhibition of the vacuolar H^+/Ca^{2+}-antiporter is responsible for the above effects (Ohya et al., 1991b).

The Ca^{2+}-permeable channels Cch1p and Mid1p have both been found to be located at the plasma membrane by immunofluorescence microscopy (Paidhungat and Garrett, 1997; Fischer et al., 1997; Locke et al., 2000) and are involved in a capacitative Ca^{2+} entry-like mechanism, which refills Ca^{2+} stores within the secretory pathway of *S. cerevisiae*. Depletion of Ca^{2+} from the ER stimulates Ca^{2+} influx through the Cch1p-Mid1p Ca^{2+}-channel (Bonilla et al., 2002). It has been shown, by systematic deletions, that the carboxyl-terminal domain is important for Mid1 function (Maruoka et al., 2002). $[Ca^{2+}]_c$ transients induced by hyperosmotic stress caused by NaCl, LiCl, or sorbitol are a result of external Ca^{2+} influx via Mid1p and Cch1p. The amplitude of these osmotically induced Ca^{2+} transients, as measured using aequorin, is attenuated by the addition of chelating agents EGTA or BAPTA, cation channel pore blockers, competitive

inhibitors of Ca^{2+} transport, or mutations (*cch1*Δ or *mid1*Δ) that reduce Ca^{2+} influx, indicating that external Ca^{2+} is a source for the transient (Matsumoto et al., 2002).

Both high- and low-affinity Ca^{2+} influx systems (HACS and LACS, respectively) exist in *S. cerevisiae*. The Cch1p-Mid1p Ca^{2+}-channel comprise the HACS. The HACS is regulated by calcineurin as it shows a large increase in activity after calcineurin inactivation or inhibition. LACS is calcineurin insensitive and Cch1p-Mid1p independent suggesting that not all the *S. cerevisiae* Ca^{2+}-permeable channels have yet been identified (Muller et al., 2001).

Two potential homologues of the *S. cerevisiae* Mid1/Cch1 Ca^{2+}-permeable channel have been identified in *Schizosaccharomyces pombe*. These are Ehs1p and Yam8p. Ehs1p is 30% identical to *S. cerevisiae* Mid1p and is involved in intracellular Ca^{2+} accumulation. High external Ca^{2+} concentrations suppress all phenotypes associated with the *ehs1* null mutation and the lethality associated with Pck2p overproduction (deleterious to wild-type cells as a result of promoting accumulation of extremely high levels of $[Ca^{2+}]_c$) is dependent upon a functional copy of *ehs1* (Carnero et al., 2000). Yam8 has been shown to partially complement the mating pheromone-induced death (mid) phenotype of the *S. cerevisiae mid1* mutant (Tasaka et al., 2000) and is therefore also likely to be a homologue of *S. cerevisiae* Mid1p.

S. cerevisiae Yvc1p is a vacuolar Ca^{2+}-permeable channel and exhibits homology to animal transient receptor potential (TRP) Ca^{2+}-permeable channels. It is necessary for an exclusively vacuolar cation conductance measured by patch-clamp techniques on vacuoles released from *S. cerevisiae* spheroplasts (Palmer et al., 2001). Yvc1p is also responsible for a hypertonic shock provoked transient increase in cytosolic Ca^{2+}. The observed transient is absent in *yvc1*Δ strains. This increase was shown to originate from internal Ca^{2+} stores as mutations in *MID1* and *CCH1* and the application of extracellular cation chelators did not affect the transient (Denis and Cyert, 2002).

A putative $InsP_3$ gated Ca^{2+}-permeable channel has been detected in purified membrane vesicles derived from *S. cerevisiae* vacuoles. These vesicles accumulate Ca^{2+} *in vitro* and release a small portion in response to $InsP_3$, suggesting a similarity to the $InsP_3$ receptors of animal cells (Belde et al., 1993). Plc1p, the yeast phospholipase C (Andoh et al., 1995), is also essential for glucose-induced Ca^{2+} influx in *S. cerevisiae*. Glucose-induced Ca^{2+} influx, as measured by aequorin, was completely abolished in a *plc1*Δ strain and was also absent in an isogenic wild-type strain treated with 3-nitrocoumarin, a phosphatidylinositol-specific phospholipase C inhibitor (Tisi et al., 2002). It has also been found that both $InsP_3$-dependent and -independent Ca^{2+} mobilisation pathways exist at the vacuolar membrane of *Candida albicans* (Calvert and Sanders, 1995). In these experiments *C. albicans* vacuoles were isolated from protoplasts, loaded with $^{45}Ca^{2+}$ and subjected to $InsP_3$ or the lipophilic cation $TPMP^+$ (which generates an inside-positive membrane potential). Both treatments resulted in release of $^{45}Ca^{2+}$ from the vacuoles. These two pathways were shown to be distinct with respect to the amount of Ca^{2+} released, the nature of response to successive stimuli, and their respective pharmacological profiles (Calvert and Sanders, 1995).

The *S. cerevisiae* Ca^{2+}-ATPase Pmr1p occurs primarily at the Golgi and associated secretory compartments. This is indicated by its co-migration with Golgi markers in subcellular fractionation experiments and its immunofluorescent punctate pattern resembling Golgi staining (Antebi and Fink, 1992). Pmr1p functions in both Ca^{2+} and Mn^{2+} transport and has been found to play a role in ER-associated processes such as the degradation of a misfolded ER protein (CpY*), which does not occur in *pmr1* mutants (Durr et al., 1998). The steady-state Ca^{2+} concentration in the ER of *S. cerevisiae* was shown to be 10 μM. Mutants lacking the *PMR1* gene showed severely reduced levels of ER Ca^{2+} demonstrating that this pump controls at least in part, the Ca^{2+} concentration in the yeast ER (Strayle et al., 1999). An N-terminal EF hand-like motif in Pmr1p binds Ca^{2+} and is essential for Pmr1p function as in-frame deletions

of the Ca^{2+}-binding motif resulted in a complete loss of Pmr1p function (Wei et al., 1999). Experiments manipulating Pmr1p activity within *S. cerevisiae* strains carrying the *vps33* mutation, which results in the absence of vacuoles and increased small vesicular and Golgi-like structures, indicate that the Golgi apparatus plays a significant role in maintaining Ca^{2+} homeostasis when vacuolar biogenesis is compromised (Miseta et al., 1999a). Cod1p/Spf1p is an another ion pump and likely to be involved in Ca^{2+} homeostasis (Cronin et al., 2002, 2000). It has been localised to the ER membrane by both immunofluorescence microscopy and density gradient fractionation (Cronin et al., 2002). The *cod1*Δ mutant is disrupted in cellular Ca^{2+} homeostasis, causing increased transcription of Ca^{2+}-regulated genes and a synergistic increase in $[Ca^{2+}]_c$ when paired with disruption of Pmr1p (Cronin et al., 2002).

A *Yarrowia lipolytica* (*Candida lipolytica*) *PMR1* gene (*YlPMR1*) has been cloned (Park et al., 1998) and is a *S. cerevisiae PMR1* homolog that encodes a putative secretory pathway Ca^{2+}-ATPase (Sohn et al., 1998). The yeast *Kluyveromyces lactis* has also been found to contain a *PMR1* homologue (*KlPMR1*). *KlPMR1* mutant phenotypes can be rescued by the introduction of *S. cerevisiae PMR1* demonstrating that *KlPMR1* encodes for a functional Pmr1p homologue (Uccelletti et al., 1999). The *S. pombe cta3* gene has been shown to encode a homologue of the *S. cerevisiae PMR2* gene (Ghislain et al., 1990), but unlike in *S. cerevisiae* where *PMR2* encodes a Na^{2+}-ATPase, the null mutation of *S. pombe cta3* reduces the level of ATP-dependent Ca^{2+} uptake into non-vacuolar intracellular storing organelles suggesting that it encodes a Ca^{2+}-ATPase located in intracellular membranes (Halachmi et al., 1992).

The vacuole is the major site of intracellular Ca^{2+} storage in yeast and functions to maintain cytosolic Ca^{2+} levels within a narrow physiological range via Pmc1p and a H^+/Ca^{2+}-antiporter (Vcx1p) driven by the vacuolar H^+-ATPase (V-ATPase) (Cunningham and Fink, 1994b; Ohsumi and Anraku, 1983; Dunn

et al., 1994; Ohya et al., 1991b; Antebi and Fink, 1992). The long term loss of V-ATPase triggers compensatory mechanisms, which are dependent on calcineurin, and mediated primarily by Pmc1p (Forster and Kane, 2000). *VCX1* encodes the major vacuolar H^+/Ca^{2+}-exchanger in *S. cerevisiae*, and is a direct or indirect target of calcineurin inhibition (Cunningham and Fink, 1996). Both the *S. cerevisiae* Ca^{2+}-ATPase Pmc1p and the Ca^{2+}/H^+-exchanger Vcx1p/Hum1p, a Ca^{2+}/H^+ antiporter, facilitate Ca^{2+} sequestration into the vacuole (Pozos et al., 1996), however, Vcx1p is much faster at sequestering a sudden pulse of $[Ca^{2+}]_c$ into the vacuole, while Pmc1p carries out this function much less efficiently. This supports the hypothesis that Vcx1p is a high capacity, low affinity Ca^{2+}-transporter that may act to attenuate the propagation of Ca^{2+} signals in this yeast (Miseta et al., 1999b)

1.2.1.2 Ca^{2+} signal effectors and Ca^{2+} regulated processes

Numerous processes are regulated by Ca^{2+} in yeasts. For many of these processes the exact signal-transduction pathways are not yet known, however many of the proteins involved in effecting these responses have been identified.

Calmodulin (CaM) and calcineurin are two of the most important proteins operating downstream of the Ca^{2+}-signal. CaM is required for numerous functions in yeasts. In *S. cerevisiae* it is involved in the correct functioning of the spindle pole body, the spindle, and the integrity of nucleus (Sun et al., 1992) and is required for the progression of nuclear division. CaM repressed yeast cells cease growing after 12-15 h. This growth arrest has been associated with a decrease in intracellular CaM levels and analysis of the terminal phenotype showed the defect was mainly in nuclear division (Ohya and Anraku, 1989). Ca^{2+} and CaM are essential for correct chromosome segregation in *S. cerevisiae* and *S. pombe* (Stirling and Stark, 2000; Sundberg et al., 1996; Flory et al., 2002). The *S. pombe* ER cation ATPase (Cta4p) is required for control of cell shape and microtubule dynamics. The *cta4*Δ mutant displays several morphological defects

in cell polarity and cytokinesis. Fluorescence resonance energy transfer (FRET) experiments in living cells using the yellow cameleon Ca^{2+} indicator showed that Cta4p regulates the cellular Ca^{2+} concentration. These results indicate that Ca^{2+} is a key ion controlling the control of cell shape, microtubule dynamics, and cytokinesis in *S. pombe* (Facanha et al., 2002). Work based on mutant screens has shown that Ca^{2+} and phosphoinositide signalling pathways (amongst others), are also crucial for the normal functioning of the *S. pombe* ultradian clock (Kippert, 2001). The maintenance of cell polarity in *S. cerevisiae* requires CaM and it has been demonstrated through genetic studies that vertebrate CaM can functionally replace yeast CaM (Ohya and Anraku, 1992). The *cam1*$^+$ gene, encoding CaM in *S. pombe*, is essential. However the Ca^{2+}-binding properties of individual sites could not be easily correlated with their functional importance for viability (Moser et al., 1995). Ca^{2+} and CaM are also required for dimorphism in *C. albicans* where a yeast-mycelium transition was induced by addition of $CaCl_2$ but was not induced by the same treatment in the presence of the calmodulin inhibitor R24571 (Sabie and Gadd, 1989). It has also been postulated that the inhibition of germ tube formation in *C. albicans* by local anaesthetics is likely to be a result of ion channel blockade as both general (lanthanum) and selective (nifedipine and verapamil) Ca^{2+}-permeable channel blockers as well as the anaesthetics lidocaine and ropivacaine inhibit germ tube formation while addition of Ca^{2+} revert such effects (Rodrigues et al., 2000). Directional hyphal growth responses in *C. albicans* to surface microtopography is also attenuated by exposure to blockers of stretch-activated ion channels and L-type calcium channels (Watts et al., 1998)

The catalytic and/or regulatory subunits of calcineurin have been cloned in *S. cerevisiae* (Cyert et al., 1991; Cyert and Thorner, 1992; Kuno et al., 1991; Liu et al., 1991; Ye and Bretscher, 1992; Ohya et al., 1987; Lee and Klevit, 2000), *S. pombe* (Yoshida et al., 1994; Cyert and Thorner, 1992; Kuno et al., 1991; Sugiura et al., 2002), *C. albicans* (Cruz et al., 2002) and *Cryptococcus neoformans* (Odom et al., 1997; Fox et al., 2001). Calcineurin function is necessary for the

growth of *S. cerevisiae* in media containing high levels of Na^+ and Li^+ (Nakamura et al., 1993). Calcineurin also effects Ca^{2+}-dependent changes in gene expression through regulation of the Crz1p transcription factor (Stathopoulos-Gerontides et al., 1999; Yoshimoto et al., 2002), which is required for the calcineurin-dependent induction of Pmc1p, Pmr1p, Pmr2ap and Fks2p. These proteins confer tolerance to high Ca^{2+}, Mn^{2+}, Na^+, and cell wall damage, respectively (Matheos et al., 1997). Ca^{2+} and calcineurin are involved in cell-cycle control in *S. cerevisiae* where a delay in the onset of mitosis is induced through the Swe1p, a negative regulatory kinase that inhibits the Cdc28-Clb complex. Calcineurin and Mpk1p activate Swe1p at the transcriptional and post-translational level, respectively, and both pathways are essential for the cell cycle delay (Mizunuma et al., 1998, 2001). The β subunit of calcineurin is also required for the function of calcineurin in promoting adaptation of haploid *S. cerevisiae* cells to mating pheromone *in vivo* (Cyert and Thorner, 1992). The *S. cerevisiae* Ca^{2+}-permeable channel, Cch1p in is involved in Ca^{2+} influx and the late stage of the mating process (Fischer et al., 1997). In *S. pombe*, a calcineurin-like protein phosphatase (Ppb1) is thought to play a role in cytokinesis, mating, transport, nuclear and spindle pole body positioning, and cell shape. Deletion of this gene caused defects in the above processes and wild-type strains treated with calcineurin inhibitors showed similar defects (Yoshida et al., 1994). In *C. albicans* and *Cryptococcus neoformans* calcineurin has been found to play an essential role in pathogenesis and calcineurin-deficient mutants are attenuated for virulence in a murine model of candidiasis (Fox and Heitman, 2002; Cruz et al., 2002).

Several other proteins involved in Ca^{2+}-signalling transduction in yeasts also have been found. For example, the Ca^{2+}/CaM kinase II (CaMKII) regulates G2/M progression in *S. pombe* (Rasmussen and Rasmussen, 1994). Two genes (*CMK1* and *CMK2*) isolated from *S. cerevisiae* encode CaM-dependent protein kinases (Ohya et al., 1991a). The essential *FRQ1 S. cerevisiae* gene is a Ca^{2+}-binding protein belonging to the recoverin/frequenin branch of the EF-hand

superfamily and regulates a yeast phosphatidylinositol 4-kinase isoform (Ames et al., 2000). *S. cerevisiae* also expresses enzymes that can synthesise and degrade sphingosine 1-phosphate (S1P) and related molecules. Treatment of yeast cells with exogenous sphingosine stimulates Ca^{2+} accumulation through two distinct pathways and it has been suggested that phosphorylated sphingoid bases might serve as messengers of Ca^{2+}-signalling in yeast during an unknown cellular response. (Birchwood et al., 2001; Brownlee, 2001)

1.2.2 Filamentous fungi

In filamentous fungi, Ca^{2+} is thought to be involved in the control of sporulation, cyst germination, dimorphism, zoospore motility, pheromone-mediated sexual reproduction, the cell cycle, circadian rhythms, cytokinesis, tip growth, hyphal branching and hyphal reorientation towards localised stimuli (Hyde, 1998; Miller et al., 1990).

Some of the discoveries made regarding Ca^{2+}-signalling in filamentous fungi are described below. Oomycetes exhibit hyphal growth and are considered by some to be 'part of the union of fungi' (Heath and Steinberg, 1999) despite the fact that they are not true eufungi (Bhattacharya et al., 1992). Although they are commonly studied by many mycologists and show hyphal tip growth, they will not be included in this report due to their different phylogenetic origin to that of true fungi (see Table 1.1 in Deacon, 1997 for a comparison (Deacon, 1997)).

1.2.2.1 Ca^{2+} influx, efflux and homeostasis

Ca^{2+} entry into the cytoplasm is thought to occur primarily at the plasma membrane, where SA-channels permeable to Ca^{2+} have been identified in fungal hyphae using electrophysiological techniques on isolated membranes and whole cells (Zhou et al., 1991; Levina et al., 1995). The presence of two $InsP_3$-activated Ca^{2+}-channels has been demonstrated in *N. crassa* membranes using electrophysiological techniques, and it has been suggested that these channels

could be responsible for the generation of the tip-high apical Ca^{2+} gradients thought to be necessary for hyphal tip growth (Silverman-Gavrila and Lew, 2002). However, it is clear that the majority of Ca^{2+}-permeable channels remain to be discovered in filamentous fungi (Jackson and Heath, 1993) as currently only one filamentous fungal Ca^{2+}-permeable channel has been cloned (NCBI accession number: AF393474).

The vacuole of filamentous fungal cells is thought to be a major Ca^{2+} storage organelle for the cell because it contains a high concentration of Ca^{2+} (Cornelius and Nakashima, 1987). In the growing fungal hypha, the vacuole has the potential to act as an infinitely expandable Ca^{2+} store. The vacuole continually enlarges with the extending hyphae thereby increasing its capacity to store Ca^{2+} (Jackson and Heath, 1993). Kinetic analysis of the vacuolar H^+/Ca^{2+}-exchanger from *S. cerevisiae* suggested that this enzyme would be sufficient to account for the levels of Ca^{2+} sequestration observed over a wide range of environmental conditions (Dunn et al., 1994). Similar conclusions were reached concerning the vacuolar H^+/Ca^{2+}-exchangers of filamentous fungi and higher plants (Blackford et al., 1990; Miller et al., 1990). *N. crassa* vacuoles have also been shown to release Ca^{2+} in response to $InsP_3$ (Cornelius et al., 1989; Schultz et al., 1990) suggesting that $InsP_3$ mediated Ca^{2+} release from internal stores may be an important part of Ca^{2+}-signalling in filamentous fungi (Kallies et al., 1998; Silverman-Gavrila and Lew, 2002), as it is in plants and animals. The fact that PLC has been cloned from several filamentous fungi (*N. crassa*, *A. nidulans*, *B. fuckeliana* (Jung et al., 1997) and *M. grisea* [NCBI accession number: AAC72385]) and the recent detection two $InsP_3$-activated Ca^{2+}-channels in *N. crassa* membranes (Silverman-Gavrila and Lew, 2002) supports this idea.

Active transport of Ca^{2+} across *N. crassa* membranes takes place via Ca^{2+}/H^+ antiporters (Stroobant and Scarborough, 1979; Stroobant et al., 1980) and Ca^{2+}-ATPases, which function to pump Ca^{2+} out of the cell or into internal storage organelles. Ca^{2+}/H^+ antiporters rely upon proton-translocating ATPases

(Bowman and Bowman, 2000; Bowman et al., 2000) to generate a transmembrane electrical potential and pH gradient, which can then be utilised to energise the active transport of Ca^{2+} (Stroobant et al., 1980). One such filamentous fungal Ca^{2+}/H^{+} antiporter, CAX, has been cloned (Margolles-Clark et al., 1999). The function of this protein is to transport Ca^{2+} into the vacuole. Five Ca^{2+}-ATPases (NCA-1, NCA-2, NCA-3, PMR-1, PH-7) have been cloned in *N. crassa* and experiments examining the suppression of *S. cerevisiae* null Ca^{2+} mutants by some of these proteins, phylogenetic analysis and induction of gene expression by Ca^{2+}, were used to indicate their function as Ca^{2+}-ATPases (Benito et al., 2000). A Ca^{2+}-ATPases has also been identified in *Ustilago maydis* and has been shown to be responsible for pumping Ca^{2+} into plasma membrane vesicles (Hernandez et al., 1994; Benito et al., 2000). In *Aspergillus niger pmrA* has been identified as a homologue of the yeast *PMR1* gene. It encodes a functional homologue of the yeast Ca^{2+}-ATPase (Pmr1p) involved in the secretory pathway as it restored the growth defect of a *Yarrowia lipolytica pmr1* null mutant (Yang et al., 2001a).

1.2.2.2 Ca^{2+} signal effectors and Ca^{2+} regulated processes

CaM and calcineurin have been cloned in *N. crassa* (Capelli et al., 1993; Melnick et al., 1993; Higuchi et al.; Kothe and Free, 1998; Prokisch et al., 1997) and *A. nidulans* (Rasmussen et al., 1990, 1994). CaM has also been cloned in *Fusarium proliferatum* (NCBI accession number: AAK69619) (Kwon et al., 2001) and calcineurin has been cloned in *A. oryzae* (Juvvadi et al., 2001). These proteins clearly play a significant role in many important processes. For example circadian rhythms are inhibited by Ca^{2+} ionophores and CaM inhibitors in *N. crassa* (Techel et al., 1990; Sadakane and Nakashima, 1996; Yang et al., 2001b) and CaM mediated phosphorylation is required for conidial germination in *N. crassa* (Muthukumar and Nickerson, 1984; Rao et al., 1997). Ca^{2+} and calcineurin are thought to play a regulatory role in aflotoxin production in *Aspergillus parasiticus* as the Ca^{2+}-permeable channel blockers verapamil and

diltiazem prevented incorporation of [^{14}C]-acetate into aflotoxin B_1 in a dose-dependent manner (Rao and Subramanyam, 1999). Aflatoxin production was also accompanied by enhanced (26-fold) activity of calcineurin concomitant with a lowered (6-fold) activity of CaM-dependent protein kinase (Jayashree et al., 2000). Contact with hard surfaces induces Ca^{2+}/CaM signalling in *Colletotrichum gloeosporioides* and primes the conidia to respond to host signals by germinating and differentiating into appressoria (Kim et al., 1998). Ca^{2+} and CaM are thought to be involved in xylanase formation and secretion in *Trichoderma reesei* based on work done with Ca^{2+}-antagonists -agonists and CaM inhibitors (Mach et al., 1998). Ca^{2+} and CaM are required for dimorphism in *Ceratocystis ulmi* (Muthukumar et al., 1987) and *Sporothrix schenckii* (Gadd and Brunton, 1992; Alsina and Valle, 1984). CaM is an essential gene in all eukaryotes so far examined. Unlike in *S. cerevisiae* (Davis, 1992), however, the essential function of CaM in *A. nidulans* is dependent on its binding Ca^{2+} (Joseph and Means, 2002). Ca^{2+} and CaM are required for cell cycle progression in *A. nidulans* (Lu et al., 1992, 1993) and mitotic spindle formation of the fungal centrosome in *A. fumigatus* is likely to involve a recently discovered homologue to the calmodulin-binding yeast Spc110p/Nuf1p protein (Flory et al., 2002).

There are many other important proteins involved in transducing Ca^{2+}-signals for the control of various processes. Examples include Ca^{2+}- and/or CaM-dependent protein kinases (CaMK), which are present in *N. crassa* (Favre et al., 1991; Yang et al., 2001b) and *Arthrobotrys dactyloides* (Tsai et al., 2002), *A. nidulans* (Kornstein et al., 1992; Joseph and Means, 2000) and *Colletotrichum gloeosporioides* (Kim et al., 1998). CaMK has been partially purified from *Fusarium oxysporum* and shown to exhibit Ca^{2+}/CaM-dependent phosphorylation and to bind anti-rat brain Ca^{2+}/CaM-dependent protein kinase II antibodies (Hoshino et al., 1992). Ca^{2+} is thought to play a role in phospholipid synthesis in *Microsporum gypseum* (Giri et al., 1994). This regulation might be achieved through Ca^{2+}/CaM-dependent phosphorylation by Ca^{2+}/CaM-kinase

(CaMPK) as addition of KN-62 (a specific inhibitor of Ca^{2+}/CaM-dependent protein kinases) and polyclonal antibodies raised against purified CaMPK of *M. gypseum* leads to the inhibition in the incorporation of labelled acetate into total phospholipids in this fungus (Giri and Khuller, 1999). The Ca^{2+}/CaM-regulated protein kinases CMKB and CMKC from *A. nidulans* play a role in control of the cell cycle. When CMKB expression is postponed spores germinate with delayed kinetics. A lag is observed in the G1-phase activation of the cyclin-dependent kinase $NIMX^{cdc2}$. Spores lacking CMKC also germinate with delayed kinetics and a lag in the activation of $NIMX^{cdc2}$ suggesting that both CMKB and CMKC are required for the proper temporal activation of $NIMX^{cdc2}$ as spores enter the cell cycle from quiescence (Joseph and Means, 2000).

Low external Ca^{2+} and Ca^{2+} inhibitors reduce the induction of conidiation in *Penicillium spp.* (Pitt and Barners, 1999) and *Trichoderma viride* (Krystova et al., 1995) and conidial germination in *N. crassa* (Muthukumar and Nickerson, 1984; Rao et al., 1997) and *Sporothrix schenckii* (Rivera-Rodriguez and Valle, 1992) are all strongly influenced by Ca^{2+}. Both germination and appressorium formation in *Phyllosticta ampelicida* pycnidiospores are regulated by Ca^{2+}-signalling (Shaw and Hoch, 2000) and several inhibitors of K^+ and Ca^{2+} ion channels have been found to inhibit ascospore discharge in *Gibberella zeae* (Trail et al., 2002).

Hyphal elongation and branching is thought to be regulated by Ca^{2+} in several species of filamentous fungi, including *N. crassa* (Gow et al., 1992; Dicker and Turian, 1990; Reissig and Kinney, 1983; Silverman-Gavrila and Lew, 2000, 2001), *Fusarium graminearum* (Robson et al., 1991c,b) and *Botrytis cinerea* (Hudecoca et al., 1994) (discussed in detail in Section 1.5). Other morphological process thought to be affected by Ca^{2+}-signalling in filamentous fungi include gravitropic responses in *Corprinus cinereus*, which are affected by Ca^{2+} modulators (Frazer and Moore, 1993) and the development of *Erysiphe pisi* on pea leaves, which is affected by Ca^{2+} and CaM modulators (Singh and ad B. K. Sarma, 2001).

Phytoparasitism in *Botrytis cinerea* is radically affected by Ca^{2+}(Elad and Kirshner, 1992). It has also been proposed that zoospores of phytopathogenic fungi perceive host signals by specific G-protein-coupled receptors and translate the signals into responses by way of the phosphoinositide-Ca^{2+}-signalling cascade. However, this remains to be proved experimentally (Islam and Tahara, 2001). The nematode trapping fungus *Arthrobotrys dactyloides* is thought to trap nematodes via a mechanism whereby pressure exerted by a nematode activates G-proteins leading to an increase in $[Ca^{2+}]_c$, activation of CaM, and finally the opening of water channels causing ring cells to constrict and immobilise the nematode (Chen et al., 2001).

1.3 *Neurospora* as an Experimental System

The filamentous fungus *N. crassa* has seven chromosomes between 4.0 and 10.9 Mbp in size and a total genome size of about 43 Mbp. It has been the subject of scientific research since 1843 (Perkins, 1992) and today boasts the greatest number of scientists devoted to one species of filamentous fungus (Nelson, 2000). *N. crassa* has several attributes that make it popular for use as a model organism. Some examples are its ease of growth (its hyphal extension rate can exceed 4 mm h^{-1}) and the fact that it is haploid throughout most of its life cycle and thus recessive mutated alleles are not masked by dominant alleles on homologous chromosomes. It produces propagules suitable for plating and can easily be maintained in suspended animation with no need for periodic transfers (Perkins, 1992). Furthermore, *N. crassa* can reproduce either sexually or asexually. DNA-mediated transformation is efficient and repeat-induced point mutation (RIP), a phenomenom whereby G:C to A:T mutations occur in duplicated DNA sequences, can be harnessed to achieve *in vivo* mutagenesis of specific chromosomal regions in *N. crassa* (Selker, 1991). Together these characteristics make *N. crassa* highly amenable to genetic manipulation and biochemical characterisation. Further

important resources have been made available by the Fungal Genetics Stock Centre (FGSC) who carried over 7000 *N. crassa* strains in 1990, and who distribute a wide selection of mutants and genetic libraries (Perkins, 1992). The entire *N. crassa* genome has been sequenced and throughly annotated (Galagan et al., 2003). *N. crassa* is the first filamentous fungus for which this has been achieved. The genetic map of *N. crassa* is also very well documented and includes over 1000 genes mapped relative to each other and over 500 cloned genes.

Overall there is a wealth of tools, resources and information for those studying *N. crassa*. Information on *N. crassa* is also readily applicable to other agriculturally or industrially important fungi. Although *N. crassa* is nonpathogenic, it is phylogenetically very closely allied with and genetically similar to several important plant pathogens including *Cochliobolus carbonum* (Southern corn leaf blight), *Fusarium spp.*, and *Magnaporthe grisea* (the rice blast fungus).

1.4 The Filamentous Fungal Lifestyle

1.4.1 Hyphal growth and branching

N. crassa is a filamentous fungus. Filamentous fungi are made up of many cellular filaments, called hyphae, that growth and branch to form a network called a mycelium. The vegetative hyphae of filamentous fungi present outstanding examples of polarised growth and branching. The polarised growth of fungal hyphae (along with cells as diverse as pollen tubes, algal rhizoids and root hairs (Bibikova et al., 1999) is characterised by extension which is confined to the cell tip. The tip of the hypha extrudes out into the environment from the subapical tube in a continuous growth process that involves the synthesis of new cell wall and cell membrane. This involves massive exocytosis of vesicles which contribute to cell wall synthesis, along with the production, localisation, and activation of the enzymes which synthesise the fibrillar cell wall polymers (Heath and Steinberg,

1999). A common rate of hyphal extension in *N. crassa* in open-culture is 36 μm min^{-1}. In order for a 10 μm wide hyphae to supply sufficient plasma membrane to the hyphal tip to maintain this growth rate it has been estimated that about 600 secretory vesicles per second would have to fuse with the apical plasma membrane (Collinge and Trinci, 1974).

Tip growth, with the accompanying ability to grow in a straight line or change direction, enables the hypha to explore and penetrate its environment (Heath and Steinberg, 1999). During tip growth, the diameter of the hyphal tube is precisely regulated. It is coordinated with growth rate and direction and is generally maintained at a constant value through varying extension rates and direction changes (López-Franco et al., 1994; Riquelme et al., 1998).

Hyphal morphogenesis is thought to be controlled by the position of the Spitzenkörper (Spk), a phase-dark body found at the tip of elongating hyphae in higher fungi (Riquelme et al., 1998; Brunswick, 1924; Girbardt, 1969; López-Franco and Bracker, 1996). The Spk is a complex assemblage of organelles containing amongst other things a central core of variable composition, a cluster of vesicles surrounding the core, and an outer cloud of vesicles with imprecise boundaries (Reynaga-Peñüia et al., 1997).

Branching in filamentous fungi is generally either *lateral*, most common in wild-type strains that have not been subjected to stress, or *dichotomous*. Dichotomous branching (see Fig.1.1) is usually observed under stress conditions or in some mutant strains.

1.4.2 Branching mutants of *Neurospora crassa*

Amongst the thousands of strains of *N. crassa* carried by the FGSC there are many mutants showing altered hyphal branching and morphology. Table 1.1 shows a selection of these mutants. In several cases Ca^{2+} is, or is thought to be, in some way involved with generating the mutant phenotype.

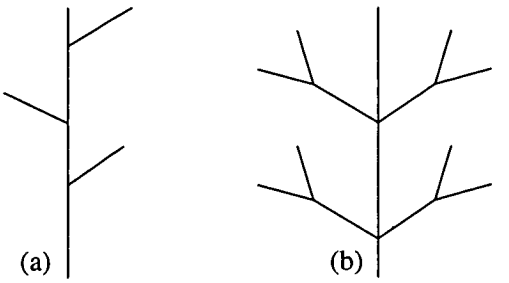

Figure 1.1: The two most common branching types in *N. crassa*: (a) lateral branching, and (b) dichotomous branching.

Table 1.1: Some hyperbranching mutants of *N. crassa*

cot-1	Colonial growth at or above 32°C, but normal growth below this temperature. At the restrictive temperature, colonies grow slowly with excessive hyphal branching and do not conidiate. The *cot-1* gene encodes a protein kinase (Yarden et al., 1992). A possible functional linkage between COT1 kinase, calcineurin and a cytoskeletal motor protein has been proposed (Gorovits et al., 1999).
cot-2	Another colonial temperature-sensitive mutant. Colonial growth at or above 32°C and a more wild-type phenotype at 25°C. Mapped to linkage group V between *ser-2 ad-7* by classical genetics (Perkins et al., 1982).
cot-3	Colonial growth at or above 32°C and a more wild-type phenotype at 25°C. The (*cot-3*) gene encodes a protein elongation factor 2 (Propheta et al., 2001).
cot-4	Small colonies at 34°C, spreading at 25°C. Morphology at 25°C resembles that of the mutant *spray*. Mapped to linkage group V between *rol-3 ini* by classical genetics (Perkins et al., 1982).
cot-5	Little or no growth at 34°C; colonial at 30°C. Morphology still not normal at 25°C. The *cot-5* gene encodes a mannosyltransferase and the mutant phenotype can be suppressed by increased medium osmoticum (Resheat-Eini et al., 2003).
spray	The *spray* mutant of *N. crassa* branches profusely under conditions of normal growth in the wild-type. This phenotype can be partially corrected by addition of 50-500 mM Ca^{2+} (Dicker and Turian, 1990). The *spray* gene has been cloned but shows no homology to other genes in the database (Bok et al., 2001).
frost	Similar to *spray* although hyperbranching is more profuse. The *frost* gene is homologous to the yeast *cdc1* gene and affects hyphal branching via manganese homeostasis (Sone and Griffiths, 1999).
pvn1-121A	A *vma-1* (V-ATPase encoding subunit) null strain. *pvn1-121A* colonies grow very slowly in comparison to wild-type colonies and show intense hyperbranching (Bowman and Bowman, 2000; Bowman et al., 2000).
pvn2-53-19A	Another *pvn* mutant. V-ATPase activity could not be detected in *pvn2-53-19A* membrane extracts (E. J. Bowmann, personal communication). This mutant also exhibits slow growth and hyperbranching.

1.4.3 Factors affecting hyphal branching

1.4.3.1 Increasing hyphal branching frequency

Many factors affect hyphal branching in filamentous fungi. For example, the addition of 1 mM verapamil to a *N. crassa* growth medium caused hyphal swelling and branching (Dicker and Turian, 1990). The Ca^{2+}-selective ionophores A23187 and ionomycin cause the emergence of multiple branches shortly after addition (Schmid and Harold, 1988; Reissig and Kinney, 1983; Harold and Harold, 1986).

Low concentrations of cytochalasins have been reported to induce branching in a number of fungi (Betina et al., 1971; Allen et al., 1980). Cytochalasins are thought to act by blocking the elongation of actin filaments or by disrupting microfilament networks (Bray, 1979; Lin et al., 1980; Brown and Spudich, 1981; Schliwa, 1982).

Phosphoinositide turnover inhibitors lysocellin, piericidin B_1*N*-oxide and the inositol analogue (2S, 3R, 5R)-3-azido-2-benzoyloxy-5-hydroxycyclohexanone, all reduce hyphal extension and cause increased branching (Hosking et al., 1995).

Cantharidin and calyculin A, inhibitors of protein phosphatase type 1 (PP1) and PP2A respectively, induce an increase in hyphal branching (Yatzkan et al., 1998). Genetic reduction of PP2A activity by ectopic expression of *pph-1* has similar effects (Yatzkan et al., 1998).

Genetic impairment of *cna-1*, *cnb-1* or treatment of wild-type *N. crassa* with anti-calcineurin drugs cyclosporin A and FK506 causes loss of apical dominance and hyperbranching followed by growth arrest (Prokisch et al., 1997). Genetic and chemical impairment of the vacuolar ATPase of *N. crassa* also increases branching frequency dramatically (Bowman and Bowman, 2000; Bowman et al., 2000).

The chitin synthase inhibitors polyoxin D and nikkomycin Z cause hyphal ballooning and hyperbranching in both *N. crassa* and *Coprinus cinereus* (Gooday, 1990). Another proposed inhibitor of chitin synthesis, Edifenphos (or Hinosan) increases branching in *Fusarium graminearum*. This effect can be counteracted by

the simultaneous addition of 20 μM choline chloride to the growth medium (Wiebe et al., 1992). Tight colonial morphology and a dramatic increase in branching were observed when 10 to 25 mM cAMP was added to *Fusarium graminearum* growth media (Robson et al., 1991a). Again, it was possible to counteract this effect with choline chloride. It seems therefore, that the morphological effects of choline are independent from the morphological effects of cAMP, and that the morphological effects of choline are independent from the morphological effects of Edifenphos. On the bases of these and other observations, it was suggested that branch initiation and hyphal extension can be regulated independently (Markham et al., 1993).

Sorbose has also been found to cause a massive increase in branching frequency and a reduction in hyphal extension rate in *N. crassa* (Crocken and Tatum, 1968; Mishra and Tatum, 1972; Trinci and Collinge, 1973).

1.4.3.2 Reducing hyphal branching frequency

There are very few treatments known which *inhibit* hyphal branching. This is perhaps because the usual fungal response to stress and many other stimuli is an increase in the frequency of branching rather than a decrease.

Addition of as little as 1-5 μM choline chloride to the growth medium of *Fusarium graminearum* inhibits branch formation without affecting specific growth rate or the mean hyphal extension rate. Similar effects were observed using the related compounds betaine, ethanolamine, monomethylethanolamine (MME) and dimethylethanolamine (DME) (Wiebe et al., 1990, 1992). Choline chloride inhibits branch formation in *Aspergillius nidulans* in a similar way (Binks et al., 1992; Markham and Bainbridge, 1992; Markham, 1992).

cGMP was found to reduce hyphal branching when added to *Fusarium graminearum* A 3/5 at a concentration of between 10 and 50 mM (Robson et al., 1991a). Furthermore, the fungal response when both cGMP and choline were

added together was even grater than the additive product that would be expected if the two compounds were added separately (Markham et al., 1993).

1.5 Ca^{2+} and Hyphal Branching in *Neurospora* and other Filamentous Fungi

A tip high Ca^{2+} gradient, peaking at about 3 μm behind the tip, has been observed in growing but not in non-growing hyphae of *N. crassa* (Levina et al., 1995) using flourescent dyes which report free Ca^{2+} (Silverman-Gavrila and Lew, 2000, 2001). Wild-type hyphae show a strong fluorescence with a clear apical gradient in mediums containing chlortetracycline (CTC) (Schmid and Harold, 1988; Dicker and Turian, 1990), which reports membrane bound Ca^{2+} (Jackson and Heath, 1993). In one case, the addition of 1 mM verapamil (a Ca^{2+}-channel blocker) to a CTC containing medium caused hyphal swelling, branching and the dissipation of the CTC fluorescence. Addition of Ca^{2+} alleviated these effects (Dicker and Turian, 1990). The hyperbranching mutants '*frost*' (*fr*) and '*spray*' (*sp*) show a similar phenotype and CTC fluorescence to verapamil treated wt, and like the treated wt, this phenotype can be corrected by treatment with 50-500 mM Ca^{2+} (Dicker and Turian, 1990). Reducing the extracellular [Ca^{2+}] of *N. crassa* growth media resulted in shorter, wider hyphae eventually leading to a total loss of polarised growth in 20% of the population at 0.1 μM-Ca^{2+} (Schmid and Harold, 1988). The Ca^{2+} ionophore A23187 caused dissipation of CTC fluorescence and the emergence of multiple branches shortly after addition (Schmid and Harold, 1988; Reissig and Kinney, 1983).

Voltage clamping has shown that the direction of ion transport across the *N. crassa* plasma membrane is not important for the regulation of tip growth (Silverman-Gavrila and Lew, 2000), but that intracellular Ca^{2+} was essential.

It has also been shown, using electrophysiological techniques, that two $InsP_3$-activated Ca^{2+}-permeable channels exist in *N. crassa* membranes (Silverman-Gavrila and Lew, 2002). A range of inhibitor experiments indicated that one of these Ca^{2+}-permeable channels was necessary to generate the hyphal tip-high Ca^{2+} gradient required for hyphal growth (Silverman-Gavrila and Lew, 2001; Silverman-Gavrila and Lew, 2002). It has been proposed that the Ca^{2+} gradient may be maintained by "Ca^{2+} shuttling" from wall-building vesicles which are concentrated in hyphal tips (Torralba et al., 2001).

Phosphoinositide turnover inhibitors lysocellin, piericidin B_1N-oxide and the inoisotol analogue (2S, 3R, 5R)-3-azido-2-benzoyloxy-5-hydroxycyclohexanone, all reduce hyphal extension and cause increased branching (Hosking et al., 1995). It has been shown that $InsP_3$ causes the release of Ca^{2+} from isolated *N. crassa* vacuoles (Cornelius et al., 1989). Heat shock leads to a transient increase of $InsP_3$ and a drastic decrease in the amount of vacuolar Ca^{2+} (Kallies et al., 1998).

In *N. crassa*, genes homologous to 2 subunits of calcineurin, *cna-1* (calcineurin A) and *cnb-1* (calcineurin B) have been cloned and shown to play roles in hyphal development (Sone and Griffiths, 1999; Kothe and Free, 1998). Impairment of either gene or treatment of wild-type with anti-calcineurin drugs cyclosporin A and FK506 causes loss of apical dominance and hyperbranching followed by growth arrest (Prokisch et al., 1997). Genetic or chemical impairment of the vacuolar ATPase, thought to be necessary for generation of the electrochemical gradient required for the operation of the vacuolar Ca^{2+}/H^+ antiporter, CAX, caused a massive reduction in hyphal extension rate and a profoundly hyperbranched phenotype (Bowman and Bowman, 2000; Bowman et al., 2000).

There is also evidence that Ca^{2+} plays a role in the regulation of tip growth and hyphal branching in other filamentous fungi including *Fusarium graminearum* (Robson et al., 1991c,b) and *Botrytis cinerea* (Hudecoca et al., 1994).

1.6 Measuring Intracellular Ca^{2+}

Due to its toxicity at μM concentrations $[Ca^{2+}]_c$ is strongly buffered in the cytoplasm. Resting $[Ca^{2+}]_c$ concentrations of 70-92 nM (Levina et al., 1995; Miller et al., 1990) in *N. crassa*, and transient increases in $[Ca^{2+}]_c$ that are over in minutes, make the measurement of Ca^{2+} in living cells problematic. Furthermore, the use of fluorescent dyes within living cells is difficult as the dyes may result in cell damage, be cytotoxic, leak out of cells, or be sequestered into organelles (Read et al., 1992). Many experiments using such dyes have induced altered growth and morphology in their subjects (Jackson and Heath, 1993; Silverman-Gavrila and Lew, 2000, 2001). The evidence for a role for Ca^{2+}-signalling in regulating hyphal branching, was either derived indirectly (e.g. using pharmocological agents), or through the direct measurement of $[Ca^{2+}]_c$ using Ca^{2+} selective fluorescent dyes. Much of the evidence indicating the presence of an apical Ca^{2+} gradient in *N. crassa* hyphae, and its requirement for normal hyphal morphology, is based on CTC staining. As CTC fluoresces only when bound to Ca^{2+} in the vicinity of a membrane (Jackson and Heath, 1993), such evidence may not provide the whole picture relating to $[Ca^{2+}]_c$ concentrations in fungal hyphae. Due to the difficulties mentioned above, there are currently "few compelling reports and numerous uncertainties" regarding the measurement of Ca^{2+} distribution and concentration in growing hyphal tips (Jackson and Heath, 1993). One technique, which has the potential to overcome these problems uses the Ca^{2+}-sensitive luminescent protein aequorin, and it is this technology that I have used in my study.

1.6.1 Measuring intracellular Ca^{2+} with recombinant aequorin

Aequorin is a 22 kDa photoprotein from the jelly fish *Aequorea victoria*, which also produces the green fluorescent protein (Kendall and Badminton, 1998). Active aequorin is composed of apoaequorin (the apoprotein), coelenterazine

(the luciferin) and bound oxygen. On binding Ca^{2+}, aequorin is converted into apoaequorin, carbon dioxide and coelenteramide, and energy from this reaction is released as blue light (see Fig. 1.2). Because the amount of luminescence

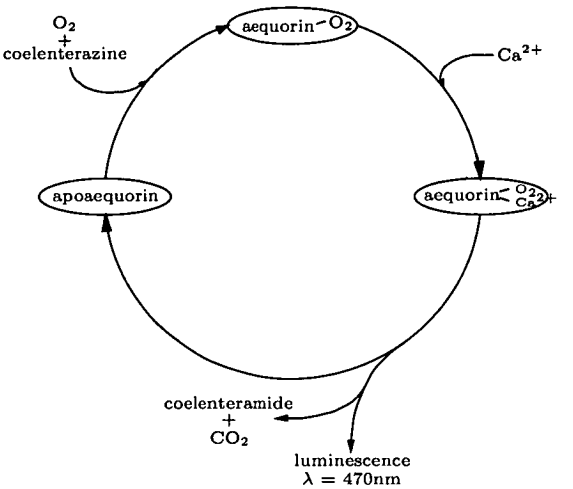

Figure 1.2: Apoaequorin, coelenterazine and molecular oxygen form the complex 'aequorin'. The combination of aequorin and Ca^{2+} initiates an intramolecular oxidation reaction that results in CO_2, coelenteramide, apoaequorin and the emission of blue light (λ = 470 nm). Adapted from a slide by Ann Haley.

is dependent upon the concentration of free Ca^{2+} (see Fig. 1.3), aequorin can be used to report $[Ca^{2+}]_c$ inside cells. Properties of aequorin which make it a useful intracellular Ca^{2+} reporter include its: high selectivity for free Ca^{2+}; very large dynamic range over which Ca^{2+} can be measured; retention within the cell compartment it has been targeted to; lack of $[Ca^{2+}]_c$ buffering; and non-cytotoxicity (Miller, 1994). Further advantages become available when aequorin is expressed in an organism by DNA-mediated transformation (Kendall and Badminton, 1998).

The cloning and characterisation of two apoaequorin genes (*aeqA* [also called *aeq1*] (Prasher et al., 1985) and *aeqD* [also called *aq440*], (Inouye et al., 1985) led to recombinant aequorin expression in plants (Knight et al., 1991b), yeast (Nakajima-Shimada et al., 1991a,b), bacteria (Knight et al., 1991a), mammalian cell lines (Kendall et al., 1992; Rizzuto et al., 1992) and slime moulds (Saran

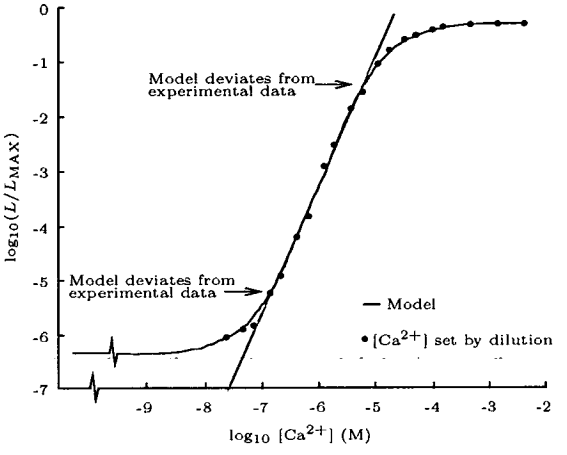

Figure 1.3: The relationship between light emission and Ca^{2+} for aequorin. Ca^{2+} was determined by dilutions of 1 M $CaCl_2$. The red line indicates the relationship between light emission and Ca^{2+} (Allen et al., 1977).

et al., 1994). Using appropriate promoters and signal sequences, aequorin can be expressed in all or selected cell types (Rosay et al., 1997), or targeted to specific subcellular locations including organelles (Rizzuto et al., 1994; Kendall and Badminton, 1998). Cytosolic or organellar free Ca^{2+} may then be analysed in single cells, tissues, organs or whole organisms using luminometry (Knight and Knight, 1995) or low light imaging (Knight et al., 1993). Luminescence is converted into $[Ca^{2+}]$ using Equation 1.3 below (Allen et al., 1977; van der Luit, 1998).

$$\frac{L}{L_{\mathrm{MAX}}} = \left(\frac{(1 + K_R \cdot [\mathrm{Ca}^{2+}])}{1 + K_{TR} + K_R \cdot [\mathrm{Ca}^{2+}])} \right)^3 \tag{1.3}$$

L = counts s^{-1}, L_{MAX} = total counts measured during the course of the experiment, $[Ca^{2+}]$ = the calculated $[Ca^{2+}]$, K_R is the equilibrium association constant and K_{TR} = [T]/[R], where T and R are the 2 possible states of the Ca^{2+}-binding sites in aequorin (Allen et al., 1977). Values used were $K_R = 2 \cdot 10^6$ M^{-1} and K_{TR} =55 (van der Luit, 1998).

1.7 Genomics - The Recent Revolution

Over the last decade, the number of organisms whose genomes have been sequenced has been growing at an ever increasing rate. The genome of the first filamentous fungus to be completely sequenced in the public sector, *N. crassa*, was recently published (Galagan et al., 2003) and more filamentous fungal genome sequencing projects are reaching completion. *Magnaporthe grisea* is the first fungal plant pathogen to have had its genome sequenced and *A. fumigatus* is the first human filamentous fungal pathogen to have its genome sequenced. The genome sequences of the non-filamentous fungal model organisms *S. cerevisiae* and *S. pombe* were published in 1996 and 2002, respectively (Goffeau et al., 1996; Wood et al., 2002).

The list of sequenced fungal organisms is growing rapidly and partial genome sequences of several other fungi are currently available. Table 1.2 lists both completed and ongoing fungal genome sequencing projects. References are given where genome sequencing projects have been completed and published in peer reviewed journals.

Table 1.2: Past and present fungal genome sequencing projects

Organism	Web Site	Reference
N. crassa	http://www-genome.wi.mit.edu/annotation/fungi/neurospora	(Galagan et al., 2003)
F. graminearum	http://www-genome.wi.mit.edu/annotation/fungi/fusarium	-
M. grisea	http://www-genome.wi.mit.edu/annotation/fungi/magnaporthe	-
P. chrysosporium	http://www.jgi.doe.gov/programs/whiterot.htm	-
A. fumigatus	http://www.tigr.org/tdb/e2k1/afu1	-
A. nidulans	http://www-genome.wi.mit.edu/annotation/fungi/aspergillus	-
C. albicans	http://genome-www.stanford.edu/fungi/Candida	-
C. neoformans	http://www.tigr.org/tdb/e2k1/cna1	-
P. carinii	http://www.uky.edu/Projects/Pneumocystis	-
S. cerevisiae	http://genome-www.stanford.edu/Saccharomyces	(Goffeau et al., 1997)
S. pombe	http://www.sanger.ac.uk/Projects/S_pombe	(Wood et al., 2002)

The availability of such large filamentous fungal genome databases has made it

possible, for the first time, to gain detailed insights into the molecular machinery of filamentous fungi through genomic analysis.

1.8 Introduction to the Research Carried out in this Thesis

Despite the obvious importance of Ca^{2+}-signalling in filamentous fungi, and in contrast to the situation in budding yeast, there is very little direct knowledge about Ca^{2+}-signalling or the molecular components involved in Ca^{2+}-signalling in filamentous fungi. The aims of this research were:

- To develop and an aequorin-based approach for measuring $[Ca^{2+}]_c$ in living *N. crassa* hyphae
- To quantitaivly characterise the Ca^{2+}-signatures in response to various stimuli over a range of environmental conditions and to develop a sensitive method for detecting perturbations in Ca^{2+}-signalling machinery
- To use the tools and methods developed to:
  - investigate the contribution of internal Ca^{2+} stores in the observed Ca^{2+}-signatures
  - analyse the role of Ca^{2+}-signalling in hyphal branching using hyperbranching mutants
- To genetically and phenotypically analyse selected hyperbranching mutants of *N. crassa*
- To perform a genomic analysis of the Ca^{2+}-signalling machinery in *N. crassa*, *A. fumigatus*, *M. grisea* and *S. cerevisiae* based on the available genome sequences

Chapter 2

Materials and Methods

2.1 Chemicals

The chemicals used in this study, and their sources, are described in Appendix A.1.

2.2 Organisms and Media

Genetically modified *Neurospora crassa* (*N. crassa*) and *Escherichia coli* (*E. coli*) were containment level 1 organisms and the relevant procedures for their handling and disposal[1] were followed at all times. Established sterile technique was used when appropriate.

All media and salt solutions were made using distilled water (dH_2O) and sterilised before use by autoclaving at 121°C, 15 pounds per square inch (psi) for 20 min. Heat-sensitive components were filter sterilised (using Sartorius Minisart 0.2 μm filters, Goettingen, Germany) and added to the main solution after the latter was autoclaved.

[1]Published by the Genetic Manipulation and Biological Safety Committee, University of Edinburgh.

2.3 Fungal Strains

Ten strains of *N. crassa* were used in this study. These were: wild-type (wt) strain 74-OR231A, *cot-1*, *cot-2*, *cot-3*, *cot-4*, *cot-5*, *frost* (*fr*), *spray* (*sp*), *pvn1-121* (*pvn1*) and *pvn2-53-19* (*pvn2*) and their genotypes are described in Table 2.1. The *pvn* strains were kindly supplied by Dr. Emma Bowman (Bowman and Bowman, 2000; Bowman et al., 2000).

Table 2.1: *Neurospora crassa* strains used in this study

Strain	FGSC Number	Mating Type	Genotype	Mutagen
74-OR231A	987	A and a	no mutations	-
cot-1	4065	A	*cot-1 allele C102(t)*	UV
cot-2	1512	a	*cot-2 allele R1006(t)*	UV
cot-3	1517	A	*cot-3 allele R2006(t)*	UV
cot-4	3600	A	*cot-4 allele R2101(t)*	UV
cot-5	1362	A	*cot-5 allele R2479(t)*	UV
frost	102	a	*fr allele B110*	UV
spray	68	A	*sp allele B132*	UV
pvn1-121	-	A	am_{132} $vma\text{-}1^{RIP1}$	-
pvn2-53-19	-	A	$vma\text{-}1^{RIP2}$	-

2.4 Cosmid Libraries and Genetic Complementation

The Orbach/Sachs pMOcosX genomic DNA cosmid library of *N. crassa* linkage group V was used for complementation experiments with *cot-2* and *cot-4*, both of which have been mapped to chromosome V by classical genetics (Perkins et al., 1982). This cosmid library was obtained from the Fungal Genetics Stock Center[2]. The vector pMOcosX has dominant selectable markers for fungi (hygromycin resistance) and *E. coli* (ampicillin resistance) (Orbach, 1994).

[2]http://www.fgsc.net

2.5 Culture Media and Growth Conditions

2.5.1 Culturing *E. coli*

2.5.1.1 Culture media

E. coli was grown on solid or in liquid Luria-Bertani (LB) medium (Appendix D). Solid nutrient agar (Table D) and glycerol stocks (0.5ml liquid LB culture + 0.5ml 80% glycerol) were used for long term storage of *E. coli.*

2.5.1.2 Inoculation procedure

Liquid medium was inoculated with a sterile wooden stick, which was used to capture individual colonies growing on solid medium. Solid LB plates were inoculated with 50-100 μl of LB-bacterial cell suspension. A sterile bent glass rod was used to disperse the inoculum. Nutrient agar tubes were inoculated with a sterile wooden stick which had been dipped in a liquid culture. The stick was inserted in the centre of the tube to half the depth of the agar and then removed.

2.5.1.3 Antibiotics and other selective media

For selection of plasmids containing hygromycin, ampicillin or chloramphenicol resistance genes, 150 μg ml^{-1} hygromycin B (Roche Diagnostics, GmbH, Germany), 100 μg ml^{-1} ampicillin (Sigma Chemical Co., USA) or 170 μg ml^{-1} chloramphenicol (Sigma Chemical Co., USA), respectively, was added to the media after autoclaving. When the acetamidase-encoding gene (*amdS*) was used as a selectable marker (Yamashiro et al., 1992), acetamide was used as the sole nitrogen source in all selective media.

2.5.1.4 Types of culture and growth conditions

Solid LB plates contained 15 to 20 ml LB per 8.5 cm Petri dish. Media were made, autoclaved and allowed to cool to 40°C before addition of the appropriate

antibiotics. Plates were poured before medium solidification, inoculated, and incubated upside down at 37°C.

Liquid LB cultures were 5 ml liquid LB in a 20 ml test tube with a plastic lid. Antibiotics were added, when appropriate, before inoculation. Cultures were incubated upright in a shaking incubator at 37°C and 200 revolutions per minute (rpm).

Solid nutrient agar cultures were 5 ml of autoclaved nutrient agar, which was poured into a 20 ml screw cap glass test tube. Once set, the culture was inoculated and stored at room temperature. Glycerol stocks were prepared, mixed throughly and stored at -80°C.

2.5.2 Culturing *N. crassa*

2.5.2.1 Culture media

N. crassa was grown on solid or in liquid Vogel's medium (Vougel, 1956) (Appendix D). Transformed *N. crassa* protoplasts were mixed with molten (40°C) regeneration medium and grown on solid plating medium (Appendix D).

2.5.2.2 Inoculation procedure

When inoculating with conidia, conidiating cultures were left in the light at room temperature for 1 week after the formation of conidia prior to harvesting. Conidial suspensions were rehydrated in dH_2O or liquid VgS overnight at 4°C prior to use as innocula.

A sterile wooden stick was used to remove conidia from a mature colony to inoculate solid VgS slants. Conical flasks of solid and liquid VgS were inoculated with a suspension of conidia in dH_20. Solid VgS plates were inoculated with 100 to 200 μl conidia in dH_2O, which were spread evenly around the plate using a sterile bent glass rod. For characterisation of *N. crassa* growth, solid VgS plates were inoculated by placing an 8 mm disc of mycelium in the centre of each

plate. Mycelial discs were cut from a fungal colony growing on solid VgS prior to conidiation using a cork borer of 8 mm diameter. Where cellophane was used to prevent the growth of aerial hyphae, 4 mm disks were cut and a scalpel used to remove the layer of medium containing the mycelia, which was then placed between two sheets of cellophane on solid VgS plates[3].

Liquid VgS microwell plates (flat bottomed 96 well opaque white 12.8 cm x 8.8 cm plates [DYNEX Technologies, Inc., Chantily, UK]) were inoculated, using a 12-channel pipette (Anachem, Luton, UK), with 100 μl of liquid VgS containing 2.5 μM native coelenterazine[4] (Cambridge Bioscience, Cambridge, UK or Biosynth AG, Staad, Switzerland) and 1x10^6 conidia ml^{-1}.

Solid VgS microwell plates contained 100 μl solid VgS per well. Coelenterazine was added to a concentration of 2.5 μM before solidification and this medium was loaded into the microwell plates, using a 12-channel pipette (Anachem, Luton, UK), and allowed to solidify. Plates were then inoculated with 25 μl of the liquid VgS/conidia/coelentrazine solution used to inoculate liquid VgS microwell plates.

2.5.2.3 Antibiotics and other selective media

For selection of strains containing the bacterial hygromycin phosphotransferase (*hph*) gene, which confers resistance to hygromycin B (hyg). 150 μg ml^{-1} hygromycin was added to the plating medium (regeneration medium was not drugged). The same concentration of hygromycin was used in liquid and solid VgS when required.

[3]Purchased from a stationary shop, boiled in dH_2O for 20 min and autoclaved before use.

[4]30 nmol aliquots of native coelenterazine were each dissolved in 25 μl pre-cooled methanol in the dark before addition to VgS. The final methanol concentration was not more than 0.1%, which is known not to affect spore germination or hyphal growth.

2.5.2.4 Types of culture and growth conditions

Solid VgS plates contained 20 ml solid VgS per 8.5 cm Petri dish. Plates were poured before medium solidification, inoculated, and incubated at the required temperature.

Solid VgS flasks comprised of 50 ml solid VgS in a 250 ml conical flask with a cotton wool bung. Flasks were inoculated and grown for 7 to 14 days at 34 or 24°C by which time maximal conidiation had occurred.

Liquid VgS *N. crassa* cultures were grown in 125 ml conical flasks, which were inoculated, plugged with cotton wool and grown in a shaking incubator at 200 rpm.

Slants consisted of 1 ml solid VgS in a 75 x 12 mm glass tube. Tubes were tilted before medium solidification. After inoculation, slants were incubated at 34 or 24°C for 5 to 10 days, until the maximal amount of conidia had been produced and were then stored at -20°C until required.

Microwell plates were covered with a microplate lid (Labsystems, Helsinki, Finland), after inoculation, individually wrapped in tin foil and incubated in the dark at the appropriate temperature.

2.6 Characterisation of *Neurospora* Growth

2.6.1 Qualitative growth characterisation

2.6.1.1 Light microscopy

An epifluoresence Zeiss Axioscope microscope (fitted with a DVC 1301 CCD camera) was used in conjunction with a Macintosh computer and NIH Image software[5] to obtain digital brightfield images of fungal strains.

[5]http://rsb.info.nih.gov/nih-image

2.6.1.2 Confocal microscopy

Solid VgS plates containing 2 or 3% agar were inoculated centrally with conidia or mycelia. 10 x 20 mm blocks of agar were cut from the outer 1 cm of the colony and placed upside-down on a 24 x 50 mm glass cover slip (Chance propper Ltd., England). FM4-64 (Molecular Probes Inc., Eugene, OR, USA) stock dye solution (16 mM) was diluted 1:10 (dye:medium) to produce a sub-stock of 1.6 mM[6]. The sub-stock was diluted 2:100 (sub-stock:medium) to produce a working dye solution of 32 μM, 10 μl of which was dropped onto the centre of each cover slip before addition of the fungal sample. Samples were left for a minimum of 15 min in a humidity chamber[7] to acclimatise to their new environment and to allow dye loading.

For staining with propidium iodide blocks of agar were immersed in 100% ethanol for 10 min before a further 10 min emersion in 50% ethanol (in dH_2O). Agar blocks were emmersed in 100% dH_2O for 10 min longer, before being inverted onto a coverslip on a drop of 50 μg ml $^{-1}$ propidium iodide (Sigma Chemical Co., USA).

Images were gathered using a Bio-Rad MRC 600 confocal laser scanning microscope fitted with a 25 mW argon laser and connected to a Nikon Diaphot TMD inverted microscope with epiflorescence equipment (all supplied by Bio-Rad Microscience, Hemel Hempstead, U.K.). The laser power used was 1 or 3% of full intensity. Excitation was at 514 nm, and fluorescence was detected at >550 nm. A x40 dry plan apo (NA 0.95) and a x60 oil immersion plan apo (NA 1.4) objective were used. A Dell PC running Bio-Rad MRC 600 CoMos software was used to capture images.

2.6.2 Quantitative growth characterisation

The following parameters were calculated for each colony:

[6]This sub-stock lasts 1 month at 4°C.

[7]An inverted Petri dish containing a water saturated disk of filter paper in its top.

Hyphal Extension Rate Colony diameter was measured at frequent time intervals and the hyphal extension rate calculated based on these measurements. 8 to 10 replicates were performed for each fungal strain.

Hyphal Width The hyphal width of 100 hyphae within the outermost 2 cm of 8 to 10 fungal colonies were measured using digital images gathered as described in Section 2.6.1 and a PC running ImageJ[8] software.

Distance Between Septa 100 measurements of the distance between two septa were made using an an eye piece graticule.

Hyphal Growth Unit The length of hyphae and how many branches occurred along their lengths was calculated. Out-growths were not regarded as a branch unless the exceeded the width of the hypha from which they were protruding. Equation 2.1 was used to calculate the Hyphal Growth Unit from from these data. One hundred replicas were performed for each fungal strain.

$$\text{Hyphal Growth Unit} = \frac{\text{Total length of a hypha or mycelium } (\mu\text{m})}{\text{Number of tips}} \quad (2.1)$$

2.7 Protoplast Production

Two hundred and fifty ml flasks containing 50 ml solid VgS medium were prepared and grown as described in Section 2.5.2. Conidia were harvested with 50 ml liquid VgS and the resulting solution was passed through a funnel containing a cheesecloth filter into a 1 l flask and incubated at 4°C overnight for rehydration. Germination of the conidia was initiated by incubating at the 34 or 24°C on a shaker (120 rpm). Once a large proportion of the conidial population had produced germ tubes about 4 conidial diameters in length, the solution was decanted into sterile 50 ml tubes and centrifuged at room temperature at 1400 rpm

[8]http://rsb.info.nih.gov/ij

for 8 min. For each tube, the supernatant was removed, the pellet resuspended in 30 ml sterile dH_2O (distilled water), and the centrifugation repeated. This wash was performed twice more. After the final wash conidia from all the tubes were combined, resuspended in one of the following solutions and incubated horizontally on a shaker at 55 rpm.

- 1 mg Novozyme^{TM}[9] in 2 ml 1 M sorbitol per $2*10^9$ (filter sterilised). Incubation temperature: 31°C.
- 40 mg Glucanex[10] in 2 ml 1 M sorbitol per $2*10^9$ conidia (filter sterilised). Incubation temperature: 37°C.

Once protoplasts had formed (i.e. spherical cells that burst upon addition of dH_2O were visible when the solution was examined under the microscope) the solution was centrifuged for 10 min at 800 rpm, 4°C. The supernatant was removed and the protoplasts washed twice by re-suspending in 10 ml chilled 1 M sorbitol and repeating the centrifugation. The pellet was then resuspended in 10 ml chilled STC and the number of protoplasts per ml estimated using a haemocytometer. The solution was centrifuged once more and the pellet resuspended in a volume of storage solution that gave a final concentration of approximately 10^7 protoplasts ml^{-1}. Protoplasts were stored at -80°C.

2.8 *Neurospora* Protoplast Transformation

For each transformation, 20 μl of 5 mg ml^{-1} heparin (Amersham Life Sciences, UK) plus 3 μg of DNA were added to 100 μl of protoplasts and incubated on ice for 30 min. One ml of PTC was added to the reaction mixture, which was then incubated at room temperature for 20 min. The reaction mixture was mixed with 8 to 10 ml regeneration medium, poured into a Petri dish containing 15 to 20 ml

[9]Novozyme^{TM} 234 Cell Wall Lysing Enzyme, *Trichoderma harzianum.* Calbiochem-Novabiochem Corporation La Jolla, CA 92039-2087.

[10]Glucanex, Novo Nordisk Ferment Ltd., CH4 243, Dittingen, Switzerland.

plating medium (amended with the appropriate antibiotic) and incubated at 34 or 24°C for 5 to 10 days.

2.9 Purification of Homokaryon Transformants

After transformation, resistant colonies were transfered to drug amended solid VgS plates and allowed to grow. Conidia were harvested and spread on to drug amended plating medium. The resulting colonies were picked and transfered to drugged VgS slants. Conidia from such slants were used to inoculate drug amended solid VgS plates and the process was repeated until each transformed colony had grown on plating medium for at least 3 generations.

2.10 Replication, Extraction and Analysis of Plasmid and Cosmid DNA

2.10.1 Transforming *E.coli*

Replication of plasmid and cosmid DNA was done by transforming competent *E. coli* cells with the DNA of interest as described by Sambrook et al. (1989).

2.10.2 Growth of *E. coli* and extraction of plasmid and cosmid DNA

A single transformed *E. coli* colony was used to inoculate 5 ml of liquid LB-amp medium. The inoculated medium was incubated overnight at 37°C, 200 rpm and the resulting colony centrifuged for 1 min at 8,000 rpm. The supernatant was discarded and plasmid DNA was extracted from the pellet using the NucleoSpin system for the purification of plasmid DNA (Macherey-Nagel & Co. KG, Germany) according to the manufacturers instructions. Plasmid DNA was eluted with dH_2O. Cosmids were extracted using the High Pure Plasmid Isolation Kit

(Roche Diagnostics, GmbH, Mannheim, Germany) according to manufactures instructions. Cosmid DNA was eluted in the elution buffer provided.

2.10.3 Determination of DNA concentration

Five hundred μl of a 1:100 dilution of DNA:dH_2O was placed in a quartz cuvette in a spectrophotometer (Pharmacia LKB, Ultrospec II). The A_{260} and A_{280} was measured and the concentration (in $\mu g\ \mu l^{-1}$) of plasmid DNA in the original sample was calculated by multiplying the A_{260} reading by 5. Calibration was performed at both wavelengths using 500 μl dH_2O. The sample purity was estimated by calculating the ratio of A_{260}:A_{280}. A ratio less than 1.8 indicates some protein contamination.

2.10.4 Restriction and analysis DNA

Restriction reactions were performed according to the manufacturers instructions for the enzymes used. All restriction enzymes were purchased from Boehringer Mannheim GmbH Germany, or from New England Biolabs GmbH Germany. DNA was separated according to size by agarose gel electrophoresis. The gel contained 0.25 to 0.4 g of agarose in 40 ml of TAE*1 buffer. Ethidium bromide was used to stain DNA (Sambrook et al., 1989). The gels were loaded with a 5:1 mixture of DNA:loading buffer (MBI Fermentas, Lithuania). Marker was Lambada DNA/Eco91I (Bst EII) Marker 15, MBI Fermentas, Lithuania. Gels were run at a fixed voltage of 2 to 12 volts per cm and viewed on a UV light box.

2.10.5 Purification of DNA from agarose gel

DNA bands were excised from agarose gel, weighed and placed in a 1 ml Eppendorf tube. DNA was purified from the band using a JETsorb DNA Extraction kit (Genomed, GmbH, Germany) according to the manufacturers instructions.

2.10.6 DNA extraction

An equal volume of phenol was added to the DNA sample in an Eppendorf tube and mixed well. Once an emulsion had formed the mixture was centrifuged in a microfuge (Hettich Mikroliter, Zentrifugen, Germany) at maximum speed for 1 min or until the organic and aqueous phases were well separated. The aqueous phase was transfered to a fresh Eppendorf tube and the whole process repeated using phenol:chloroform in place of the phenol.

2.10.7 Ethanol precipitation of DNA

10% 3 M sodium acetate (pH 5.2 unless otherwise stated) was added to DNA in an Eppendorf tube. Two and a half volumes of chilled ethanol were then added and the solution was incubated at -20°C for 2 h and centrifuged at 13,000 rpm 4°C for 20 min. The supernatant was discarded and the pellet resuspended in 1 ml 75% chilled ethanol and incubated as before for 15 min followed by a further 15 min centrifugation. The supernatant was removed and the Eppendorf tube left to dry upside down on filter paper. The DNA pellet was eluted with the appropriate volume of dH_2O.

2.11 Cloning in Plasmid Vectors

2.11.1 Genes and plasmids

The DNA and amino acid sequences of the *aeqS* synthetic aequorin gene are shown in Appendix B.1. Plasmids pCSN43, pAEQS1-15, pAN7-1, pGNAEQD3 and LBS6 were used in this study. pCSN43 contains the *E. coli hph* gene under the control of *Aspergillus nidulans TrpC* transcription signals. It is known to work in *N. crassa* (Staben et al., 1989) and was used as a positive control in transformations. pAEQS1-15 (Appendix C Fig. C.1) was produced by Glyn Nelson (Nelson, 1999) and contains the *aeqS* synthetic aequorin and

amdS genes under the control of the *gpdA* promotor and *TrpC* terminator from *A. nidulans*. pAN7-1 (Genebank accession number, Z32698) contains the gene encoding glyceraldehyde-3-phosphate dehydrogenase under the control of the *gpdA* promotor and *TrpC* terminator from *A. nidulans*. pGNAEQD3 (Appendix C Fig. C.1) contains the *aeqS* synthetic aequorin gene inserted into the T-cloning vector, pTAg (R&D Systems, UK). The LBS6 plasmid, kindly provided by Dr. D. Ebbole, (Appendix C Fig. C.2), was constructed by Lori Bailey Shrode and contains the *hph* gene under the control of the *N. crassa cpc-1* promotor, modified for constitutive expression, and the *TrpC* terminator from *A. nidulans* (D. Ebbole, Texas, A&M University, personal communication).

2.11.2 Preparation and ligation of DNA

DNA fragments to be ligated were prepared by digestion with the appropriate restriction enzymes, separated by agarose gel electrophoresis and purified from the gel as described in Sections 2.10.4 and 2.10.5. DNA was dephosphorylated by incubation with calf intestinal alkaline phosphatase (CIP) (Boehringer Mannheim GmbH, Germany) where appropriate (see (Sambrook et al., 1989)). CIP was removed by incubation with 100 μg μl^{-1} proteinase K (Boehringer Mannheim GmbH, Germany) for 30 min at 56°C. Dephosphorylated DNA was then cleaned as described in Section 2.10.4. DNA was ligated using T4 DNA ligase and buffer (Boehringer Mannheim GmbH, Germany) according to the manufacturers instructions. After ligation the reaction mixture was added to 100 μl of competent *E. coli* cells and transformed as described in Section 2.10.1.

2.11.3 Primer design and DNA sequencing

All primers were designed using Primer3, a web based primer design program based at[11]. Dissociation temperatures, stable trimers and hairpins were calculated

[11]http://www-genome.wi.mit.edu/cgi-bin/primer/primer3_www.cgi

using Oligo v. 4.0 for the Macintosh. Primers were produced by Sigma Genosys[12]. DNA sequencing was performed by The Laboratory of DNA Analysis, The Institute of Life Sciences, The Hebrew University of Jerusalem, Jerusalem.

2.12 Extraction and Analysis of Genomic DNA

2.12.1 Genomic DNA extraction

N. crassa was grown in 25 ml liquid VgS at 24 or 34°C and 200 rpm, collected by vacuum filtration through a Buchner funnel, frozen at -80°C, freeze-dried and ground to a fine powder with a pestle and mortar. Three hundred μl of this powder was added to an Eppendorf tube, mixed with 500 μl of DNA Extraction Buffer and incubated for 15 min at 60°C. The Eppendorf tube was then filled with a 24:1 chloroform:octanol mixture, vortexed and centrifuged at 12,000 rpm for 5 min. Of the resulting 3 phases, the uppermost was transfered to a new Eppendorf tube and a volume of 3 M sodium acetate (pH 5.2) equal to 1/10 of the collected volume of the uppermost phase plus 1 volume of isoproponal (-20°C) were gently mixed in. The Eppendorf tube was incubated at -20°C for 5 min followed by centrifugation at 12,000 rpm, 4°C for 5 min. The supernatant was discarded and the Eppendorf tube filled with 75% ethanol (-20°C) inverted several times and centrifuged as before. The supernatant was discarded and the pellet dried at 37°C for several min before being resuspended in 100 μl dH_2O at 4°C overnight. The resulting solution was analysed for protein contamination using a spectrophotometer as described in Section 2.10 above. DNA concentration was estimated by running samples on a 0.7% agarose gel along side digested and undigested Lambda DNA (MBI Fermentas). Approximate DNA concentration was calculated by comparing the relative luminescence of sample and control DNA.

[12]http://www.sigma-genosys.com

2.12.2 Southern analysis

Eight μl of genomic DNA extract plus 0.5 μl RNAase (2 μg μ^{-1}) (Boehringer Mannheim GmbH, Germany) were incubated overnight with 1.5 μl concentrated *Apa*I (40 Units μl^{-1} Boehringer Mannheim GmbH, Germany), or 3 μl *Kpn*I (10 Units μl^{-1} Boehringer Mannheim GmbH, Germany), in a total volume of 20 μl according to the manufacturers instructions. A 0.9% agarose gel containing 5 μl ethidium bromide was loaded with digested genomic DNA extracts, λ-DNA marker and 5 μl of a 1:300 dilution of ApaI digested plasmid pAZ6, run for 5 h at 100 volts and photographed on a UV light box. The gel was exposed to UV light for a further 3 min before being transfered to a Magnacharge nylon transfer membrane (Micron Seoeration Inc., USA) using a VacuGene XL (Pharmica LKB) vacuum blotter in accordance with the manufacturers instructions. After transfer, the membrane was cross-linked using a Spectrolinker XL-1000 UV crosslinker (Spectronics Corporation, USA). The membrane was then incubated with 20 ml Hybridisation Solution at 42°C. After 4 h the solution was removed and *aeqS* specific ($\alpha-^{32}$P)dNTP labelled DNA probe was added to 10 ml of the hybridisation solution and returned to the membrane. The probe was made according to the manufacturers instructions using the Prime-a-Gene Labelling System (Promega Corperation, USA). Gel purified *aeqS* extracted from pAZ6 using *Eco*RI was used as the DNA template. The membrane was hybridised overnight, washed twice for 15 min at room temperature in 2*SSC 0.1% SDS, and twice for 30 min at 42°C in 0.1*SSC 0.25% SDS (see Sambrook et al., 1989, for content).

2.12.3 PCR amplification

For PCR amplification of genomic *cot-4* DNA, the following reaction mixture was prepared in 500 μl Eppendorf tubes on ice: 33.5 μl dH_2O, 5 μl Taq DNA Polymerase 10X reaction buffer without $MgCl_2$ (Promega Corporation, WI, USA),

5 μl of 2 mM DNTPs mix, 3 μl of 25 mM $MgCl_2$ (Promega Corporation, WI, USA), 0.5 μl Promega Taq DNA Polymerase, 2 μl primer mix and 1 μl template mix. DNTPs mix was produced by mixing a set of 100 mM dATP, dCTC, dGTP and dTTP (Promega Corporation, WI, USA) and diluting the mixture to a concentration of 2 mM in dH_2O. Primer mix consisted of 25 pmoles of each of the two primers in 2 μl dH_2O. Template mix was 20 μl genomic DNA extract plus 1 μl of 2 $\mu g\ \mu l^{-1}$ RNAase. A negative control was set up with no template DNA, and a positive control was set up using cosmid pMOcosX X15:E10 DNA. Several reactions were run simultaneously in an Eppendorf mastercycler gradient (Eppendorf AG, Hamburg, Germany) PCR machine. Samples were denatured for 30 s at 94°C. Annealing was performed for 1 min at 58°C $\pm$ 2°C (according to the position in the PCR machine temperature gradient). Elongation was done for 2 min at 72°C (the optimal temperature for the Taq used). Thirty rounds of annealing and elongation were done in total.

2.13 Extraction and Analysis of Fungal Protein

2.13.1 Protein extraction

N. crassa strains were grown in 50 ml liquid VgS at 24 or 34°C and 150 rpm for 2 days, collected by vacuum filtration through a Buchner funnel, and ground to a fine powder in a pestle and morter containing liquid nitrogen. Powder was transfered to pre-weighed pre-cooled Eppendorf tubes and 1 ml protein extraction buffer (Appendix D) was added per 0.2 g mycelial powder. Each Eppendorf tube was vortexed for 1 min followed by 5 min centrifugation at 13,000 rpm. Resulting supernatant was transfered to fresh Eppendorf tubes flash-frozen in liquid nitrogen and stored at -80°C for future use.

2.13.2 Analysis of protein concentration

Total protein determination was performed using the Bio-Rad Standard Assay Procedure (Bio-Rad Laboratories Ltd., Hemel Hempstead, UK). BSA protein standards were prepared by dissolving BSA in protein extraction buffer at 50 μg ml^{-1} intervals from 0 to 1300 μg ml^{-1}. Ten μl of each sample was mixed with 500 μl diluted Bio-Rad dye reagent (1 part Bio-Rad dye concentrate plus 4 parts dH_2O) in an Eppendorf tube and 200 μl of the resulting solution was transfered to 1 well in a 12.8 x 8.6 cm, 96 well transparent microtiter plate (Dynex Technologies, Inc., Chantily, UK). Unknown samples were protein extract prepared according to Section 2.13.1. Blanks were protein extraction buffer (Appendix D).

The A_{590} of each well was measured using a Dynatech MR5000 densitometer/plate reader (Dynatech Laboratories Ltd., Sussex, UK). A standard curve was constructed and used to determine the concentration of protein in the unknown samples. For this purpose, a software program was written (getproteinunkns.sh, Appendix E) in csh[13]. This program took a plain text file containing sample names and A_{590} readings. It calculated protein concentration of the unknown samples using the equation $y = ax + c$, where a=slope and c=intercept as calculated from the standard curve this program calculated the protein concentration of the unknown samples. It also calculated amount of protein extraction buffer (Appendix D) to add to each sample to obtain the final concentration of 40 μg total protein per 100 μl of solution (desired for aequorin discharge experiments).

2.14 Luminometry

Luminometry was done using a EG&G Berthold (Bad Wildbad, Germany) LB96P Microlumat luminometer controlled by a dedicated PC running the Microsoft Windows based Berthold WinGlow software. The luminometer allowed a maximum of two 100 μl injections into each well through built-in injectors.

[13]A shell (command interpreter) with C-like syntax (DuBois, 1995).

Such injections were used to stimulate (or discharge aequorin from) samples when required. The luminometer was calibrated to the optimal working voltage of 1496 volts.

Flat-bottomed 96 well opaque white 12.8 cm x 8.8 cm microtiter plates (Dynex Technologies, Inc., Chantily, UK) were used in all experiments involving microwell plate luminometry. Each well has a capacity of 350 μl.

Two types of luminometer protocol were used in this study: (a) kinetic and (b) repeated. The kinetic protocol measures light emitted by a sample in one well continuously until the end of the experiment. The repeated protocol measures light emitted from a number of samples over the course of one experiment. To achieve this, the detector of the luminometer must move from one sample to the next. The time it takes to measure every sample in the experiment and return to the starting sample is called the cycle time. The time that each sample is measured for per cycle is called the measurement time.

2.14.1 *In vitro* Measurement of aequorin luminescence

2.14.1.1 Calculating the amount of aequorin as a fraction of total protein

Growth of strains, protein extraction and determination of protein concentration of samples was carried out as described in Sections 2.13.1 and 2.13.2. Stock coelenterazine was first dissolved in 25 μl methanol before being added to the appropriate volume of protein extraction buffer (Appendix D) and protein extract to attain 100 μl aliquots of protein extract containing 40 μg total protein and 2.5 μM coelenterazine (ratio of protein extract to protein extraction buffer was calculated by getproteinunkns.sh, Appendix E). Aliquots were loaded into a 96 well plate, constituted in the dark for 4 h at 4°C and placed in the luminometer. Luminescence was measured at 30°C for 60 s using a kinetic protocol. A 100 μl injection of 100 mM $CaCl_2$ was given after 10 s to discharge all the aequorin

present in the protein sample. Blank wells (100 μl protein extraction buffer) were used to estimate background light levels. The average of 12 such wells was subtracted from the results of each sample tested. Six replicas of each sample were measured, luminescence emitted over the first 20 s after $CaCl_2$ injection was integrated and the mean $\pm$ S.E. recorded for each sample (units were RLU/20 s/40 μg total protein).

Conversion of RLU to μg aequorin per g total protein was done using a calibration curve (Fig. 2.1). This curve was made by discharging aliquots of commercial aequorin D (Cambridge Bioscience, UK) dissolved in dH_2O to concentrations ranging from 10^{-17} M to 10^{-8} M. One hundred μl aliquots of each aequorin concentration were loaded, constituted and discharged as described above for total protein extracts. The best method of performing this conversion

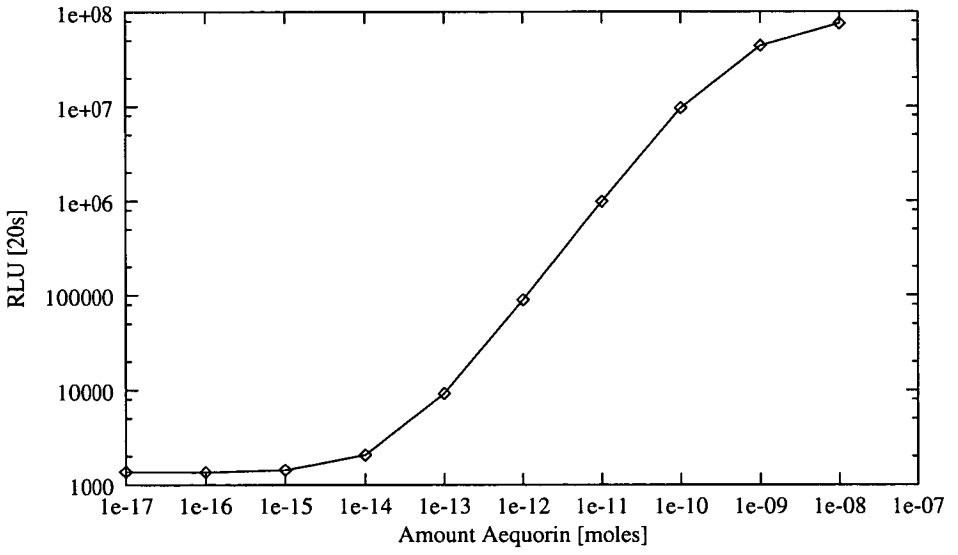

Figure 2.1: Aequorin calibration curve. Commercial aequorin was dissolved in dH_2O. One hundred μl aliquots were placed in a microwell plate, constituted (using 2.5 μM native coelenterazine for 4 h at 4°C) and discharged using 100 μl 100 mM $CaCl_2$. Luminescence was integrated for 20 s after injection (calibration curve generated with assistance from Dr. O. Kozlova-Zwinderman).

accurately was found to be through the use of a computer program. A program

was therefore written in perl[14] to perform this task. The program (getaeqamnt.pl, see Appendix E) took the aequorin calibration curve and aequorin sample discharge data as input and calculated the amount of aequorin in each aequorin discharge sample. This eliminated the need to read such values from the calibration curve by hand, a potential source of serious errors.

2.14.1.2 Influence of temperature on aequorin luminescence

Constitution, discharge and integration of RLU was carried out as described in 2.14.1.1. After constitution, protein samples were placed in the luminometer and given 15 min to reach the set temperature of 24°C after which the aequorin in the first set of samples was discharged at this temperature. The plate was then heated to 37°C, given 15 min to equilibrate after which aequorin in the next set of samples was discharged at this new temperature. This process was repeated at 42°C. The plate was then cooled to 37°C and the equilibration and discharge steps repeated. Finally the plate was cooled to 24°C, given 15 min to reach the set temperature, and the aequorin in the remaining samples was discharged at 24°C.

2.14.2 *In vivo* Ca^{2+} measurement by luminometry

2.14.2.1 *In vivo* optimisation of aequorin luminescence

Liquid VgS cultures were inoculated and grown in microwell plates as described in Section 2.5.2 except that spore concentrations of $1x10^4$, $1x10^5$, $5x10^5$, $1x10^6$ or $5x10^6$ conidia ml^{-1} were used. Cultures were incubated at 24°C for 14, 18, 22, 26 or 30 h before being discharged as described below.

[14]http://www.perl.com

2.14.2.2 Standard *in vivo* luminometry

Microwell plates containing *N. crassa* colonies (inoculated and grown as described in Section 2.5.2) were placed in the temperature-controlled luminometer and luminescence was measured for 10 min with one of three stimuli being provide after 57 s. Stimuli consisted of one 100 μl injection of liquid VgS medium (mechanical perturbation), VgS medium diluted in dH_2O [1:20; v/v] (hypo-osmotic shock) or 100 mM $CaCl_2$ (high external Ca^{2+}) (Nelson et al., 2003). A kinetic measurement protocol was used to follow the exact changes in culture luminescence over the entire 10 min measurement period. Six extra wells in each plate were inoculated to allow the total amount of luminescence per colony to be determined. For this purpose luminescence was integrated over 10 min with one 100 μl injection of 3 M $CaCl_2$ plus 20% ethanol after 57 sec and one 100 μl injection of 100 mM $CaCl_2$ after 5 min 57 s. This treatment discharges all the aequorin present in mature *N. crassa* colonies. Background light levels were measured in six wells containing medium only and subtracted from fungal aequorin luminescence measurements.

2.14.2.3 *In vivo* luminometry with chemical treatments

All chemical treatment concentrations given refer to the final concentration of the treatment after addition to the *N. crassa* colony in the microwell plate. The following treatments were used in this study:

- sorbose (0 to 0.25%)(Sigma Chemical Co., UK), dissolved in VgS
- FK506 (0 to 248 nM)(Calbiochem, UK), dissolved in DMSO (dimethyl sulfoxide, Fluka Chemie, Switzerland)
- CsA (0 to 250 nM)(cyclosporin A, Sigma Chemical Co., UK), dissolved in DMSO
- caffeine (0 to 25 mM)(Sigma Chemical Co., UK), dissolved in VgS

- CPA (0 to 50 μM)(cyclopiazonic acid, Sigma-Aldrich, UK), dissolved in methanol
- 2-APB (0 to 50 μM)(2-aminoethoxy-biphenylborate, Calbiochem, UK), dissolved in methanol

Final solvent concentrations were not more than 0.1%, which is known not to affect spore germination or hyphal growth. For each treatment, controls were also performed in which cultures were treated with solvent only.

Three types of experiment were performed involving chemical treatments: (a) growth on amended media; these experiments were performed normally except that all cultures were grown on amended media. (b) Drug pretreatment; 100 μl liquid VgS cultures were grown in microwell plates. Cultures were pretreated by the gentle addition 25 μl of drug or control solution 10 min before the microwell plate was placed in the luminometer. Stimuli and measurements were then given as previously described. (c) Drug injection; cultures were grown normally, placed in the luminometer and then exposed to one 100 μl injection of drug in liquid VgS after 57 s in place of the usual stimulus.

2.14.2.4 *In vivo* luminometry after a temperature shift

These experiments were performed exactly as described for standard luminometry except that cultures were grown at 24°C and then shifted to 37°C for a fixed time before being placed in the temperature-controlled luminometer at 37° for further stimulation and measurement.

2.14.2.5 *In vivo* luminometry before, during and after temperature shifts

Microwell plates containing four sets of six wild-type and six *cot-1 N. crassa* colonies were grown for 17 h at 24°C before being placed in the temperature-controlled luminometer at 24°C. Sample set 1 luminescence was measured at

24°C for 1 h after which sample set 2 was discharged at 24°C. Luminescence measurement was then continued on sample set 1 for a further 4 h as the temperature of the luminometer was raised to 37°C. At the end of this period sample set 3 was discharged at 37°C. Microwell plates were briefly transferred to a 37°C incubator, while the luminometer was cooled back to 24°C. Plates were then put back in the luminometer and luminescence measurement continued on sample set 1 for one h at 24°C. Finally, sample set 4 was discharged at 24°C. When converting these data into $[Ca^{2+}]_c$ concentrations using the equation described by Fricker et al. (1999) (Fricker et al., 1999), total RLU available for emission was calculated from the appropriate discharge sample for each point during the experiment. In short, the experiment can be divided into three stages: measurement of sample set one at (a) 24°C for 1 h; (b) 37°C for 4 h; (c) 24°C for 1 h. There are three discharge samples that correspond to these three sections: discharge of (a) sample set two at 24°C; (b) sample set 3 at 37°C; (c) sample set 4 at 24°C. This method is used to overcome the differences in aequorin luminescence resulting from different measurement temperatures as described later in this thesis. A separate experiment was performed in which 100 μl samples of medium in microwell plates were placed inside the luminometer during temperature shifts while the actual temperature of the medium in the microwell was measured using an electronic temperature probe.

2.14.3 Conversion and analysis of luminometer data

2.14.3.1 Conversion of RLU to Ca^{2+} concentrations and subsequent quantification of Ca^{2+}-signatures

A software program was developed to (a) convert the data produced by our luminometer from RLU to Ca^{2+} concentrations, (b) quantify various parameters of the Ca^{2+}-signature, and (c) perform statistical analysis on these data. The

program was written in perl[15] and used the perl data language [PDL][16] for complex multidimensional data manipulation and gnuplot[17] for graph production. The source code for this program is in Appendix E. It was written and run on a standard PC running SuSE Linux version 7.3[18]. Fig. 4.1 summarises the main functions of this program, which accepted plain text input, generated by the WinGlow software running the luminometer. These files contained measurement times and luminescence in RLU. Three files were read into the program for each experiment: (1) background data, from measurement of wells containing medium only; (2) sample data, from the actual experimental samples; and (3) discharge data, from samples assigned for discharge. Error type could be set to variance, standard deviation or standard error. Output graphs could be generated in FIG or PostScript™ format[19] and a number of other options could be set, including the use of error bars and graph size.

Input data were converted, by my program, into Ca^{2+} concentrations using the following empirically derived calibration formula, Equation 2.2 based on Equation 1.3 was used (Fricker et al., 1999).

$$\mathrm{p}Ca = 0.332588(-\log\, k) + 5.5593 \tag{2.2}$$

where

$$k = \frac{\mathrm{RLU\,s^{-1}}}{\text{total RLU available}}$$

Calibration coefficients for Equation 2.2 were determined at 25°C using the AEQ1

[15]http://www.perl.com
[16]http://pdl.perl.org
[17]http://www.gnuplot.info
[18]http://www.suse.com and http://www.linux.org
[19]The FIG graphics format is a vector drawing format that can be used with programs such as xfig (http://www.xfig.org) to produce simple figures for documents. PostScript is a programming language optimised for printing graphics and text and is made by Adobe[20].

aequorin isoform encoded by pMAQ2 (Badminton et al., 1995). The discharge data was used to determine k for each time point. All discharge data were multiplied by 1.24 to correct for the fact that the ethanol in the discharge solution quenches aequorin luminescence by 24% (Kozlova-Zwinderman, 2002).

All *in vivo* luminometry was performed using a repeated measurement protocol where each sample was measured once every measurement cycle. In order to calculate the total amount of light emitted by a sample over the course of the experiment, it was assumed that each measurement point was connected by a straight line and the total area under the resulting graph (A_{tot}) (see Fig. 2.2) was calculated as follows:

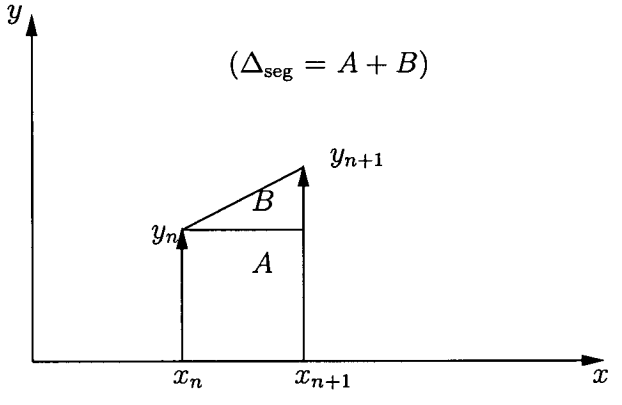

Figure 2.2: A diagram of the method used to estimate the amount of light emitted from a sample between measurements. Each sample was measured once every cycle. To estimate the amount of light emitted between measurements, each measurement point was assumed to be connected by a straight line. The total area under the graph (A_{tot}) was then calculated.

$$A_{\text{tot}} = A + B \tag{2.3}$$

$$= (x_{n+1} - x_n) \cdot y_n + \frac{1}{2}(x_{n+1} - x_n) \cdot (y_{n+1} - y_n) \tag{2.4}$$

$$= \frac{1}{2}(x_{n+1} - x_n) \cdot (y_{n+1} + y_n) \tag{2.5}$$

The sampling period is constant, i.e. $(x_{n+1} - x_n) = \Delta$, so Equation 2.5 can be further simplified to:

$$= \frac{1}{2}\Delta(y_{n+1} + y_n) \tag{2.6}$$

If we have $N + 1$ data, i.e. $y_0, y_1, \ldots, y_{N+1}$, then the total area underneath the graph (linearly interpolating between the points) is:

$$A_{\text{tot}} = \sum_{i=0}^{N-1} \frac{1}{2}\Delta(y_{i+1} + y_i) \tag{2.7}$$

As well as converting RLUs to Ca^{2+} concentrations and saving this data in plain text format, the program automatically calculates means and standard errors for all data points and displays these values as a graph. Furthermore, it calculates the following quantitative parameters (see Fig. 2.3) of the Ca^{2+}-signature along with their means and standard errors: (1) average resting $[Ca^{2+}]_c$ concentration before the stimulus is provided; (2) maximum $[Ca^{2+}]_c$ concentration reached during the entire experiment; (3) lag time (the time from the stimulus to the point when $[Ca^{2+}]_c$ concentration starts rising); (4) rise time (the time for the $[Ca^{2+}]_c$ concentration to reach a maximum from the time it begins to rise following the stimulus); (5) maximum $[Ca^{2+}]_c$ amplitude; and (6) the full width half maximum (FWHM) (the width of the $[Ca^{2+}]_c$ transient at half maximum amplitude). Amplitude (amp) was calculated using the following equation:

$$\text{amp} = y_{\text{max}} - y_{\text{min}} \tag{2.8}$$

Half maximum amplitude (HM) was calculated as follows:

$$\text{HM} = \frac{\text{amp}}{2} \tag{2.9}$$

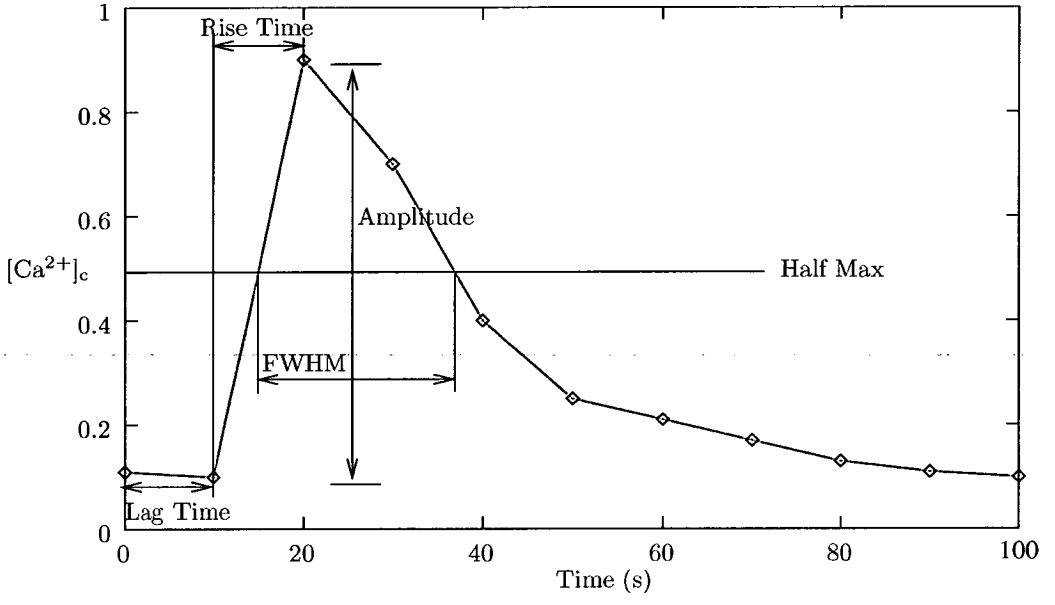

Figure 2.3: Some quantitative parameters of the Ca^{2+}-signature.

FWHM was then calculated:

$$\text{FWHM} = \left(\frac{(h-c)}{a}\right) + x_n \tag{2.10}$$

where h is HM, c is y_n and a is the slope, calculated as follows:

$$a = \frac{(y_{n+1} - y_n)}{(x_{n+1} - x_n)} \tag{2.11}$$

All statistical data is also written to the output file, along with data from the individual repetitions. Finally, this program will warn the user if their experimental data is unsuitable for conversion into Ca^{2+} concentrations. Data is unsuitable for use if the majority of the aequorin in the sample was discharged during an experiment.

2.15 Genome Analysis

A range of Ca^{2+}-signalling proteins and genes from plants, animals and fungi were blasted against the (a) *N. crassa* genome database; (b) *M. grisea* genome database; (c) *A. fumigatus* genome database; and (d) *S. cerevisiae* genome database using the BLASTN, TBLASTN and BLASTP algorithms (see Table 1.2 for database web addresses). Potential hypothetical protein homologues from *N. crassa*, *M. grisea* and *A. fumigatus* and *S. cerevisiae* were identified based on: (a) *E*-values, (b) percent identities, positives and gaps, and (c) conserved domains present. Hypothetical proteins and DNA coding sequences obtained in this way were entered into my database[21] of potential Ca^{2+}-signalling proteins. These data were stored under their locus numbers, as defined by each organism's genome project's web page. In the case of *A. fumigatus*, a database of hypothetical proteins was unavailable. Homologous DNA sequences, plus 1000 bp on each side of the homologous region, were therefore entered into our database for further analysis. These data were stored under our own names. The format of this name is: contig_start-stop, where "contig" is the contig number of the homologous region, as provided by the *A. fumigatus* TIGR blast result, and "start" and "stop" define the range of DNA in this contig entered into our database.

Potential Ca^{2+}-signalling proteins and regions of DNA from our database were blasted back against the GenBank, EMBL, DDBJ and PDB databases through NCBI using the TBLASTN and (in the case of *A. fumigatus*) BLASTX algorithms to check for similar proteins or DNA sequences in other organisms. This information was also entered into my database.

Conserved protein domains were analysed using the NIH tools: CDD and CDART[22]. Hydrophilicity plots were performed using the Kyte-Doolittle method using a web-based program provided by the Weizmann Institute of Science[23].

[21] http://www.fungalcell.org/FDF/
[22] http://www.ncbi.nlm.nih.gov
[23] http://bioinformatics.weizmann.ac.il/hyd-bin/plot_hydroph.pl

Prediction of putative transmembrane segments was done using PredictProtein, from the server at EMBL[24]. Multiple sequence alignment and generation of phylogenetic trees was done using the `clustalx` program (Thompson, 1997).

A MySQL database was used for data storage[25]. The web interface and underlying software to my database was written in perl[26] and html[27]. It was written and run on a standard PC running SuSE Linux version 7.3[28].

[24]http://www.embl-heidelberg.de/predictprotein/submit_def.html
[25]http://www.mysql.com
[26]http://www.perl.com
[27]http://www.w3.org
[28]http://www.suse.com and http://www.linux.org

Chapter 3

Development of the Aequorin Method for Ca^{2+} Measurement in *Neurospora*

3.1 Introduction

The cloning and characterisation of aequorin genes (Inouye et al., 1985; Prasher et al., 1985), and the subsequent codon-optimisation of aequorin D for expression in filamentous fungi has paved the way for easy and routine measurement of Ca^{2+} in living fungal cells expressing the aequorin gene (Nelson et al., 2003). The use of Ca^{2+}-sensitive photoproteins (e.g. aequorin) to measure Ca^{2+}, has now begun to be applied to filamentous fungi (Shaw et al., 2001; Greene et al., 2002; Nelson et al., 2003). The essential requirement for such measurements is that the level of aequorin expression is: (a) sufficient to produce detectable levels of light at resting Ca^{2+} concentrations; and (b) sufficient to be able to report large changes in Ca^{2+} concentration without the majority of the aequorin being using up.

The first transformations of a filamentous fungus (*N. crassa*) with the native aequorin A and D genes resulted in very low aequorin expression levels (0.15 and 0.05 μg aequorin per g total protein, respectively (Nelson et al., 2003))

making it difficult to observe changes in $[Ca^{2+}]_c$ (Collis, 1996). Subsequent codon-optimisation of aequorin D for expression in filamentous fungi increased the level of aequorin expression more than ten times. However a comprehensive set of aequorin expressing *N. crassa* strains, and the methods to work with them, had not yet been developed.

The aims of the work described in this chapter were: (1) to obtain high levels of aequorin expression in hyphae of three *N. crassa* strains (wild-type, *cot-1* and *spray*) using the synthetic filamentous fungal codon-optimised aequorin D gene (*aeqS*); (2) to analyse the level of aequorin expression in transformants from each strain and to confirm that no phenotypic abnormalities resulted from transformation; (3) to estimate the number of *aeqS* inserts in selected transformants; (4) to determine a suitable set of growth conditions for optimal *in vivo* luminescence in *N. crassa*.

3.2 Results

3.2.1 Protoplasts

Wild-type, *cot-1*, and *spray* protoplasts were made from germinating conidia and transformed with the pCSN43 plasmid (see Section 2.11.1). The resulting colonies were able to grow on hygromycin amended medium and thus judged to be successfully transformed. Transformations using the pAEQS1-15 and pAN7-1 plasmids were unsuccessful, based on inability to grow on selective medium. A new plasmid was therefore constructed to transform *N. crassa* with *aeqS*. This plasmid contained the *aeqS* synthetic aequorin gene under the control of the *N. crassa cpc-1* promotor modified for constitutive expression.

3.2.2 Plasmids

*Eco*RI was used to excise *aeqS* from pGNAEQD3 (see Appendix C Fig. C.1 [b]) and to linearise LBS6 at polylinker2 (see Appendix C Fig. C.2). Linearised LBS6 was dephosphorylated and *aeqS* was ligated into the resulting DNA to produce the pAZ plasmid. Plasmids were extracted from 10 *E. coli* colonies and designated pAZ1 to pAZ10. Restriction analysis with *Sal*I (see Fig. 3.1) showed that six plasmids contained *aeqS* in the correct orientation (pAZ1, 2, 3, 5, 6 and 8), three in reverse orientation (pAZ4, 7 and 9) and one plasmid, pAZ10, contained no insert (see Fig. 3.1). The correct orientation and reading frame were verified

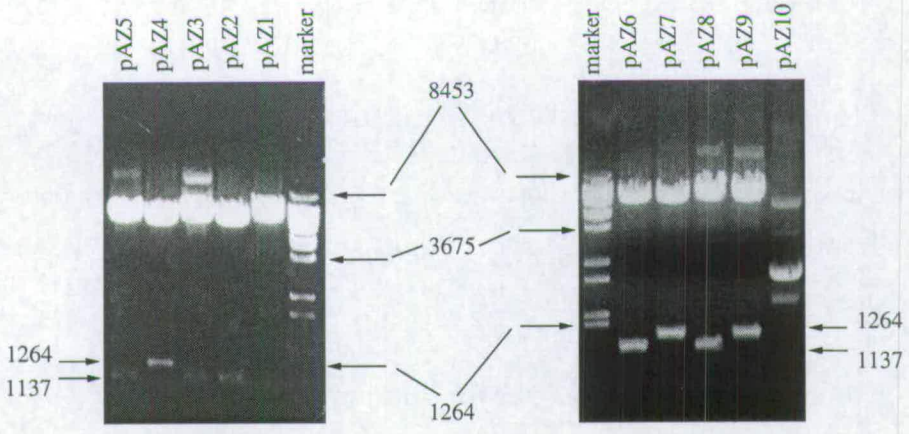

Figure 3.1: Restriction analysis of pAZ1-10 using *Sal*I. Insertion of *aeqS* in the correct orientation gives fragments of sizes 1137 and 6192 bp. Insertion of the gene in reverse orientation gives bands at 1252 and 6077 bp. pAZ2, 3, 5, 6 & 8 contain the gene in the correct orientation.

in pAZ2 and pAZ6 by sequencing the junction region using the primer: 5'-ATC TTG CCG TTG TGG TTG AC-3'. Both sequences were identical and and showed 100% similarity to their respective *aeqS* and *cpc-1* components. The *aeqS*/*cpc-1* junction contained all the restriction sites in LBS6 polylinker2 including an intact *Eco*RI site. The pAZ6 plasmid (Fig. 3.2) was chosen for further use.

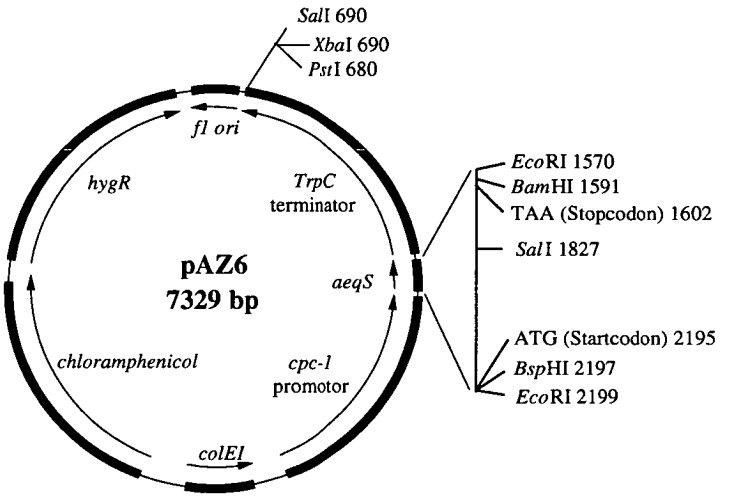

Figure 3.2: pAZ6. A plasmid containing the *aeqS* synthetic aequorin gene under the control the *cpc-1* promotor from *N. crassa* and *TrpC* terminator from *A. nidulans*.

3.2.3 *Neurospora* pAZ6 transformants

pAZ6 was successfully used to transform wild-type, *cot-1* and *spray* protoplasts (based on hygromycin resistance). Twenty to thirty transgenic homokaryons were then purified from each strain.

3.2.3.1 Determination of aequorin production

To determine the exact amount of aequorin produced by transformants from each strain as a proportion of total protein, *in vitro* luminometry was performed on total protein extracts. A 4 h aequorin constitution (production of the aequorin holoenzyme from the apoprotein by addition of coelenterazine) period was found to be sufficient to constitute all the aequorin in a 40 μg total protein sample (Fig. 3.3). The majority of aequorin was constituted after a 60 min incubation with coelenterazine at 4°C and optimal constitution was reached after 90 min. Further constitution, within the time frame examined, made no difference to the amount of active aequorin present in the protein extracts. This experiment was repeated using different protein extracts and results were almost identical.

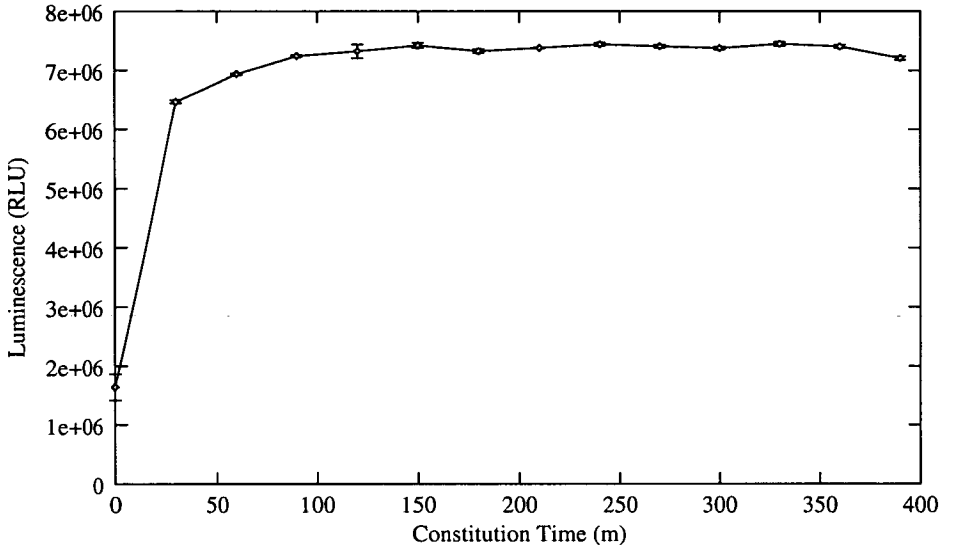

Figure 3.3: Constitution of active aequorin in protein extracts for pAZ6 transformed *N. crassa* strains. Samples were prepared as described in Section 2.14.1.1, except that discharge was performed at various time points after coelenterazine addition (0 m). Values are mean ± S.E. (n=3).

Luminometry was then performed on protein extracts from all transformants, using a 4 h constitution period as described in Section 2.14.1.1. Table 3.1 shows a selection of results from the transformants analysed. Following this screening process, one transformant representing each of the strains analysed, was chosen (on the basis of high aequorin luminescence) for further studies. The best wild-type transformant was 22A3AWTAZ6, and produced 2.9 ± 0.03 μg (S.E. n=3) of aequorin per g total protein. The best *cot-1* transformant, AZ63211cot1, produced 4.1 ± 0.04 and the best *spray* transformant, 18B1ASPAZ6, produced 6.9 ± 0.02 μg (S.E. n=3) of aequorin per g total protein. This experiment was repeated with protein extracts from fungal colonies grown on another occasion and yielded almost identical results. During the purification of homokaryons and the luminescence screening process, a strain exhibiting partial phenotypic suppression of *cot-1* was also isolated. This strain was named AZ63131cot1 and produced 5.7 ± 0.11 (S.E. n=3). Overall, the transformants analysed showed a

Table 3.1: *In vitro* aequorin discharge of total protein extracts from *aeqS* transformed wild-type, *cot-1* and *spray* strains of *N. crassa*. Values are mean ± S.E.

Strain	Transformant Name	Amount of Aequorin (μg aequorin per g total protein)
wild-type	Untransformed Control	0.0 ± 0.00
wild-type	AZ61211wt	0.5 ± 0.02
wild-type	35D3BWTAZ6	2.6 ± 0.03
wild-type	22A3AWTAZ6	2.9 ± 0.03
cot-1	AZ63211cot1	4.1 ± 0.04
cot-1	AZ63131cot1*	5.7 ± 0.11
spray	AZ62311spray	1.0 ± 0.01
spray	22C2ASPAZ6	6.2 ± 0.09
spray	18B1ASPAZ6	6.9 ± 0.02

* This strain exhibited partial phenotypic suppression of *cot-1*.

range of aequorin expression as can be expected from the ectopic transformation technique used to produce them.

3.2.3.2 Morphological analysis

Hyphal extension rate and hyphal/colonial morphology were examined on solid VgS to determine if there were any observable effects of transformation and aequorin expression on the fungal phenotype. There was no observed differences between the extension rates of aequorin-expressing transformants compared with untransformed controls (wild-type and *cot-1* grew between 4.5 ± 0.69 and 4.7 ± 0.51 mm/h at 24°C; wild-type grew between 6.3 ± 1.05 and 6.9 ± 0.86 mm/h at 24°C; *spray* grew between 1.07 ± 0.09 and 1.06 ± 0.12 mm/h at 24°C; and *cot-1* grew between 0.086 ± 0.008 and 0.091 ± 0.01 mm/h at 37°C; values are means ± S.D., n=6). Fungal hyphae, stained with the membrane selective dye FM4-64, were imaged using confocal laser scanning microscopy. The morphologies of transformed and untransformed strains were indistinguishable (see Fig. 3.4).

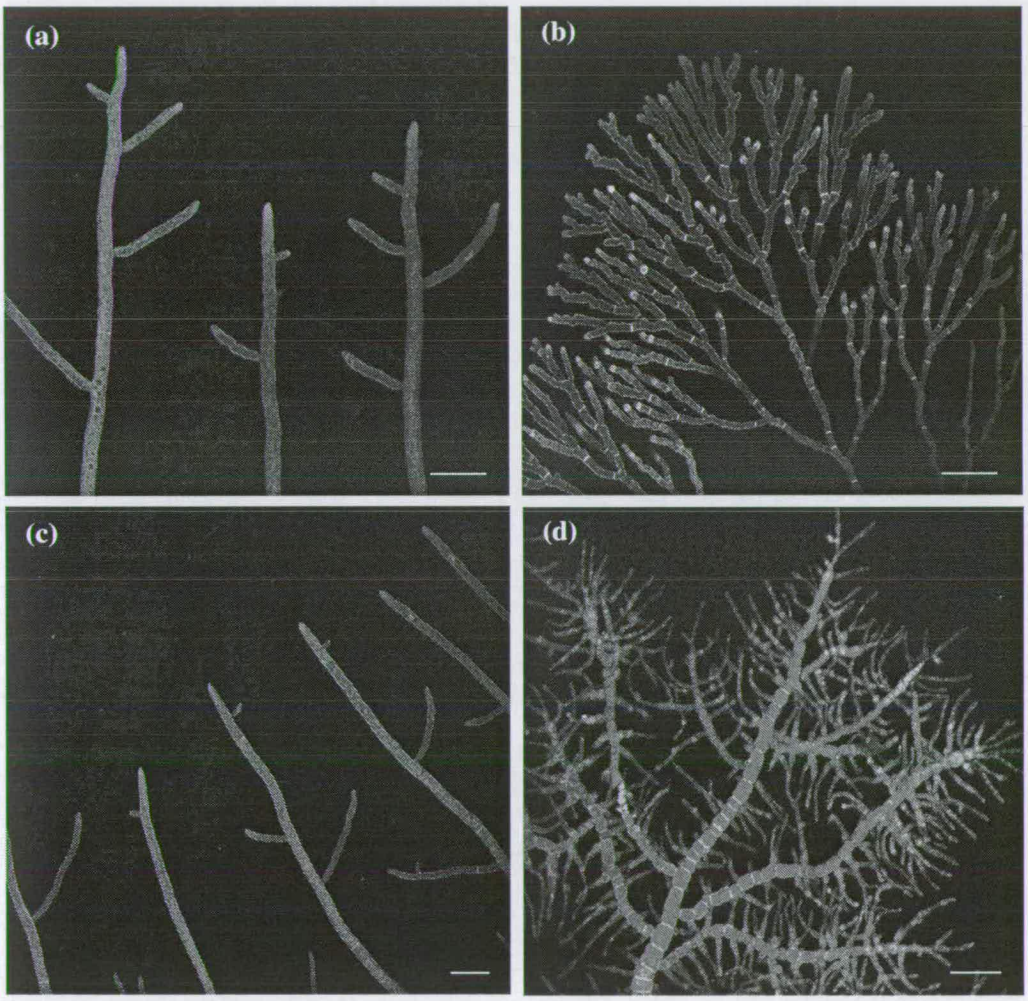

Figure 3.4: Confocal images showing morphologies of (a) wild-type at 24°C; (b) *spray* at 24°C; (c) *cot-1* at 24°C and (d) *cot-1* at 37°C for 4 h after shifting from 24°C. Samples were stained with FM4-64. Bar = 50 μm.

3.2.3.3 Southern analysis

Southern analysis was performed on a number of pAZ6 transformants in order to confirm the presence of the *aeqS* gene in the transformants, and to determine whether there was a correlation between the number of *aeqS* insertions and the level of aequorin expression.

Genomic DNA was extracted from transformants (see Section 2.12.1) and Southern analysis performed as described in Section 2.12.2. Figs. 3.5 a and b

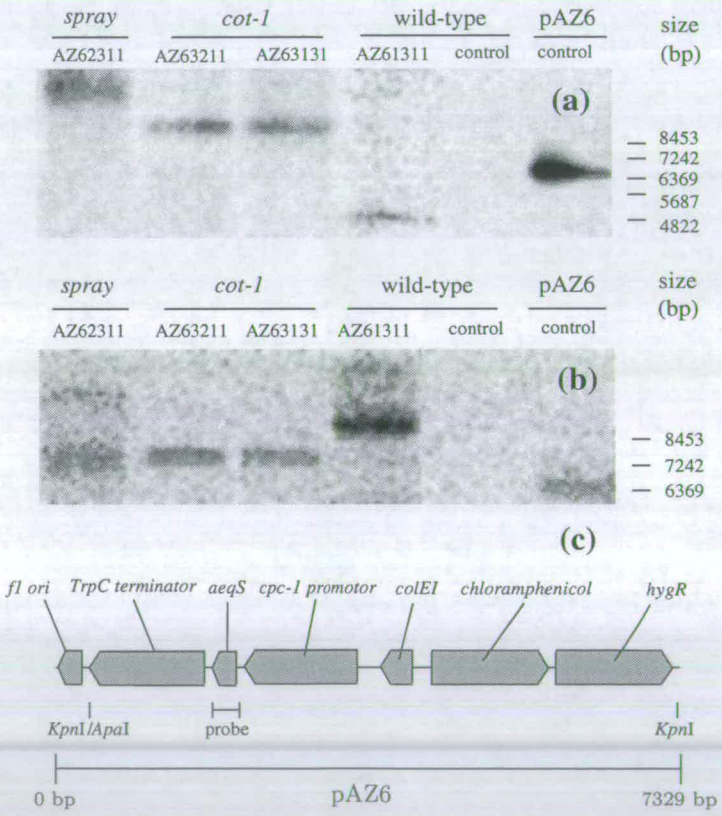

Figure 3.5: A Southern analysis of (a) *Apa*I and (b) *Kpn*I digests of genomic DNA extracted from wild-type, *cot-1* and *spray* pAZ6 transformants plus non-transformed wild-type and *spray* controls. *Apa*I cuts once in pAZ6. *Kpn*I cuts twice, liberating a 1000 bp fragment (not visible). The probe was random-primed, ^{32}P-labelled 629 bp *aeqS* extracted from pAZ6 by *Eco*RI digestion and agarose gel purification. (c) A schematic diagram of pAZ6 indicating the features relevent to this Southern analysis.

show the results of two southern blots performed using genomic DNA digested

with *Apa*I and *Kpn*I, respectively. In each case the positive controls produced a single band in agreement with the pAZ6 plasmid size of 7329 bp. *Kpn*I liberates a 1000 bp fragment from pAZ6 (not visible) and therefore the control band was proportionately smaller. Wild-type untransformed controls remained blank. The wild-type transformant (AZ61311wt) showed one band at about 4700 bp (Fig. 3.5 a) or one band at about 8500 bp (Fig. 3.5 b). The *spray* transformant (AZ62311spray) showed one band of greater than 8500 bp (Fig. 3.5 a) or two bands, one within a fragment about 7500 bp in size, the second within a fragment of greater than 8500 bp (Fig. 3.5 b). The *cot-1* transformants (AZ63211cot1 and AZ63131cot-1) showed one band each, at about 8500 bp or 7800 bp (Figs. 3.5 a and b, respectively).

3.2.3.4 *In vivo* optimisation of aequorin luminescence

No previous work has been done using an aequorin-based system to measure $[Ca^{2+}]_c$ concentrations in *N. crassa*. The optimal spore concentration for medium inoculation and subsequent growth time of the colony therefore had to be determined to obtain the best luminescence from the *N. crassa* transformants produced (see Section 2.14.2). Figure 3.6 shows that for optimal luminescence, our *cot-1* transformant should be inoculated at a concentration of $1x10^6$ conidia ml^{-1} and grown for 18 h at 24°C. A similar experiment was done for wild-type and *spray* aequorin transformants. Fig. 3.7 shows that the optimal incubation time for wild-type at 24°C was 18 h, the same as for *cot-1*. Incubation time did not affect *spray* luminescence to the same extent as with wild-type and *cot-1*. The effect of spore concentration on wild-type and *spray* strains was similar to *cot-1*. It was therefore decided that the standard spore concentration and incubation time for wild-type, *cot-1* and *spray* cultures should be $1x10^6$ conidia ml^{-1} and 18 h, respectively.

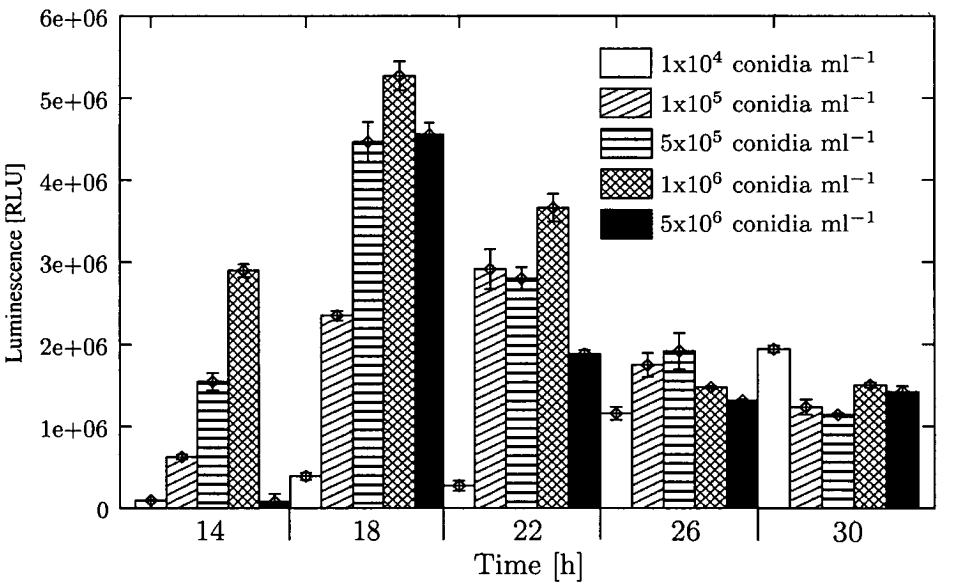

Figure 3.6: The effect of spore concentration and growth time on aequorin luminescence in *cot-1* colonies. Microwell plates were innoculated with liquid VgS containing *cot-1* spores as described in Section 2.5.2 except that spore concentrations of $1x10^4$, $1x10^5$, $5x10^5$, $1x10^6$ or $5x10^6$ conidia ml^{-1} were used. Cultures were incubated at 24°C for 14, 18, 22, 26 or 30 h before being discharged as described in Section 2.14.2. Values are means ± S.E. (n=6).

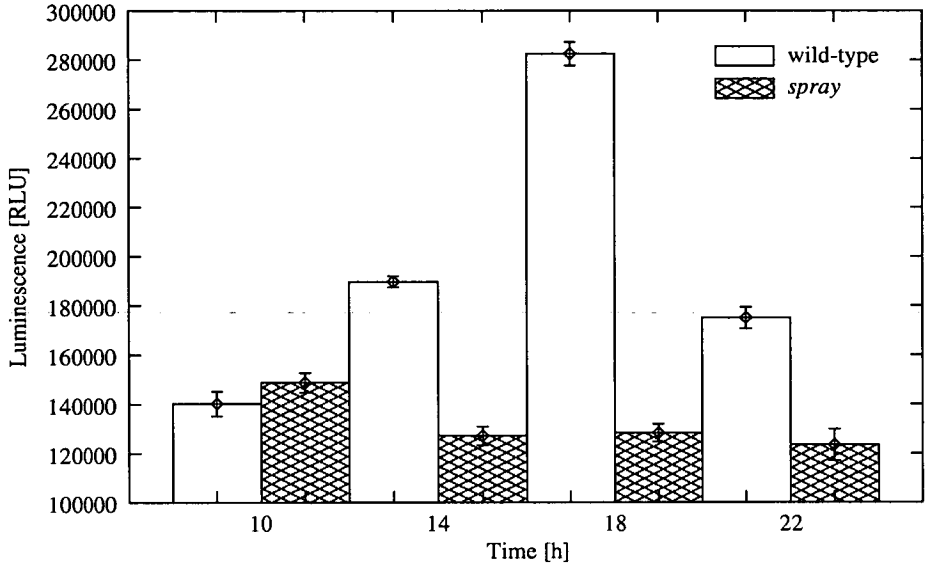

Figure 3.7: The effect of growth time on aequorin luminescence in wild-type and *spray* colonies. Microwell plates were innoculated and grown in microwell plates as described in Section 2.5.2. Cultures were incubated at 24°C for 10, 14, 18 or 22 h before being discharged as described in Section 2.14.2. Values are means ± S.E. (n=6).

3.3 Discussion

Transformable protoplasts were made from wild-type, *cot-1* and *spray* strains of *N. crassa*. Attempts to transform these protoplasts with pAEQS1-15 (which contains the synthetic filamentous fungal codon-optimised aequorin D gene [*aeqS*] (Nelson, 1999; Nelson et al., 2003)) were unsuccessful. Rather than spend time investigating the reasons for this, a plasmid (pAZ6) was produced, which contained *aeqS* under the control of the *N. crassa cpc-1* promotor (see Fig. 3.2). The promotor region of the *cpc-1* gene in pAZ6 included the first open reading frame but not the second, thereby negating the need for amino acid starvation to induce transcription and resulting in a constitutive promotor (D. Ebbole, Texas, A&M University, personal communication) (Paluh et al., 1988). Restriction analysis (Fig. 3.1) and sequencing confirmed the presence and orientation of *aeqS* in pAZ6, which was then used to transform *N. crassa*.

Previous transformations of filamentous fungi with *aeqS* have resulted in levels of aequorin expression ranging from 2.26 (*N. crassa*) to 21.8 μg aequorin per g total protein (*A. awamori*) (Nelson et al., 2003). Here, a set of transformants of the *N. crassa* strains: wild-type, *cot-1*, and *spray*, along with a partial phenotypic suppressor of *cot-1*, have been produced. It was shown that aequorin constitution in protein extracts from these transformants reaches its maximum after 90 min and that further constitution does not affect aequorin luminescence (in the time frame examined). A method for the rapid determination of the amount of aequorin in transformants was developed. These transformants, in which *aeqS* was driven by a modified *N. crassa cpc-1* promotor, contained between 2.9 and 6.9 μg aequorin per g total protein. No morphological abnormalities of differences in hyphal extension rate could be observed between transformed and non-transformed strains. The amount of aequorin in these strains was higher than previous transformants of *N. crassa* expressing the *aeqS* gene driven by the *N. crassa* clock controlled gene (*ccg-1* formally *grg-1* (Wang et al., 1994; McNally and Free, 1988)) promoter (Nelson et al., 2003). This is the first time that mutant strains of *N. crassa* have been transformed with an aequorin encoding gene.

Southern analysis of wild-type, *cot-1* and *spray* transformants showing a range of aequorin production (0.5 to 5.7 μg aequorin per g total protein), confirmed the presence of chimeric *aeqS* insertions but could not show a correlation between the number of *aeqS* insertions and the level of aequorin production (see Table 3.1 and Fig. 3.5). Both *Apa*I and *Kpn*I genomic DNA digestions showed wild-type (AZ61311wt) and *cot-1* (AZ63211cot1 and AZ63131cot1) transformants to have one *aeqS* insertion despite the fact that the wild-type transformant produced only 0.5 μg aequorin per g total protein and the *cot-1* transformant (AZ63131cot1) produced more than 10 times this amount. The *spray* transformant (AZ62311spray), on the other hand, appeared to have two *aeqS* insertions but only produced 1.0 μg aequorin per g total protein. Although Fig. 3.5 (a) showed only one *aeqS* containing band for *spray*, this band was heavy (> 8500 bp and therefore out of

the linear range of separation of a 0.9% agarose gel, which is from 500 to 7000 bp (Sambrook et al., 1989)) and could therefore have contained both *aeqS* insertions. A second blot in which a different preparation of genomic DNA was digested with *Apa*I showed the same results. The size of the *aeqS* containing bands in the *cot-1* transformants was identical in both Southern blots. Both these transformants were isolated from the same primary transformant during the purification of homokaryons. Together these results suggest that the AZ63211cot1 and AZ63131cot1 are the same transformant, and that the partial phenotypic suppression of *cot-1* was unrelated to the *aeqS* insertion but occurred during the purification process.

In vivo luminometry was carried out to determine the spore concentration for medium inoculation and the subsequent growth period that would provide maximum aequorin activity in the *N. crassa* transformants produced, while standardising the growth conditions between strains. It was found that transformants should be inoculated at a concentration of $1x10^6$ conidia ml^{-1} and grown for 18 h at 24°C (Figs. 3.6 and 3.7). These conditions are different from those used previously in *aeqS* transformed filamentous fungi. Examples include *N. crassa*: spore concentration not controlled (Nelson, 1999); *Aspergillus spp.*: $1x10^5$ spores ml^{-1} incubated at 30°C for 24 h (Nelson et al., 2003); and *Phyllosticta ampelicida*: inoculation with mycelia followed by 5 days growth at 25°C prior to transfer of colonies to a microwell plate and incubation with coelenterazine for 4 h before experiment (Shaw et al., 2001). These differences show the importance of determining the optimum conditions for fungal growth and aequorin luminescence for each new strain or species of fungus transformed.

3.4 Summary

- A new plasmid, pAZ6, designed for the constitutive expression of *aeqS* (the synthetic filamentous fungal codon-optimised aequorin D gene) in *N. crassa* was produced.
- This plasmid produced high levels of aequorin expression when transformed into several strains of *N. crassa*.
- No correlation between the number of ectopic *aeqS* insertions and the amount of aequorin produced by transformed strains could be shown.
- To achieve both high levels of *in vivo* luminescence and standardised growth conditions in the transformants produced, it was determined that transformants should be inoculated at a concentration of $1x10^6$ conidia ml^{-1} and grown for 18 h at 24°C.

Chapter 4

Characterisation of Ca^{2+}-Signalling in Wild-type and Hyperbranching Strains of *Neurospora*

4.1 Introduction

A $[Ca^{2+}]_c$ transient induced by an external stimulus is comprised of two main phases: a period of $[Ca^{2+}]_c$ increase when CPC activity predominates followed by a period of $[Ca^{2+}]_c$ decrease when Ca^{2+}-pump and -transporter activity predominate. The timing and regulation of CPC, Ca^{2+}-pump and -transporter activities will define the Ca^{2+}-signature generated by a specific external stimulus.

It has recently been shown that three external stimuli (mechanical perturbation, hypo-osmotic shock and high external calcium) produce three distinct Ca^{2+}-signatures in *A. awamori* (Nelson et al., 2003), and that these Ca^{2+} responses are sensitive to different Ca^{2+} agonists and antagonists suggesting that they originate from the activity of different combinations of CPC, Ca^{2+}-pump and -transporter proteins. Current thinking suggests that information encoded in

the Ca^{2+}-signature is an important factor in providing the necessary specificity for a particular stimulus to illicit a defined response (Sanders et al., 2002). However, a thorough quantitative analysis of Ca^{2+}-signatures and their relationship with environmental conditions, Ca^{2+} modulators and genetic background has not yet been performed in any organism. Furthermore, although Ca^{2+}-signalling has been implicated in playing a role in regulating branch formation in *N. crassa* and other filamentous fungi (see Section 1.5), an analysis of Ca^{2+}-signalling during hyperbranching has not yet been done.

The aims of the work carried out in this chapter were: (1) to determine the robustness and reproducibility of the wild-type *N. crassa* Ca^{2+}-signature in response to different stimuli when the fungus is grown under different environmental conditions; (2) to use the Ca^{2+}-signature as an indicator of what components of the Ca^{2+}-signalling machinery may have been disrupted in hyperbranching mutants for which there is some evidence for Ca^{2+}-signalling having been compromised (Dicker and Turian, 1990; Bok et al., 2001; Gorovits et al., 1999; Prokisch et al., 1997); (3) to use pharmacological agents to investigate the properties of the components involved in the generation of $[Ca^{2+}]_c$ transients in response to different stimuli; and (4) to determine whether $[Ca^{2+}]_c$ transients are associated with branch initiation in wild-type and hyperbranching mutant strains of *N. crassa*.

4.2 Results

4.2.1 Temperature and aequorin luminescence

Because my intention was to measure Ca^{2+} in aequorin-transformed strains at 24°C and 37°C, it was necessary to establish whether temperature influenced aequorin luminescence. It has previously been found that incubating purified aequorin for 0 to 60 min at 45 or 50°C had no significant effect on the amount of luminescence detected when these aequorin samples were all measured at 25°C (Gong et al., 1998). However, whether the light detected from measuring aequorin

luminescence at different temperatures (e.g. 24°C vs 37°C) will also be unaffected, has not been determined. Luminescence measurements of protein extracts from aequorin-expressing wild-type *N. crassa* incubated at 24 or 37°C were very similar when all samples were measured at 24°C. However, luminescence measured at 24°C was reduced to $\sim$ 80% when measurement was performed at 37°C (Table 4.1). Despite these findings, data gathered at 24 and 37°C can still be compared

Table 4.1: The effect of temperature on luminescence emitted by wild-type protein extracts. 100 μl samples each containing 40 μg total protein were constituted in 2.5 μM native coelenterazine for 4 h at 4°C before measurement. Luminescence was integrated for 20 s after injection of 100 mM $CaCl_2$

Incubation Temperature (°C)	Measurement Temperature (°C)	Mean Luminescence (% of maximum)	S.D. (n=6)
24	24	96	0.05
37	37	82	0.02
37	24	100	0.05
42	42	70	0.02
42	24	99	0.02

as conversion from RLUs to $[Ca^{2+}]_c$ concentrations results in the normalisation of the data converted.

Kinetic analyses was also performed to determine if temperature caused changes in the rate of light detected. No changes in the rate of light emission were observed at the temperatures tested.

4.2.2 Quantitative analysis of Ca^{2+}-signatures

4.2.2.1 Development of a rapid and accurate quantification system

In order to (a) convert the data produced by our luminometer from RLUs to Ca^{2+} concentrations, (b) quantify various parameters of the Ca^{2+}-signature, and (c) perform statistical analyses on these data on the large scale required by this study, it was necessary to develop a software package in order to automate these requirements. Figure 4.1 summarises the main functions of this program,

which accepted plain text input, generated by the WinGlow software running the luminometer (see Section 2.14.3 for details and Appendix E for the program source code).

4.2.2.2 The Ca^{2+}-signature - unique and robust

The initial question I addressed in this study concerned how robust and reproducible Ca^{2+}-signatures are under different growth conditions. Ca^{2+}-signatures were therefore compared in response to mechanical perturbation, hypo-osmotic shock, and high external Ca^{2+} in 12 or 18 h cultures at different temperatures (24 or 37°C) in liquid or on solid medium.

Each of the three stimuli produced a unique Ca^{2+}-signature (Fig. 4.2) and quantification of each signature resulted in a characteristic combination of rise time, amplitude and FWHM (Fig. 4.2, histograms). The small error bars highlight the highly reproducible nature of $[Ca^{2+}]_c$ transients in response to the stimuli tested. As the errors were of a similar magnitude in all other experiments error bars have been omitted in subsequent Figures for the sake of clearer graphical presentation.

In general, the Ca^{2+}-signatures detected in response to any one stimulus retained their basic characteristics with cultures of different ages, at different temperatures and in liquid or on solid medium (Figs. 4.2 and 4.3) although differences were noted. The basic characteristics of the Ca^{2+}-signatures were as follows (data from cultures grown in liquid medium for 18 h at 24°C; mean ± S.D. n=6). Mechanical perturbation resulted in a small (0.31 ± 0.02 μM) $[Ca^{2+}]_c$ transient that returned to its non-stimulated (or resting) level quite slowly (as shown by its quite large FWHM 55.8 ± 8.1 s); hypo-osmotic shock produced a larger (0.38 ± 0.02 μM) $[Ca^{2+}]_c$ transient that took a long time (FWHM was 76.8 ± 5.9 s) to return to its original level; high external Ca^{2+} produced a very large (0.59 ± 0.02) $[Ca^{2+}]_c$ transient that reached its maximum very fast (1.7 ± 0.00 s), and dropped back to its non-stimulated level very quickly (FWHM 25.8 ± 1.32 s).

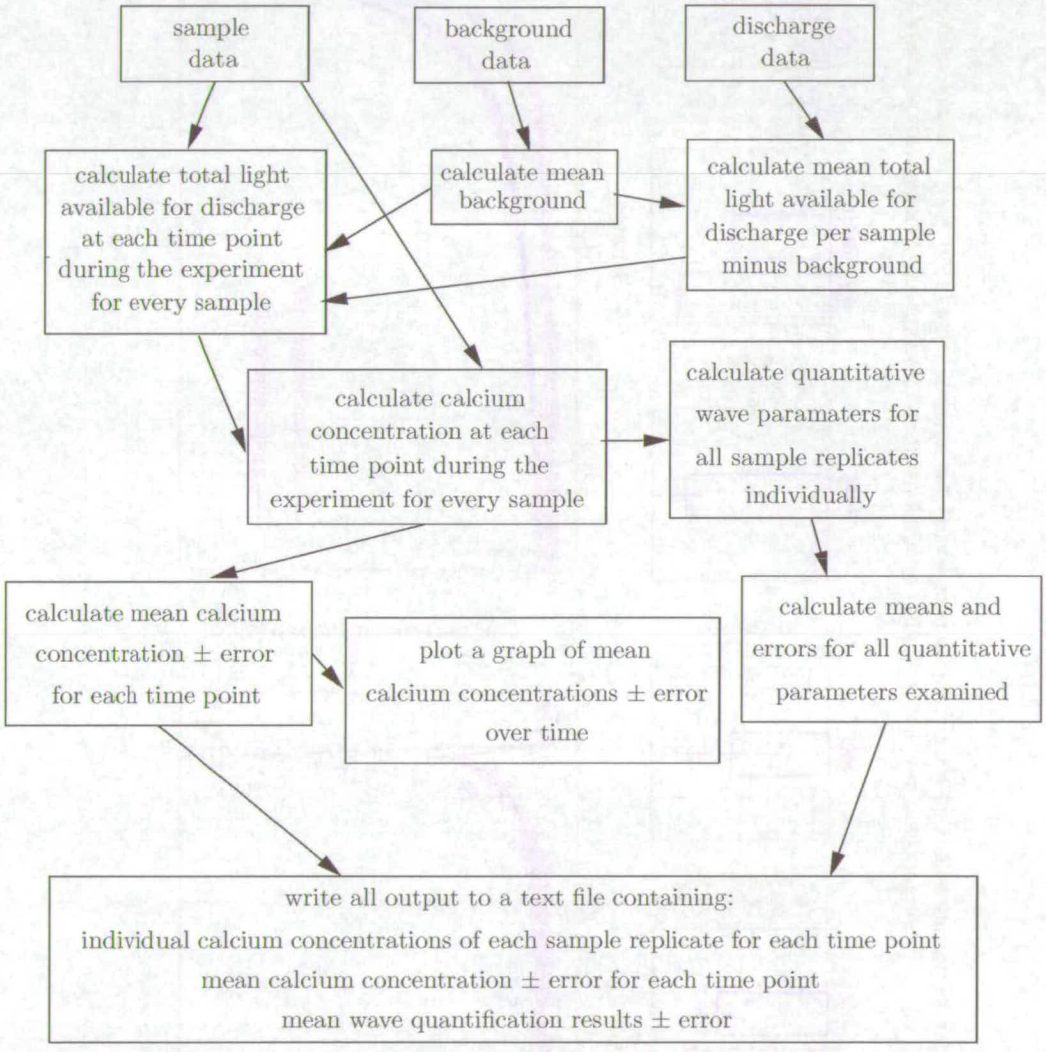

Figure 4.1: Summary of a program written to (a) convert the data produced by our luminometer from RLU to Ca^{2+} concentrations, (b) quantify various parameters of the Ca^{2+}-signature, and (c) perform statistical analysis on these data.

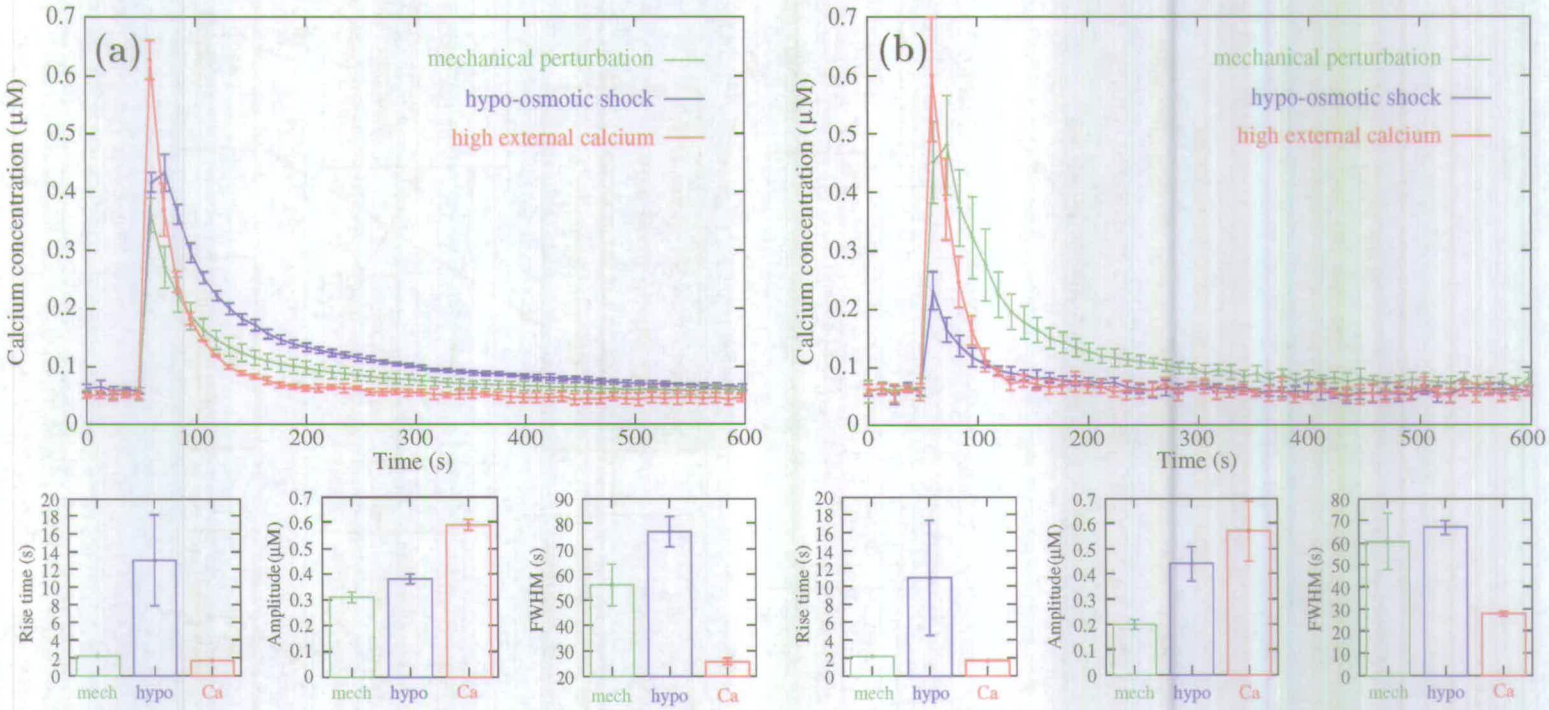

Figure 4.2: The effect of stimulation by mechanical perturbation, hypo-osmotic shock, and high external Ca^{2+} on $[Ca^{2+}]_c$ transients in 18 h old *N. crassa* wild-type colonies grown at 24°C in (a) liquid medium and (b) on solid medium. Error bars represent means ± S.D. of 6 replicates.

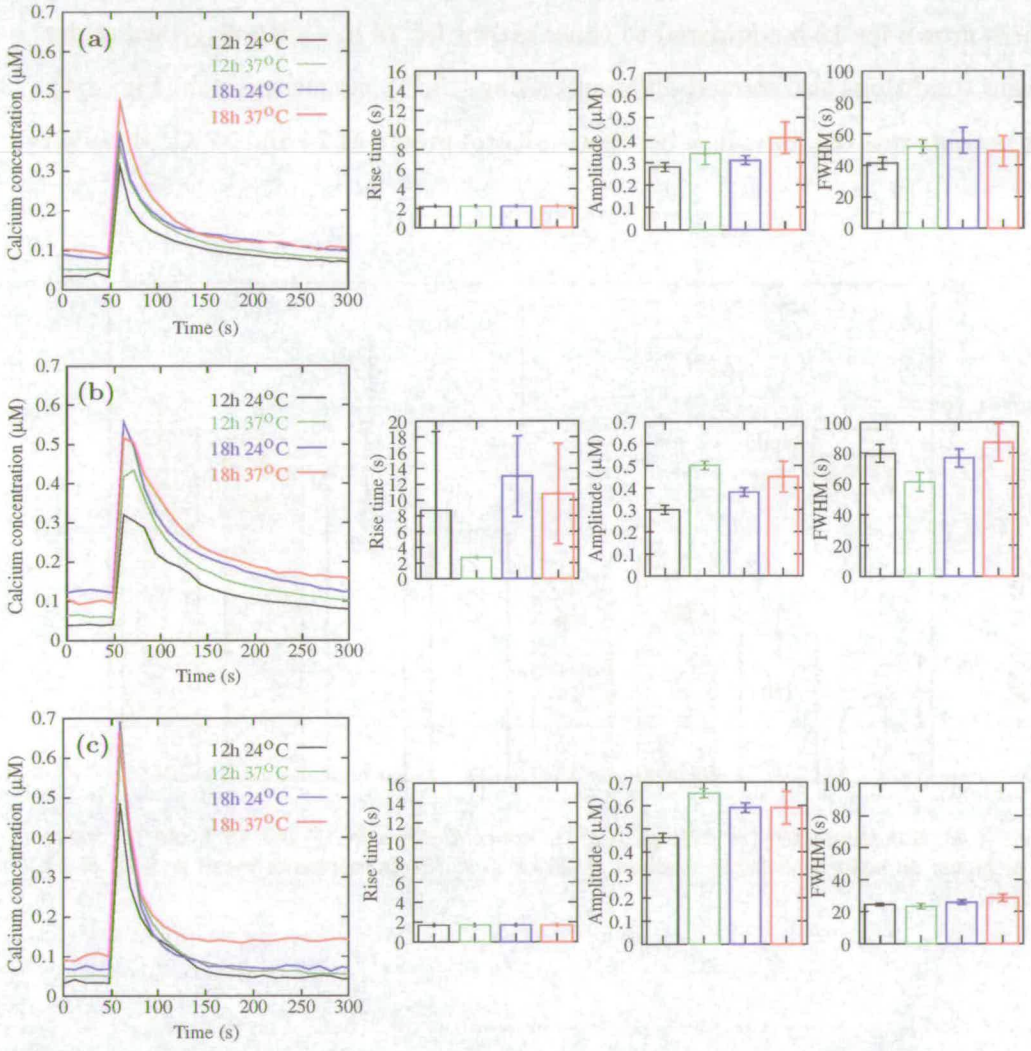

Figure 4.3: The effect of stimulation by (a) mechanical perturbation, (b) hypo-osmotic shock and (c) high external Ca^{2+} on $[Ca^{2+}]_c$ transients in 12 and 18 h old *N. crassa* wild-type colonies grown in liquid medium at 24 and 37°C. Lines are means of 6 replicates. Bars represent S.D. of 6 replicates.

The main difference noted between Ca^{2+}-signatures in colonies grown at different temperatures was that amplitudes were sometimes greater (from 0 ± 16.7% to 40 ± 9.8% [mean ± S.D. n=6]) in cultures grown at 37°C compared to those grown at 24°C (Fig. 4.3 histograms). These differences were more pronounced in cultures grown for 12 h compared to those grown for 18 h. Cultures grown under different conditions also showed different resting $[Ca^{2+}]_c$ concentrations (Fig. 4.4). Most notable was the difference between cultures grown at 24 and 37°C, although

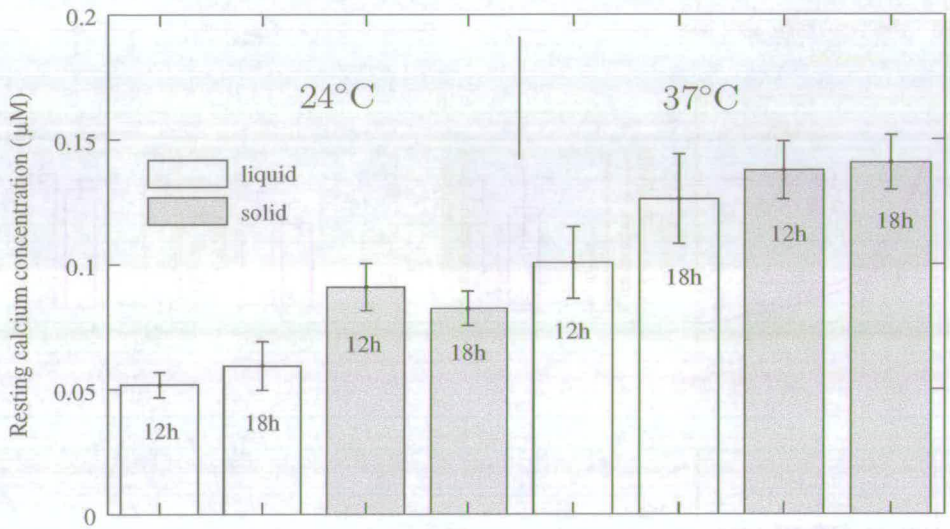

Figure 4.4: Non-stimulated (or resting) $[Ca^{2+}]_c$ concentrations in 12 and 18 h old *N. crassa* cultures grown on solid or in liquid medium at 24 or 37°C. Error represents mean ± S.D. of 12 replicates.

cultures grown on solid medium also had higher resting $[Ca^{2+}]_c$ concentrations than those grown in liquid medium.

Based on results obtained from repeated experiments, we found that the variations in signatures obtained from cultures grown on solid medium were typically slightly higher than those obtained from liquid medium. We therefore performed subsequent experiments using cultures grown in liquid medium.

4.2.2.3 The Ca^{2+}-signature reports disruptions in Ca^{2+}-signalling machinery

Genetic and pharmacological approaches were used to investigate the effect of disruptions in Ca^{2+}-signalling machinery on Ca^{2+}-signatures. The morphological mutants *spray* and *cot-1* were transformed with aequorin and their Ca^{2+}-signatures examined. *spray* has a hyperbranching phenotype (Fig. 3.4 b) and a hyphal extension rate about 20% that of the wild-type on solid medium at 24°C. The *spray* gene is thought to encode a 'Ca^{2+}-controlling protein' (Dicker and Turian, 1990) and although its sequence shows no match to genes of known function, pharmacological evidence suggests that the SPRAY protein regulates the distribution of Ca^{2+} via calcineurin (Bok et al., 2001). The *cot-1* mutant (Collinge et al., 1978; Yarden et al., 1992) has a hyphal extension rate and morphology almost indistinguishable from that of the wild-type (see Section 3.2.3 and Fig. 3.4 c) at the permissive temperature (< 24°C). However, 1-2 h after shifting a *cot-1* culture to the restrictive-temperature (> 37°C) hyphal extension ceases and massive induction of hyphal branching occurs (Fig. 3.4 d). The newly formed hyphal tips are unable to continue elongating at the restrictive-temperature, but returning the culture to the permissive-temperature results in rapid restoration of normal hyphal growth (Collinge et al., 1978; Yarden et al., 1992). The *cot-1* gene has been isolated and, based on the deduced COT1 amino acid sequence, it encodes a Ser/Thr-specific protein kinase (Yarden et al., 1992; Gorovits et al., 1999).

Ca^{2+}-signatures in *spray* had significant differences from those of the wild-type after 18 h of growth at 24°C in liquid medium (Fig. 4.5). The amplitudes of Ca^{2+}-signatures in response to mechanical perturbation, hypo-osmotic shock and high external Ca^{2+} in *spray* were reduced by 28 ± 25, 41 ± 39 and 46 ± 5.4% (mean ± S.D. n=6) respectively, compared to those of the wild-type. Rise time was also reduced, especially in response to hypo-osmotic shock. FWHM, however,

Figure 4.5: The effect of stimulation by (a) mechanical perturbation, (b) hypo-osmotic shock and (c) high external Ca^{2+} on $[Ca^{2+}]_c$ transients in 18 h old wild-type and *spray* colonies grown in liquid medium at 24°C. Lines are means of 6 replicates. Bars represent S.D. of 6 replicates.

was less affected. Despite these major differences, the basic characteristics of the Ca^{2+}-signatures in *spray* were very similar to those of the wild-type.

To determine whether the decreased amplitudes observed in *spray* Ca^{2+}-signatures were potentially mediated via calcineurin, Ca^{2+}-signatures were measured in wild-type colonies grown in the presence of 124 nM of the calcineurin inhibitor FK506 (Prokisch et al., 1997). This concentration reduced the wild-type hyphal extension rate by 40 ± 12% (mean ± S.D. n=6) and caused *spray*-like hyperbranching (Fig. 4.6 a). The FK506 medium amendment conferred a reduction

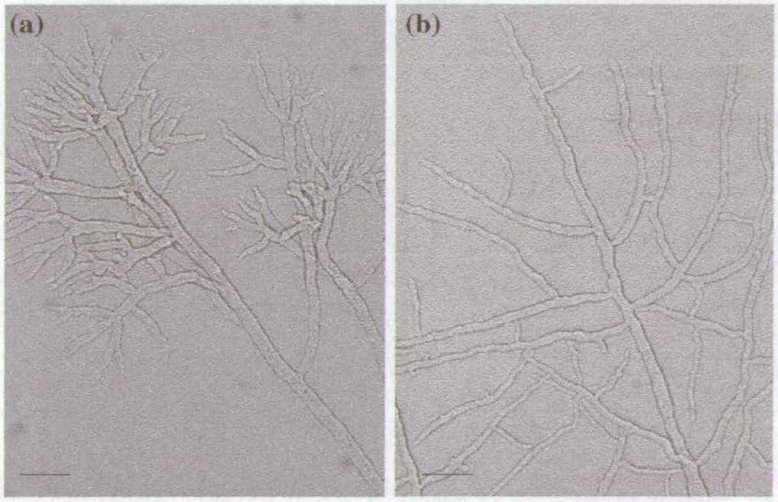

Figure 4.6: The effect of (a) 124 nM FK506 or (b) 0.25% sorbose on wild-type *N. crassa* morphology grown at 24°C on solid Vogel's medium. Bars are 50 μm.

in wild-type amplitudes in response to mechanical perturbation, hypo-osmotic shock and high external Ca^{2+} by 16 ± 13.2, 30 ± 31.8 and 16 ± 10% (mean ± S.D. n=6) respectively, compared to the untreated wild-type control (Fig. 4.7). These reductions, however, were not as large as observed in the untreated *spray* control (27 ± 6.6, 46 ± 31.8, and 53 ± 7.6% (mean ± S.D. n=6), in response to mechanical perturbation, hypo-osmotic shock and high external Ca^{2+}, respectively). A further control in the form of wild-type grown on 0.25% sorbose was also used. This concentration of sorbose, like the FK506, causes a 38 ± 12%

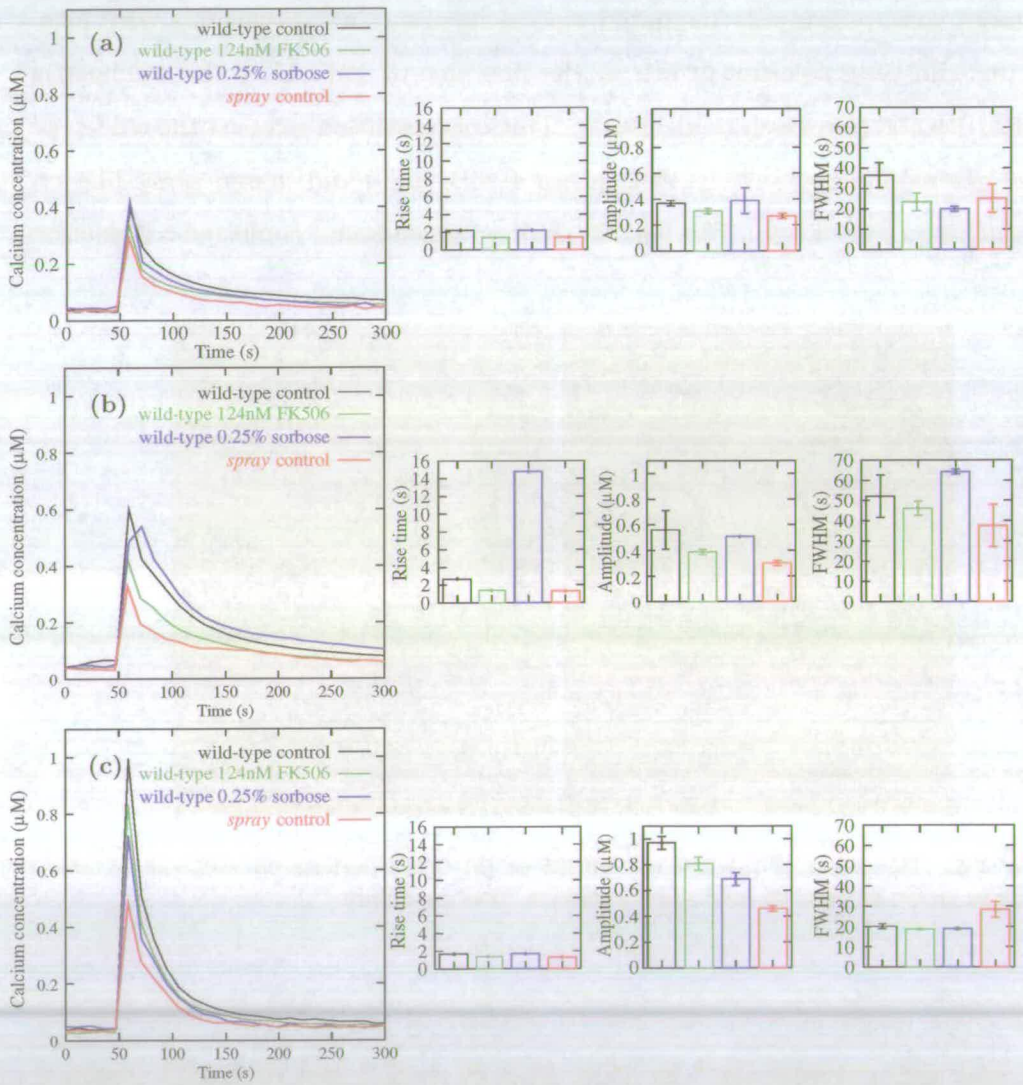

Figure 4.7: The effect of 0.25% sorbose or 124 nM FK506 on wild-type $[Ca^{2+}]_c$ transients induced by (a) mechanical perturbation, (b) hypo-osmotic shock and (c) high external Ca^{2+} in 18 h old *N. crassa* colonies grown in liquid medium at 24°C. Non-treated wild-type and *spray* controls are also shown. Lines are means of 6 replicates. Bars represent S.D. of 6 replicates.

(mean ± S.D. n=6) reduction in hyphal extension rate and *spray*-like hyperbranching (Fig. 4.6 b) but has no known link to Ca^{2+}-signalling. The amplitudes of Ca^{2+}-signatures in response to mechanical perturbation, hypo-osmotic shock and high external Ca^{2+} in wild-type colonies grown in sorbose amended medium showed a 5.1 ± 32% increase, an 8.9 ± 27% decrease and a 29 ± 7.6% (mean ± S.D. n=6) decrease compared to the untreated wild-type control (Fig. 4.7). In the case of the response to mechanical perturbation and hypo-osmotic shock these amplitudes were not significantly different to those of the untreated wild-type control. Finally, Ca^{2+}-signatures in response to mechanical perturbation, hypo-osmotic shock and high external Ca^{2+} were measured in wild-type cultures grown for 18 h at 24°C in liquid VgS after a 10 min pretreatment with either 248 nM FK506 or another calcineurin inhibitor, 250 nM cyclosporin A. No difference in Ca^{2+}-signatures could be observed in comparision with control cultures (data not shown).

To confirm that the decreased amplitude of the $[Ca^{2+}]_c$ transients observed in *spray* is related to a disruption of the Ca^{2+}-signalling machinery, and not a result of a difference in maturity or biomass between the two strains (given that *spray* has a hyphal extension rate 80% slower than the wild-type), Ca^{2+}-signatures were measured in *spray* colonies grown for 10, 14, 18 and 22 h at 24°C. The Ca^{2+}-signatures measured at these times were very similar (Fig. 4.8), although quantification of these Ca^{2+}-signatures (Fig. 4.8, histograms) showed that amplitudes decreased with increasing growth time. After 22 h, amplitudes had decreased by 36 ± 12, 37 ± 0.0 and 23 ± 3.7% (mean ± S.D. n=6) in response to mechanical perturbation, hypo-osmotic shock and high external Ca^{2+} respectively, as compared to 10 h cultures. However, as amplitudes in *spray* do not increase with time, the differences observed between wild-type and *spray* amplitudes can not be said to be related to maturity or biomass and are likely to represent a genuine difference in the composition or behaviour of Ca^{2+}-signalling machinery present in the *spray* mutant.

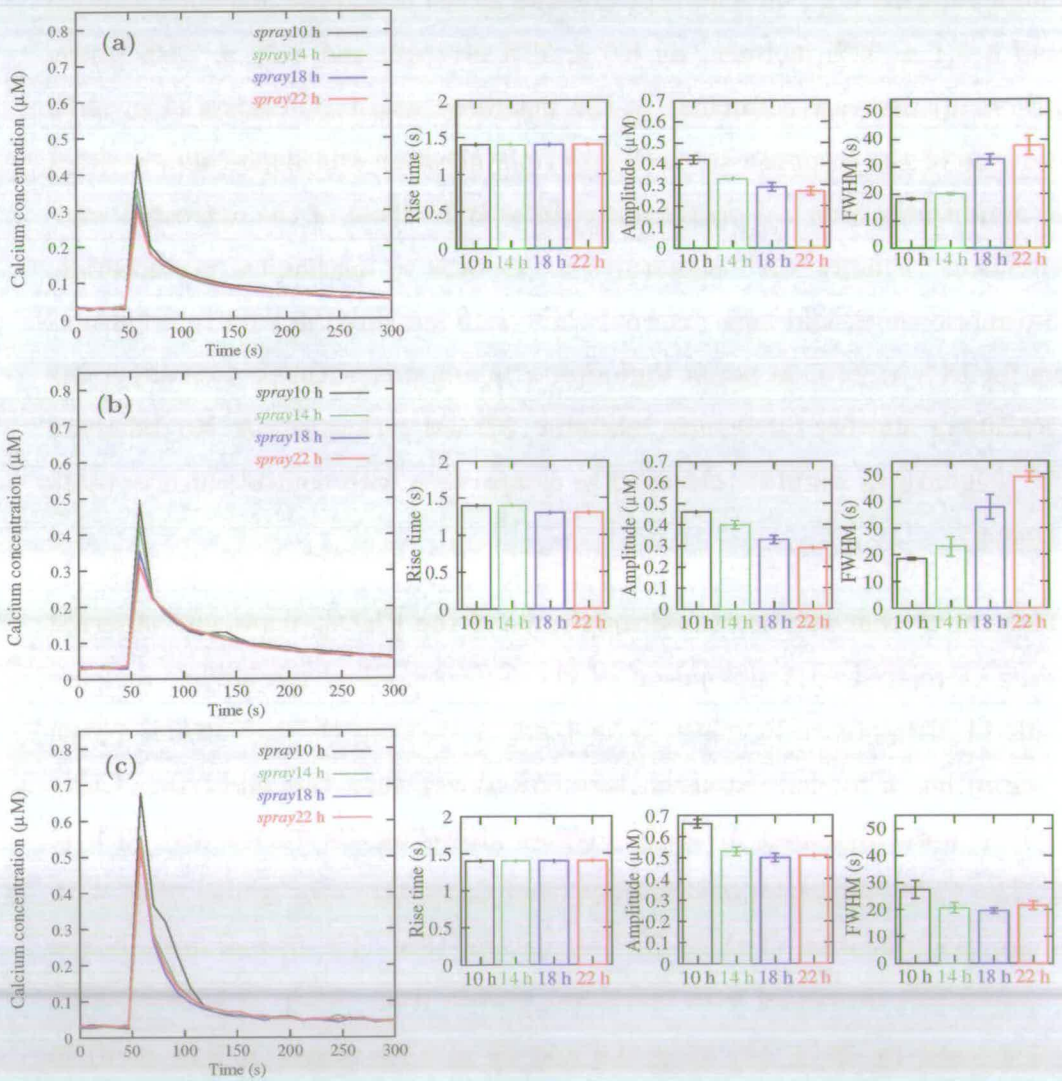

Figure 4.8: The effect of growth time on $[Ca^{2+}]_c$ transients induced by (a) mechanical perturbation, (b) hypo-osmotic shock and (c) high external Ca^{2+} in *N. crassa spray* colonies grown in liquid medium at 24°C. Lines are means of 6 replicates. Bars represent S.D. of 6 replicates.

The effects of three known Ca^{2+} modulators on wild-type Ca^{2+}-signatures were also examined: (a) cyclopiazonic acid (CPA) reversibly inhibits Ca^{2+}-ATPases that fill internal Ca^{2+} stores (Okorokov et al., 1997); (b) 2-APB is known to inhibit IP_3-induced Ca^{2+} release from Ca^{2+} stores in animal cells (Maruyama et al., 1997); and (c) caffeine causes the release of Ca^{2+} from internal Ca^{2+} stores in diverse organisms (Komori et al., 1995; Bauer et al., 1999; Arora and Ohlan, 1997).

Injection of 10 to 50 μM CPA into 18 h old wild-type *N. crassa* cultures inside the luminometer was found to cause dose-dependent prevention of recovery of the resting $[Ca^{2+}]_c$ concentration after the injection-induced $[Ca^{2+}]_c$ transient (see Fig. 4.9). A 10 min pretreatment with 25 μM CPA was found to raise resting

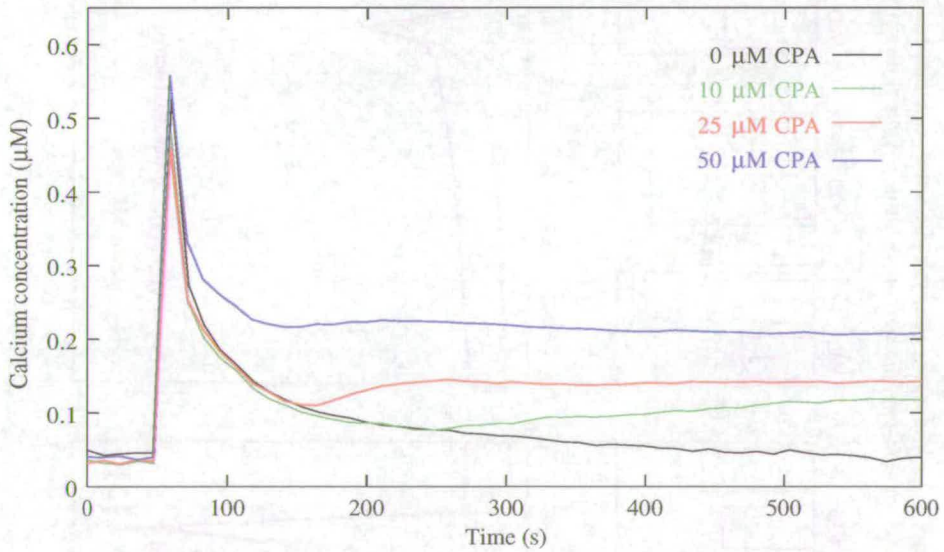

Figure 4.9: Differences in $[Ca^{2+}]_c$ transients induced by one 0 to 50 μM injection of CPA into 18 h old wild-type *N. crassa* cultures inside the luminometer. Lines are means of 6 replicates.

$[Ca^{2+}]_c$ concentrations by 74 $\pm$ 8.6% (mean $\pm$ S.D. n=6) over the control (data from Fig. 4.10). Ca^{2+}-signatures in the CPA pretreated colonies in response to mechanical perturbation, hypo-osmotic shock and high external Ca^{2+} differed from untreated controls in showing slightly reduced amplitudes and dramatically

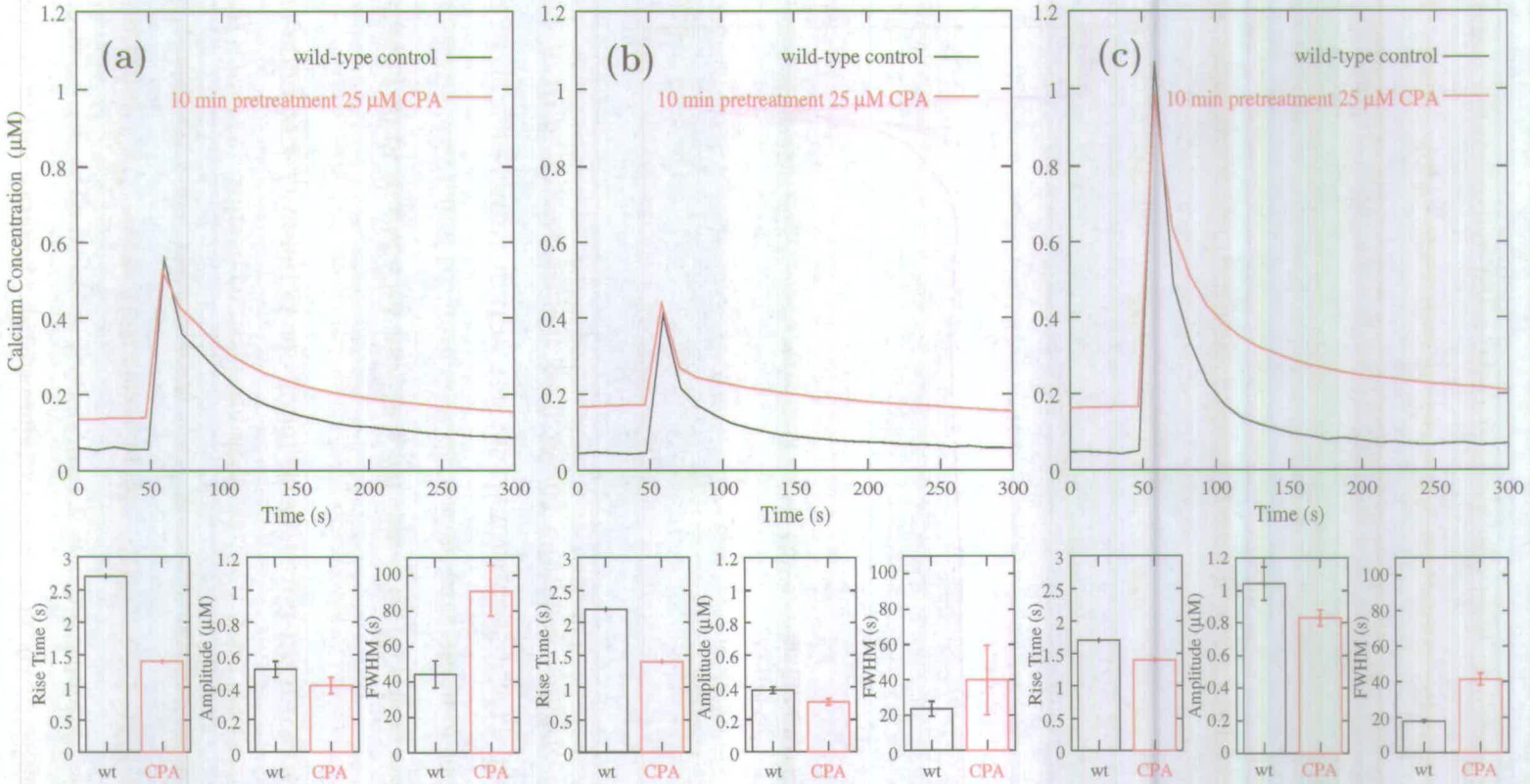

Figure 4.10: The effect of 10 min pretreatment with 25 μM CPA on $[Ca^{2+}]_c$ transients in 18 h old wild-type *N. crassa* colonies grown in liquid medium at 24°C and stimulated by (a) mechanical perturbation, (b) hypo-osmotic shock and (c) high external Ca^{2+}. Lines are means of 6 replicates. Bars represent S.D. of 6 replicates.

increased FWHMs, especially in response to mechanical perturbation and high external Ca^{2+} (Fig. 4.10).

Injection of 50 μM (but not 10 or 25 μM) 2-APB into 18 h old wild-type *N. crassa* cultures inside the luminometer prevented recovery of the resting $[Ca^{2+}]_c$ concentration after the injection-induced $[Ca^{2+}]_c$ transient (see Fig. 4.11). A

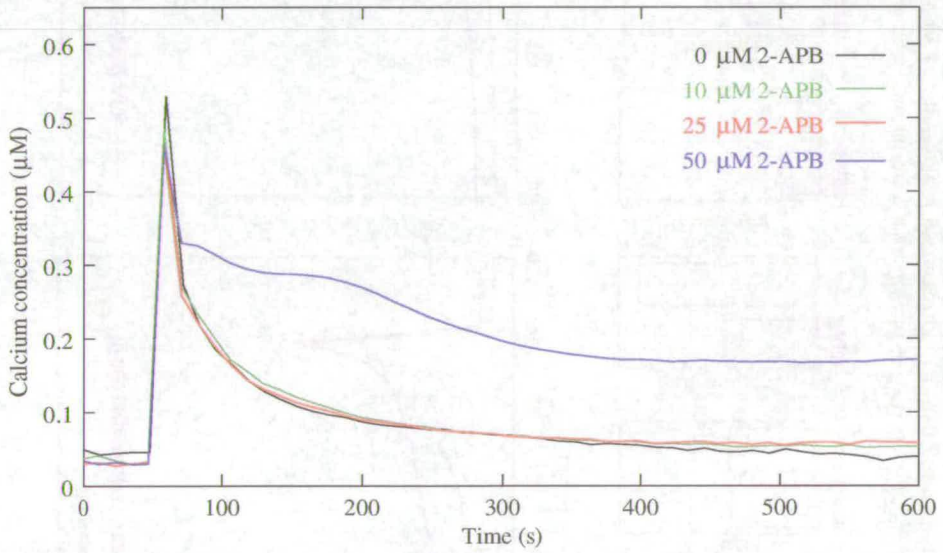

Figure 4.11: Differences in $[Ca^{2+}]_c$ transients induced by one 0 to 50 μM injection of 2-APB into 18 h old wild-type *N. crassa* cultures inside the luminometer. Lines are means of 6 replicates.

10 min pretreatment with 25 μM 2-APB was found to raise resting $[Ca^{2+}]_c$ concentrations by 60 $\pm$ 16% (mean $\pm$ S.D. n=6) over the control (data from Fig. 4.12). Ca^{2+}-signatures in the 2-APB pretreated colonies in response to mechanical perturbation, hypo-osmotic shock and high external Ca^{2+} differed from untreated controls in showing slightly increased amplitudes and dramatically increased FWHMs (Fig. 4.10). These effects were more profound in $[Ca^{2+}]_c$ transients resulting from stimulation by hypo-osmotic shock and high external Ca^{2+}.

Injection of 0 to 10 mM caffeine into 18 h old wild-type *N. crassa* cultures inside the luminometer had no observable effect on $[Ca^{2+}]_c$ transients (see Fig.

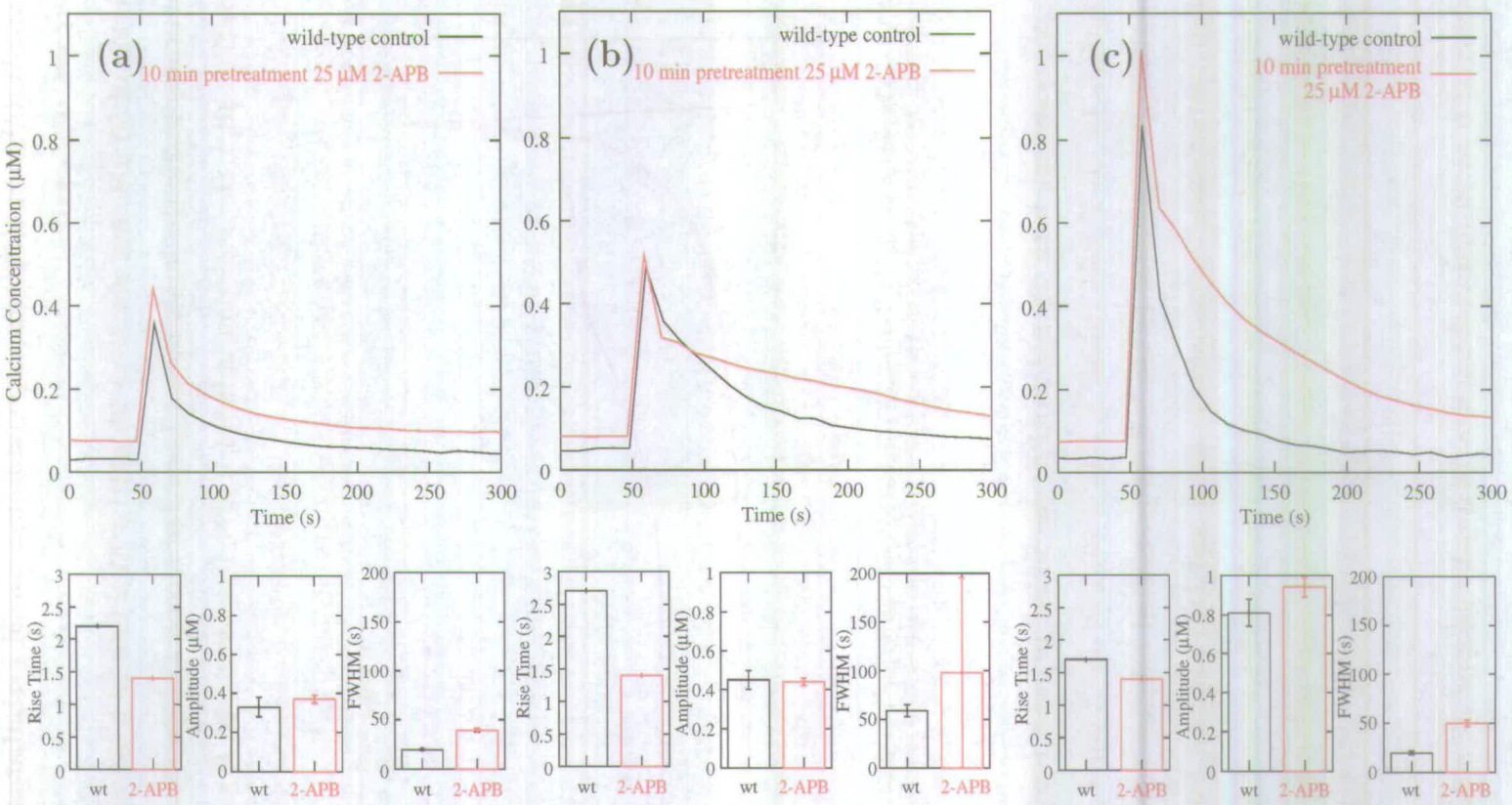

Figure 4.12: The effect of 10 min pretreatment with 25 μM 2-APB on $[Ca^{2+}]_c$ transients in 18 h old wild-type *N. crassa* colonies grown in liquid medium at 24°C and stimulated by (a) mechanical perturbation, (b) hypo-osmotic shock and (c) high external Ca^{2+}. Lines are means of 6 replicates. Bars represent S.D. of 6 replicates.

4.13). Injection of 25 mM caffeine, the maximum amount I was able to dissolve in

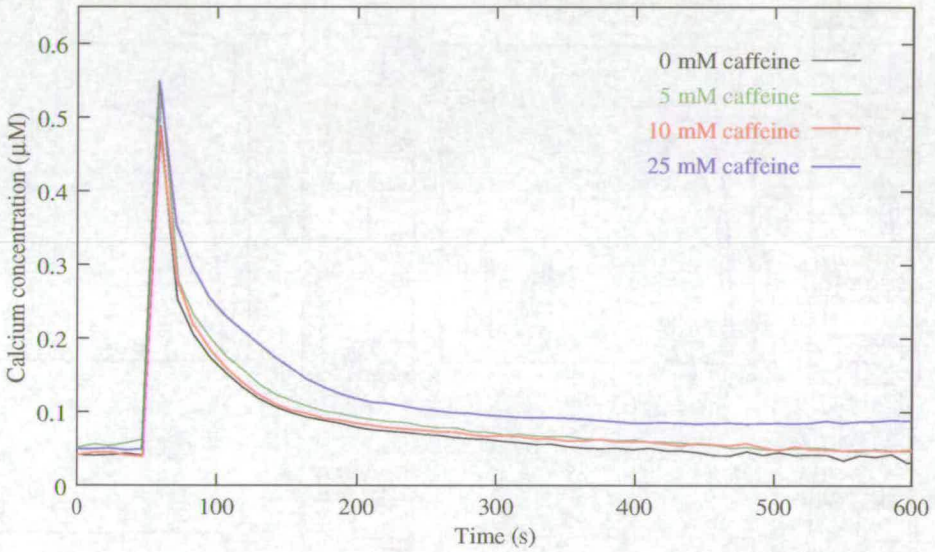

Figure 4.13: Differences in $[Ca^{2+}]_c$ transients induced by one 0 to 25 mM injection of caffeine into 18 h old wild-type *N. crassa* cultures inside the luminometer. Lines are means of 6 replicates.

liquid VgS medium, caused a 49 ± 22% (mean ± S.D. n=6) increase in FWHM in comparison to the control (data from Fig. 4.13) but no observable changes in amplitude. A 10 min pretreatment with 10 mM caffeine had no observable effect on either resting $[Ca^{2+}]_c$ concentrations or on Ca^{2+} transients in response to mechanical perturbation, hypo-osmotic shock or high external Ca^{2+} (data not shown).

At the permissive temperature, *cot-1* is morphologically almost indistinguishable from wild-type. This was reflected in terms of Ca^{2+}-signatures, which were also very similar in the two strains at the permissive temperature (Figs. 4.14 a to c and corresponding histograms). After 4 h at the restrictive temperature, however, Ca^{2+}-signatures in *cot-1* showed significantly smaller amplitudes than the wild-type in response to mechanical perturbation and hypo-osmotic shock, and high external Ca^{2+} (Figs. 4.14 d to f and corresponding histograms), indicating that impaired COT1 function alters the Ca^{2+}-signature.

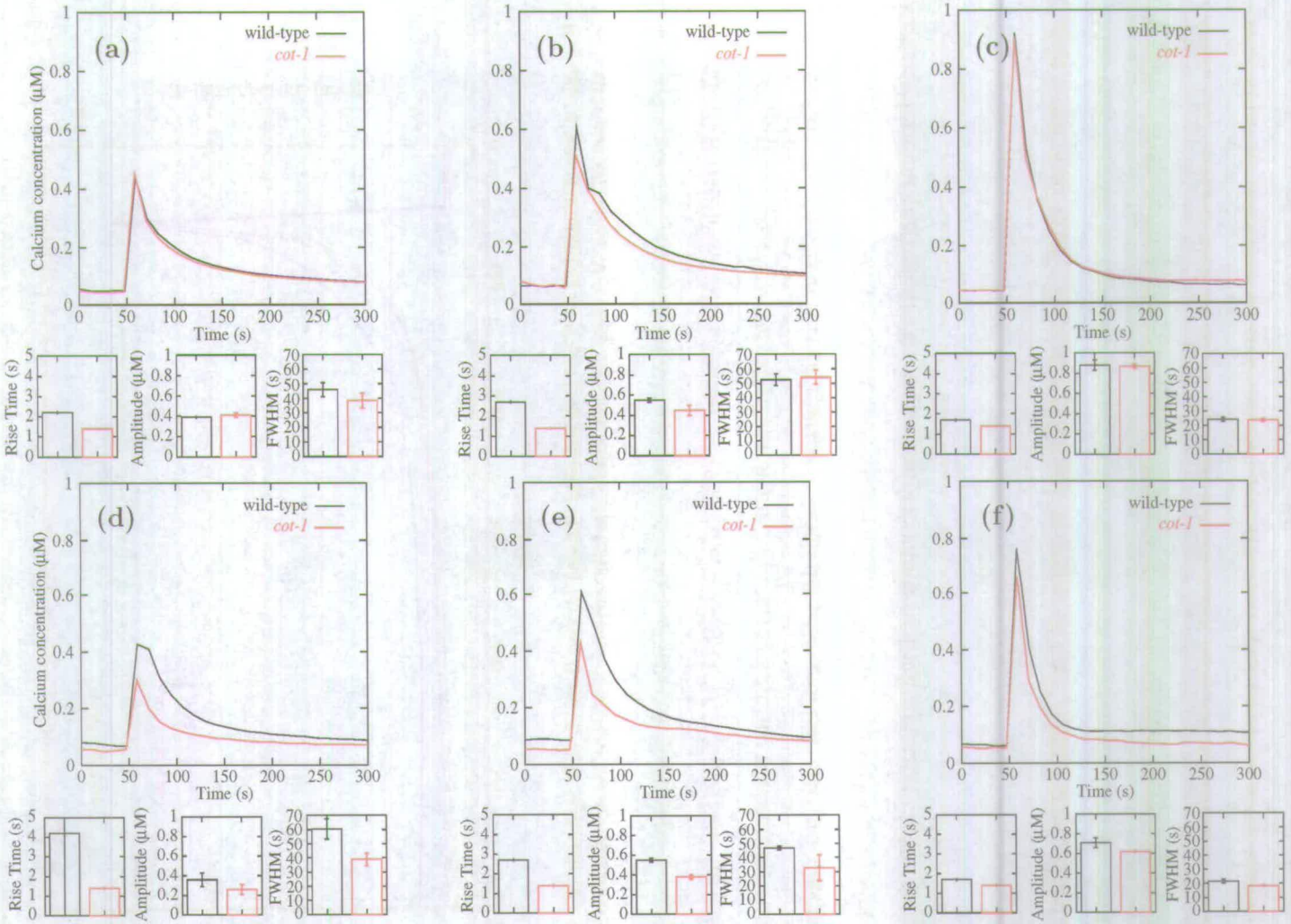

Figure 4.14: The effect of a 24 to 37°C temperature shift on $[Ca^{2+}]_c$ transients of wild-type and *cot-1* colonies. Strains were grown in liquid medium at 24°C for 22 h and stimulated by (a) mechanical perturbation, (b) hypo-osmotic shock and, (c) high external Ca^{2+} or grown at 24°C for 18 h as above and then shifted to 37°C for 4 h and stimulated by: (d) mechanical perturbation, (e) hypo-osmotic shock and (f) high external Ca^{2+}. Lines are means of 6 replicates. Bars represent S.D. of 6 replicates.

4.2.2.4 $[Ca^{2+}]_c$ transients are not associated with hyphal branch induction

The Ca^{2+} measurements made during this work are an average of $[Ca^{2+}]_c$ changes across the thousands of fungal microcolonies thriving in each microwell. Despite the fact that studies in plants and animals have established that changes in $[Ca^{2+}]_c$ following stimulation are typically very localised within cells (Berridge et al., 2000; Sanders et al., 2002) the general measurements made during this work provide a great deal of information. The non-stimulated (or resting) $[Ca^{2+}]_c$ concentration of many hyphal colonies will change according to the frequency and magnitude of the 'house-keeping' Ca^{2+}-signalling going on. Ca^{2+}-signalling has been implicated in the regulation of tip growth and hyphal branching for many years (see Section 1.5). The observation of resting $[Ca^{2+}]_c$ concentrations in hyperbranching strains may therefore provide an indication of changes in the frequency of branch induction signals if Ca^{2+}-signals do regulate hyphal branch induction.

To determine whether higher resting levels of $[Ca^{2+}]_c$ accompany the regulation of polarised cell extension (tip growth) or its induction (hyphal branching) in *N. crassa*, the non-stimulated $[Ca^{2+}]_c$ concentration was measured in hyperbranching and non-hyperbranching strains. Resting $[Ca^{2+}]_c$ concentrations were not significantly different the hyperbranching mutant *spray* (34.3 ± 3.9 nM [mean ± S.D. n=6]) or in wild-type colonies treated with 0.25% sorbose (33.8 ± 8.6 nM [mean ± S.D. n=6]) or to wild-type colonies treated with 124 nM FK506 (41.4 ± 4.6 nM [mean ± S.D. n=6]). Both sorbose and FK506 treatments induced hyperbranching phenotype (Fig. 4.6) and reduced hyphal extension rate by ~ 40%. The untreated wild-type control had an average, non-stimulated $[Ca^{2+}]_c$ concentration of 33.8 ± 8.3 nM (mean ± S.D. n=6). After 4 h at 37°C wild-type and *cot-1* colonies had an average $[Ca^{2+}]_c$ concentration of 63.8 ± 2.7 nM and 54.3 ± 3.4 nM (mean ± S.D. n=6), respectively. Furthermore, no change in resting $[Ca^{2+}]_c$ concentrations accompanies either the cessation (upon shifting

to the restrictive temperature) or the resumption (upon shifting back to the permissive temperature) of hyphal elongation in *cot-1* (Fig. 4.15). It should also be noted that prolific hyperbranching is induced in *cot-1* colonies shortly after shifting them to the restrictive temperature (Fig. 3.4), and that no change in average $[Ca^{2+}]_c$ concentrations was observed during this process (Fig. 4.15).

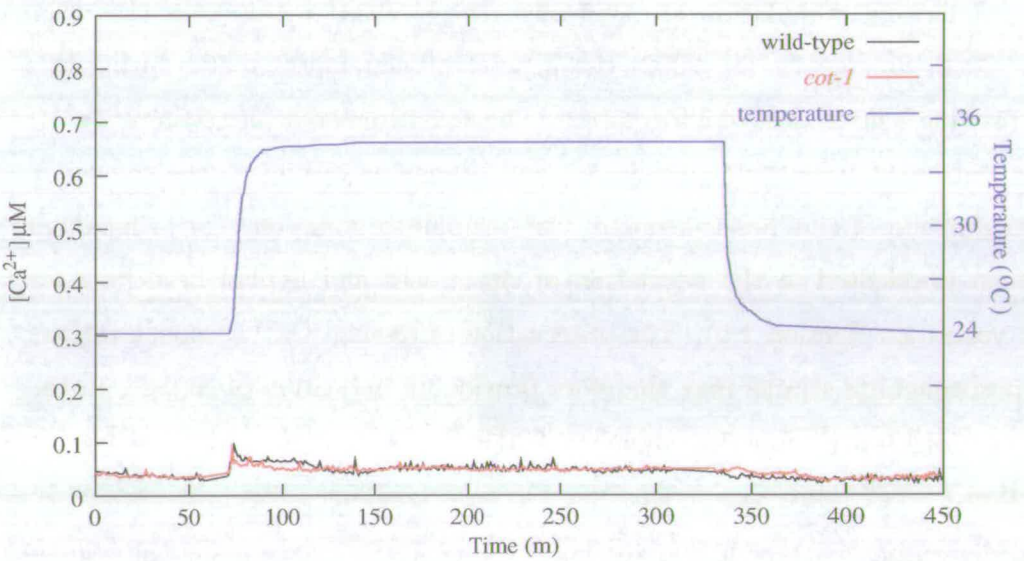

Figure 4.15: The induction of hyperbranching in *cot-1* (achieved by shifting cot-1 from 24 to 37°C for 4 h) does not correspond to changes in $[Ca^{2+}]_c$ resting concentrations. Lines (except temperature) are means of 6 replicates.

4.3 Discussion

Increasing measurement temperature from 24 to 37°C was found to reduce aequorin luminescence by about 20%, however, data gathered at the two temperatures are still comparable after conversion from RLUs to $[Ca^{2+}]_c$ concentrations as data is normalised during the conversion process. The equation used to convert luminescence in RLUs to Ca^{2+} concentrations is based on the amount of luminescence at a point in time, divided by the amount of luminescence available for emission at that point in time (see Section 2.14.3). This is necessary

for accurate conversion into Ca^{2+} concentrations because active aequorin is used up during the course of an experiment, the probability of an interaction between a Ca^{2+} ion and and active aequorin molecule decreases. Thus, towards the end of an experiment, lower levels of luminescence represent higher concentrations of Ca^{2+}. In the case of the reduction of aequorin luminescence by measurement temperature, the amount of luminescence available for discharge is reduced from the beginning of the experiment, and is taken into account from the beginning of the experiment. Data gathered at different temperatures is therefore comparable. Data in RLUs gathered at different temperatures should not be compared. Kinetic analyses showed no changes in the rate of light emission at the temperatures tested. I therefore conclude that aequorin is a suitable indicator for use in detecting differences in Ca^{2+}-signatures at these temperatures.

Using aequorin it was recently shown that three external stimuli (mechanical perturbation, hypo-osmotic shock and high external calcium) produce three distinct Ca^{2+}-signatures in *A. awamori* (Nelson et al., 2003). Nelson et al. (2003) used a spreadsheet to convert RLUs to Ca^{2+} concentrations and subsequent quantification of Ca^{2+}-signatures was done by hand. Here I have developed a computer program that converts RLUs to Ca^{2+} concentrations, quantifies various parameters of the Ca^{2+}-signature, statistically analyses and plots data directly from the luminometer (see Section 2.14.3). This program has a number of important improvements on the spreadsheet:

- Data interpolation is done in a more realistic manner. As *in vivo* luminometry was performed using a repeated measurement protocol (see Section 2.14.3) each sample was measured once every measurement cycle. In order to estimate the amount of light emitted from a sample between measurements, the spreadsheet used by Nelson et al. (2003) assumes that the rate of luminescence emitted by a sample is constant throughout the measurement cycle. Luminescence is thus assumed to change in a step-wise manner at each measurement point. The program developed here assumes that the

rate of light emission changes in a linear fashion between each measurement point (see Fig. 2.2) and interpolates the data based on that assumption. This method will give much more accurate results when the change in light emission between measurement points is large.

- Background luminescence is subtracted from all data. This was not done by the spreadsheet.

- The user is warned of unsuitable data. Data is unsuitable for conversion into Ca^{2+} concentrations if the majority of the aequorin in the sample is discharged during an experiment. For example, if all the aequorin was used up during an experiment luminescence would drop to zero but this would not necessarily correspond to a decrease in Ca^{2+} concentration. This program allows the user to set a percentage of the total aequorin available (calculated from the discharge data) that is allowed to be used up during the course of an experiment. If this value is exceeded the user is warned that the data conversion is likely to be inaccurate.

- Quantitative parameters of the Ca^{2+}-signature are calculated automatically. Previous quantification of Ca^{2+}-signatures had to be done by hand. The accurate derivation of parameters such as FWHM from printed graphs of $[Ca^{2+}]_c$ transients is both difficult and time consuming. This is reflected by the absence of means and standard errors for the parameters of Ca^{2+}-signatures (except amplitude) quantified by Nelson et al. (2003) and Kozlova-Zwinderman (2002). My software calculates six quantitative parameters from each replicate of every experiment and then calculates means and performs statistics on these results. Furthermore, data from the luminometer does not need to be copy-pasted into the program as data files produced by the luminometer are read directly. Much larger datasets can therefore be processed more accurately in less time.

- Experiments with different numbers of repetitions can be processed. This

program automatically calculates the number of replicates (n) in each data file. Means and statistics are calculated using this value. Previously, a new spreadsheet had to be created for every experiment that did not have 6 or less replicates. My software is therefore more flexible than the old approach.

- This program was written in a modular fashion to allow new quantitative parameters of the Ca^{2+}-signature to be easily introduced for automated analysis as they are thought of or required.

Using this program it is now possible to accurately and quantitatively process data from hundreds of experiments, providing for the first time, the amount of data needed to study Ca^{2+}-signatures in depth.

The Ca^{2+}-signatures of $[Ca^{2+}]_c$ transients induced by mechanical perturbation, hypo-osmotic shock and high external Ca^{2+} were shown to be (a) highly reproducible; (b) readily quantifiable, and (c) have distinct characteristics regardless of growth time, growth temperature or growth in liquid vs on solid medium. Although the actual values of these signatures changed slightly in colonies grown under different conditions, the overall characteristic response to each stimulus was maintained. The reproducibility of Ca^{2+}-signatures on solid medium was less good than in cultures grown on liquid medium and day-to-day variability was also greater. This is likely to be a result of (1) much less mycelium in solid cultures due to the fact they grow only on the surface of solid medium therefore reducing the overall fungal biomass, and (2) the application of liquid stimuli to cultures growing on solid medium involves two phases that do not reach equilibrium quickly, resulting in a protracted and potentially more variable stimulus.

Cultures grown in liquid or on solid medium at 24 or 37°C consistently had different resting $[Ca^{2+}]_c$ concentrations. This may reflect the different 'housekeeping' Ca^{2+}-signalling needed for growth in these different conditions.

The fact that Ca^{2+}-signatures have quantitatively definable reproducible characteristics offers a unique opportunity to use these signatures to gain insights into the state of the Ca^{2+}-signalling machinery. Here I have looked at three

aspects of the Ca^{2+}-signature: (1) the rise time, (2) amplitude, and (3) FWHM. Each parameter tells a different story. Rise time and amplitude are likely to be most affected by Ca^{2+}-channel activity, while FWHM is more indicative of the action of Ca^{2+}-pumps and transporters. A genetic and pharmacological dissection of the exact elements of the Ca^{2+}-signalling machinery involved in the different aspects of the Ca^{2+}-signature will allow even more information to be gained from changes in Ca^{2+}-signatures.

In this study Ca^{2+}-signatures have been analysed with a high degree of quantitation. However, there are some important limitations in the current method. Firstly, the repeated protocol needed to measure a number of experimental replicates simultaneously, results in a resolution equal to the time between each measurement of a given replicate (the cycle time). In the case of the data presented here, the cycle time was 11.6 s. This must be taken into account when drawing conclusions from the quantitative data. Rise time, especially, often had a S.D. of zero, as the maximum amplitude was always reached by the second measurement after the stimulus. However, given a cycle time of 11.6 s, a rise time of 2 $\pm$ 0.0 s (mean $\pm$ S.D. n=6) is not necessarily different from a rise time of 10 $\pm$ 0.0 s (mean $\pm$ S.D. n=6). For this reason, I have limited the conclusions drawn from rise time data. FWHM and amplitude are less susceptible to this type of problem, although if the maximum amplitude occurs between measurement points it will not be observed. These problems can be avoided by using a continuous measurement protocol. However, it is then much more time consuming to perform a number of replicates and the data set will be proportionately smaller. The current method is therefore useful for the identification of interesting results, high throughput screening, and for drawing general conclusions, while a continuous protocol might be used to repeat certain experiments at a higher temporal resolution. My software will analyse results from both types of experiment. Secondly, the description of a $[Ca^{2+}]_c$ transient using three quantitative parameters is clearly a simplified picture of reality. FWHM, is best suited to data that exhibits

a Gaussian distribution. Future development of the software written here should involve the mathematical description of regions of Ca^{2+}-signature. The program could then do curve fitting based on how well each signature fits the equations that describes it, providing a less digital analysis of the Ca^{2+}-signature.

Based on, amongst other things: (1) hypersensitivity to calcineurin inhibitors FK506 and cyclosporin A (CsA); (2) the fact that 50-500 mM exogenously added Ca^{2+} corrected the mutant phenotype to an essentially wild-type appearance (Dicker and Turian, 1990); and (3) the presence of presumptive transmembrane domains, Bok et al. (2001) suggested that the SPRAY protein is an internal membrane protein that regulates Ca^{2+}-transport across organellar membranes and this is mediated by calcineurin. Here it has been shown that Ca^{2+}-signatures in *spray* had significantly reduced amplitudes and rise times compared to those of the wild-type after 18 h growth at 24°C in liquid medium. These results were not due to reduced biomass or immaturity of *spray* colonies compared to the wild-type controls as amplitudes in *spray* colonies were found to change very little in 10 to 22 h old colonies. The differences in amplitudes observed are therefore likely to represent a real difference in the composition or behaviour of the Ca^{2+}-signalling machinery present in the *spray* mutant. These data support the idea that Ca^{2+}-signalling is perturbed in the *spray* mutant, but point toward *spray* having decreased Ca^{2+}-channel activity rather than decreased Ca^{2+}-transporter activity as rise time and amplitude are the most affected elements of the *spray* Ca^{2+}-signature. If active transport of Ca^{2+} into internal organelles were perturbed, one would expect to see the time for Ca^{2+} concentration to return to resting levels increase significantly, as observed in CPA-treated wild-type colonies (CPA inhibits Ca^{2+}-ATPase activity). This increase in recovery time would be reflected in a much longer FWHM, which was not observed in *spray* Ca^{2+}-signatures.

Ca^{2+}-signatures in wild-type colonies grown in medium amended with 124 nM FK506 showed a reduction in amplitudes in response to all stimuli tested. Medium amendment with 0.25% sorbose caused reduced amplitudes in response

to high external Ca^{2+}. These results suggest that Ca^{2+}-signalling is abnormal in both FK506-treated and, to a lesser extent, sorbose-treated wild-type *N. crassa* colonies. Ca^{2+}-signatures in wild-type colonies given a 10 min pretreatment with 248 nM FK506 or 250 nM CsA, however, showed no observable differences in Ca^{2+}-signatures compared to untreated controls. The effect of calcineurin on Ca^{2+}-signatures is therefore a result of long-term exposure and could be indirect. These results suggest that calcineurin does not play an important role in the generation or kinetics of $[Ca^{2+}]_c$ transients in *N. crassa* in response to the stimuli tested. Furthermore, it is unlikely that the SPRAY protein influences Ca^{2+}-signalling through the regulation of calcineurin activity as short-term exposure of wild-type colonies to high concentrations of FK506 and CsA did not result in Ca^{2+}-signatures similar to *spray*, while long-term exposure to FK506 had a much less potent effect on Ca^{2+}-signalling than the *spray* mutation.

Treatment of wild-type colonies with CPA caused a massive increase in resting $[Ca^{2+}]_c$ concentrations and also significantly increased the FWHM of Ca^{2+}-signatures in response to all stimuli tested. These results indicate that CPA inhibits Ca^{2+}-ATPases that fill internal Ca^{2+} stores in *N. crassa*, as it does in animal and plant cells (Seidler et al., 1989; Okorokov et al., 1997; Liang and Sze, 1998). CPA had previously been shown to radically reduce *N. crassa* hyphal extension within two minutes upon addition to liquid cultures at concentrations of 10 to 100 μM and to cause multiple subapical branching (Silverman-Gavrila and Lew, 2001). However, until now its effect on Ca^{2+}-signatures in *N. crassa* had not been analysed, although it has been found to increase $[Ca^{2+}]_c$ concentrations in *A. awamori* (Kozlova-Zwinderman, 2002; Nelson et al., 2003). These experiments with CPA clearly illustrate the probable role of Ca^{2+}-ATPases in: (a) maintaining low resting $[Ca^{2+}]_c$ concentrations and (b) removing Ca^{2+} from the cytoplasm after $[Ca^{2+}]_c$ concentration has increased. The results also quantitatively show the specific changes in the Ca^{2+}-signature that results from Ca^{2+}-ATPase inhibition on $[Ca^{2+}]_c$ transients caused by the stimuli tested. Interestingly, although CPA

treated *N. crassa* cultures did show increased resting $[Ca^{2+}]_c$ concentrations and slower recovery from $[Ca^{2+}]_c$ transients, CPA pretreated colonies were able to recover their (elevated) resting $[Ca^{2+}]_c$ concentrations, after a stimulus-induced $[Ca^{2+}]_c$ transient, during the 600 s measurement time. This indicates that additional mechanisms other than the Ca^{2+}-ATPase(s) inhibited by CPA are able to remove Ca^{2+} from the cytoplasm.

The results shown in this chapter raise some questions regarding the effects of 2-APB in *N. crassa*. 2-APB is known to inhibit IP_3-induced Ca^{2+} release from internal Ca^{2+} stores in animal cells (Maruyama et al., 1997), and concentrations of 10 to 50 μM 2-APB have been shown to almost completely inhibit *N. crassa* hyphal extension in liquid medium within two minutes after addition, and to cause hyphal widening and apical hyperbranching (Silverman-Gavrila and Lew, 2001). More recently, the presence of two IP_3-activated CPCs was demonstrated in *N. crassa* membranes under voltage clamp conditions using the bilayer lipid membrane (BLM) technique (Silverman-Gavrila and Lew, 2002). The activity of these channels was inhibited by 25 μM 2-APB and this effect was correlated with the effect of 2-APB on hyphal growth and Ca^{2+} gradients (2-APB was found to dissipate the tip high Ca^{2+} gradient observed with chlortetracycline [CTC] and to increase Ca^{2+} fluorescence behind the tip). The effect of 25 μM 2-APB on *N. crassa* resting $[Ca^{2+}]_c$ concentrations and Ca^{2+}-signatures in response to external stimuli observed in this chapter does not indicate that 2-APB inhibits IP_3-activated CPCs. Conversely, 2-APB has an agonistic effect on $[Ca^{2+}]_c$ concentration, resulting in Ca^{2+} measurements similar to those from experiments using CPA (e.g. increased resting $[Ca^{2+}]_c$ concentrations and slower recovery from $[Ca^{2+}]_c$ transients). These results are more in line with the idea that 2-APB prevents Ca^{2+} from being removed from the cytosol, rather than preventing it from being released into the cytosol.

The Ca^{2+}-signalling machinery of *N. crassa* has a major difference to that of *A. awamori*. Caffeine causes the release of Ca^{2+} from internal Ca^{2+} stores in

diverse organisms (Komori et al., 1995; Bauer et al., 1999; Arora and Ohlan, 1997) and 5 mM caffeine was found to have a profound effect on both hyphal growth and $[Ca^{2+}]_c$ transients in *A. awamori* (Nelson et al., 2003; Kozlova-Zwinderman, 2002). Experiments in *N. crassa*, however, have shown that 1 mM caffeine had no effect on hyphal extension rate or morphology (Silverman-Gavrila and Lew, 2001). My data adds to these observations by showing that caffeine has almost no effect on $[Ca^{2+}]_c$ in *N. crassa*. Observable effects were only attained at concentrations of 25 mM caffeine (a near saturated caffeine solution) and these were still very minor compared to results using 6 mM caffeine with *A. awamori* (Nelson et al., 2003), which results in a 70% increase in $[Ca^{2+}]_c$ concentration over the control as opposed to a 10% increase observed for *N. crassa* with 25 mM caffeine. These results demonstrate the danger of extrapolating observations across species.

Examination of Ca^{2+}-signatures in *cot-1* colonies at permissive and restrictive temperatures shows a correlation between induction of the mutant phenotype, and altered Ca^{2+}-signalling. Co-imunoprecipitation experiments by Gorovits *et al.* (1999) suggested a physical interaction between COT1 kinase and the catalytic subunit of calcineurin (Gorovits et al., 1999). However based on the results shown in this chapter using calcineurin inhibitors, the changes in Ca^{2+}-signatures observed in *cot-1* are unlikely to be mediated via calcineurin. The mechanism by which impaired COT1 function alters the Ca^{2+}-signature remains to be determined.

Resting $[Ca^{2+}]_c$ concentrations were measured in two different hyperbranching mutants of *N. crassa* and in wild-type colonies exposed to two different branch-inducing treatments (a total of four different means of inducing hyperbranching). Resting $[Ca^{2+}]_c$ concentrations were only higher than the untreated wild-type controls in one of the four cases (e.g. long-term treatment with FK506) despite the large differences in hyphal extension rate and branching frequency observed in every case. FK506 inhibits calcineurin activity and therefore affects an important part of the fungal Ca^{2+}-signalling machinery. It could be that the small increase

resting $[Ca^{2+}]_c$ observed was an attempt, by the fungus, to overcome the reduction in calcineurin activity resulting from the FK506 treatment. If tip growth or hyphal branching in *N. crassa* was positively regulated by $[Ca^{2+}]_c$ signalling, it is unlikely that all the other methods of reducing hyphal extension rate and causing hyperbranching would have failed to increase resting $[Ca^{2+}]_c$ concentrations. In addition to this it was shown that no change in resting $[Ca^{2+}]_c$ concentrations accompanied either the cessation of hyphal elongation and the induction of hyperbranching or the return to normal hyphal elongation and branching in *cot-1*. Together these results suggest that one branch induction event in *N. crassa* is not the result of one $[Ca^{2+}]_c$ transient, because if this were true increasing branching frequency would necessitate an increase in the frequency of these $[Ca^{2+}]_c$ transients, which would result in a higher resting $[Ca^{2+}]_c$ concentration. In fact, slightly lower $[Ca^{2+}]_c$ concentrations were observed in both *spray* colonies and in *cot-1* colonies at the restrictive (but not the permissive) temperature. The negative regulation of hyphal branch induction by $[Ca^{2+}]_c$ transients is unlikely (but cannot be ruled out by these data), as this would require the presence of $[Ca^{2+}]_c$ transients to prevent branch induction. The result would be a lower resting $[Ca^{2+}]_c$ concentration - observed in *spray* and *cot-1* at the restrictive temperature, but not in sorbose or FK506 treated colonies. Finally, these data cannot rule out the possibility that information encoded in hypothetical branch-inducing $[Ca^{2+}]_c$ transients, rather than the frequency or magnitude of the transients controls the frequency of branch induction.

4.4 Summary

- Aequorin luminescence in transformed *N. crassa*, and in protein extracted from transformed *N. crassa*, is reduced with increased ambient temperature. However once converted into Ca^{2+} concentrations, data gathered at different temperatures can be compared.

- A computer program was written that enabled large amounts of data from the luminometer to be rapidly and accurately converted into Ca^{2+} concentrations and performed a range of quantitative analyses on the converted data.
- Unique, reproducible and characteristic Ca^{2+}-signatures resulted from stimulation of *N. crassa* colonies under a range of environmental conditions.
- The Ca^{2+}-signature provided an indicator of what components of the Ca^{2+}-signalling machinery were affected by different environmental stimuli, mutations or pharmacological treatments.
- The SPRAY is unlikely to influence Ca^{2+}-signalling through calcineurin.
- CPA inhibits Ca^{2+}-ATPases in *N. crassa* as in other fungi, plants and animals.
- *N. crassa* does not possess caffeine-sensitive Ca^{2+} stores with similar properties to plants, animals and *A. awamori.*
- 2-APB has an unexpected agonistic effect on $[Ca^{2+}]_c$ signalling in *N. crassa.*
- Increased $[Ca^{2+}]_c$ concentration does not accompany hyperbranching in *N. crassa.*

Chapter 5

Characterisation of *Neurospora* Hyperbranching Mutants

5.1 Introduction

Many papers have been published over the past few years that cover the topics of hyperbranching or increased branching frequency in *N. crassa* (Sone and Griffiths, 1999; Bok et al., 2001; Watters et al., 2000; Propheta et al., 2001; Lauter et al., 1998; Bowman et al., 2000; Prokisch et al., 1997). Indeed, *N. crassa* mutants are often named on the basis of their morphological phenotypes. Some examples are: *cot-1* through to *cot-5* (*cot* referring to their 'colonial temperature sensitive' phenotype), *frost*, *spray* and *snowflake* (Perkins et al., 1982). Despite the diversity of branching mutants and their equally diverse genetic causes, it is rare that their phenotypic diversity is appreciated. Changes in branching frequency and morphology are mostly referred to in general terms such as 'hyperbranching' or 'colonial morphology'. In some cases the names of mutants imply major similarities. For example, classical genetics has mapped all the *cot* genes to different chromosomal locations and in the case of *cot-1*, *cot-3* and *cot-5* sequencing of the mutant genes have shown them to be completely unrelated (Yarden et al., 1992; Propheta et al., 2001; Resheat-Eini et al., 2003).

Until now, papers discussing hyperbranching mutants in *N. crassa* have focused primarily on aspects other than the phenotypes of the strains examined. Advances in microscopy and the availability of specific vital dyes and reporter genes now enable examination of these phenotypes at a resolution that was not previously possible.

The evidence for the regulation of hyphal branching by Ca^{2+} was outlined in Section 1.5 and the relationship between $[Ca^{2+}]_c$, tip growth and hyphal branching in *N. crassa* was investigated experimentally in Chapter 4. Although a large number of *N. crassa* hyperbranching mutants have been isolated many have not yet been genetically characterised.

The aims of the work carried out in this chapter were: (1) to highlight some of the subtle phenotypic differences between several hyperbranching strains of *N. crassa* (described in Table 1.1) and (2) to determine whether the *cot-2* and *cot-4* mutants have mutations in Ca^{2+}-signalling related genes.

5.2 Results

5.2.1 Phenotypic characterisation of hyperbranching mutants

5.2.1.1 Qualitative characterisation of hyperbranching mutants

Confocal and light microscopy were used to characterise wild-type and mutant strains of *N. crassa*. In general, wild-type hyphae had a consistent width, a uniform distance between branches (which were mostly of a lateral nature), and branch angles of $\sim 70°$ relative to the main hyphae (Fig. 5.1 a and b). The wild-type colony periphery was quite uniform. The mature regions of the colony, although still uniform, showed different characteristics including adventitious hyphae and hyphal fusion, which were not observed in the colony periphery (Fig.

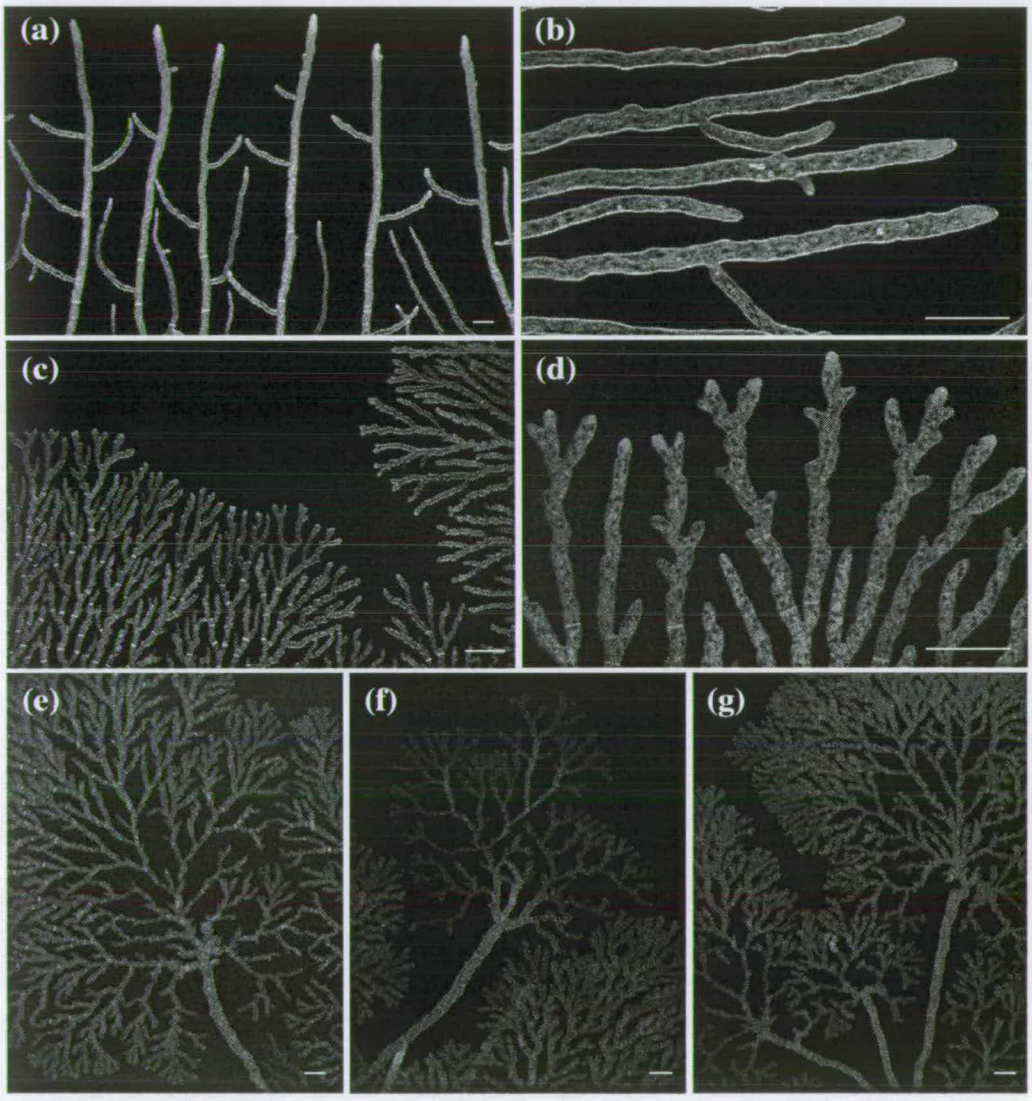

Figure 5.1: Morphology of wild-type [(a) and (b)] and hyperbranching [(c) and (d) *spray*; (e), (f) and (g) *frost*] strains of *N. crassa* grown on solid VgS at 34°C. Fungi were stained with FM4-64 and imaged using a confocal microscope. Bars are 50 μm.

5.2) or in any part of the colonies of the hyperbranching strains (except *cot-1* at the permissive temperature).

Figure 5.2: A mature region of wild-type mycelia grown at 34°C showing main and adventitious hyphae. Bar = 50 μM.

The hyphae of *spray* (Fig. 5.1 c and d), *frost* (Fig. 5.1 e, f and g), *pvn1*, *pvn2*, *cot-1* at the restrictive temperature (Fig. 5.3 b), *cot-4* (Fig. 5.3 h and i) and *cot-5* (Fig. 5.3 j and k) (at both permissive and restrictive temperatures) were small, thin and uneven in width relative to the wild-type. Both *spray* and *frost* showed purely dichotomous branching, a form of branching almost non-existent in the wild-type, *cot-5* showed a mixture of dichotomous and lateral branching, whereas *pvn1* showed mostly lateral branching but at a very high frequency with many small ($\sim$ 25 μm) aborted branches. The phenotype of *pvn2* was comparable to *pvn1* but less extreme (as indicated by the quantitative data in Figs. 5.5 to 5.8). Aborted branches were also seen in *spray* and *frost*, however unlike the *pvn* mutants, these were normally no longer than the width of the hyphae. Branch angles in all hyperbranching strains except the *cot* strains were similar to the wild-type. Of the *cot* strains *cot-1* (at the restrictive temperature only), *cot-3* and *cot-4* (at both temperatures) had branch angles of near 90° (*cot-2* and *cot-5* had wild-type like branch angles of $\sim$ 70°). At the restrictive temperature *cot-1* and *cot-2* showed swollen hyphae but *cot-5* had swollen hyphae at both

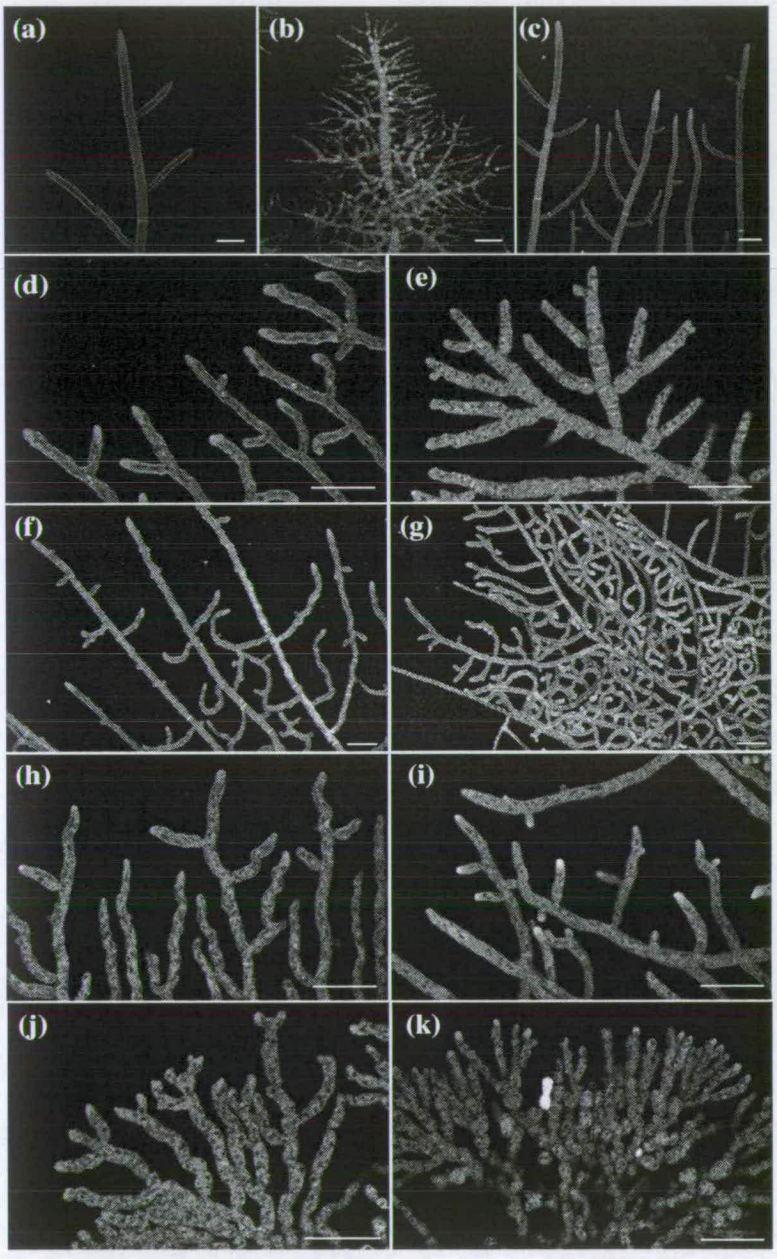

Figure 5.3: Morphology of wild-type and colonial temperature-sensitive strains of *N. crassa* at permissive (24°C) and restrictive (37°C) temperatures. Fungi were stained with FM4-64 and imaged using a confocal microscope: (a) *cot-1* grown at 24°C; (b) *cot-1*, 37°C; (c) wild-type, 37°C; (d) *cot-2*, 24°C; (e) *cot-2*, 37°C; (f) *cot-3*, 24°C; (g) *cot-3*, 37°C; (h) *cot-4*, 24°C; (i) *cot-4*, 37°C; (j) *cot-5*, 24°C; (k) *cot-5*, 37°C. Bars are 50 μm.

temperatures. The hyphae of *cot-3* had a tendency to curl and this tendency was exaggerated to the extreme at the restrictive temperature. Finally, while most of the strains examined had an overall growth pattern similar (but proportionately more branched) to the wild-type (e.g. an even density of hyphae increasing towards the more mature regions of the colony), *frost* and to a lesser extent *cot-5* (at both temperatures) grew as a very dense mat of hyphae, from which individual hyphae would escape unbranched to start a 'new' profusely hyperbranched phase. Over time the main colony caught up with and enveloped these subcolonies.

The distribution of nuclei in wild-type, *cot-1* and *spray* was investigated in ethanol fixed cells using propidium iodide. Wild-type, *cot-1* (Fig. 5.4 a) and *spray* were found to have an even distribution of nuclei within their hyphae at 24°C (although nuclei were not present at the very tips of the hyphae). At 37°C (the restrictive temperature for *cot-1*) the distribution of nuclei in wild-type and *spray* were unaffected. However, in *cot-1* the nuclei were found to be entirely absent from the middle of the hyphae. Figure 5.4 b and d show the top and bottom optical sections of a *cot-1* hypha at restrictive temperature. Fig. 5.4 c shows the middle section. This distribution of nuclei can not be easily observed using conventional widefield fluorescence microscopy because of its lack of optical sectioning capability.

5.2.1.2 Quantitative characterisation of hyperbranching mutants

Detailed quantitative characterisation was done on wild-type, *cot-1*, *frost*, *spray*, *pvn1* and *pvn2* strains of *N. crassa*. The methods used are described in Section 2.6.2 and are based on techniques developed by Trinci and others in the 1970's (Trinci, 1973a,b; Trinci and Collinge, 1973; Trinci, 1974), however here the fungi were grown between two sheets of cellophane to force 2-dimensional growth. Under these conditions wild-type and *cot-1* had almost identical hyphal extension rates when grown at 24°C (2.02 ± 0.25 and 2.05 ± 0.19 m h^{-1}, respectively [mean $\pm$ S.D. n=10]). At the restrictive temperature, however, *cot-1* had an hyphal

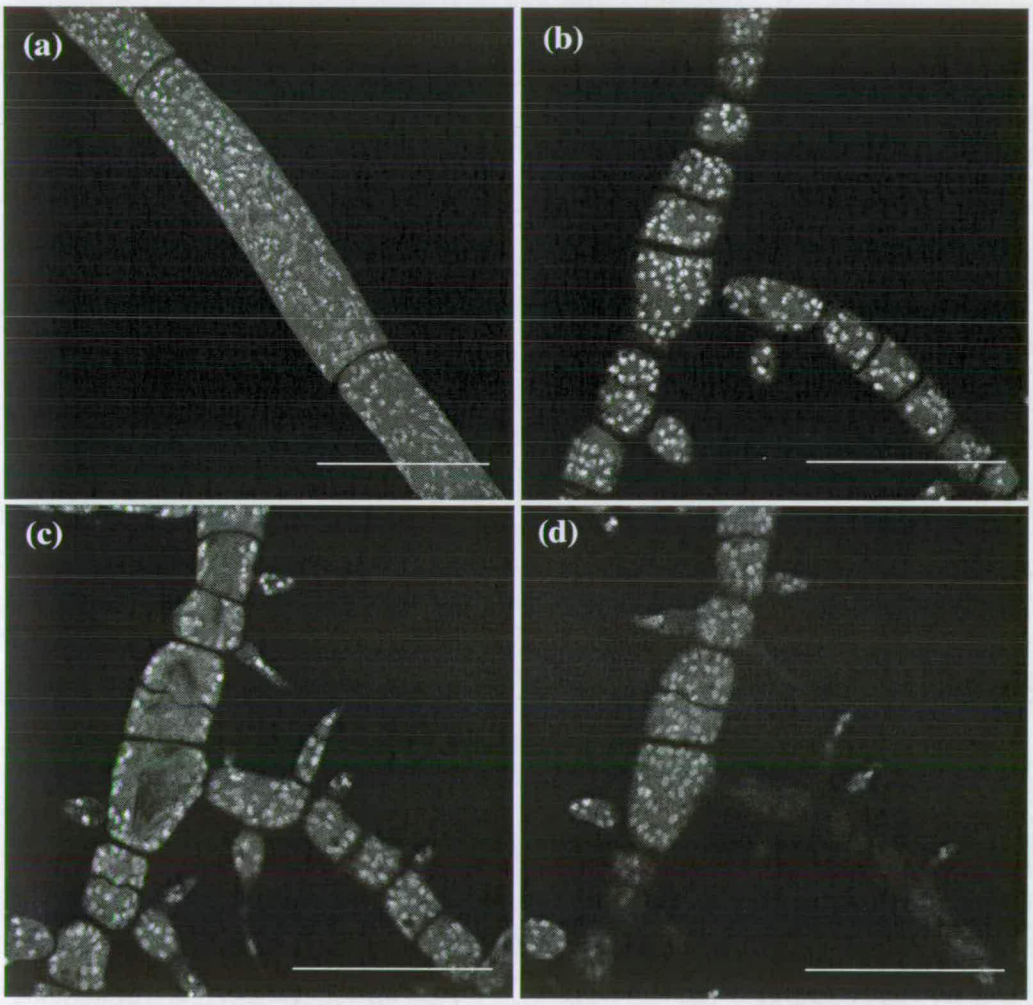

Figure 5.4: Nuclear morphology of *cot-1* at permissive (24°C) (a) and restrictive (37°C) (b), (c) and (d) temperatures. Images (b), (c) and (d) are the top, middle and bottom sections, respectively, of a series of optical sections through the same hyphae. Fungi were fixed in ethanol, stained with propidium iodide and imaged using a confocal microscope. Bars are 50 μm.

extension rate of just 0.13 ± 0.03 mm h^{-1} compared to the wild-type hyphal extension rate of 3.18 ± 0.28 mm h^{-1} (see Fig. 5.5). The other hyperbranching

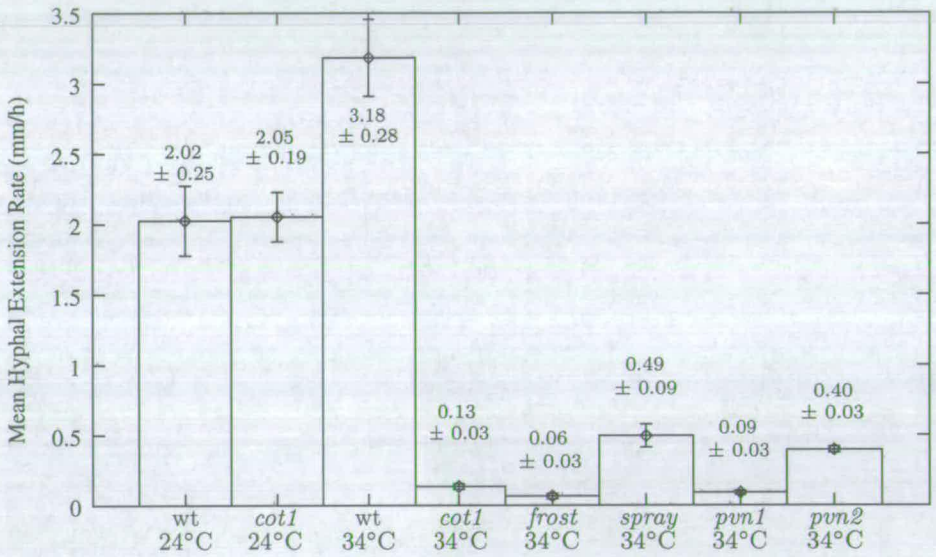

Figure 5.5: Hyphal extension rate of wild-type plus several hyperbranching strains of *N. crassa* on solid medium between two sheets of cellophane. Lines are means of 10 replicates ± S.D. (except *frost* where n=8).

strains examined all had significantly reduced hyphal extension rates compared to those of the wild-type (see Fig. 5.5). The hyphal width of wild-type grown at 24 and 34°C was not significantly different to *cot-1* grown at 24°C (16.6 ± 3.2 and 16.0 ± 3.2 versus 13.8 ± 2.4, respectively [mean ± S.D. n=100]) (see Fig. 5.6). When grown at the restrictive temperature, however, *cot-1* showed very narrow hyphae compared to the wild-type (7.8 ± 2.0 vs 16.0 ± 3.2, respectively [mean ± S.D. n=100]). The other hyperbranching strains also had narrow hyphae, similar in width to *cot-1* at the restrictive temperature. The distance between septa in *cot-1* grown at the permissive temperature was similar (81.3 ± 25 [mean ± S.D. n=100]) to the wild-type grown at both 24°C (105 ± 41 μm [mean ± S.D. n=100]) and 34 °C (89.2 ± 33 μm [mean ± S.D. n=100]) (see Fig. 5.7). At the restrictive temperature, however, the distance between septa in *cot-1* was much smaller (24.1 ± 5.6 vs the wild-type value of 89.2 ± 33 μm [mean ± S.D. n=100]). The distance

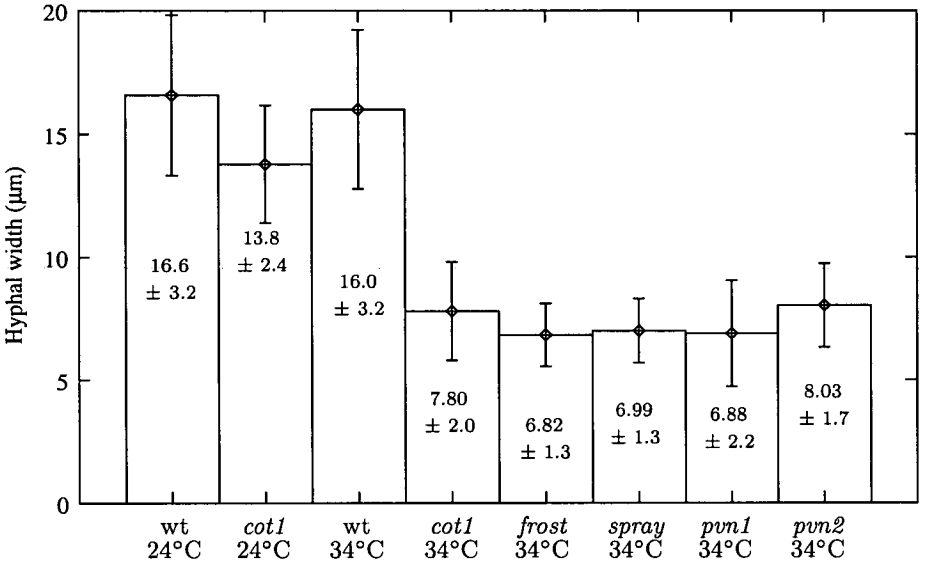

Figure 5.6: Hyphal width of wild-type plus several hyperbranching strains of *N. crassa* on solid medium between two sheets of cellophane. Lines are means of 100 replicates ± S.D.

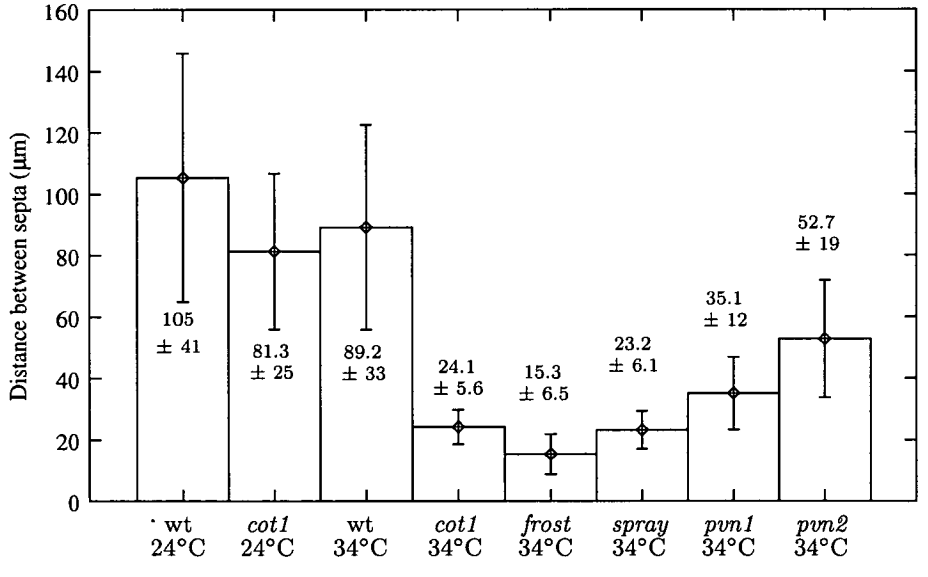

Figure 5.7: Distance between septa of wild-type plus several hyperbranching strains of *N. crassa* on solid medium between two sheets of cellophane. Lines are means of 100 replicates ± S.D.

between septa of the other hyperbranching strains varied quite widely, but were all less than the wild-type. There was no correlation between hyphal extension rate and distance between septa in the the strains analysed (Figs. 5.7 and 5.5). The hyphal growth unit (HGU) was largest for the non-hyperbranching strains (wild-type and *cot-1* at the permissive temperature). All the hyperbranching strains had similar sized hyphal growth units and all were $\sim$ 80% smaller than the wild-type (see Fig. 5.8).

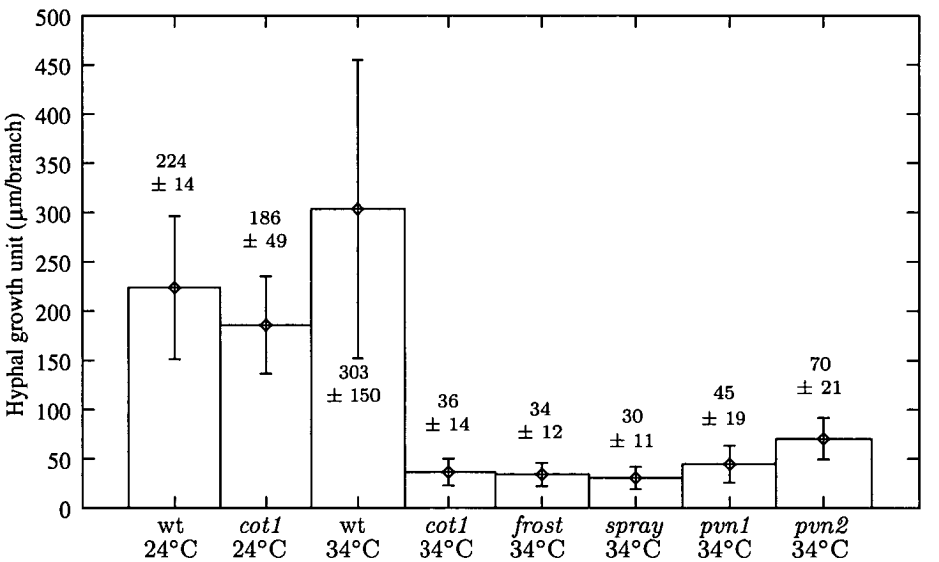

Figure 5.8: Hyphal growth unit of wild-type plus several hyperbranching strains of *N. crassa* on solid medium between two sheets of cellophane. Lines are means of 25 replicates ± S.D.

The hyphal extension rates of the *N. crassa* colonial temperature sensitive mutants (*cot-1*, *cot-2*, *cot-3*, *cot-4* and *cot-5*) were measured on standard solid VgS medium at permissive and restrictive temperatures (see Fig. 5.9). All the *cot* mutants showed reduced hyphal extension rates at restrictive vs permissive temperatures. However only *cot-1* and *cot-3* showed hyphal extension rates close to that of the wild-type at permissive temperatures.

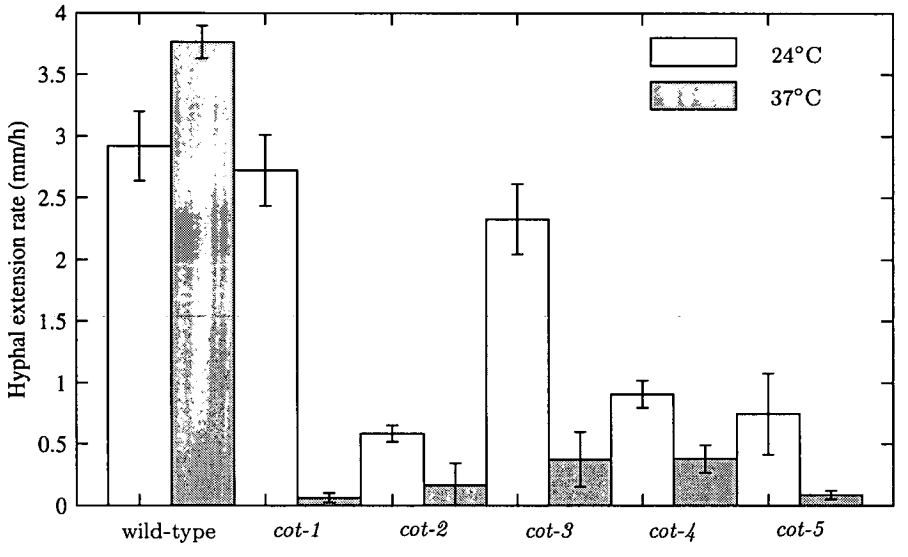

Figure 5.9: Hyphal extension rate of wild-type plus the colonial temperature sensitive *N. crassa* mutants of *N. crassa* on solid medium. Lines are means of 5 replicates ± S.D.

5.3 Genotypic Characterisation of *cot-2* and *cot-4*

Apart from *cot-2* and *cot-4*, all the mutants described in Section 5.2.1 have mutations in single cloned genes. Classical genetics has shown that both *cot-2* and *cot-4* have mutations in single, but different, genes in linkage group V (Perkins et al., 1982). Until now, however, these genes have remained unknown. In order to determine whether the *cot-2* or *cot-4* strains had mutations in genes involved in Ca^{2+}-signalling I attempted to clone these genes by complementation. Complementation was carried out as previously described by Propheta et al. (2001) (also see Section 2.4).

The Orbach/Sachs pMOcosX library cosmids G23:G5 and X15:E10 were found to complement *cot-2* and *cot-4*, respectively. Mutants transformed with their respective cosmids gave rise to hygromycin-resistant colonies that displayed wild-type phenotypes at permissive and restrictive temperatures and were therefore regarded as *cot-2*$^+$ and *cot-4*$^+$.

T3 and T7 primers were used to sequence each end of the genomic DNA in both cosmids. The resulting sequences were compared to the entire *N. crassa* genome sequence (http://www-genome.wi.mit.edu/annotation/fungi/neurospora) using the BLASTN algorithm. Four 100% matches, one for each sequence submitted, were obtained thus pinpointing the beginning an end of each cosmid's genomic DNA insertion to a location in the *N. crassa* genome sequence. This information was used to predict[1] the remaining sequence in each cosmid. The T3 and T7 ends of Cosmid G23:G5 matched *N. crassa* contig 3.219 bp 57473-57981 and bp 93193-93648, respectively. The DNA complementary to *cot-2* is therefore likely to reside within the 36175 bp fragment in contig 3.219 bp 57473-93648; the T3 and T7 ends of cosmid X15:E10 matched contig 3.203 bp 27026-27637 and bp 71493-72195, respectively. The DNA complementary to *cot-4* is therefore likely to reside within the 45169 bp fragment in contig 3.203 bp 27026-72195. DNA sequences corresponding to these regions were retrieved from the *N. crassa* genome database and blasted against the the GenBank, EMBL, DDBJ and PDB databases using NCBI's BLAST facility (http://www.ncbi.nlm.nih.gov/BLAST) in order to determine which regions of these cosmids were homologues to known genes. Furthermore, the hypothetical proteins corresponding to these regions were obtained from the *N. crassa* genome database and examined.

The DNA for G23:G5 matched hypothetical proteins NCU04189.1 to NCU04200.1. Amongst these were no proteins related to Ca^{2+}-signalling on the bases of sequence homology to other known proteins.

The DNA thought to be contained in cosmid X15:E10 matched hypothetical proteins NCU03794.1 to NCU03810.1. Of the proteins that could be assigned a preliminary function based on homology to other known proteins one, NCU03804.1, was a E=0 hit against the *N.crassa* calmodulin-dependent protein phosphatase mRNA, catalytic subunit of calcineurin (Higuchi et al.). Due to

[1]The method used to make the pMOcosX library (Orbach, 1994) does not preclude a number of unrelated fragments being ligated into the same cosmid. However, the possibility is not high.

the presence of a Ca^{2+}-signalling related gene in this cosmid, and the absence of such a gene in the other, it was decided to focus further efforts on the *cot-4* complementary cosmid X15:E10.

Separate digests of X15:E10 were made using several restriction enzymes. Part of each digest was run on an agarose gel (Fig. 5.10) and part was mixed with a plasmid bearing a hygromycin resistance cassette (pAZ6) and used to co-transform *cot-4* protoplasts. Based on complementation resulting from transformation with

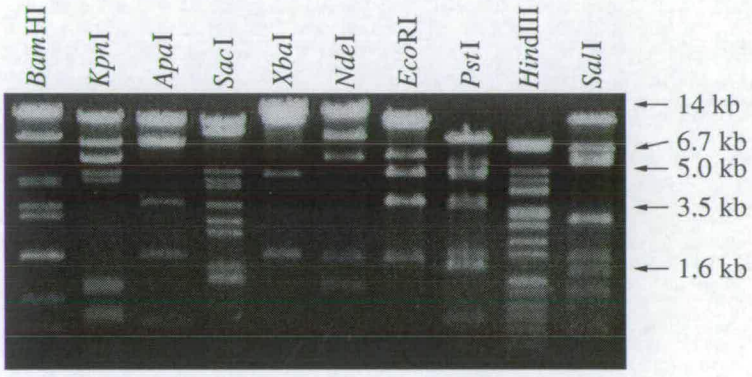

Figure 5.10: Agarose gel showing various digests of the X15:E10 cosmid.

cosmid digests it was determined that *Bam*HI, *Apa*I, *Xba*I, *Nde*I and *Sal*I did not cut within the complementary gene contained cosmid X15:E10. Further experiments revealed that a X15:E10/*Apa*I band of $\sim$ 8 kb was sufficient to complement *cot-4*. This band was ligated into the Bluescript cloning vector (GenBank X52331) and sequenced using M13-20 and SK primers. The resulting sequence data was blasted against the *N. crassa* genome database and matched contig 3.203 bp 60907-61809 and 53099-53751, respectively, giving an overall probable sequence of 53099-61809, a total of 8710 bp, and in good agreement with the $\sim$ 8 kb fragment ligated into Bluescript. This 8.7 kb complementary fragment was found to contain three hypothetical *N. crassa* open reading frames (ORFs): NCU03803.1, NCU03804.1 and NCU03805.1. Based on restriction maps of these ORFs and data from transformation with various cosmid digests it appeared likely that the DNA encoding NCU03804.1 was in fact the *cot-4* gene. This

was confirmed by successful complementation using a *Bam*HI/*Apa*I generated 4.2 kb band cut from the Bluescript cloning vector containing my 8.7 kb fragment. This band contained only *N. crassa* contig 3.203 bp 55355-59536. The only hypothetical ORF in this region of DNA was NCU03804.1.

Genomic DNA was extracted from *cot-4* and primers were designed (1L: 5'-CAG CTT TGG AGG AGA AGT GG-3'; 1R: 5'-CCA AGA AAT GAC AAG CAG CA-3'; 2L: 5'-ACC CGG TGA CTT TTA TGC AG-3'; and 2R: 5'-TTG GCG AGC TAT TCG ATC TT-3') in order to amplify the mutant gene plus flanking regions (see Fig. 5.11). PCR

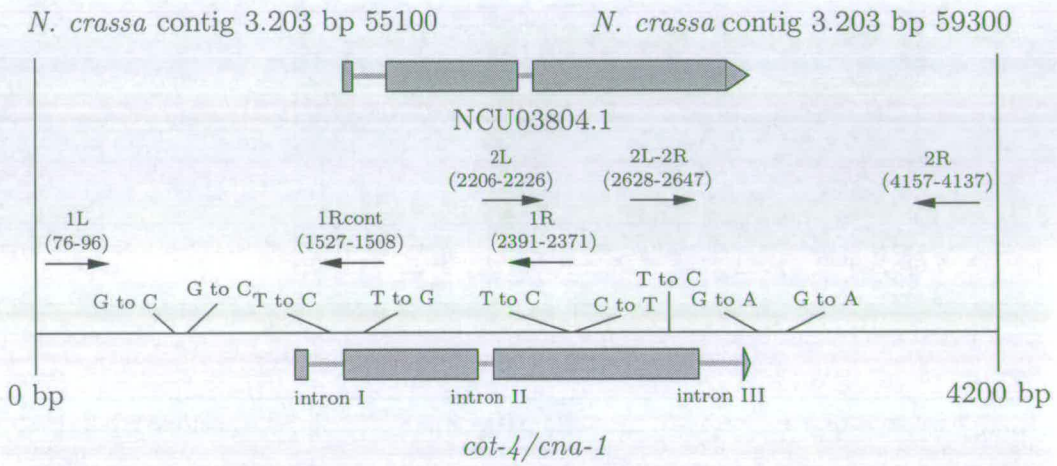

Figure 5.11: *N. crassa* contig 3.203 bp 55100-59300 with the hypothetical ORF NCU03804.1 and the *cot-4/cna-1* proteins marked. Primers used in PCR reactions and potential mutations in the *cot-4* gene are also indicated. Figure is to scale except for length of primer arrows, which start in correct location but are longer than in reality.

products of 2315 and 1905 bp were obtained using primers 1L plus 1R and 2L plus 2R, respectively. Both fragments obtained were sent for direct sequencing with their respective primers. The resulting sequences covered the entire 4081 bp region. The *N. crassa* genomic DNA sequence for that region (contig 3.203 bp 55176-59257) and the published sequence for *cna-1* mRNA (GenBank accession number M73032 (Higuchi et al.)) were in good agreement. Three introns were found in the genomic DNA sequence. Intron I was from 1203-1365; intron II was from 1950-2025 and intron III was from 2940-3115. The coding sequence was from

1157-3121. A comparison of the published sequence data with my own sequence data revealed a number of potential mutations. Two more primers were therefore designed (1Rcont: 5'-AGC TTG GTA CCC TCC CTG AT-3'; and 2L-2R: 5'-CCT TGC TAT CGG TCG TCT GT-3') in order to resequence some ambiguous regions (see Fig. 5.11). The final differences observed between my sequence data, the *N. crassa* genome sequence and the published sequence for the wild-type *cna-1* mRNA are recorded in (Table 5.1).

Table 5.1: Potential mutations in *cot-4* (*cna-1*) and their effects on the translated amino acid sequence.

Location*	Mutation	Effect on amino acid sequence	Comments
620	G to C	n/a	537 bp upstream of ATG
663	G to C	n/a	494 bp upstream of ATG
1302	T to C	n/a	in intron I
1452	T to G	L to W (TGG)	in coding region
2364	T to C	no change of codon	in coding region
2373	C to T	no change of codon	in coding region
2787	T to C	no change of codon	in coding region
3172	G to A	n/a	54 bp downstream of TAA
3286	G to A	n/a	168 bp downstream of TAA

* Location 0 corresponds to *N. crassa* contig 3.203 bp 55100.

To test the effect of the *cot-4* mutation on the sensitivity of *cot-4* colonies to calcineurin inhibitors, *cot-4* colonies were grown at the permissive temperature on FK506 and cyclosporin A amended solid VgS medium. *cot-4* was hypersensitive to both FK506 and cyclosporin A, relative to the wild-type, but not to hygromycin B, a general protein synthesis inhibitor (see Fig. 5.1).

5.4 Discussion

In this chapter the phenotypes of ten strains of *N. crassa* (the wild-type and 9 hyperbranching mutants) were compared. General similarities between the hyperbranching strains included significantly reduced hyphal extension rates,

1157-3121. A comparison of the published sequence data with my own sequence data revealed a number of potential mutations. Two more primers were therefore designed (1Rcont: 5'-AGC TTG GTA CCC TCC CTG AT-3'; and 2L-2R: 5'-CCT TGC TAT CGG TCG TCT GT-3') in order to resequence some ambiguous regions (see Fig. 5.11). The final differences observed between my sequence data, the *N. crassa* genome sequence and the published sequence for the wild-type *cna-1* mRNA are recorded in (Table 5.1).

Table 5.1: Potential mutations in *cot-4* (*cna-1*) and their effects on the translated amino acid sequence.

Location*	Mutation	Effect on amino acid sequence	Comments
620	G to C	n/a	537 bp upstream of ATG
663	G to C	n/a	494 bp upstream of ATG
1302	T to C	n/a	in intron I
1452	T to G	L to W (TGG)	in coding region
2364	T to C	no change of codon	in coding region
2373	C to T	no change of codon	in coding region
2787	T to C	no change of codon	in coding region
3172	G to A	n/a	54 bp downstream of TAA
3286	G to A	n/a	168 bp downstream of TAA

* Location 0 corresponds to *N. crassa* contig 3.203 bp 55100.

To test the effect of the *cot-4* mutation on the sensitivity of *cot-4* colonies to calcineurin inhibitors, *cot-4* colonies were grown at the permissive temperature on FK506 and cyclosporin A amended solid VgS medium. *cot-4* was hypersensitive to both FK506 and cyclosporin A, relative to the wild-type, but not to hygromycin B, a general protein synthesis inhibitor (see Fig. 5.1).

5.4 Discussion

In this chapter the phenotypes of ten strains of *N. crassa* (the wild-type and 9 hyperbranching mutants) were compared. General similarities between the hyperbranching strains included significantly reduced hyphal extension rates,

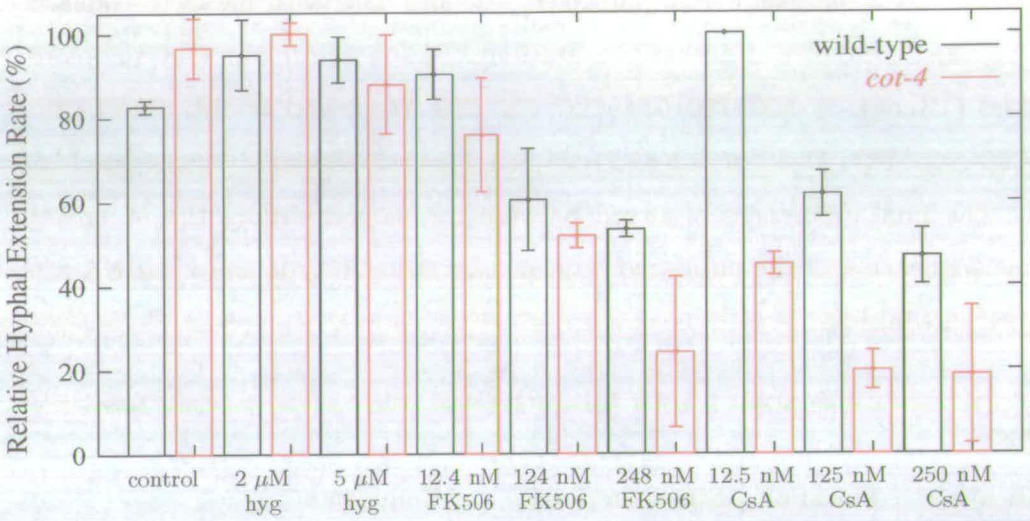

Figure 5.12: The effect of two calcineurin inhibitors, FK506 and cyclosporin A, on the hyphal extension rate of wild-type and *cot-4* colonies grown on solid medium at 24°C. Hygromycin B (hyg), a general protein synthesis inhibitor, was used as a control. Boxes are means ± S.D. of 6 replicates.

narrower hyphae with less distance between septa and reduced hyphal growth unit (e.g. more branches per unit length of hyphae). Of the quantitative parameters measured, distance between septa and hyphal extension rate varied the most. Despite these general quantitative similarities the actual phenotypes of the different mutants varied considerably. This was ture on a gross morphological level (e.g. the curled hyphae of *cot-3*, the escaping hyphae and satellite colonies of *frost*, the aborted branches of *pvn1* and the swollen hyphae of *cot-1* at the restrictive temperature) and at a subcellular level (e.g. the different distribution of nuclei in *cot-1* at the restrictive temperature compared to *spray* and wild-type). One interesting similarity of all the hyperbranching strains examined, however, was an absence of adventitious hyphae in the mature regions of the colonies. The reason for this is unknown.

The colonial temperature sensitive (*cot*) mutants of *N. crassa* were found to have very different hyphal extension rates and morphologies at both permissive and restrictive temperatures. The only *cot* mutant to show wild-type like

morphology and hyphal extension rate at the permissive temperature was *cot-1*. All the other *cot* mutants had significantly reduced hyphal extension rates at both temperatures, although as their names suggest, their mutant phenotypes were less profound at the permissive temperature.

The phenotypic diversity observed in the strains examined is not surprising given the fact that each strain was subject to mutations in a different gene (with the exception of *pvn1* and *pvn2*, which were both *vma-1*-linked mutants [see Table 1.1]).

Of all the mutants examined, only *cot-2* and *cot-4* had not been cloned. Complementation of *cot-2* and *cot-4* was achieved with the Orbach/Sachs pMOcosX genomic DNA cosmids G23:G5 and X15:E10, respectively (Orbach, 1994). The *cot-2* complementary cosmid contained a number of potential genes. However, none were thought to be related to Ca^{2+}-signalling and therefore the exact complementary gene was not identified. The gene for which *cot-4* is mutant was found to be *cna-1*, the catalytic subunit of calcineurin, a Ca^{2+}/calmodulin-dependent protein phosphatase (Higuchi et al.). The mutant gene was amplified from *cot-4* genomic DNA by PCR and a number of mutations identified, four of which were in the coding region but only one of which resulted in a change of codon (leucine to tryptophan). The number of differences between the wild-type DNA sequence (as derived from two independent published sources (Higuchi et al.; Galagan et al., 2003)) and the *cot-4* DNA sequence, however, was higher than expected (9 mutations were found in just 4081 bp). It is thought that several of these potential mutations were due to errors during the PCR amplification of the native *cot-4* gene, rather than bona fide mutations, and thus require further analysis.

cot-4 colonies were hypersensitive to the calcineurin inhibitors FK506 and cyclosporin A. These results further support the cloning results which indicate that the *cot-4* mutation is in the catalytic subunit of calcineurin.

5.5 Summary

- Nine genetically-unlinked hyperbranching strains of *N. crassa* were examined. These strains demonstrated differences in hyphal form, branching frequency, hyphal extension rate, hyphal width and distance between septa.
- The *cot-2* strain can be complemented with the Orbach/Sachs pMOcosX cosmid G23:G5. Based on the *Neurospora* genome project, sequence from this cosmid matches that found to be on linkage group V, which is in agreement with the location of *cot-2* based on the genetic map.
- The *cot-4* strain can be complemented with the Orbach/Sachs pMOcosX cosmid X15:E10. Based on the *Neurospora* genome project, sequence from this cosmid matches that found to be on linkage group V, in agreement with the location of *cot-4* based on the genetic map.
- The *cot-4* gene was cloned and a mutation in the catalytic subunit of calcineurin, a Ca^{2+}/calmodulin-dependent protein phosphatase, was found to be responsible for the *cot-4* phenotype.

Chapter 6

Genomic Analysis of the Ca^{2+}-Signalling Machinery in Filamentous Fungi

6.1 Introduction

Despite the obvious importance of Ca^{2+}-signalling in filamentous fungi, and in contrast to the situation in budding yeast, only a handful of Ca^{2+}-signalling genes have been cloned or characterised in filamentous fungi to date (see Table 6.1). These include genes encoding a Ca^{2+}-permeable channel (NCBI #AF393474), Ca^{2+}-ATPases (Benito et al., 2000), a Ca^{2+}/H^{+} exchanger (Margolles-Clark et al., 1999), calcineurin (Higuchi et al.; Kothe and Free, 1998; Juvvadi et al., 2001; Rasmussen et al., 1994; Fox et al., 2001) and calmodulin (CaM) (Capelli et al., 1993; Melnick et al., 1993; Rasmussen et al., 1990).

Due to recent genome sequencing efforts across the world, the complete (or, in some cases, incomplete) genome sequences of several filamentous and non-filamentous fungi are now available on the internet (see Table 1.2). The availability of such large filamentous fungal genome databases has made it

possible, for the first time, to gain detailed insights into the molecular machinery of filamentous fungi through genomic analysis.

The aims of the work carried out in this chapter were: (1) to determine the Ca^{2+}-signalling proteins encoded in the genomes of *N. crassa*, *A. fumigatus* and *M. grisea* based on an analysis of their entire genomes; (2) to analyse in detail the Ca^{2+}-permeable channels, Ca^{2+}-transporters and Ca^{2+}-pumps in *N. crassa*; (3) to compare these Ca^{2+}-signalling proteins with those in *M. grisea* and *A. fumigatus*, and with those in *S. cerevisiae* as a "model" system as a fungus with a large amount of associated Ca^{2+}-signalling literature; and (4) to provide a comprehensive web-based database resource on all Ca^{2+}-signalling proteins in *N. crassa*, *A. fumigatus*, *M. grisea* and *S. cerevisiae*.

6.2 Results

6.2.1 Data storage and access

A database with a web interface was made[1] and used as a repository for detailed information regarding all the proteins identified in this chapter. This website should be used to supplement all the information presented below. The advantages of this approach for data storage and access are the provision of: (1) a dynamic and convenient interface for the public to access (and potentially contribute to) these data; (2) numerous ways for the user to filter the data to view or search for what one wants; (3) access to sequence data for all the proteins and genes described in the database; (4) hyperlinks to other sources of information specific to the data within the database (e.g. automatic searches for conserved domains within a protein and other functions); (5) the flexibility to add unlimited additional functions in the future. A local blast facility was also set up (software

[1] http://fungalcell.org/FDF/

provided courtesy of NCBI[2] to enable the sequence data deposited in my database to be searched by the public using the NCBI blast software package[3].

6.2.2 Ca^{2+}-signalling proteins previously identified in filamentous fungi and budding yeast

A search of the literature and the NCBI Entrez-Protein database revealed a number of previously identified filamentous fungal Ca^{2+}-signalling proteins (Table 6.1).

Table 6.1: Ca^{2+}-signalling proteins previously identified in filamentous fungi

Protein Class	Protein Name	Organism	Reference(s)
Ca^{2+}-permeable channel	CCH1	*A. nidulans*	NCBI #AF393474
Ca^{2+}-ATPase	pmrA	*A. niger*	Yang et al. (2001a)
Ca^{2+}-ATPase	NCA-1, NCA-2, NCA-3, PMR-1, PH-7	*N. crassa*	Benito et al. (2000)
Ca^{2+}/H^{+}-exchanger	CAX	*N. crassa*	Margolles-Clark et al. (1999)
calmodulin	CMD	*N. crassa*	Capelli et al. (1993); Melnick et al. (1993)
calmodulin	CMDA	*A. nidulans*	Rasmussen et al. (1990)
calmodulin	AAK69619	*Fusarium proliferatum*	Kwon et al. (2001)
calcineurin A	CNA	*N. crassa*	Higuchi et al.
calcineurin A	CNAA	*A. nidulans*	Rasmussen et al. (1994)
calcineurin A	CNA1	*Filobasidiella neoformans*	Odom et al. (1997)
calcineurin A	CNAA	*A. oryzae*	Juvvadi et al. (2001)

[2]http://www.ncbi.nlm.nih.gov/Ftp/
[3]http://fungalcell.org/blast/

calcineurin A	CNA	*Exophiala dermatitidis*	NCBI #AAL47191
calcineurin B	CNB	*N. crassa*	Kothe and Free (1998)
calcineurin B	CNB1	*Filobasidiella neoformans*	Fox et al. (2001)
Ca^{2+}/CaM-dependent protein kinase	FCaMK	*Arthrobotrys dactyloides*	Tsai et al. (2002)
Ca^{2+}/CaM dependent protein kinase B	CaMK I/IV homolog cmkB	*A. nidulans*	Joseph and Means (2000)
Ca^{2+}/CaM dependent protein kinase C	CaMKK a/b homolog cmpk	*A. nidulans*	Joseph and Means (2000)
Ca^{2+}/CaM dependent protein kinase	CMKA	*A. nidulans*	Kornstein et al. (1992)
Ca/CaM-dependent kinase-1	CAMK-1	*N. crassa*	Yang et al. (2001b)
CaM-dependent protein kinase	CgCMK	*Colletotrichum gloeosporioides*	Kim et al. (1998)
Calnexin	CLXA	*A. niger*	Wang et al. (2003)
phospholipase C	NCPLC-1, NCPLC-2, NCPLC-3	*N. crassa*	Jung et al. (1997)
phospholipase C	ANPLC1	*A. nidulans*	Jung et al. (1997)
phospholipase C	BCPLC1	*B. fuckeliana*	Jung et al. (1997)
phospholipase C	MPLC1	*M. grisea*	NCBI #AAC72385

In all filamentous fungi only one Ca^{2+}-permeable channel, CCH1, has been previously identified (NCBI accession #AF393474). Six Ca^{2+}-ATPases and one Ca^{2+}/H^{+}-exchanger comprise the total number of these types of proteins

previously described in filamentous fungi. Calcineurin has been identified in five species of filamentous fungi, and calmodulin (CaM) in three. Several putative isozymes of phospholipase C (PLC) have been identified in *N. crassa*, *A. nidulans*, *M. grisea* and *Botryotinia fuckeliana*, although their actual cellular functions have not yet been tested experimentally.

In budding yeast three Ca^{2+}-permeable channels, four Ca^{2+}-ATPases, one Ca^{2+}/H^{+}-exchanger, one Ca^{2+}/Na^{+}-exchanger, one PLC and several other proteins involved in Ca^{2+}-transport and homeostasis have all been previously identified (Table 6.2). In contrast to the case with filamentous fungi, all of these

Table 6.2: Ca^{2+}-signalling proteins previously identified in budding yeast

Protein Class	Protein Name/Locus	Reference(s)
Ca^{2+}-permeable channel	Cch1p, Mid1p, Yvc1p	Fischer et al. (1997); Maruoka et al. (2002); Palmer et al. (2001)
Non-specific cation channel	Pmp3p	Navarre and Goffeau (2000)
Ca^{2+}-ATPase	Pmc1p, Pmr1p, Spf1p, Neo1p	Degand et al. (1999); Park et al. (2001); Cronin et al. (2002); Catty and Goffeau (1996)
Ca^{2+}-transporter	Ccc1p	Lapinskas et al. (1996)
Ca^{2+}/H^{+}-exchanger	Vcx1p	Miseta et al. (1999b)
Calmodulin	Cmd1p	Davis et al. (1986)
calcineurin A	Cna1p, Cna2p	Cyert et al. (1991)
calcineurin B	Cnb1p	Cyert and Thorner (1992)
CaM-dependent protein kinase	Cmk1p	Cyert (2001)
CaM-dependent protein kinase	Cmk2p	Cyert (2001)
Calnexin	Cne1p	de Virgilio et al. (1993)
phospholipase C	Plc1p	Flick and Thorner (1993)

proteins have been investigated experimentally, and had their cellular functions confirmed.

The genome size of budding yeast ($\sim$ 13 Mbp) is 60 to 70% smaller than that of *N. crassa*, *M. grisea* and *A. fumigatus* ($\sim$ 43, 40 and 35 Mbp, respectively). The fact that far more Ca^{2+}-signalling proteins have been described in the literature and are present in the Entrez-Protein database for budding yeast, than all the filamentous fungi put together, is thus highly unlikely to reflect the true ratio of Ca^{2+}-signalling proteins present in these groups. To begin to rectify this apparent imbalance in knowledge of Ca^{2+}-signalling related proteins between yeast and filamentous fungi, I performed an exhaustive BLAST analysis of three filamentous fungal genomes (*N. crassa*, *A. fumigatus* and *M. grisea*) and budding yeast.

6.2.3 Ca^{2+}-signalling proteins present in filamentous fungi and budding yeast

My blast analysis discovered 46, 38, 40 and 40 Ca^{2+}-signalling proteins in *N. crassa*, *A. fumigatus*, *M. grisea* and *S. cerevisiae*, respectively (Tables 6.3 and 6.4).

In *N. crassa*, *A. fumigatus* and *M. grisea* 78, 100 and 95% of these proteins, respectively, were previously unknown and uninvestigated. In *S. cerevisiae* only 15% were previously unknown and of these 10% had not been previously investigated. The number of Ca^{2+}-signalling proteins discovered in *N. crassa* represents almost 0.5% of the total 10,000 proteins thought to be encoded by the *N. crassa* genome (Galagan et al., 2003). Clearly then, genes encoding Ca^{2+}-signalling proteins are an important component of fungal genomes.

The proteins discovered were divided into several categories for further analysis. These were: (1) Ca^{2+}-permeable channels; (2) Ca^{2+}-pumps; (3) Ca^{2+}-transporters; and (4) other proteins important for Ca^{2+}-signalling. Many of the Ca^{2+}-signalling proteins discovered will not be discussed here, however, they are all available on the website provided[4]. Hypothetical proteins were not available

[4]http://www.fungalcell.org/FDF/

from the *A. fumigatus* database and have therefore been excluded from the detailed protein analysis in the following sections.

6.2.3.1 Ca^{2+}-permeable channels

Ca^{2+}-permeable channels are made from several subunits and commonly contain pore-forming Shaker-like domains (Kreusch et al., 1998) consisting of 6 transmembrane (TM) spans, within which is a putative "pore" region. Ca^{2+}-, CaM- and/or cyclic nucleotide-binding domains may also be present, depending on the type of channel. Our BLAST analysis revealed 3 Ca^{2+}-permeable channels in each of the four fungi investigated (Table 6.3). All of these proteins were previously unknown in filamentous fungi. A phylogenetic tree constructed with the *N. crassa*, *M. grisea* and *S. cerevisiae* proteins had 2 branches (Fig. 6.1), and showed that the proteins fell into 3 separate groups. In each case the *N. crassa* and *M. grisea*

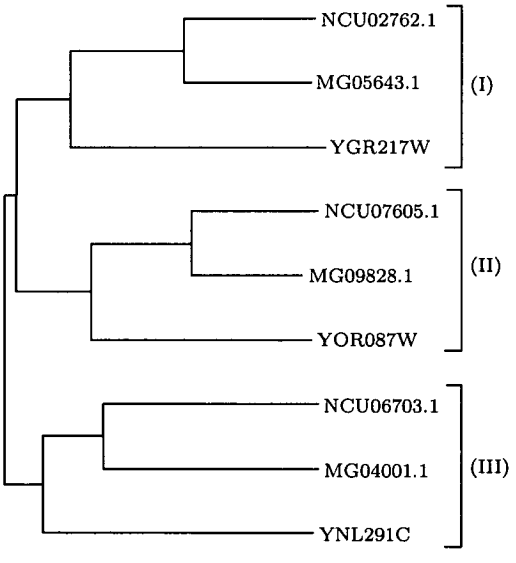

Figure 6.1: Phylogenetic tree of Ca^{2+}-permeable channels identified in *N. crassa*, *M. grisea* and *S. cerevisiae*. (Neither rigorous calculation of evolutionary distances nor phylogenetic relationship can be inferred with confidence from this tree.)

proteins were more closely related to each other than to the *S. cerevisiae* protein.

Group I Ca^{2+}-permeable channels included the yeast Cch1p protein. Cch1p

Table 6.3: Ca^{2+}-permeable channels, -pumps and -transporters in *N. crassa*, *A. fumigatus*, *M. grisea* and *S. cerevisiae*

Protein Class	Proteins in *N. crassa*		Homologues in: *A. fumigatus*		*M. grisea*		*S. cerevisiae*	
	Name	No.	Name	No.	Name	No.	Name	No.
Ca^{2+}-permeable channel	NCU02762.1 NCU06703.1 NCU07605.1	3	4837_44838-51270 4903_95811-98584 4925_476666-479554	3	MG05643.1 MG04001.1 MG09828.1	3	Cch1p Mid1p Yvc1p	3
Cation-pumps (Ca^{2+} unless otherwise indicated)	NCA-1 NCA-2 NCA-3 PMR1 PH-7 NCU04898.1 NCU03818.1 NCU07966.1 NCU01437.1† ENA-1*	9	4963_51054-55386 4897_59083-63769 4944_55012-59497 4801_29807-34346 4927_125721-129900 4925_401457-406276 4899_407390-410352 4899_471968-476447 4882_6919-10658 4826_49523-53702*	9	MG04550.1, 2.852_18780-19520 MG02487.1, MG07971.1 MG04890.1 MG09892.1 MG10730.1†, 2.1107_34917-37626 2.1792_25841-29738† MG04066.1 MG05078.1* MG06925.1† MG02074.1†	12	Pmr1p Pmc1p Pmc1p Pmr1p Ena2p* Spf1p Neo1p Ena2p* YOR291W† Ena5p*	5
Ca^{2+}-transporters (Ca^{2+}/H^+ unless otherwise indicated)	CAX NCU00916.1 NCU00795.1 NCU06366.1 NCU07711.1 NCU05360.1 NCU02826.1‡ NCU08490.1‡	8	4932_1025450-1028316 4882_219707-223976 4882_219707-223976 4856_44229-47908 4932_1025450-1028316 4882_587414-592053 4901_620762-623217	5	2.175_3011-3697 MG01193.1 MG08710.1 MG04159.1 MG04159.1 MG01381.1 MG01638.1 MG08710.1, MG01193.1	6	Vcx1p Vcx1p Vcx1p Vcx1p Vcx1p YNL321W YDL206W‡,Ecm27p‡ YNL321W	4

*Na^+-ATPase; †undefined cation-ATPase; ‡Ca^{2+}/Na^+-exchanger.

Table 6.4: Phospholipase C's and important Ca^{2+} and/or CaM binding proteins in *N. crassa*, *A. fumigatus*, *M. grisea* and *S. cerevisiae*

Protein Class	Proteins in: *N. crassa*		Homologues in: *A. fumigatus*		*M. grisea*		*S. cerevisiae*	
	Name	No.	Name	No.	Name	No.	Name	No.
Phospholipase C	NCU01266.1		4836_319018-323704		MG02444.1		Plc1p	
	NCU06245.1	4	4871_107810-112364	2	MG05332.1	4	Plc1p	1
	NCU09655.1		4806_73778-76479		MG05905.1		Plc1p	
	NCU02175.1		4871_107810-112364		MG02682.1		Plc1p	
Calmodulin	CMD	1	4840_243470-246367	1	MG06884.2	1	Cmd1p	1
Calcineurin (catalytic)	CNA-1	1	4938_684630-687160	1	MG07456.2	1	Cna1p, Cmp2p	2
(regulatory)	CNB-1	1	4899_233789-236133	1	MG06933.1	1	Cnb1p	1
Ca^{2+}/CaM	NCU02283.1		4861_105606-107947		MG00925.1		Cmk1p, Cmk2p	
dependent	NCU09123.1		4829_85272-88063		MG09912.1		Cmk1p, Cmk2p	
protein kinase	NCU06177.1		4903_144856-147683		MG06421.1		Pak1p	
	NCU09212.1	7	4800_5925-8603	7	MG08547.1	7	Rck2p, Rck1p	10
	NCU00914.1		4942_397345-402284		MG01196.1		Kin4p, Arp8p	
	NCU02814.1		4901_679884-682486		MG01596.1.1		Dun1p, Rad53p	
	NCU06347.1		4836_394664-398651		MG06180.1		End3p	
Calnexin	NCU09265.1	1	4865_210410-230126	1	MG01607.1	1	Cne1p	1

bears sequence similarity to the α1, catalytic subunit of voltage-gated Ca^{2+}-permeable channels and was localised to plasma membrane by Locke et al. (2000). The filamentous fungal homologues of Cch1p (*N. crassa* NCU02762.1, *A. fumigatus* 4837_44838-51270 and *M. grisea* MG5643.1) were very similar to the yeast protein (E=0, E=1e^{-112} and E=0, respectively). Like the α1 subunits, the fungal proteins contain four repeat units (I to IV) of six TM domains (Fig. 6.2 a) that tetramerize to form the core of the Ca^{2+}-channel (a Shaker-like domain). Most of the sequence identity between the fungal and mammalian calcium channel subunits is present within regions thought to play key roles in defining channel specificity (domain P) and voltage dependence (TM domain S4) (Paidhungat and Garrett, 1997). All four hydrophobic domains (I, II, III, and IV) contain amino acid residues indicative of the Ca^{2+}-selective P segment, and three (II, III, and IV) of the four (Fig. 6.2 b) contain a highly conserved glutamate residue that is thought to play a critical role in Ca^{2+} coordination (Paidhungat and Garrett, 1997). Each of the S4 segments of domains I, II, and III contain repeated motifs of a positively charged residue followed by two hydrophobic residues (Fig. 6.2 c). Similar segments have been shown to act as voltage sensors in ion channels of higher eukaryotes (Paidhungat and Garrett, 1997). The hydrophobic domains (I, II, III, and IV) matched the pfam00520 domain, found in Na^{+}-, K^{+}-, and Ca^{2+}-permeable channels and consists of 6 TM helices in which the last two helices flank a loop which determines ion selectivity.

Group II Ca^{2+}-permeable channels included the yeast Mid1p protein. Mid1p is a stretch-activated, plasma membrane based, Ca^{2+}-permeable channel. The filamentous fungal homologues of Mid1p (*N. crassa* NCU06703.1, *A. fumigatus* 4903_95811-98584 and *M. grisea* MG04001.1) were quite similar to the yeast protein (E=4e^{-28}, E=3e^{-36} and E=1e^{-32}, respectively) although the filamentous fungal proteins were larger (NCU06703.1 by 22% and MG04001.1 by 38%). None of the Ca^{2+}-permeable channels in this class had overall sequence similarity with known plant or animal ion channels. Several features are thought to be important

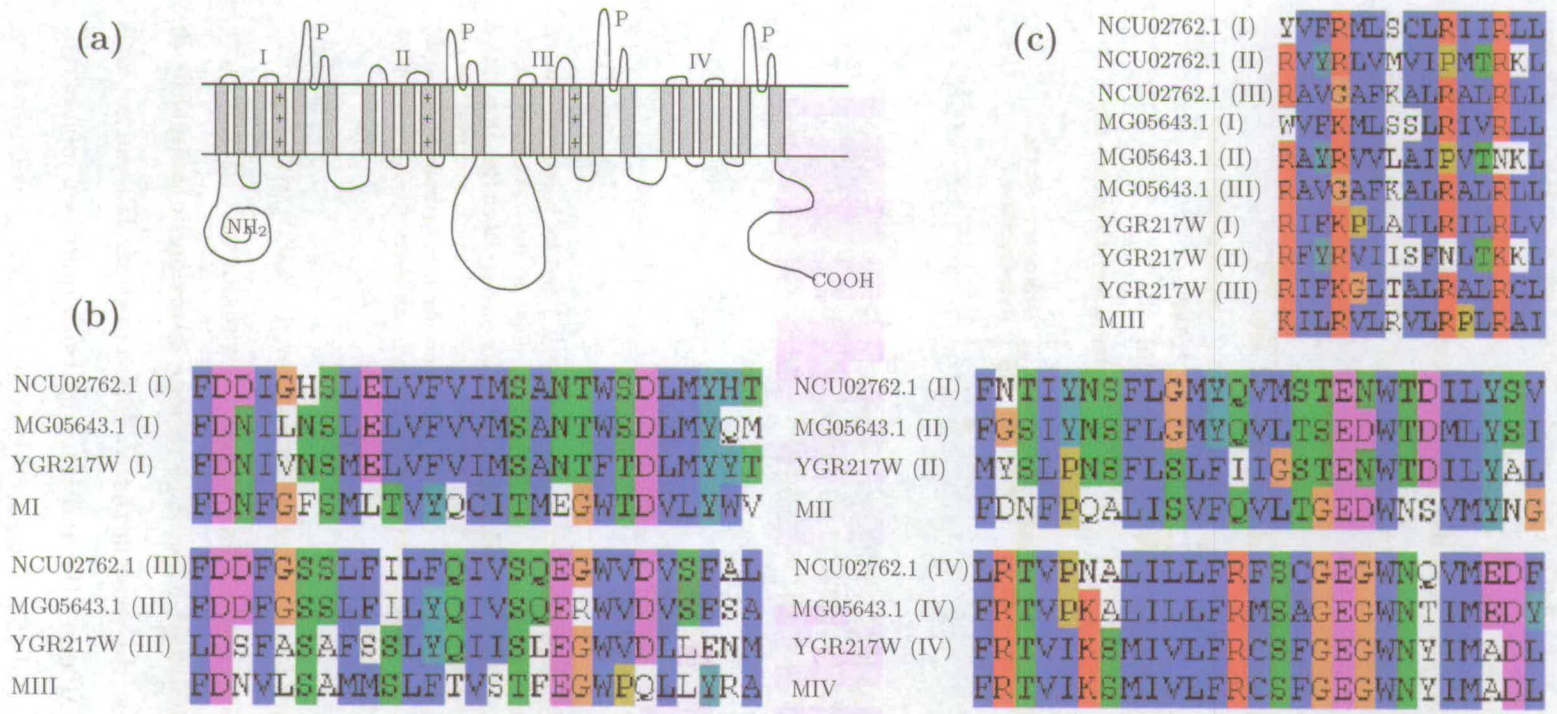

Figure 6.2: Characteristics of *S. cerevisiae* Cch1p (YGR217W) and its homologues in *N. crassa* (NCU02762.1) and *M. grisea* (MG5643.1). (a) A schematic diagram of Cch1p in *S. cerevisiae*. The four hydrophobic repeats are marked I to IV. The S4 and P domains of each hydrophobic repeat were assigned by analogy with mammalian Ca^{2+}-permeable channels. The S4 domains of repeats I, II, and III are marked with plus signs to indicate the positively charged amino acids. (b) Lower left and right panel: sequence alignment of the predicted P domains of Cch1p [YGR217W (I) to YGR217W (IV)], and homologues in *N. crassa* and *M. grisea*, with the corresponding P domains (MI to MIV) of a skeletal muscle Ca^{2+}-permeable channel (Tanabe et al., 1987). (c) Sequence alignment of the positively charged S4 transmembrane segments of Cch1 (YI, YII, and YIII), and homologues in *N. crassa* and *M. grisea*, with the S4 segment of the third hydrophobic repeat (MIII) of a rat brain Ca^{2+}-channel (Snutch et al., 1991). Diagram adapted from Paidhungat and Garrett (1997).

in Mid1p function (Maruoka et al., 2002; Tada et al., 2003) (see Fig. 6.3 a). These are (a) four hydrophobic segments named H1 to H4; (b) a carboxy-terminal region containing three possible functional motifs; and (c) a cysteine-rich region at the carboxy end of the protein. The hydrophobic regions of Mid1p, partially similar

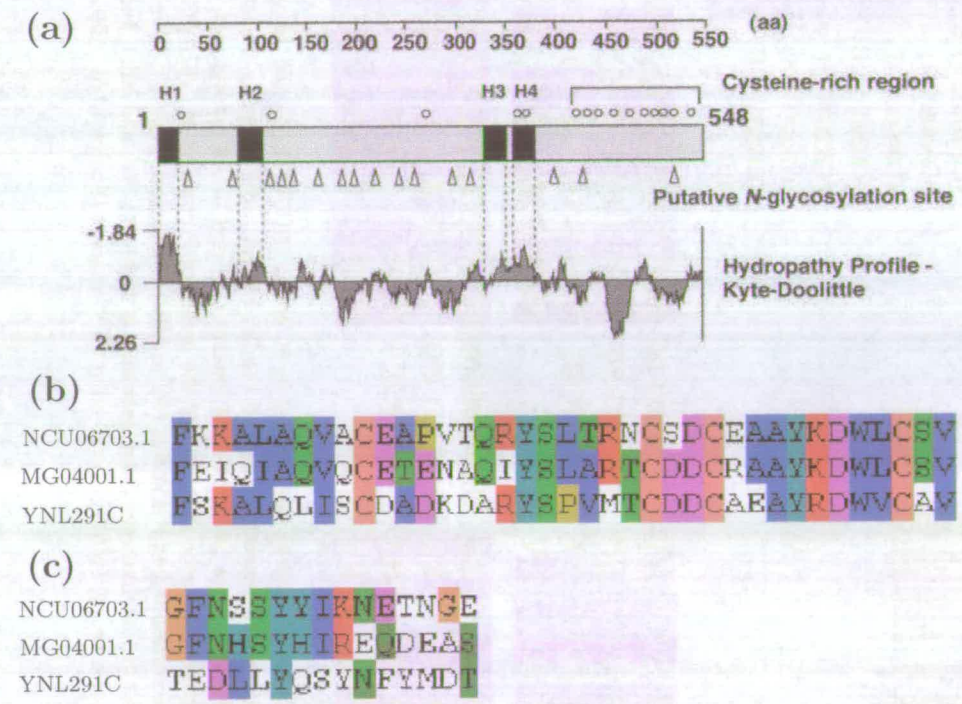

Figure 6.3: Characteristics of *S. cerevisiae* Mid1 protein (YNL291C) and its homologues in *N. crassa* (NCU06703.1) and *M. grisea* (MG04001.1). (a) A schematic diagram and hydropathy profile of Mid1p (from Tada et al. (2003)). The four hydrophobic regions are marked HI to H4, 16 putative N-glycosylation sites (△), and 15 cysteine residues (○). Position numbers of amino acid residues are indicated at the top of the figure. (b) Alignment of Mid1p EF-hand-like motif (residues 408-445) with filamentous fungal homologues. (c) Alignment of Mid1p sheet-turn-sheet structure (residues 512-526) with filamentous fungal homologues.

to the TM segments of known ion channels (Maruoka et al., 2002), were found to be partially conserved in the *N. crassa* and *M. grisea* homologues. H1 was quite well conserved. However, MG04001.1 had a 15 residue insertion in the middle of this region not found in either the yeast or the *N. crassa* protein. H2 was not well conserved between the three fungi. H3 and H4 were both quite well conserved. The carboxy-terminal region of the protein preceeding H4 has previously been

postulated to be a regulatory region for the Mid1p channel (Iida et al., 1994). Every cysteine residue within the cysteine-rich region previously defined in Mid1p (Maruoka et al., 2002) was conserved in all three fungal homologues. This region is essential (Tada et al., 2003) and contains a putative casein kinase 2 phosphorylation motif which is absent from the filamentous fungal homologues examined and was found to be non-essential to Mid1p function (Tada et al., 2003). An EF-hand like structure, also in this region, has been shown to be essential for Mid1p function (Tada et al., 2003) and was was well conserved between the three fungi (see Fig. 6.3 b). There is conflicting data on the importance of the sheet-turn-sheet motif in Mid1p. However, my analysis suggests that it is not important in *N. crassa* and *M. grisea* as it was not conserved between budding yeast and filamentous fungi (see Fig. 6.3 c).

Group III Ca^{2+}-permeable channels included the yeast Yvc1p protein. Yvc1p is a voltage-dependent Ca^{2+}-activated Ca^{2+}-permeable channel located in the budding yeast vacuolar membrane. The filamentous fungal homologues of Yvc1p (*N. crassa* NCU07605.1 , *A. fumigatus* 4925_476666-479554 and *M. grisea* MG09828.1) were very similar to the yeast protein (E=$9e^{-90}$, E=$2e^{-94}$ and E=$1e^{-114}$, respectively). NCU07605.1 was $\sim$ 50% larger than MG09828.1 and Yvc1p. However the first 50% (650 residues) of NCU07605.1 has no homology to known proteins. Yvc1p, and its filamentous fungal homologues, have significant homology to the transient receptor potential (TRP) family of ion channels. Hydrophilicity and domain prediction indicate that Yvc1p (Palmer et al., 2001), MG09828.1 and the last 50% of NCU07605.1 contain six TM domains (see Fig. 6.4 a and b). The most significant homology to other TRP channels is found in the predicted sixth TM domain (see Fig. 6.4 d), which forms part of the ion conduction pathway and is intimately associated with deactivation gating in cation channels (Palmer et al., 2001). All six TM domains were highly conserved in the proteins examined, although NCU07605.1 was missing large parts of TM domain 4 and 5 (see Fig. 6.4 c). The C-terminal portion of Yvc1p contains a

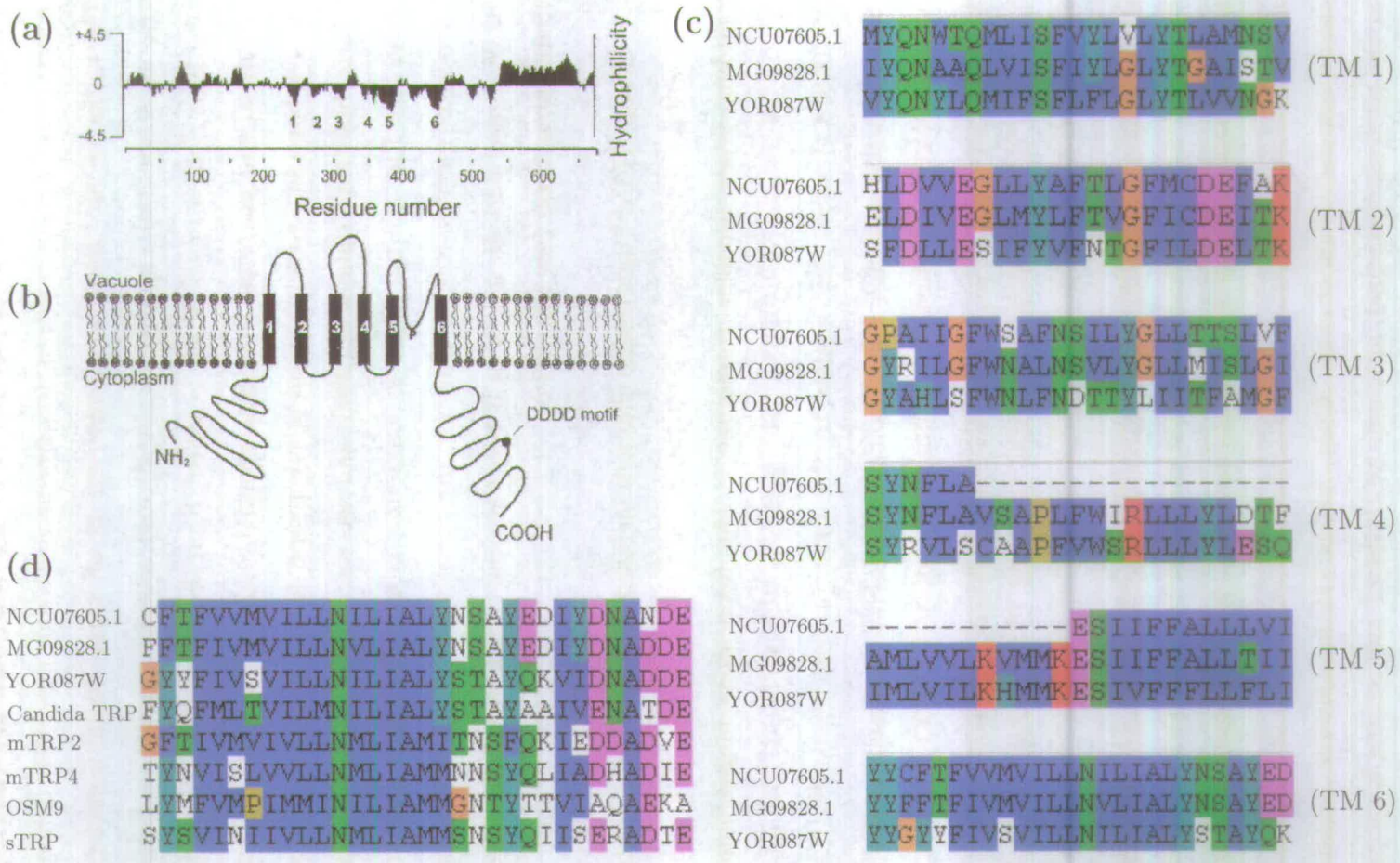

Figure 6.4: Characteristics of *S. cerevisiae* Yvc1p protein (YOR087W) and its homologues in *N. crassa* (NCU07605.1) and *M. grisea* (MG09828.1). (a) Hydrophilicity plot of the predicted protein encoded by YVC1 from Palmer et al. (2001). Six potential TM domains are marked (1-6). (b) Model structure for the protein encoded by the YVC1 gene (Palmer et al., 2001); six TM domains (1-6) and a putative pore region (P) are labelled. (c) Alignment between the six predicted fungal TM domains. (d) Alignment between the predicted sixth TM region of NCU07605.1, MG09828.1 and Yvc1p and the predicted sixth TM regions of other TRPs: *Candida TRP*, a homologue in *C. albicans*; mTRP2 and mTRP4, mouse homologues (Vannier et al., 1999; McKay et al., 2000); OSM9, a homologue in *Caenorhabditis elegans* (Colbert et al., 1997); dTRP, the *Drosophila* TRP (Hardie and Minke, 1992).

DDDD motif that may be involved in Ca^{2+} regulation similar to the Ca^{2+}-binding bowl in Ca^{2+}-activated K^+-channels (Palmer et al., 2001; Schreiber and Salkoff, 1997). This motif is absent from MG09828.1. Interestingly, NCU07605.1 has a DDDD motif in its N-terminal region. Whether this plays a role in Ca^{2+}-binding is unknown.

6.2.3.2 Ca^{2+}-pumps

Ca^{2+}-ATPases hydrolyse ATP to drive the active transport of Ca^{2+} across biological membranes. They reduce $[Ca^{2+}]_c$ concentrations by pumping Ca^{2+} into internal stores, or across the cell membrane and out of the cell. Ca^{2+}-ATPases fall into the superfamily of P-type (or E1-E2 type) ATPases. Although there are large differences in primary structure and low overall similarity within the P-type ATPase family, eight conserved regions (A - H) have been identified (Axelsen and Palmgren, 1998, 2001). Most Ca^{2+}-ATPases are either type P_{2A} or type P_{2B} ATPases. Type P_5 ATPases are a recently discovered, but currently biochemically uncharacterised, class of ATPases that may be Ca^{2+}-transporting (Axelsen and Palmgren, 2001). Type P_{2A} Ca^{2+}-ATPases are mainly present in the sarcoplasmic and endoplasmic reticulum and are similar to animal sarcoplasmic reticulum Ca^{2+}-ATPases (SERCA) but in addition include a plant pump apparently present in both the vacuolar and plasma membranes (Ferrol and Bennett, 1996). Type P_{2B} Ca^{2+}-ATPases are most similar to mammalian plasma membrane Ca^{2+}-ATPases (PMCA) but this family also includes pumps present in the vacuolar membrane (Cunningham and Fink, 1994a; Moniakis et al., 1995; Malmström et al., 1997). It is important to note, however, that fungal Ca^{2+}- and Na^+-ATPases can only be distinguished by functional analysis (Benito et al., 2000). The results presented below should be interpreted with this in mind.

My BLAST analysis revealed nine Ca^{2+}- or cation-ATPases in *N. crassa* (four of which were novel), nine Ca^{2+}-/cation-ATPases in *A. fumigatus* (all novel)

and twelve[5] (all novel) in *M. grisea* (see Table 6.3). In budding yeast, my analysis identified only five Ca^{2+}-/cation-ATPases of which one, YOR291W, was of unknown function but had been previously described (Catty et al., 1997). Eleven other ATPases have been identified in *S. cerevisiae*, although none of these have been classified as Ca^{2+}-ATPases (Catty et al., 1997). Five of the *N. crassa* Ca^{2+}-ATPases had been previously discovered (Benito et al., 2000) and found to be distributed in all branches of type P_2 ATPases except the branch of animal Na^+/K^+-ATPases (P_{2C}) (Benito et al., 2000). NCA1 conserved all the amino acids involved in Ca^{2+}-binding in SERCA (sarcoplasmic reticulum Ca^{2+}) (see Fig. 6.5) and showed a motif of ER retention in the carboxy terminus (KKKDL) (Benito et al., 2000). This motif was not present in any of the *M. grisea* or *S. cerevisiae* P-type ATPases analysed. NCA2 contained a sequence indicative of an N-terminal calmodulin-binding autoinhibitory domain (residues 165-182) (Benito et al., 2000). The five *N. crassa* type P_{2A} and P_{2B} ATPases identified by my analysis showed very good homology with animal, plant and yeast SERCA and PMCA type Ca^{2+}-ATPases (Fig. 6.5). The two *M. grisea* type P_{2A} and three P_{2B} ATPases were also well conserved. However two proteins, MG04550.1 and MG02074.1, had only 4 TM regions (all other P-type ATPases analysed here had between 7 and 10 TM regions) and showed a complete absence of TM 4 and TM 4-6, respectively. These proteins were also very short, having only 588 and 221 residues, respectively, while the other P-type ATPases analysed ranged between 1094 and 2005 amino acids in length. I think that these hypothetical proteins may have been predicted incorrectly.

Also revealed in *N. crassa* were an additional one type P_{2D}, one P_4 and two P_5 ATPases (see Fig. 6.5). *M. grisea* showed one type P_{2D}, one P_4 and one P_5 ATPase. The type P_{2D} ATPases showed close homology to *S. pombe* CTA3, a known Ca^{2+}-ATPase (Ghislain et al., 1990). The five novel P_4 and P_5

[5]Three of the *M. grisea* Ca^{2+}-/cation-ATPases did not correspond to hypothetical proteins in the *M. grisea* database and were therefore not analysed in detail during this study.

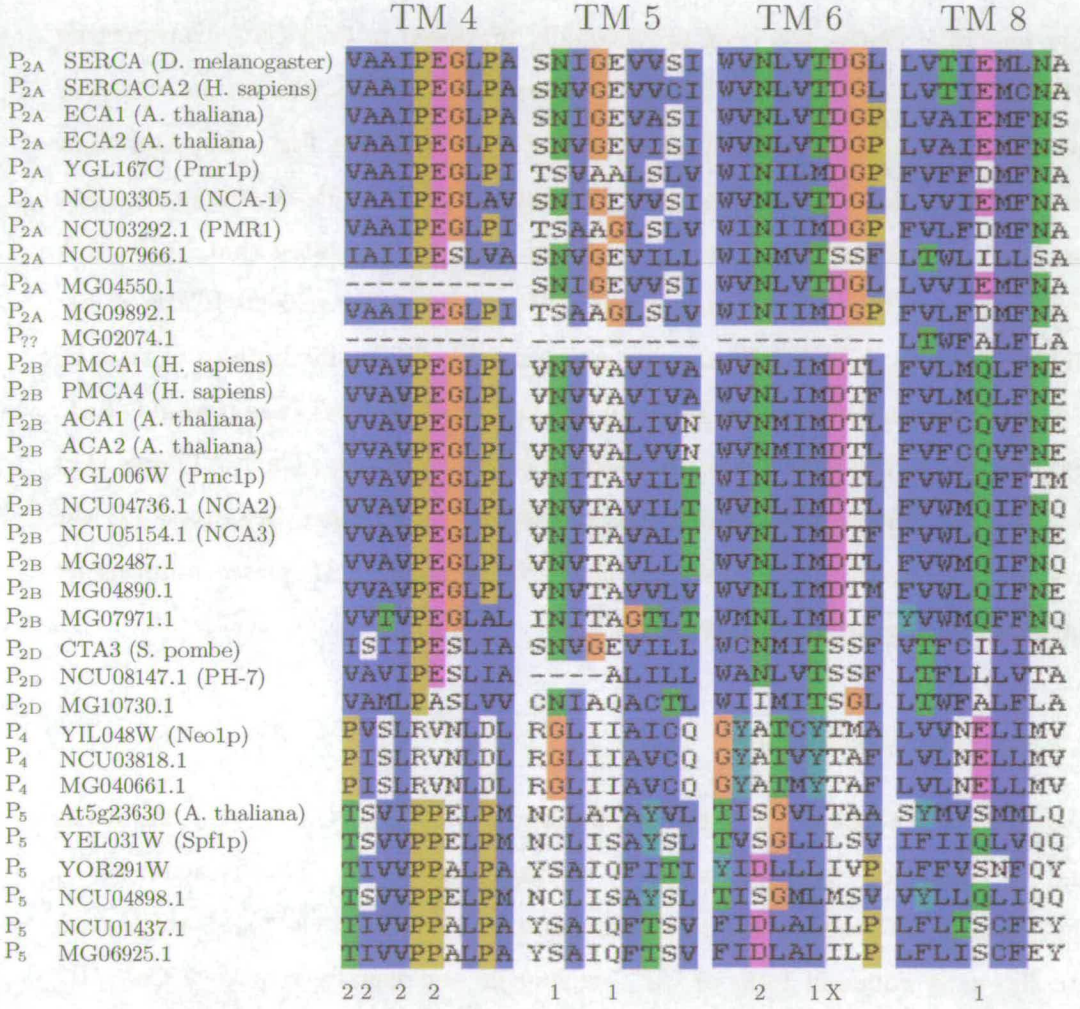

Figure 6.5: Sequence alignments of potential Ca^{2+}-ATPases of *N. crassa*, *M. grisea* and *S. cerevisiae* in conserved TM segments containing amino acids putatively involved in Ca^{2+}-binding. Examples of Ca^{2+}-ATPases from other organisms are: (a) SERCA (type P_{2A}) sequences were *D. melanogaster* SERCA (NCBI #A36691), *H. sapiens* SERCACA2 (NCBI #P16615) and *A. thaliana* ECA1 (NCBI #AAF36087) and ECA2 (NCBI #CAA10659); (b) PMCA (type P_{2B}) were *H. sapiens* PMCA1 (NCBI #P20020) and PMCA4 (NCBI #P23634), and *A. thaliana* ACA1 (NCBI #CAA49559) and ACA2 (NCBI #T04721); (c) type P_{2D} sequences were *S. pombe* CTA3 (NCBI #P22189); (d) type 5 sequences were (NCBI #At5g23630). Residues involved in coordination of Ca^{2+} in the two Ca^{2+}-binding sites (Site I and Site II) found in the 2.6 Å crystal structure of SERCA1a (Toyoshima et al., 2000) are marked with 1 and 2, respectively. The position marked X is a residue involved in coordination of both Ca^{2+} ions (Axelsen and Palmgren, 2001). $P_{??}$ indicates type unknown.

Ca^{2+}-ATPases in *N. crassa* and *M. grisea* all had homologues in *S. cerevisiae*. Neo1p (YIL048W), a *S. cerevisiae* P_4-type ATPase related to the YAL026C gene encoding Drs2p, has been provisionally proposed to be a Ca^{2+}-transporting ATPase (Catty and Goffeau, 1996). However as the TM spans do not conserve the residues thought to be involved in Ca^{2+}-binding (see Fig. 6.5) and show low homology to the same regions of mammalian Ca^{2+}-ATPases this proposition has been questioned (Catty et al., 1997). It was also suggested that YOR291W was unlikely to be a Ca^{2+}-transporting ATPase for similar reasons (Catty et al., 1997). However, YEL031W, also belonging to this unclassified group of type P_5 ATPases, has recently proved to be an ER-localised Ca^{2+}-ATPase (Cronin et al., 2000, 2002). In the light of the discovery of other new P-type Ca^{2+}-ATPases that do not show homology to animal P_{2A} and P_{2B} Ca^{2+}-ATPases (e.g. type P_5) the true role of Neo1p, YOR291W and their *N. crassa* and *M. grisea* homologues must be determined experimentally.

6.2.3.3 Ca^{2+}-exchangers

Like P-type ATPases, Ca^{2+}-exchangers serve to reduce $[Ca^{2+}]_c$ concentrations and to load Ca^{2+} into internal Ca^{2+} storage organelles. This is achieved by the-exchange of positive ions across membranes. In plants Ca^{2+}/H^+ antiporters are the most common form of Ca^{2+}-exchanger and usually require a Ca^{2+}/H^+ stoichiometry of at least three (Blackford et al., 1990). Several of the eleven putative Ca^{2+}-exchangers (CAXs) in *A. thaliana* (Mäser et al., 2001) have been localised to the vacuolar membrane (Mäser et al., 2001; Sanders et al., 2002). In animals Ca^{2+}/Na^+ antiporters are the primary Ca^{2+}-exchangers found. *Saccharomyces cerevisiae* has only one previously identified Ca^{2+}/H^+-exchanger (Vcx1p/Hum1p) and it is localised in the vacuolar membrane (Pozos et al., 1996; Cunningham and Fink, 1996; Miseta et al., 1999b). The *A. thaliana* Ca^{2+}/H^+ antiporter CAX1 is (and CAX3 and VCAX1 are probably) regulated at the posttranslational level by a mechanism of N-terminal auto-inhibition (Pittman

and Hirschi, 2001; Pittman et al., 2002b,a). However, apart from CAX1, very little is known about the posttranslational regulation mechanisms of Ca^{2+}/H^+ antiporters from any species.

My analysis identified six Ca^{2+}/H^+-exchangers and two Ca^{2+}/Na^+-exchangers in *N. crassa* (see Table 6.3). In *A. fumigatus* five Ca^{2+}/H^+-exchangers but no Ca^{2+}/Na^+-exchangers were found and in *M. grisea* five Ca^{2+}/H^+-exchangers and one Ca^{2+}/Na^+-exchanger was found[6]. Of all these proteins, only one, *N. crassa* CAX, was previously known (Margolles-Clark et al., 1999). In yeast two Ca^{2+}/H^+-exchangers (one novel) and two Ca^{2+}/Na^+-exchangers (both novel) were identified. None of the fungal Ca^{2+}-exchangers identified contained regions homologues to the N-terminal regulatory domain found in *A. thaliana* CAX1 (Pittman et al., 2002b). All the proteins analysed had between 9 and 14 predicted TM domains, in good agreement with known Ca^{2+}-transporters.

A phylogenetic tree constructed from the proteins identified, along with examples of Ca^{2+}/H^+ and Ca^{2+}/Na^+-exchangers from other organisms had two main branches (see Fig. 6.6). With the exception of NCU08490.1, Ca^{2+}/H^+-exchangers (predicted on the basis of conserved domains and homology to known proteins) were found in one branch and Ca^{2+}/Na^+-exchangers in the other. Although NCU08490.1 was found in the Ca^{2+}/H^+-exchanger branch of the tree, it was thought to be a Ca^{2+}/Na^+-exchanger as it has homology to the ECM27 Ca^{2+}/Na^+-exchanger domain (CDD #10401) (see Fig. 6.7). Homology between predicted Ca^{2+}/H^+-exchanger proteins (see Fig. 6.7) was greater than between predicted Ca^{2+}/Na^+-exchangers (see Fig. 6.8), and regions of homology between all the Ca^{2+}-transporter proteins were lower still.

[6]One of the *M. grisea* Ca^{2+}/H^+-exchangers did not correspond to a hypothetical protein in the *M. grisea* database and was therefore not analysed in detail during this study.

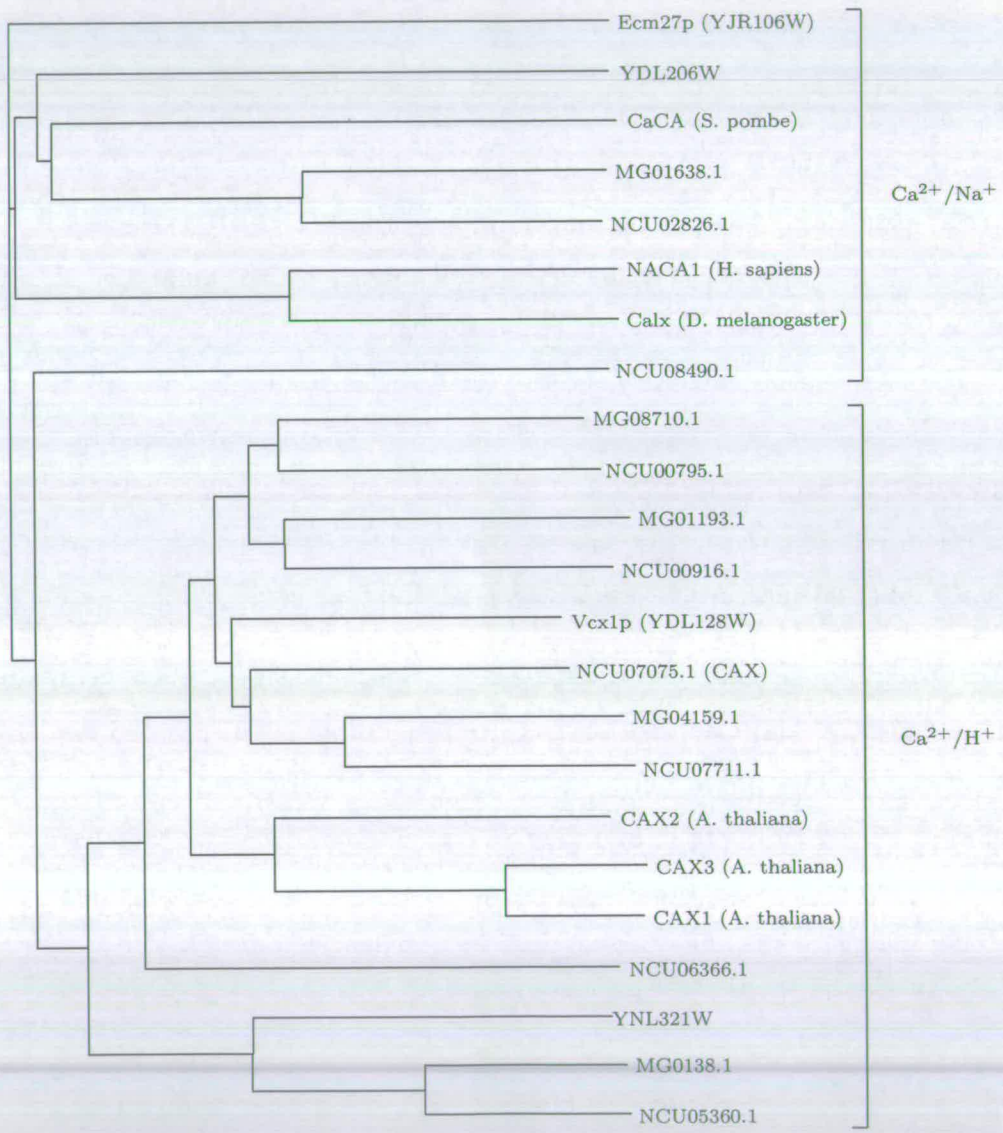

Figure 6.6: Phylogenetic tree of Ca^{2+}-transporters identified in *N. crassa*, *M. grisea* and *S. cerevisiae*. Examples of Ca^{2+}-transporters from other organisms are: (a) Ca^{2+}/Na^{+}-exchanger sequences *S. pombe* CaCA (NCBI #NP_593332), *H. sapiens* NACA1 (NCBI #P32418) and *D. melanogaster* Calx (NCBI #NP_732577); (b) Ca^{2+}/H^{+}-exchanger sequences *A. thaliana* CAX2 (NCBI #AAM19859), CAX3 (NCBI #At3g51860) and CAX1 (NCBI #AAL66749). (Neither rigorous calculation of evolutionary distances nor phylogenetic relationship can be inferred with confidence from this tree.)

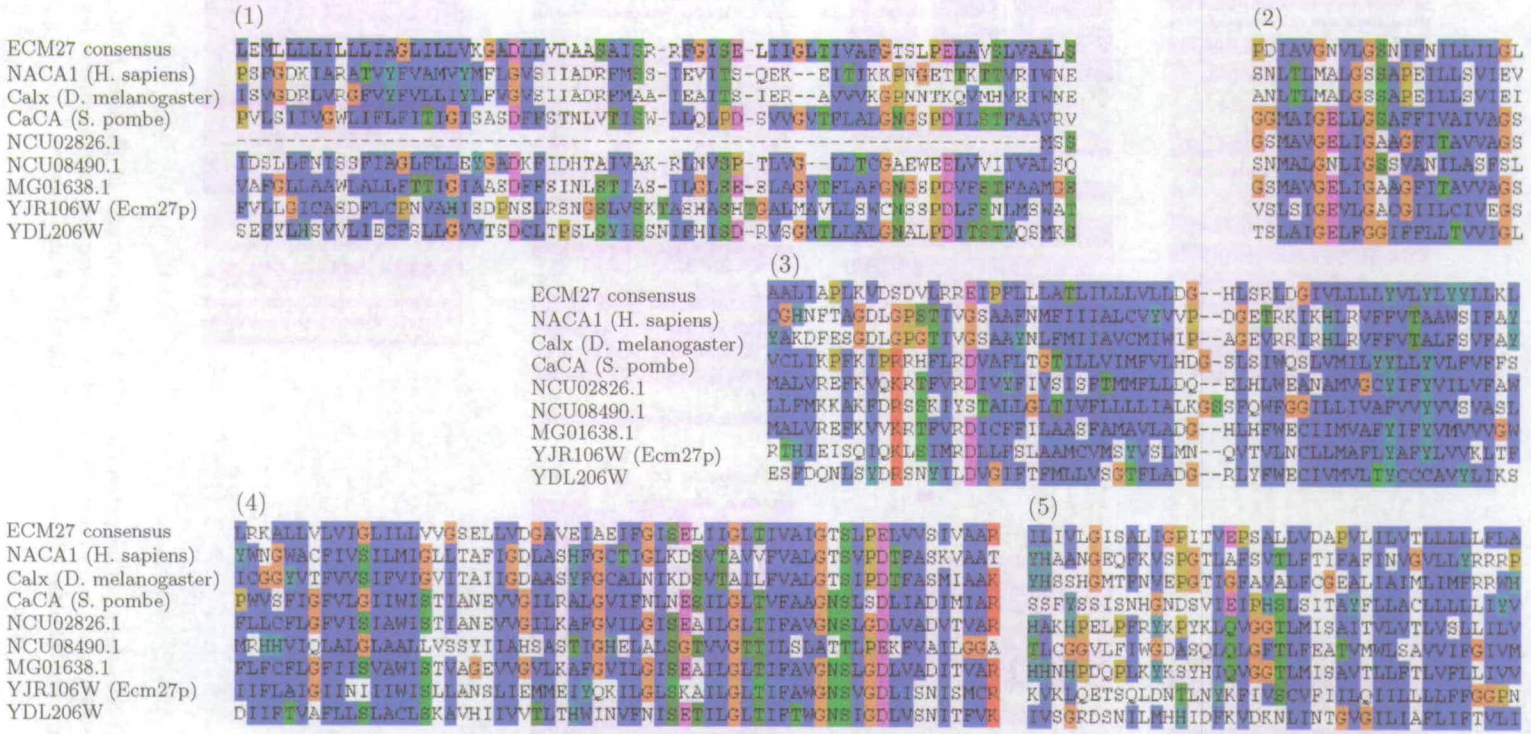

Figure 6.7: Regions of homology within potential Ca^{2+}/Na^{+}-exchangers of *N. crassa*, *M. grisea* and *S. cerevisiae*. Examples of Ca^{2+}/Na^{+}-exchangers from other organisms are as described in Fig. 6.6. Consensus Ca^{2+}/Na^{+}-exchanger domain ECM27 domains (CDD #10401) is also shown.

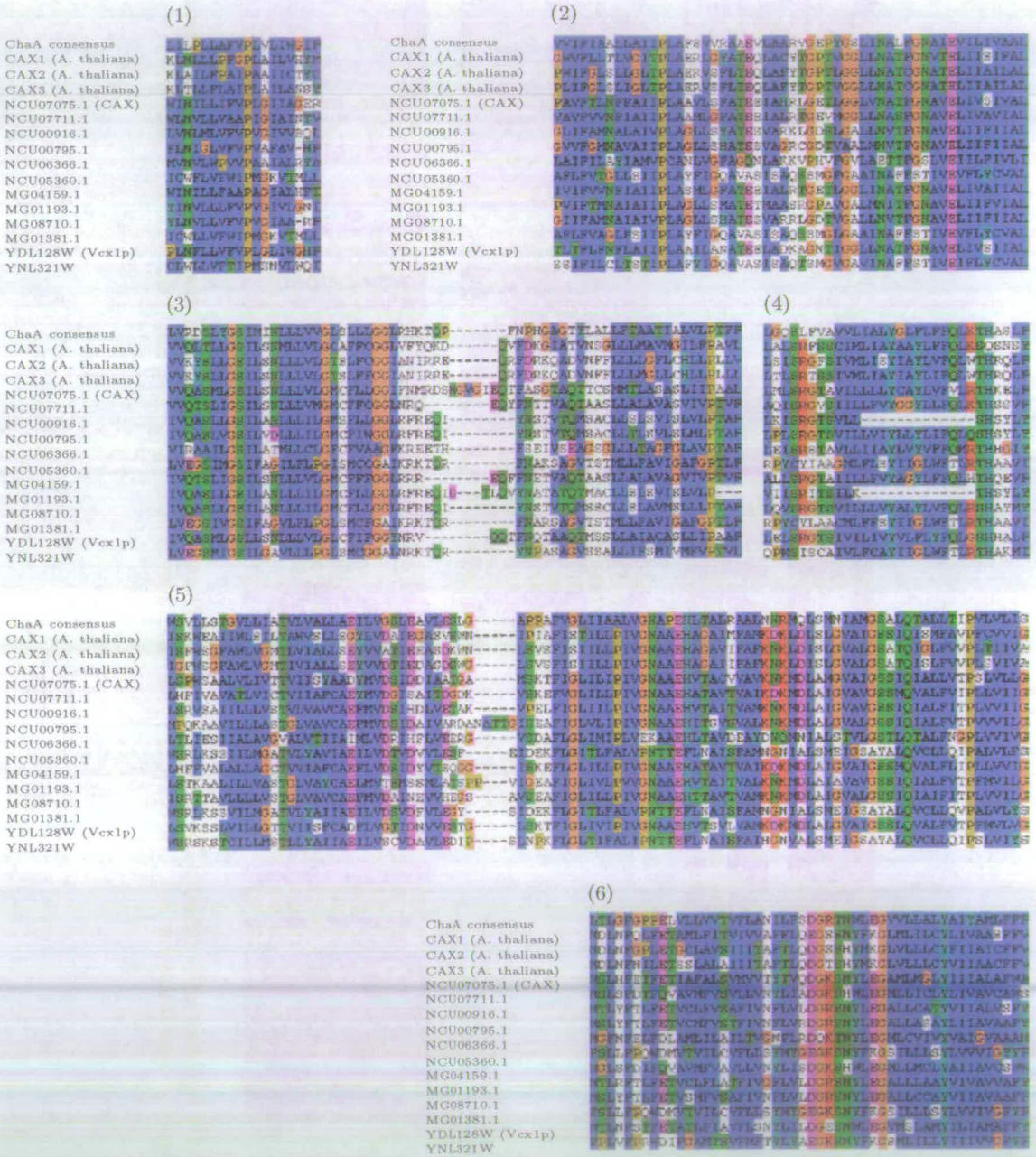

Figure 6.8: Regions of homology within potential Ca^{2+}/H^{+}-exchangers of *N. crassa*, *M. grisea* and *S. cerevisiae*. Examples of Ca^{2+}-transporters from other organisms are as described in Fig. 6.6. Consensus Ca^{2+}/H^{+} antiporter domain ChaA (CDD #COG0387) is also shown.

6.2.3.4 Other important Ca^{2+}-signalling proteins found

Many other important Ca^{2+}-signalling proteins were discovered during this analysis. Table 6.4 summarises the phospholipase C, calmodulin, calcineurin, Ca^{2+} and/or calmodulin dependent protein kinase and calnexin proteins found. The remaining Ca^{2+}-signalling proteins not described here are a diverse range of Ca^{2+} and/or calmodulin binding proteins that play important roles in transducing the Ca^{2+}-signals resulting from the activity of the proteins described in detail in this chapter.

6.2.3.5 Important Ca^{2+}-signalling proteins not found

A surprising difference between Ca^{2+}-signalling in the fungi examined as compared with plants and animals was also revealed by this analysis. An important aspect of Ca^{2+}-signalling in plant and animal cells involves Ca^{2+} release from internal stores. This is commonly mediated by the second messengers inositol 1,4,5 trisphosphate ($InsP_3$) and cADP ribose, sphingolipids, NAADP or by Ca^{2+}-induced Ca^{2+} release (Bootman et al., 2001). $InsP_3$ is present within *N. crassa* hyphae (Lakin-Thomas, 1993) and physiological evidence, including intracellular membrane associated $InsP_3$-activated Ca^{2+}-channel activity, supports a role in Ca^{2+}-signalling (Schultz et al., 1990; Cornelius et al., 1989). In spite of this, none of the fungi analysed here possessed recognisable $InsP_3$ receptors. In addition none of the following components of Ca^{2+} release from plant and animal internal stores were found in the fungi analysed: (a) ADP ribosyl cyclase, which synthesises cADP ribose or NAADP; (b) ryanodine receptor proteins, key components of Ca^{2+}-release mechanisms in plant and animal cells; (c) sphingosine kinases, which catalyse the formation of sphingosine 1-phosphate (Spiegel and Milstien, 2002); and (d) SCaMPER homologues, SCaMPER is a sphingolipid-activated protein that causes the release of Ca^{2+} from the ER of animal cells (Mao et al., 1996). These observations raise the question of whether other, perhaps novel, second

messenger systems responsible for Ca^{2+}-release from internal stores remain to be discovered in fungi.

6.3 Discussion

This analysis has identified many of the proteins likely to be necessary for Ca^{2+}-signalling in three important filamentous fungi: *N. crassa*, *A. fumigatus* and *M. grisea* (see Fig. 6.9). These proteins include previously unknown Ca^{2+}-permeable channels, Ca^{2+}-ATPases, Ca^{2+}/H^{+}-exchangers, Ca^{2+}/Na^{+}-exchangers, phospholipase C proteins and Ca^{2+} and/or CaM binding proteins. A web-based resource[7] has been made available containing detailed information regarding all of the proteins discovered during this analysis.

Although the total number of proteins found in the filamentous fungi is similar to the number found in budding yeast, this is unlikely to represent reality. Many more Ca^{2+} and/or CaM binding proteins were found in budding yeast than in the filamentous fungi. These proteins are difficult to identify by protein homology alone and the greater number found in yeast reflects the greater number reported in the literature compared with those reported for the three filamentous fungi, rather than the greater number present in their respective genomes. Looking at Ca^{2+}-permeable channels, Ca^{2+}-pumps and transporters, PLC's, CaM and calcineurin alone, *N. crassa*, *A. fumigatus* and *M. grisea* have 35, 19 and 37% more Ca^{2+}-signalling proteins than budding yeast, respectively. These results highlight both the potential importance and likely greater complexity of Ca^{2+}-signalling in filamentous fungi. Overall, therefore, the Ca^{2+}-signalling machinery in the filamentous fungi was more complex than in budding yeast. Given the greater diversity and heterogeneity of environments that filamentous fungi inhabit when compared to budding yeast, and also the greater complexity of the organisms themselves, this finding is not surprising.

[7] http://www.fungalcell.org/FDF/

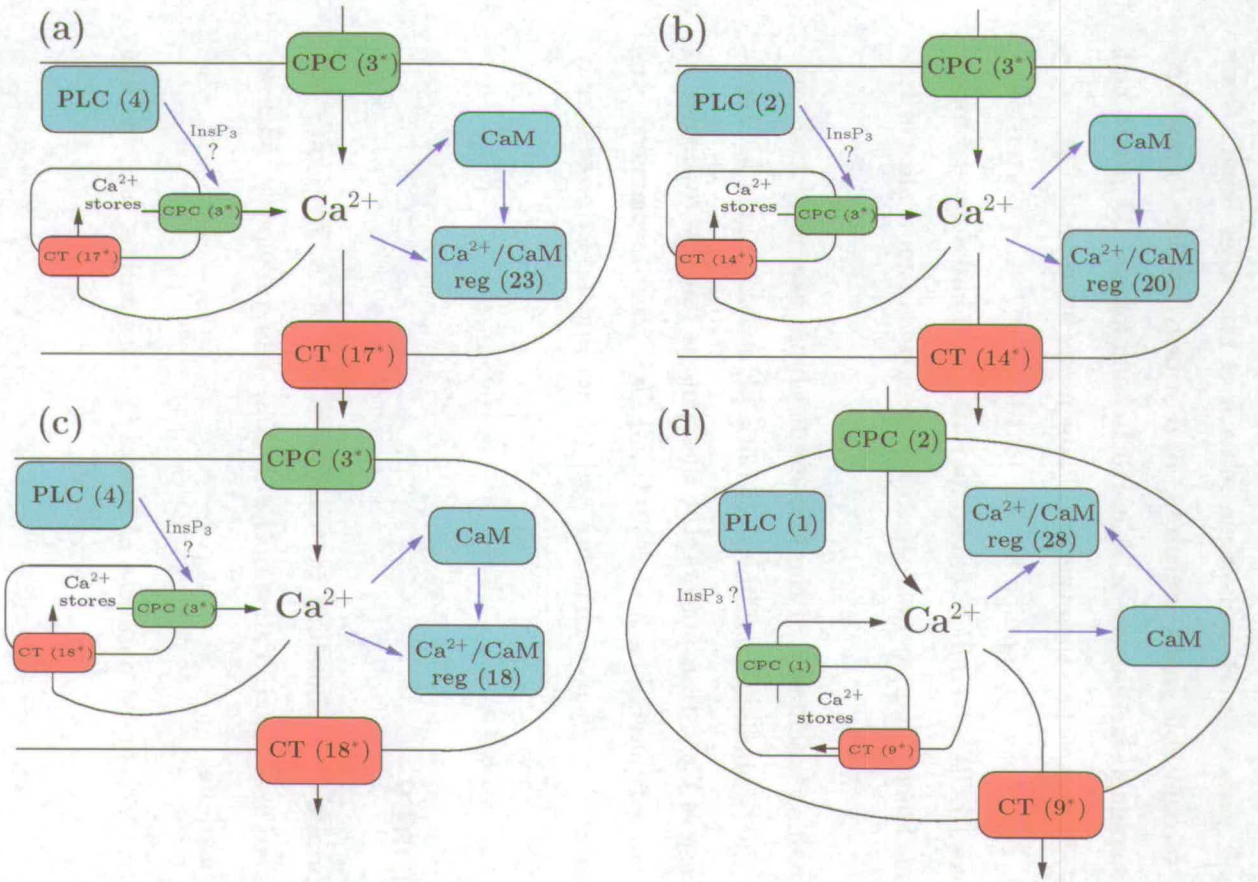

Figure 6.9: Overview of major intracellular Ca^{2+}-signalling proteins in (a) *N. crassa*, (b) *A. fumigatus*, (c) *M. grisea* and (d) *S. cerevisiae*. Asterisk, location in plasma membrane and/or organelle membranes not determined; CPC, Ca^{2+}-permeable channel; CT, Ca^{2+}-transporter; PLC, phospholipase C; CaM, calmodulin; Ca^{2+}/CaM reg, Ca^{2+} and/or calmodulin regulated. Numbers in brackets are number of proteins in that class. Black arrows indicate flow of Ca^{2+}. Blue arrows indicate regulation.

The Ca^{2+}-signalling machinery of the filamentous fungi had some notable similarities and differences. Ca^{2+}-permeable channel proteins were very similar between all three filamentous fungi (and budding yeast). Each fungus had 3 Ca^{2+}-permeable channels with a direct homologue in each of the other fungi. None of the fungi had recognisable $InsP_3$ receptors, ADP ribosyl cyclase, ryanodine receptor proteins, sphingosine kinases or SCaMPER homologues. *M. grisea* had more P-type Ca^{2+}-ATPases than the other two filamentous fungi but fewer Ca^{2+}-transporters than *N. crassa*. *A. fumigatus* also had few Ca^{2+}-transporters than *N. crassa* and fewer PLC's. Overall, *N. crassa* and *M. grisea* had a more complex Ca^{2+}-signalling machinery than *A. fumigatus*. The biological significance of this is unknown.

The Ca^{2+}-signalling machinery of the filamentous fungi examined had similarities with the Ca^{2+}-signalling machinery of both plants and animals. Interestingly, in the case of Ca^{2+}-transporters, the filamentous fungi were similar to both plants and animals having both Ca^{2+}/H^+ and Ca^{2+}/Na^+-exchangers. Animals have primarily Ca^{2+}/Na^+-exchangers and plants appear to possess only Ca^{2+}/H^+-exchangers.

6.4 Summary

- Many important Ca^{2+}-signalling proteins in *N. crassa*, *A. fumigatus* and *M. grisea* were discovered. The majority of these were previously unknown to filamentous fungi.
- An interactive web-based database of fungal Ca^{2+}-signalling proteins was made.
- The Ca^{2+}-signalling machinery was more complex in filamentous fungi than in budding yeast.
- None of the fungi examined had recognisable $InsP_3$ receptors, ADP ribosyl

cyclase, ryanodine receptor proteins, sphingosine kinases or SCaMPER homologues suggesting that the mechanisms of Ca^{2+}-release from internal Ca^{2+} stores may be different from that in animal and plant cells.

Chapter 7

Summary and Future Work

During this study I have developed a method for the quantitative measurement of $[Ca^{2+}]_c$ in living *N. crassa* hyphae. This involved the production of a new plasmid, pAZ6, which was shown to produced high levels of aequorin expression when transformed into several strains of *N. crassa*.

The effect of temperature on aequorin luminescence was found to be significant. However conversion of aequorin luminescence values into the Ca^{2+} concentrations using the appropriate calibration, normalised this effect. A computer program was written that enabled large amounts of data from the luminometer to be rapidly and accurately converted into Ca^{2+} concentrations. This program also performed a number of quantitative analyses on the converted data. The measurement of $[Ca^{2+}]_c$ transients and the quantification of Ca^{2+}-signatures using the methods developed was shown to be robust, reproducible and applicable to both wild-type and mutant strains of *N. crassa*. Furthermore, it was shown that it is possible to dissect the roles of different Ca^{2+}-signalling proteins through careful measurement of the Ca^{2+}-signature. These methods were used to provide evidence, in contrast to what has been previously reported (Bok et al., 2001), that the SPRAY protein is unlikely to influence Ca^{2+}-signalling through calcineurin, that CPA inhibits Ca^{2+}-ATPases in *N. crassa* as in other fungi (Nelson et al., 2003), plants (Sievers and Busch, 1992) and animals (Maruyama et al., 1997),

that *N. crassa* does not possess caffeine-sensitive Ca^{2+} stores with similar properties to plants (Arora and Ohlan, 1997), animals (Komori et al., 1995) and *A. awamori* (Nelson et al., 2003), that 2-APB has an unexpected agonistic effect on $[Ca^{2+}]_c$ signalling in *N. crassa*, and that increased $[Ca^{2+}]_c$ concentration does not accompany hyperbranching in *N. crassa*.

Studies on animal and plant cells (Berridge et al., 2000; Sanders et al., 2002), have established that changes in $[Ca^{2+}]_c$ following stimulation are typically very localised within cells. The Ca^{2+}-signatures which I have measured are a reflection of $[Ca^{2+}]_c$ changes averaged across thousands of fungal microcolonies within each plate microwell. Although aequorin-based systems are not well suited for the measurement of Ca^{2+} within individual hyphae (due to low light levels compared with what can be detected from fluorescent probes), this thesis has shown that aequorin is very well suited for Ca^{2+} measurement over an entire mycelium. My experimental approach is extremely well suited to quantitatively analysing Ca^{2+}-signatures. This is because I used multiwell plate luminometry that enabled the analysis of multiple samples in the same experiment. In most other studies involving the analysis of aequorin luminescence, light is detected from a single sample in a tube luminometer as, for example, in most studies on plants (Knight and Knight, 1995). Not only does the recombinant aequorin method now provide an easy and routine technique for Ca^{2+} measurement to experimentally study Ca^{2+}-signalling in wild type and mutant strains of *N. crassa*, it also provides a powerful analytical tool in a variety of other applications. The further analysis of mutants compromised in Ca^{2+}-signalling, and which are expressing aequorin, will allow different components of Ca^{2+}-signalling pathways to be dissected apart and identified. The genomic analysis of Ca^{2+}-signalling proteins encoded in the *N. crassa* done during this PhD (Galagan et al., 2003) will help determine which genes to mutate. Furthermore, aequorin can be used as a luminescent reporter in high throughput screens for mutants compromised in Ca^{2+}-signalling. Finally, fungi expressing recombinant aequorin can be used in high throughput screens for

the discovery of antifungal compounds which target Ca^{2+}-signalling because, as shown here, this system is ideally suited for high throughput assay development (Nelson et al., 2003).

Whether the three stimuli used in the present study caused localised $[Ca^{2+}]_c$ changes in hyphae will need further analysis at the subcellular level using low-light imaging techniques. This would best be achieved using a recombinant fluorescent probe such as a cameleon probe (Miyawaki et al., 1997) that is brighter than aequorin but still has the all the advantages of recombinant probes. One therefore needs to be very careful about extrapolating from measurements of the Ca^{2+}-signature at the global multi-colonial level to what this represents in terms of the likely heterogeneity of Ca^{2+} transients at the subcellular level.

Detailed qualitative and quantitative analyses were performed on nine genetically-unlinked hyperbranching strains of *N. crassa*. It was shown that these strains demonstrated differences in hyphal form, branching frequency, hyphal extension rate, hyphal width and distance between septa. Observations of nuclear distribution in *cot-1* showed an unusual distribution of nuclei in *cot-1* hyphae at the restrictive, but not the permissive temperature. It was shown that the *cot-2* was strain of *N. crassa* can be complemented with the Orbach/Sachs pMOcosX cosmid G23:G5 and that *cot-4* strain can be complemented with the Orbach/Sachs pMOcosX cosmid X15:E10. The *cot-4* gene was cloned and found to have a mutation in the catalytic subunit of calcineurin, a Ca^{2+}/calmodulin-dependent protein phosphatase. However several single base differences between the wild-type and *cot-4* mutant alleles of the *cna-1* gene which were found need to be confirmed. Future work on this project should therefore include the re-amplification and resequencing of the native *cot-4* gene.

An analysis of the genomes of *N. crassa*, *A. fumigatus* and *M. grisea* has identified many of the fundamental Ca^{2+}-signalling proteins present in filamentous fungi. In particular, these proteins include a number of previously unknown Ca^{2+}-permeable channels, Ca^{2+}-pumps and Ca^{2+}-transporters. The Ca^{2+}-signalling

machinery of filamentous fungi was found to be more complex than that of budding yeast. The large number of Ca^{2+}-signalling proteins found in the filamentous fungi examined highlights the importance and complexity of Ca^{2+}-signalling in these organisms. Interestingly, none of the fungi examined had recognisable $InsP_3$ receptors, ADP ribosyl cyclase, ryanodine receptor proteins, sphingosine kinases or SCaMPER homologues despite the fact that pharmacological evidence points towards the presence of internal $InsP_3$-gated Ca^{2+} stores in *N. crassa* (Cornelius et al., 1989; Schultz et al., 1990; Silverman-Gavrila and Lew, 2002). These observations raise the question of whether other, perhaps novel, second messenger systems responsible for Ca^{2+}-release from internal stores remain to be discovered in fungi. All the Ca^{2+}-signalling proteins found in *N. crassa*, *A. fumigatus*, *M. grisea* and *S. cerevisiae* were deposited in an interactive web-based database which will be available as a resource for the scientific community at large[1]. This resource also contains protein and DNA sequences and a large amount of other information on the proteins found. An inventory of Ca^{2+}-signalling proteins in filamentous fungi is an important starting point for reverse genetic and physiological approaches aiming at elucidating the biological significance of these proteins. Further development of the web-based resource made during my PhD should include software code which automatically performs a BLAST analysis of all the proteins in the database every week. This code would also add the information from these BLAST searches into the database, thus keeping it up to date with the ever-changing genomic and proteomic information available.

The future for Ca^{2+}-signalling research in filamentous fungi is bright! The aequorin system of Ca^{2+} measurement developed here will provide a convenient and sensitive method for the investigation the roles of different proteins in Ca^{2+}-signalling in living fungi. The next step in this research should therefore be the generation of mutant strains, impaired in the function of specific Ca^{2+}-signalling proteins. A careful study of all aspects of the resulting strains, especially their

[1]http://fungalcell.org/FDF/

Ca^{2+}-signatures, will reveal new and important information about the nature and biological significance of Ca^{2+}-signalling in filamentous fungi.

Appendices

Appendix A

Chemicals Used in this Study

Table A.1: Chemicals used in this study

acetamide	Sigma Chemical Co., USA
acetic acid (glacial)	Frutarom Ltd., Israel
aequorin D	Cambridge Bioscience, UK
agar	Becton Dickinson Company, USA
agarose	Techcomp Ltd., Hong Kong
ampicillin	Sigma Chemical Co., USA
2-APB	Calbiochem, UK
bacto peptone	Difco Laboratories, USA
bacto tryptone	Difco Laboratories, USA
bacto yeast extract	Difco Laboratories, USA
bicinchoninic acid solution	Sigma Chemical Co., USA
BSA	Sigma Chemical Co., USA
bromophenol blue	Merck, Germany
caffeine	Sigma Chemical Co., UK
calcium chloride	Sigma Chemical Co., USA
chitinase	Sigma Chemical Co., USA
chloramphenicol	Sigma Chemical Co., USA

chloroform	Frutarom Ltd., Israel
citric acid	Merck, Germany
coelenterazine (native)	Cambridge Bioscience, Cambridge, UK or Biosynth AG, Staad, Switzerland
copper (II) sulphate pentahydrate 4% (w/v) solution	Sigma Chemical Co., USA
CTAB	BDH Chemicals, England
$CuSO_4 \cdot 5H_2O$	J.T.Baker, USA
cyclopiazonic acid	Sigma-Aldrich, UK
cyclosporin A	Sigma Chemical Co, UK
dimethyl sulfoxide	Fluka Chemie, Switzerland
ethanol	Carlo Erba, France
ethidium bromide	Sigma Chemical Co., USA
EDTA	United States Biochem. Corp., USA
EGTA	United States Biochem. Corp., USA
$Fe(NH_4)_2(SO_4)_2 \cdot 6H_2O$	Merck
ficoll (type 400; Pharmica)	Sigma Chemical Co., USA
FK506	Calbiochem, UK
FM4-64	Molecular Probes Inc., Eugene, OR, USA
fructose(D)	Sigma Chemical Co., USA
Glucanex	Novo Nordisk Ferment Ltd., CH4 243, Dittingen, Switzerland
glucose(D)	BDH Chemicals, England

glycerol	United States Biochem. Corp., USA
H_3BO_3 (anhydrous)	J.T.Baker, USA
heparin (sodium)	Amersham Life Sciences, UK
hydrochloric acid	Frutarom Ltd., Israel
hygromycin B (in PBS 50 mg ml^{-1}	Roche Diagnostics, GmbH, Germany
KH_2PO_4 (anhydrous)	Merck, Germany
β-mercaptoethanol	Sigma Chemical Co., USA
$MgSO_4 \cdot 7H_2O$	Merck, Germany
$MnSO_4 \cdot 1H_2O$	BDH Chemicals, England
$Na_2Mo_4 \cdot 2H_2O$	Merck, Germany
NH_4NO_3 (anhydrous)	Merck, Germany
Novozyme	Calbiochem-Novabiochem Corporation La Jolla, CA 92039-2087
nutrient broth	Difco Laboratories, USA
1-octanol	Sigma Chemical Co., USA
polyethylene glycol 4000	BDH Chemicals, England
propidium iodide	Sigma Chemical Co., USA
quinic acid	Sigma Chemical Co., USA
RNAase	Boehringer Mannheim GmbH, Germany
sodium acetate	Sigma Chemical Co., USA
sodium bisulphate	Sigma Chemical Co., USA
sodium chloride	J.T.Baker, USA
sodium citrate$\cdot 2H_20$	Sigma Chemical Co., USA
sodium dodecyl sulphate	Chem-Impex International, USA
sodium hydroxide	Merck, Germany

sorbitol(D)	Sigma Chemical Co., USA
sorbose(L)	Sigma Chemical Co., UK
sucrose	Sugat Ltd., Israel
Trizma-base	Sigma Chemical Co., USA
Trizma-HCl	Sigma Chemical Co., USA
Tween 20	Sigma Chemical Co., USA
xylene cyanol FF	Sigma Chemical Co., USA
$ZnSO_4 \cdot 7H_2O$	BDH Chemicals, England

Appendix B

DNA and Amino Acid Sequences

Table B.1: The DNA and corresponding protein sequence of *aeqS*

C	CGC	AGA	CCT	G†AA	TTC	ATG	ACC	TCC	AAG	CAG	TAC	TCC	GTC	AAG
						MET	THR	SER	LYS	GLN	TYR	SER	VAL	LYS
CTT	ACC	TCC	GAC	TTC	GAC	AAC	CCC	CGC	TGG	ATC	GGC	CGC	CAC	AAG
LEU	THR	SER	ASP	PHE	ASP	ASN	PRO	ARG	TRP	ILE	GLY	ARG	HIS	LYS
CAC	ATG	TTC	AAC	TTC	CTC	GAC	GTC	AAC	CAC	AAC	GGC	AAG	ATT	TCC
HIS	MET	PHE	ASN	PHE	LEU	ASP	VAL	ASN	HIS	ASN	GLY	LYS	ILE	SER
CTC	GAC	GAG	ATG	GTC	TAC	AAG	GCC	TCC	GAC	ATC	GTC	ATC	AAC	AAC
LEU	ASP	GLU	MET	VAL	TYR	LYS	ALA	SER	ASP	ILE	VAL	ILE	ASN	ASN
CTC	GGC	GCT	ACC	CCC	GAG	CAG	GCC	AAG	CGC	CAC	AAG	GAC	GCC	GTC
LEU	GLY	ALA	THR	PRO	GLU	GLN	ALA	LYS	ARG	HIS	LYS	ASP	ALA	VAL
GAG	GCC	TTC	TTC	GGC	GGT	GCC	GGC	ATG	AAG	TAC	GGC	GTC	GAG	ACC
GLU	ALA	PHE	PHE	GLY	GLY	ALA	GLY	MET	LYS	TYR	GLY	VAL	GLU	THR
GAC	TGG	CCC	GCC	TAC	ATC	GAG	GGC	TGG	AAG	AAG	CTC	GCC	ACC	GAC
ASP	TRP	PRO	ALA	TYR	ILE	GLU	GLY	TRP	LYS	LYS	LEU	ALA	THR	ASP
GAG	CTC	GAG	AAG	TAC	GCC	AAG	AAC	GAG	CCC	ACC	CTC	ATC	CGC	ATC
GLU	LEU	GLU	LYS	TYR	ALA	LYS	ASN	GLU	PRO	THR	LEU	ILE	ARG	ILE
TGG	GGC	GAC	GCC	CTC	TTC	GAC	ATC	GTC	GAC	AAG	GAC	CAG	AAC	GGT
TRP	GLY	ASP	ALA	LEU	PHE	ASP	ILE	VAL	ASP	LYS	ASP	GLN	ASN	GLY
GCC	ATC	ACC	CTC	GAC	GAG	TGG	AAG	GCC	TAC	ACC	AAG	GCC	GCC	GGC
ALA	ILE	THR	LEU	ASP	GLU	TRP	LYS	ALA	TYR	THR	LYS	ALA	ALA	GLY
ATC	ATT	CAG	TCC	AGC	GAG	GAC	TGC	GAA	GAG	ACC	TTC	CGC	GTC	TGC
ILE	ILE	GLN	SER	SER	GLU	ASP	CYS	GLU	GLU	THR	PHE	ARG	VAL	CYS
GAC	ATC	GAC	GAG	TCC	GGC	CAG	CTC	GAT	GTC	GAT	GAG	ATG	ACC	CGC
ASP	ILE	ASP	GLU	SER	GLY	GLN	LEU	ASP	VAL	ASP	GLU	MET	THR	ARG
CAG	CAC	CTC	GGC	TTC	TGG	TAC	ACC	ATG	GAC	CCC	GCC	TGC	GAG	AAG
GLN	HIS	LEU	GLY	PHE	TRP	TYR	THR	MET	ASP	PRO	ALA	CYS	GLU	LYS
CTC	TAC	GGC	GGT	GCC	GTC	CCC	TAA	GAT	CTA	AGC	TTG	GAT	CCA	GCC
LEU	TYR	GLY	GLY	ALA	VAL	PRO	STOP							

†*Eco*RI cuts between nucleotides 11 and 12. The ATG start and TAA stop codons are underlined.

Appendix C

Plasmids

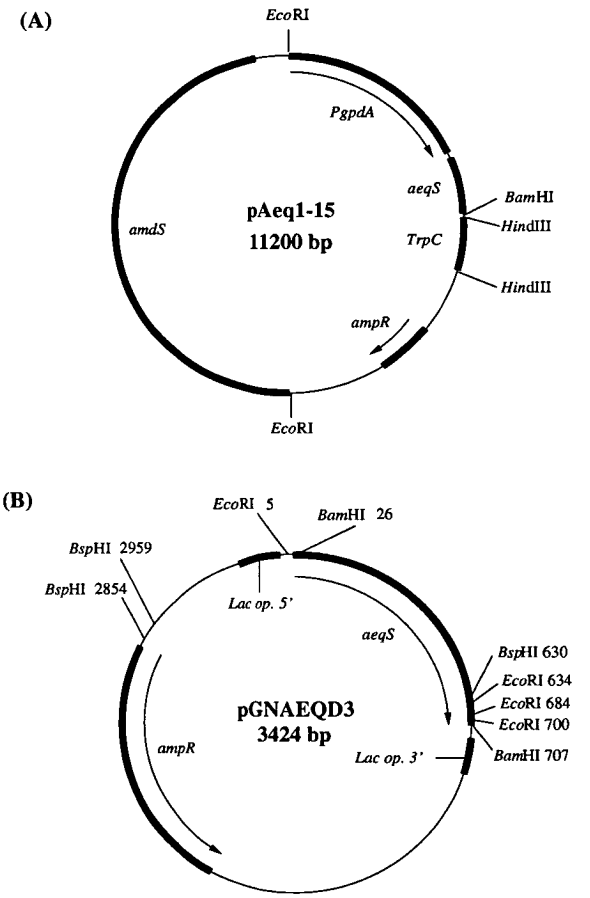

Figure C.1: (a) pAEQS1-15. A plasmid containing the *aeqS* gene (encoding apoaequorin) under the control of the *gpdA* promotor and *TrpC* terminator from *A. nidulans*; (b) pGNAEQD3. The *Eco*RI and *Bam*HI sites shown both excise the whole *aeqS* gene.

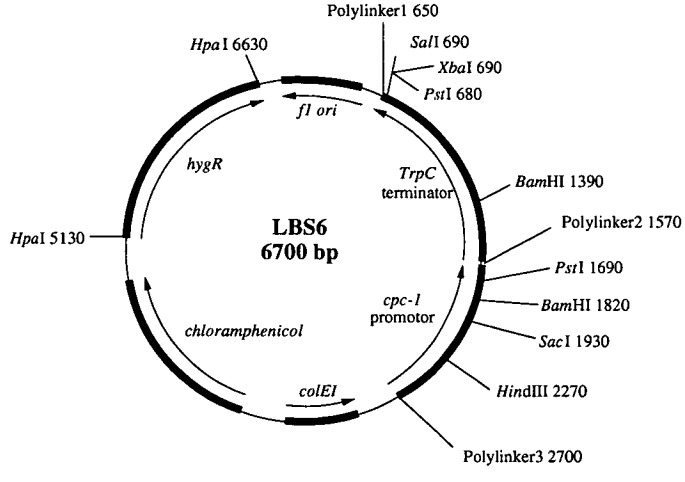

Figure C.2: Plasmid map of LBS6. Polylinker1: T7.*Kpn*I.*Apa*I.*Xho*I.*Sal*I.*Cla*I.*Hin*dIII; Polylinker2: *Eco*RI.*Pst*I.*Sma*I.*Bam*HI; Polylinker3: *Xba*I.*Not*I.*Sac*I.T3.

Appendix D

Contents of Solutions and Gels

Table D.1: Contents of solutions and gels

Solution	Ingredients
DNA Extraction Buffer	1 vol. DNA Ext. Buffer Component 1 1 vol. nuclei lysis buffer, 0.4 vol. (5% w/v) *N*-Lauroylsarcosine, 38 mg sodium bisulphate per 10 ml buffer
DNA Extraction Buffer Component 1	0.35 M sorbitol, 0.1 M Tris-base 5 mM EDTA adjust to pH 7.5 with HCL
DNA Loading Buffer	0.25% bromophenol blue, 0.25% xylene cyanol FF, 15% Ficoll in dH_2O
Hybridisation Solution	6 ml 20*SSC, 2 ml 50* Denhard's, 200 μl salmon sperm (100 $\mu g\ ml^{-1}$), 10 ml formamide 0.5 ml 20% SDS, 1.3 ml dH_2O
DTC-Ca^{2+} Medium	7.35 g $CaCl_2$, 0.5 g Bacto yeast extract 0.5 g Bacto Tryptone, 2 ml Vogel's *50 stock solution, 1.5 g sucrose 2 g agar
FGS*10	100 g sorbose, 2.5 g fructose, 2.5 g glucose dH_2O to a vol. of 500 ml

LB Medium (liquid)	10 g Bacto Tryptone, 5 g Bacto yeast extract 10 g NaCl dH_2O to final vol. of 1 litre
LB Medium (solid)	as liquid LB plus 15 mg ml^{-1} agar
Nuclei Lysis Buffer	0.2 M Tris-base, 0.05 M EDTA, 2 M NaCl 2% (w/v) CTAB‡
Nutrient Agar	0.8 g nutrient broth, 0.8 g agar dH_2O to total vol. of 100 ml
Plating Medium	4 ml Vogel's*50, 3 g agar, 176 ml dH_2O autoclave then add 20 ml FGS*10 and antibiotics if appropriate
Protein Extraction Buffer	5 ml 200 mM EGTA pH 8, 5 ml 1 M Tris pH 7.4, 10 ml 5 M NaCl, 79.8 μl stock β-mercaptoethanol, dH_2O to final vol. of 100 ml
Protoplast Storage Solution	8 ml STC, 2 ml PTC, 100μl DMSO‡ mix components and filter sterilise
PTC	40 g PEG 4000†, 5 ml 1 M Tris-HCl pH 8 5 ml 1 M $CaCl_2$ dH_2O to final vol. of 100 ml
Regeneration Medium	4 ml Vogel's*50, 36.8 g sorbitol, 3 g agar, 170 ml dH_2O, autoclave then add 20 ml FGS*10
STC	18.2 g sorbitol, 5 ml 1 M Tris-HCl pH 8 5 ml 1 M $CaCl_2$ dH_2O to final vol. of 100 ml

Trace Element Solution	5 g citric acid·1H_2O, 5 g $ZnSO_4$·7H_2O (zinc sulphate), 1 g $Fe(NH_4)_2(SO_4)_2$·6H_2O (ferrous amonium sulphate hexahydrate) 0.25 g $CuSO_4$·5H_2O (cupric sulphate), 0.05 g $MnSO_4$·1H_2O (manganese sulfate), 0.05 g H_3BO_3 (anhydrous) (boric acid), 0.05 g Na_2MoO_4·2H_2O (molybdic acid sodium salt dihydrate) dH_2O to final vol. of 100 ml plus 2 ml chloroform
TAE*50 Buffer for DNA Gels	242 g Tris Base, 57.1 g glacial acetic acid 100 ml 0.5 M EDTA§ pH 8, dH_2O to final vol. of 1 litre
Vogel*50 Solution	dissolve successively in 650 ml dH_2O: 125 g $C_6H_5Na_3O_7$·2H_2O (tri-sodium citrate dihydrate), 150 g KH_2PO_4 (monopotassium phosphate anhydrous), 250 g NH_4NO_3 (ammonium nitrate anhydrous)* 10 g $MgSO_4$·7H_2O (magnesium sulphate), 5 g $CaCl_2$·2H_2O (dissolve first in 25 ml H_2O) then add: 5 ml trace element solution, 2.5 ml biotin solution (0.1 mg ml^{-1} in dH_2O), dH_2O to a vol. of 1 litre plus 2 ml chloroform as a preservative
Vogel's Sucrose Medium (liquid)	4 ml Vogel's*50 stock solution, 3 g sucrose dH_2O to 200 ml total
Vogel's Sucrose Medium (solid)	4 ml Vogel's*50 stock solution, 3 g sucrose 4 g agar, dH_2O to 200 ml total

Working Reagent	50 vol. bicinchoninic acid solution, 1 vol. copper(II) sulphate pentahydrate 4% (w/v) solution

*Replace the 250 g of anhydrous NH_4NO_3 with 29.5 g acetamide to produce a medium which will select for the *amdS* gene (Yamashiro et al., 1992); †PEG 4000 = polyethylene glycol 4000; ‡DMSO = dimethyl sulfoxide; §EDTA = ethylenediam-inetetraacetic acid; ♯CTAB = cetyltrimethylammonium bromide

Appendix E

Software CD

This CD contains four software packages:

1. **getproteinunkns.sh**: written to (a) convert A_{590} readings of protein extracts into actual protein concentrations using a standard curve and (b) calculate the dilutions of each sample with extraction buffer to give a final concentration of 40 μg total protein per 100 μl of solution.

2. **getaeqamnt.pl**: written to convert aequorin discharge data to amount aequorin per g total protein.

3. **term-bert** and **luminometer_subs**: written to (a) convert the data produced by our luminometer from RLU to Ca^{2+} concentrations, (b) quantify various parameters of the Ca^{2+}-signature, and (c) perform statistical analysis on these data.

4. **The Fungal Cell Biology Group Database Facility**: this is a series of programs, which when used in conjunction with a web server and a MySQL database package, provide a complete web-based database as described in Chapter 6. These files can be found in the "FDF" directory.

Appendix F

Papers Published in Scientific Journals

The genome sequence of the filamentous fungus *Neurospora crassa*

James E. Galagan[1], Sarah E. Calvo[1], Katherine A. Borkovich[2], Eric U. Selker[3], Nick D. Read[4], David Jaffe[1], William FitzHugh[5], Li-Jun Ma[1], Serge Smirnov[1], Seth Purcell[1], Bushra Rehman[1], Timothy Elkins[1], Reinhard Engels[1], Shanguang Wang[1], Cydney B. Nielsen[1], Jonathan Butler[1], Matthew Endrizzi[1], Dayong Qui[1], Peter Ianakiev[1], Deborah Bell-Pedersen[6], Mary Anne Nelson[7], Margaret Werner-Washburne[7], Claude P. Selitrennikoff[8], John A. Kinsey[9], Edward L. Braun[10], Alex Zelter[A,11], Ulrich Schulte[12], Gregory O. Kothe[3], Gregory Jedd[13], Werner Mewes[14,15], Chuck Staben[16], Edward Marcotte[17], David Greenberg[18], Alice Roy[1], Karen Foley[1], Jerome Naylor[1], Nicole Stange-Thomann[1], Robert Barrett[1], Sante Gnerre[1], Michael Kamal[1], Manolis Kamvysselis[1], Evan Mauceli[1], Cord Bielke[14], Stephen Rudd[15], Dmitrij Frishman[15], Svetlana Krystofova[2], Carolyn Rasmussen[19], Robert L. Metzenberg[20], David D. Perkins[21], Scott Kroken[22], Carlo Cogoni[21], Giuseppe Macino[21], David Catcheside[22], Weibd Li[18], Robert J. Pratt[5], Stephen A. Osmani[23], Colin P. C. DeSouza[24], Louise Glass[19], Marc J. Orbach[25], J. Andrew Berglund[3], Rodger Voelker[3], Oded Yarden[11], Michael Plamann[26], Stephan Seiler[26], Jay Dunlap[27], Alan Radford[28], Rodolfo Aramayo[6], Donald O. Natvig[7], Lisa A. Alex[29], Gertrud Mannhaupt[14], Daniel J. Ebbole[30], Michael Freitag[3], Ian Paulsen[31], Matthew S. Sachs[31], Eric S. Lander[A,32], Chad Nusbaum[1] & Bruce Birren[1]

A list of author affiliations appears at the end of the paper

Neurospora crassa **is a central organism in the history of twentieth-century genetics, biochemistry and molecular biology. Here, we report a high-quality draft sequence of the *N. crassa* genome. The approximately 40-megabase genome encodes about 10,000 protein-coding genes—more than twice as many as in the fission yeast *Schizosaccharomyces pombe* and only about 25% fewer than in the fruitfly *Drosophila melanogaster*. Analysis of the gene set yields insights into unexpected aspects of *Neurospora* biology including the identification of genes potentially associated with red light photobiology, genes implicated in secondary metabolism, and important differences in Ca^{2+} signalling as compared with plants and animals. *Neurospora* possesses the widest array of genome defence mechanisms known for any eukaryotic organism, including a process unique to fungi called repeat-induced point mutation (RIP). Genome analysis suggests that RIP has had a profound impact on genome evolution, greatly slowing the creation of new genes through genomic duplication and resulting in a genome with an unusually low proportion of closely related genes.**

Research on *Neurospora* in the early part of the twentieth century paved the way for modern genetics and molecular biology. First documented in 1843 as a contaminant of bakeries in Paris[1], *Neurospora* was developed as an experimental organism in the 1920s[2,3]. Subsequent work on *Neurospora* by Beadle and Tatum[4] in the 1940s established the relationship between genes and proteins, summarized in the 'one-gene-one-enzyme' hypothesis. In the latter half of the century, *Neurospora* had a central role as a model organism, contributing to the fundamental understanding of genome defence systems, DNA methylation, mitochondrial protein import, circadian rhythms, post-transcriptional gene silencing and DNA repair[5]. Because *Neurospora* is a multicellular filamentous fungus, it has also provided a system to study cellular differentiation and development as well as other aspects of eukaryotic biology[6].

The legacy of over 70 years of research[7], coupled with the availability of molecular and genetic tools, offers enormous potential for continued discovery. The sequencing of the *N. crassa* genome was undertaken to maximize this potential. Here, we report an initial sequence and analysis of the *Neurospora* genome.

Neurospora genome sequence

The *Neurospora* genome is much larger (greater than 40 megabases (Mb)) than that of *S. pombe* and *Saccharomyces cerevisiae* (both about 12 Mb). Accordingly, first we sought to produce and analyse a high-quality draft sequence *en route* to a finished sequence.

The genome sequence was assembled from deep whole-genome shotgun (WGS) coverage obtained by paired-end sequencing from a variety of clone types (Supplementary Information). In all, the data provided an average of >20-fold sequence coverage and >98-fold physical coverage of the genome. The Arachne package[8] was used to assemble the draft genome sequence. The resulting assembly consists of 958 sequence contigs with a total length of 38.6 Mb (Table 1) and an N50 length of 114.5 kilobases (kb) (that is, 50% of all bases are contained in contigs of at least 114.5 kb). Contigs were assembled into 163 scaffolds with a total length of 39.9 Mb (including gaps between contigs) and an N50 length of 1.56 Mb.

Most of the assembly (97%) is contained in the 44 largest scaffolds, and there are 38 tiny scaffolds with lengths <4 kb. Forty-two of the large scaffolds (and one of the smaller ones) could be anchored readily to the *Neurospora* genetic map[9] by virtue of their containing genetic markers with sequence.

The assembly has long-range continuity, with the N50 scaffold size being nearly 1,000-fold larger than the average gene size. The assembly represents the vast majority of the genome, as assessed by comparison with available finished sequence and genetic markers. It contains 99.13% of available finished sequence (17 Mb from linkage groups II and V[10]) and all of the 252 genetic markers with sequence. This estimate, however, does not account for unusual genomic regions such as the ribosomal DNA repeats, centromeres and telomeres; such regions may contain about 1.7 Mb of additional sequence[10], corresponding to 2–3% of the genome that cannot be assembled readily with available techniques. The long-range continuity of the assembly was also confirmed by comparisons with previously described bacterial artificial chromosome (BAC) physical maps for linkage groups II and V[11], as only one discrepancy was noted.

The assembly also has high accuracy, with 99.9% of the sequence having Arachne quality scores ≥30. Comparison with the 17 Mb of finished sequence confirms the sequence accuracy, with a discrepancy rate for this subset of less than 10^{-5}. The comparison also largely confirms the assembly, as only 12 minor discrepancies were identified (Supplementary Information).

articles

Genes

Gene count and basic characteristics

A total of 10,082 protein-coding genes (9,200 longer than 100 amino acids) were predicted (Table 1 and Supplementary S6). This constitutes nearly twice as many genes as in *S. pombe* (about 4,800) and *S. cerevisiae* (about 6,300), and nearly as many as in *D. melanogaster* (about 14,300). Genes cover at least 44% of the genome sequence with an average gene density of one gene per 3.7 kb. The average gene length of 1.67 kb is slightly longer than the 1.4-kb average gene length for both *S. cerevisiae* and *S. pombe*. The difference in gene length is due to the greater number of introns in *Neurospora* genes—an average of 1.7 introns per gene with an average intron size of 134 nucleotides. Notably, most predicted *Neurospora* introns lack a polypyrimidine tract, which is common in other eukaryotic introns, but do contain a strong branchpoint sequence (Supplementary Information).

Comparative analysis

A total of 4,140 (41%) *Neurospora* proteins lack significant matches to known proteins from public databases (Table 1), reflecting the early stage of fungal genome exploration and the diversity of fungal genes remaining to be described. Furthermore, 5,805 (57%) *Neurospora* proteins do not have significant matches to genes in either of the sequenced yeast species (Supplementary Information). When compared to sequenced eukaryotes, a total of 1,421 (14%) *Neurospora* genes display best BLASTP matches to proteins in either plants or animals (Supplementary Information). Of these, 384 lack high-scoring hits to either sequenced yeast species. These data reflect the biology shared by filamentous fungi and higher eukaryotes, which in a number of cases is absent in the yeasts.

Epigenetics, genome defence and genome evolution

Neurospora is an important model for the study of epigenetic phenomena, possessing a wide variety of epigenetic mechanisms and related genome defence mechanisms. The most remarkable of these mechanisms is repeat-induced point mutation (RIP), a process unique to fungi.

Repeat-induced point mutation

First discovered in *Neurospora*[6,7], RIP is a process that efficiently detects and mutates both copies of a sequence duplication. RIP acts during the haploid dikaryotic stage of the *Neurospora* sexual reproductive cycle, causing numerous C•G to T•A mutations within duplicated sequences. In a single passage through the sexual cycle, up to 30% of the C•G pairs in duplicated sequences can be mutated, with a strong preference for C to T mutations occurring at CpA dinucleotides[14]. The pattern of mutations produces a characteristic skewing of dinucleotide frequencies that allows RIP-mutated sequences to be detected accurately[15]. RIP requires a minimal duplicated sequence length of about 400 base pairs (bp)[16] and greater than roughly 80% sequence identity between duplicates[17]. In addition to suffering mutations, RIP-mutated sequences are frequent targets for DNA methylation. As with mammals, DNA methylation has been shown to cause gene silencing in *Neurospora*[18]. RIP thus mutates and epigenetically silences repetitive DNA.

RIP has been proposed to act as a defence against selfish or mobile DNA[19]. However, because RIP mutation and methylation can extend beyond the bounds of duplicated sequences[17], RIP can have both mutational and epigenetic effects on neighbouring unique sequences. Furthermore, RIP acts on all duplicated sequences, including those arising from large-scale chromosomal duplications as well as gene duplications[20]. The presence of RIP thus has profound consequences for the evolution of the *Neurospora* genome. Indeed, it has been proposed that RIP might prevent gene innovation through gene duplication[18,21]. With the availability of the *Neurospora* genome sequence, we were able to address this hypothesis.

Table 1 *Neurospora crassa* genome features

Feature	Value
General	
Size (bp) (assembly 6)	39,639,760
Chromosomes	7
C + G content (%)	50
Protein-coding genes	10,082
Protein-coding genes >100 amino acids	9,200
tRNA genes	424
5S rRNA genes	74
Per cent coding	44
Per cent intron	6
Average gene size (bp)	1,673 (681 amino acids)
Average number gene clusters (bp)	1,050
Predicted protein-coding sequences	
Identified by similarity to known sequences	5,035 (50%)
Conserved hypothetical proteins	4,906 (49%)
Predicted proteins (no similarity to known sequences)	4,140 (41%)

Multigene families

To investigate the impact of RIP on protein families in *Neurospora*, genes were clustered into 'multigene families' on the basis of an all versus all comparison of protein sequences (see Methods). As shown in Fig. 1, the percentage of genes in multigene families in selected sequenced eukaryotes is correlated with genome size. However, in marked contrast to the other analysed organisms, *Neurospora* possesses many fewer genes in multigene families than expected. When the analysis is expanded to include an additional 17 sequenced prokaryotes (Supplementary Information), only *Mycoplasma genitalium*, *Mycoplasma pulmonis*, *Ureaplasma urealyticum* and *Vibrio cholerae* display a correspondingly small proportion of genes in families. This is noteworthy considering that the *Mycoplasma* genus is thought to have undergone reductive evolution and represent minimal life forms[22].

Our analysis reveals another characteristic of *Neurospora* gene families. Unlike other sequenced eukaryotes, *Neurospora* possesses only a handful of highly similar gene pairs. Figure 2 displays histograms of amino acid and nucleotide similarities between each gene in the six organisms analysed and the best-matching gene in that organism. A significant proportion of genes have best matches with greater than 80% amino acid and nucleotide identity in all the organisms considered except *Neurospora*. *Neurospora* contains only eight genes with top matches of greater than 80% amino acid or coding sequence identity. This value is significant because, as described above, RIP mutates duplicated sequences that display greater than about 80% nucleotide similarity. Thus, the small proportion of genes in multigene families and the near absence of highly similar genes are consistent with the actions of RIP.

An example of the lack of highly similar genes in multigene families is revealed in an analysis of predicted major facilitator superfamily (MFS) sugar transporters (Fig. 3). *Neurospora* has about the same number of predicted MFS sugar transporters as *S. cerevisiae*. However, a phylogenetic analysis of fungal sugar transporters indicates that the *Neurospora* proteins are substantially more divergent than those of *S. cerevisiae* as well as those of *S. pombe*. Furthermore, the *Neurospora* transporters contain no apparent instances of recent duplication. In contrast, most of the *S. cerevisiae* HXT hexose and *S. pombe* GHT transporters represent two relatively recent and independent expansions and include very recently duplicated genes. Thus, despite a diversity of MFS sugar transporters, *Neurospora* seems to lack close paralogues in this gene family, consistent with the results of the genome-wide multigene family analysis.

Analyses of other gene families yielded similar results (data not shown). Furthermore, the paucity of closely related sequences is evident not only at the level of complete genes, but even at the level of individual exons, protein domains and protein architectures (Supplementary S4).

Gene evolution through gene duplication

The above results suggest that RIP has had a powerful impact in suppressing the creation of new genes or partial genes through genomic duplication. This is consistent with the large number of mutations induced in duplicated sequences by RIP. Computer simulations (see Methods) indicate that after a gene duplication, each copy has an 80% probability of acquiring an in-frame stop codon after only a single round of RIP and a 99.5% probability by the point that RIP has mutated the copies to less than 85% nucleotide similarity. The high frequency of stop codons reflects the preference of RIP for mutating CpA to TpA, increasing the prevalence of the stop codons TAA and TAG.

These results raise the critical question of whether any significant gene duplication has occurred in *Neurospora* subsequent to the acquisition of RIP. We searched for empirical evidence of duplicated genes that have survived RIP by analysing the set of *Neurospora* coding sequences using two different measures[15] for detecting RIP-mutated sequences (see Methods). These measures use the characteristic skewing of dinucleotides produced by RIP to detect mutated sequences. According to these measures, only 39 of the 9,200 predicted genes encoding proteins ≥100 amino acids show evidence of mutation by RIP. Of these, only eight consist of pairs of predicted duplicated genes (genes in the same multigene family) in which both copies are predicted to be RIP-mutated. Thus, few pairs of duplicated genes display evidence of having both survived RIP (Supplementary Information).

Gene duplication is thought to have a primary role in the innovation of new genes[16]. However, taken together, our data support the conclusion that most, if not all, paralogous genes in *Neurospora* duplicated and diverged before the emergence of RIP, and since that point the evolution of new genes through gene duplication has been virtually arrested. This conclusion raises the question of whether and how *Neurospora* is able to evolve new genes. A number of mechanisms that do not involve gene duplication are conceivable, although ultimately a conclusive analysis may be possible only by comparing the genome of *Neurospora* with the genomes of closely related species to illuminate recent evolutionary history. Nonetheless, our results indicate that the cost to *Neurospora* of increased genome security through RIP is a significant impact on the evolution of new gene functions through gene duplication.

Repetitive DNA

An analysis of repeat sequences longer than 200 bp and with greater than 65% similarity (see Methods) revealed that 10% of the *Neurospora* assembly consists of repeat sequences, consistent with previously reported estimates[21].

The repeat sequence of *Neurospora* provides a testament to the efficiency of RIP. Applying the measures of RIP mentioned above to the *Neurospora* genome revealed that most of the repetitive sequences (81%) in *Neurospora* have been mutated by RIP. Conversely, only 18% of predicted RIP-mutated sequence is non-repetitive, potentially reflecting loss of the corresponding duplicated sequence. As described above, duplications greater than about 400 bp are susceptible to RIP[15]. In keeping with this, we observe that over 97% of genomic repeats greater than 400 bp in length are RIP-mutated. Moreover, repeats longer than 400 bp clustered by sequence similarity display an average sequence identity within clusters of 78%, with 93% of clusters displaying an average identity of less than 85%. This corresponds to previous estimates indicating

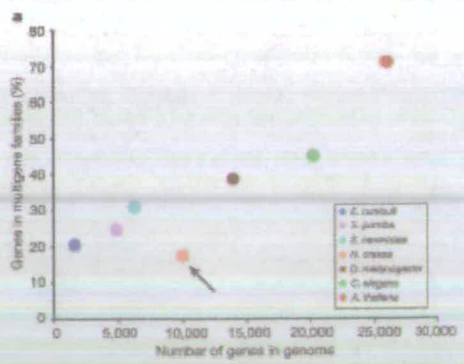

Figure 1 *Neurospora* has a low proportion of genes in multigene families. The graph displays the proportion of genes in multigene families (see Methods) as a function of the number of genes in the genomes of selected sequenced eukaryotic organisms. The arrow indicates *Neurospora*. See text for more details.

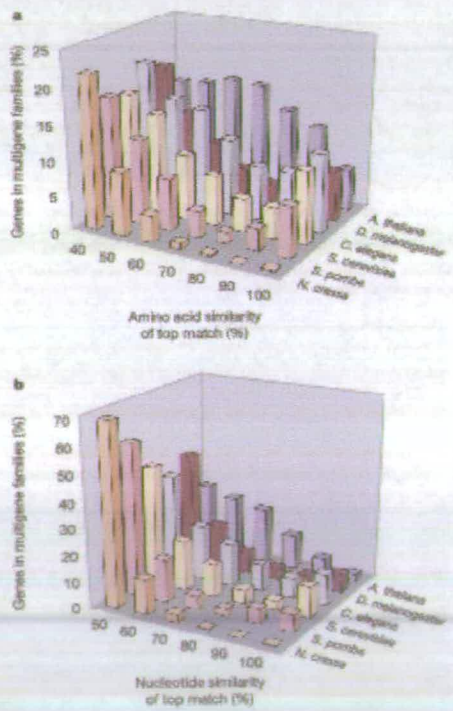

Figure 2 *Neurospora* possesses few highly similar genes. **a**, **b**, Histogram of amino acid (**a**) and nucleotide (**b**) per cent identity of top-scoring self-matches for genes in selected sequenced eukaryotic genomes. For each organism, the protein and coding regions for each gene (including paralogues) were compared to those of every other gene in the same genome using BLASTX. Top-scoring matches were aligned using ClustalW and per cent identities calculated. In contrast to other eukaryotes, *Neurospora* possesses only eight genes with a top match of greater than 80% amino acid or nucleotide identity.

that RIP requires greater than about 80% sequence identity to detect duplicated sequences.

Consistent with the hypothesis that RIP acts as a defence mechanism against selfish DNA[1,2], no intact mobile elements were identified. Furthermore, a significant proportion of the *Neurospora* RIP-mutated sequence (46% of repetitive nucleotides) can be identified as relics of mobile elements (Supplementary Information).

Ribosomal RNA

The only large repetitive sequences known to have survived RIP in *Neurospora* are the approximately 175–200 copies[10] of the large rDNA tandem repeat containing the 17S, 5.8S and 25S rRNA genes. As in higher eukaryotes, these tandem repeats occur within the nucleolar organizer region (NOR), and their resistance to RIP seems to stem from this localization[4,5]. Within the genome sequence we found several copies of the rDNA repeat outside the NOR. In every case, they display evidence of mutation by RIP, consistent with previous observations[10]. Thus, the sequence of the rDNA repeat does not in itself seem to confer resistance to RIP.

The 5S rRNA genes in *Neurospora* have survived RIP in a different manner. In contrast to most higher eukaryotes in which the 5S rRNA genes form tandem repeats, the 5S genes are dispersed throughout the genome in *Neurospora*[24]. A total of 74 copies comprising several different subtypes of 5S rDNA are dispersed through all seven chromosomes. This dispersal coupled with their small size (approximately 120 nucleotides) ensures that they are not recognized by RIP.

DNA methylation

Neurospora has been used extensively as a model for studying DNA methylation in eukaryotes[25]. The *Neurospora* genome includes two potential cytosine DNA methyltransferase genes. One, called *dim-2*, is required for all known DNA methylation[26]. The other, called *rid*, is

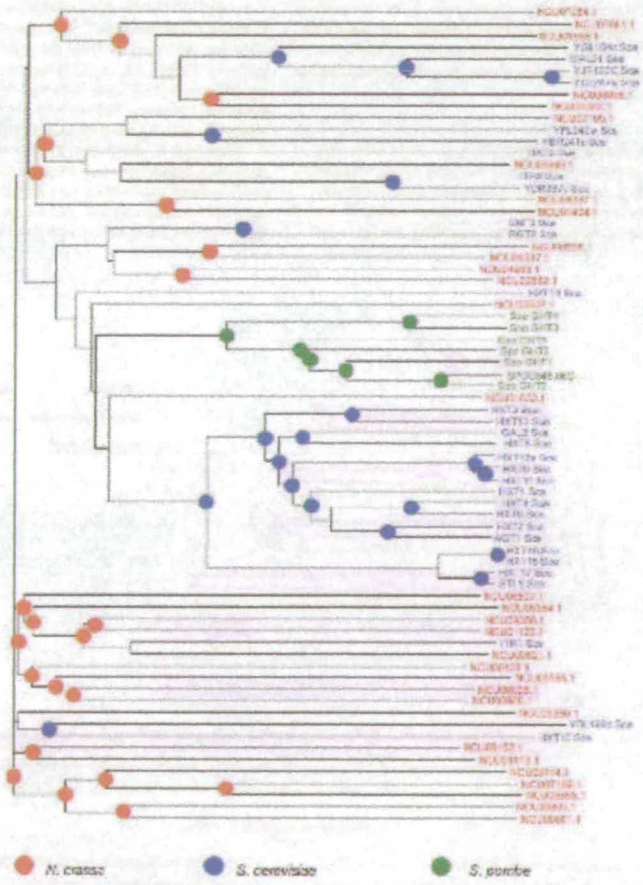

Figure 3 Examples of lack of recent duplications in a *Neurospora* gene family. Phylogenetic tree of major facilitator superfamily (MFS) sugar transporters from *S. cerevisiae*, *S. pombe* and *Neurospora*. Coloured dots represent branching points between predicted paralogous genes in *Neurospora* (red), *S. cerevisiae* (blue) and *S. pombe* (green). In contrast to both yeast species, *Neurospora* transporters contain no predicted instances of recent paralogous duplication.

required for RIP and is a member of a family found thus far only in filamentous fungi[35]. In *Neurospora*, an estimated 1.5% of cytosines are methylated[1,8,29], and it has been suggested that nearly all DNA methylation is a result of RIP[8–10,34].

Plasmid reads for *Neurospora* were sequenced from libraries cloned separately in methylation-tolerant and methylation-intolerant strains of *Escherichia coli*. Although not intended for this purpose, these libraries provided a basis for predicting DNA methylation by comparing the representation of regions in sequence obtained from each library (see Methods). Testing the accuracy of such predictions, we found that 8 of 10 regions predicted to be methylated were experimentally confirmed as such. The predictions thus have good specificity—although they lack sensitivity (see Methods).

The specificity of the predictions provides insight into the pattern of methylation in the *Neurospora* genome. Regions predicted to be methylated show a marked correspondence to regions predicted to be repetitive and RIP-mutated (Fig. 4). Fully 85% correspond to predicted RIP-mutated sequences. However, a small proportion (10%) corresponds to predicted non-repetitive and non-RIP-mutated sequence. In two out of ten such cases, both the methylation and the non-repetitive nature of these sequences were experimentally verified. This raises the possibility that methylation in *Neurospora* may also have non-defence roles, as proposed for higher organisms.

RNA silencing

Post-transcriptional gene silencing (PTGS), or RNA silencing, is widespread among organisms and is increasingly being recognized as a principal switch for controlling eukaryotic gene expression[36]. RNA-silencing pathways are thought to be derived from ancestral natural defence systems directed against invading nucleic acids[35]. Consistent with this, all known PTGS mechanisms share similar components[34].

Neurospora possesses two RNA-silencing pathways. The first, called quelling, acts during vegetative growth. This pathway was uncovered through the study of three genes, *qde-1*, *qde-2* and *qde-3*, coding respectively for an RNA-dependent RNA polymerase (RdRP), an argonaute and a RecQ helicase[36]. The second pathway, called meiotic silencing, acts during sexual reproduction[36,37]. Before our analysis, a gene called *sad-1*, encoding an RdRP, had been identified for this pathway[36].

Our analysis of the *Neurospora* genome sequence uncovered several additional genes implicated in RNA silencing (Table 2). These include one RdRP, one argonaute-like protein and one RecQ-like helicase, as well as two dicer-like ribonucleases. A phylogenetic analysis (Supplementary S7) of the predicted RdRPs, argonaute-like proteins and dicer-like proteins indicates that the *Neurospora* genes comprise two paralogous sets. One set includes the three *qde* genes and is thus predicted to correspond to the quelling pathway. The other set includes *sad-1*, and in phylogenetic trees these genes branch consistently with those of the single pathway observed in *S. pombe*[37,38]. On the basis of this analysis, we predict that one of the identified dicers, *Sms-3*, belongs phylogenetically to the meiotic silencing pathway, whereas the other, *dcl-2*, belongs to the quelling pathway (Table 2). In addition, we predicted that the identified argonaute, *Sms-2*, also belongs phylogenetically to the meiotic silencing pathway. Subsequent experimental work has supported roles for *Sms-2* (ref. 40) and *Sms-3* (M. McLaughlin, D. W. Lee, R. Pratt and R. Aramayo, manuscript in preparation) in meiotic silencing. Taken together, these results suggest that meiotic silencing and quelling represent two phylogenetically distinct RNA-dependent silencing pathways. We further hypothesize that both might have evolved from a single ancestral RNA-silencing pathway.

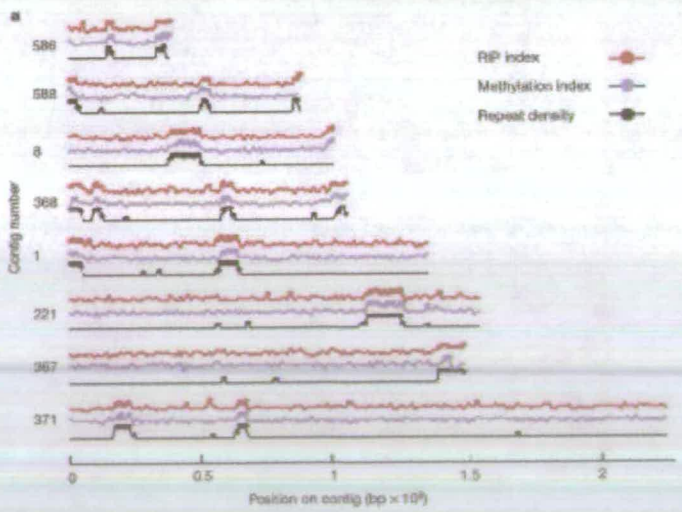

Figure 4 Correspondence between predicted RIP, methylation and repetitive DNA. Prediction of RIP, methylation and repeat sequence in 1-kb windows for selected contigs. Red lines plot the TpA/ApT RIP index (see Methods); red dots indicate windows predicted to be RIP-mutated (TpA/ApT > 1.2). Blue lines plot the proportion of reads from the methyl-tolerant library; blue dots indicate windows predicted to be methylated based on >70% methyl-tolerant reads (see Methods). Black lines plot repeat content as a fraction of nucleotides in each window that is in repetitive sequence; black dots indicate windows with >50% repeat sequence. Contigs were selected to illustrate regions predicted as methylated.

Fungal biology and evolution

The *Neurospora* genome sequence provides an opportunity to study the genetic basis underlying the extraordinary biochemical and metabolic diversity exhibited by a filamentous fungus. Our analysis of the genome sequence has resulted in a number of surprising insights into the biology and evolution of *Neurospora* and other filamentous fungi.

Cell signalling and environmental responses

Discovery of putative red-light-sensing genes

Blue light is an important regulator of *Neurospora* growth and development, affecting the circadian rhythm of conidiation, carotenogenesis of hyphae and numerous facets of sexual development[41]. Although *Neurospora* photobiology has been studied intensively for more than two decades, the genome sequence has nonetheless revealed a number of previously uncharacterized sequences with similarity to blue-light-sensing genes, including both a cryptochrome homologue and a gene whose product contains a single PAS/LOV-type domain associated with light sensing.

Furthermore, *Neurospora* possesses two putative phytochrome homologues most similar to bacteriophytochromes—genes known for their role in red light sensing in prokaryotes—and a putative homologue of the *Aspergillus nidulans velvet* gene implicated in the regulation of both red and blue light responses. The presence of these genes is unexpected given that no red light photobiology has been described for *Neurospora* so far. It has been shown recently that in addition to red light sensing, some *Arabidopsis* phytochromes associate with cryptochromes to have a role in blue light sensing and signalling[42]. Therefore, the two phytochromes and the velvet homologue may also regulate this aspect of *Neurospora* photobiology.

Importance of two-component signalling in filamentous fungi

Mitogen-activated protein kinase (MAPK) pathways integrate signals from multiple receptor pathways including two-component signalling systems[43]. The basic two-component system consists of a histidine kinase and a cognate response regulator. The nine MAPK pathway proteins identified in the *Neurospora* genome sequence (Fig. 5) correspond to those found in *S. pombe* and *S. cerevisiae*, indicating that the basic MAPK machinery is conserved between these species. In contrast, *Neurospora* has a significantly expanded complement of 11 histidine kinases, as compared with one in *S. cerevisiae* and three in *S. pombe*. Two of the 11 genes have been characterized previously in *Neurospora*[44], whereas a third is similar to proteins in *Aspergillus fumigatus* and *A. nidulans* that affect conidiation (L. A. Alex and M. I. Simon, unpublished observations; see also ref. 44). Functions for the remaining genes are unknown, although seven (including the two phytochromes discussed above) contain PAS/PAC domains, implicating them in oxygen and light responses. This number of histidine kinases suggests a larger role than previously expected, and reveals filamentous fungi to be more similar in this regard to plants, where two-component systems are abundant, than to animals, where these systems are absent.

A new family of G-protein-coupled receptors

Eukaryotic cells sense many environmental stimuli through seven-transmembrane-helix, G-protein-coupled receptors (GPCRs)[45]. Our analysis indicates that *Neurospora* possesses ten predicted seven-transmembrane-helix proteins (Fig. 5), three of which belong to a new class not previously identified in any fungus. These three genes encode proteins similar to cyclic AMP GPCRs from the protists *Dictyostelium discoideum*[46] and *Polysphondylium pallidum*, and also to predicted proteins from *Arabidopsis thaliana*[47] and *Caenorhabditis elegans*. The *D. discoideum* proteins sense cAMP levels during chemotaxis and multicellular development[48]. This suggests a possible analogous function in *Neurospora*. The existence of an extracellular cAMP signalling pathway has never been demonstrated previously in any fungal system.

In support of this hypothesis, along with the presence of putative cAMP receptors, *Neurospora* was found to possess the full complement of proteins required for the synthesis and degradation of cAMP. Furthermore, *Neurospora* wild-type strains accumulate cAMP in the extracellular medium[49], although a role in extracellular signalling has not been established. Taken together, these data suggest the possibility that cAMP or a related molecule may serve as an extracellular signal in *Neurospora*.

Ca^{2+} sensory transduction in filamentous fungi

A considerable body of evidence, primarily from pharmacological studies, indicates that Ca^{2+} signalling regulates numerous processes in filamentous fungi[50]. However, the identification of the main components of even one Ca^{2+}-mediated response pathway in filamentous fungi has remained elusive. The genome sequence of *Neurospora* has provided over 25 of the proteins likely to be necessary for Ca^{2+} signalling in filamentous fungi (Fig. 5).

A notable difference between Ca^{2+} signalling in *Neurospora* as compared with plants and animals was revealed by the genome sequence. An important aspect of Ca^{2+} signalling in plant and animal cells involves Ca^{2+} release from internal stores. This is commonly mediated by the second messengers inositol-1,4,5-trisphosphate ($InsP_3$) and cADP ribose, or by Ca^{2+}-induced Ca^{2+} release[51]. $InsP_3$ is present within *Neurospora* hyphae[52], and physiological evidence including intracellular membrane-associated, $InsP_3$-activated Ca^{2+} channel activity supports a role in Ca^{2+} signalling[53,54]. In spite of this, *Neurospora* (and *S. cerevisiae*) lacks recognizable $InsP_3$ receptors. In addition, neither ADP ribosyl cyclase nor ryanodine receptor proteins, principal components of Ca^{2+} release mechanisms in plant and animal cells, are found in *Neurospora*. These observations raise the question of whether other

Table 2 **Neurospora has two RNA-silencing pathways**

Predicted protein	*Neurospora*	*A. fumigatus**	*S. pombe*†	Pathway‡
RNA-directed RNA polymerases	*qde-1* (NCU07534.1) *sad-1* (NCU02178.1) *rrp-3* (NCU08435.1)	*rrpA* (contig 158) *rrpB* (contig 475) –	– *rdp1*+ (SPAC6F12.09) –	Quelling Meiotic silencing Unknown
Argonaute-like, related to translation initiation factors	*qde-2* (NCU04730.1) *Sms-2* (NCU09434.1)	*ppdA* (contig 730) *ppdB* (contig 126)	– *ago1*+ (SPCC736.11)	Quelling Meiotic silencing
Dicer-like, related to RNA-RNAseIII ribonuclease of the carpel factory	*dcl-2* (NCU06766.1) *Sms-3* (NCU08270.1)	*dclB* (contig 618) *dclA* (contig 310)	– *dcr1*+ (SPCC584.10C)	Quelling Meiotic silencing
RecQ helicase-like, related to Bloom's and Werner syndrome helicases	*qde-3* (NCU08598.1) *RecQ-2* (NCU03237.1)§	*rqhA* (contig 443)§ *rqhB* (contig 958)§	– *rqh1*+ (SPAC2G11.12)	Quelling Unknown

*Unfinished *A. fumigatus* genome project (http://www.tigr.org).
†*Schizosaccharomyces pombe* genome project (http://www.genedb.org).
‡Pathway assignment on the basis of either known experimental data for *qde-1*, *qde-2* and *qde-3* (quelling pathway) or *sad-1*, *Sms-2* and *Sms-3* (meiotic silencing pathway), or predicted on the basis of phylogenetic analysis.
§RecQ helicase-like protein.

second messenger systems responsible for Ca^{2+} release from internal stores remain to be discovered in filamentous fungi.

Growth and development

Hyphal growth

True hyphae produced by filamentous fungi are tubular structures consisting of cellular compartments that are usually delineated by incomplete septa[6]. In contrast, the pseudohyphae produced by yeasts consist of chains of uninucleate elongated cells[6,7] with no apparent cytoplasmic continuity. The molecular mechanisms underlying these two modes of growth are not well understood.

The two signalling pathways that regulate pseudohyphal growth in *S. cerevisiae*—the MAPK and cAMP modules—are both conserved in the *Neurospora* genome. In *Candida albicans*, capable of pseudohyphal, true hyphal and budding growth, both pathways are required for true hyphal production, suggesting a similar role in *Neurospora*[6]. However, at least three transcription factors—Tec1p, Flo8p and Sfl1p—specifically required for regulating pseudohyphal development in *S. cerevisiae*[7,8] were not found in *Neurospora*. Conversely, *Neurospora* possesses a gene with similarity to a transcription factor necessary for hyphal growth in *C. albicans*[9] (Efg1). This transcription factor is not required for pseudohyphal growth in *C. albicans*, nor is the homologous protein in *S. cerevisiae* (Phd1p)[10]. More study of the complex pathways underlying these modes of growth is required. Nonetheless, these data clarify in part the distinctions and similarities between the signalling pathways and regulatory components of hyphal and pseudohyphal growth.

The macroconidiation pathway differs from that in *A. nidulans*

Macroconidia are asexual spores common to filamentous fungi but absent from yeast[6,11]. Components of the macroconidiation pathway have been identified in both *Neurospora* and the filamentous fungus *A. nidulans*, and known upstream signalling proteins seem to be conserved in both species[6,9]. In contrast, there is little conservation of downstream components between the two fungi. In *Neurospora*, the *acon-2*, *acon-3*, *fld* and *fl* genes are essential for conidiation[6], whereas in *A. nidulans*, the FlbC, FlbD, BrlA, AbaA and WetA gene products are required. Our analysis of the genome sequence revealed that *Neurospora* possesses no FlbC, BrlA or AbaA homologues, and a protein with only very weak similarity to approximately 100 amino acids at the carboxy terminus of WetA. These data make clear that the molecular machinery underlying macroconidiation in *Neurospora* differs significantly from that in *A. nidulans*.

Secondary metabolism

The fungal kingdom produces a vast array of small, bioactive compounds termed secondary metabolites that are best known for their roles as pigments, antibiotics and mycotoxins. With the exception of carotenoid and melanin pigment synthesis, *Neurospora* has not been shown to possess secondary metabolism. It was thus surprising that the *Neurospora* genome sequence revealed a number of putative genes for secondary metabolite production.

Non-ribosomal peptide synthetases

Three predicted non-ribosomal peptide synthetase (NRPS) genes and one NRPS-related gene were identified in the *Neurospora* genome sequence (Fig. 6). By phylogenomic analysis, one NRPS gene is orthologous to an *Aureobasidium pullulans* NRPS. The most closely related NRPS of known function is *sid2* of *Ustilago maydis*, which is responsible for production of hydroxamate siderophores[12]. The remaining two are of unknown function, although one is orthologous to an NRPS in *Magnaporthe grisea*, and the other is

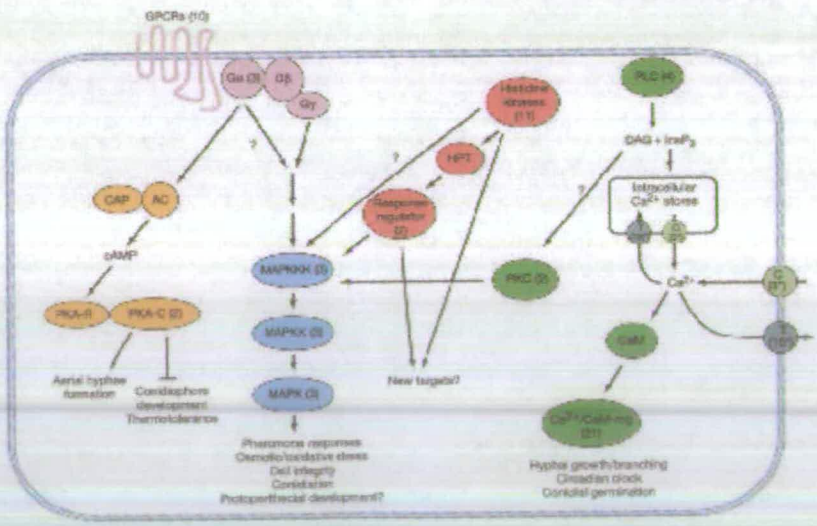

Figure 5 Overview of major intracellular signalling pathways in *Neurospora*. The numbers identified for each gene are in parentheses. An asterisk indicates that the location in the plasma membrane and/or organelle membranes is not determined. AC, adenylyl cyclase; C, Ca^{2+} channel protein; CaM, calmodulin; Ca^{2+}/CaM-reg, calcium- and calmodulin-regulated protein; CAP, cyclase-associated protein; DAG, diacylglycerol; GPCR, G-protein-coupled receptor; G_α, G protein α-subunit; Gβ, G protein β-subunit; G_γ, G protein γ-subunit; HPT, histidine-containing phosphotransfer domain protein; MAPK, MAP kinase; MAPKK, MAPK kinase; MAPKKK, MAPKK kinase; PKA-C, protein kinase A catalytic subunit; PKA-R, protein kinase A regulatory subunit; PLC, phospholipase C; PKC, protein kinase C; T, Ca^{2+} transport protein (P-type Ca^{2+}-ATPase, H^+/Ca^{2+} exchanger, or Na^+/Ca^{2+} exchanger).

orthologous to an NRPS found in all other filamentous ascomycetes with genome sequence (see Methods). The NRPS-related gene shares 66% amino acid identity with the *CPS1* gene product that contributes to the virulence of *Cochliobolus heterostrophus*, *C. victoriae* and *Gibberella zeae*[40].

Polyketide synthases

Seven polyketide synthase (PKS) genes were identified in the *Neurospora* genome, which could be classified into three groups on the basis of domain structure (Fig. 6). The first class contains genes similar to DHN-melanin PKS genes of the fungi *Exophila dermatitidis*[41], *Colletotrichum lagenarium*[42] and *Alternaria alternata*[43]. Sequence identity to numerous expressed sequence tag (EST) sequences from sexual and perithecial libraries suggest a role in melanin pigment synthesis during sexual development[44]. The genes in the second class are similar in structure to several fungal PKSs, including the *Aspergillus terreus lovF* gene required for lovastatin synthesis. The genes in the third class resemble other fungal genes, including the *A. terreus lovB* gene, which is also required for lovastatin synthesis.

Diterpene metabolism

Diterpenes comprise a diverse group of compounds, primarily in plants and fungi, with roles in defence, pathogenicity and regulation of plant growth. The genome sequence revealed several genes associated with diterpene biosynthesis in other organisms, including a terpene synthase, several genes related to gibberellin oxidases, and a member of the cytochrome P450 mono-oxygenase gene family. These genes include at least one member of each of the three enzyme classes required for the biosynthesis of gibberellic acid. Gibberellic acid, a normal growth regulator in plants, was first identified as a metabolic product of the plant pathogen *Gibberella fujikuroi*, a relative of *Neurospora* that causes 'foolish seedling' disease in rice[45]. The presence of these genes in *Neurospora* suggests that many components necessary for gibberellic acid production were present in the ancestors of *Neurospora* and *G. fujikuroi*.

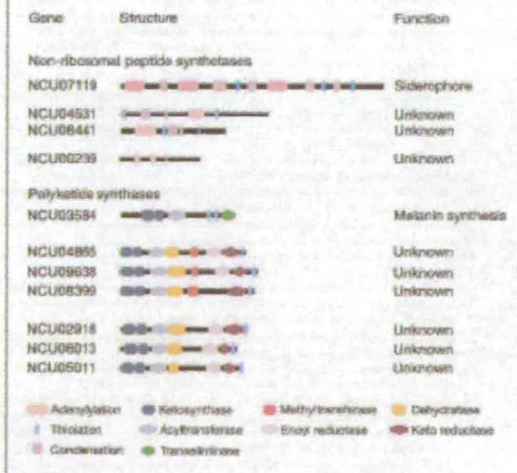

Figure 6 Domain structures of predicted *Neurospora* non-ribosomal peptide synthetase (NRPS) and polyketide synthase (PKS) genes. Domains were predicted using a combination of PFAM searches using HMMER, protein alignments and manual inspection.

We speculate that these secondary metabolism genes identified may have roles in morphogenesis and chemotropism[46], interspecies communication and possibly even chemical defence. The identification of these genes in *Neurospora* suggests that apparent major differences in lifestyles among related fungi, such as pathogenicity, may derive in part from minor modifications of gene function and expression.

Plant pathogenicity and *Neurospora*

The ability to parasitize living plants is widespread throughout the fungal kingdom. Although *Neurospora* is a saprotroph (that is, it feeds on dead or decaying matter), the genome sequence contains numerous genes similar to those required for plant pathogenesis identified in fungal pathogens. In particular, a number of genes were identified that have no known function in other organisms except in pathogenesis (Supplementary S8). *Neurospora* also possesses a wide range of extracellular enzymes capable of digesting plant cell wall polymers, although there is no clear cutinase homologue. Cutin is one of the main layers protecting the epidermis of the leaves of plants, and many, but not all, plant pathogens have cutinase activity. *Neurospora* has a wide range of cytochrome P450 enzymes that are important in some host–pathogen systems for detoxification of plant anti-fungal compounds. In addition, a large number of identified ABC (ATP-binding cassette) and MFS drug efflux systems could have a role in combating toxic plant compounds. The capability to form secondary metabolite members of the PKS, NRPS and terpenoid families, as described above, is present. Also, *Neurospora* contains all signal transduction components implicated in ascomycete pathogenesis that have been described so far. Thus, although *Neurospora* is not known to be a pathogen, the genome sequence has revealed many genes with similarity to those required for pathogenesis.

Discussion

Although *Neurospora* has been studied intensely for over 70 years, the analysis of the genome sequence has provided many new insights into a variety of cellular processes, including cell signalling, growth and differentiation, secondary metabolism and genome defence. The analysis has also uncovered surprising similarities between the saprotrophic *Neurospora* and pathogenic fungi, providing a new perspective on the molecular underpinnings of these lifestyles. Finally, the genome sequence has revealed the remarkable impact of RIP on the evolution of genes in *Neurospora*. Recent reports indicating the apparent presence of RIP in other fungi[47,48] broaden the implications of our findings. The apparent lack of functional gene duplication in *Neurospora* provides a unique opportunity to study other modes of evolution in this experimentally tractable organism.

The genome sequence of *Neurospora* provides only a first glimpse into the genomic basis of the biological diversity of the filamentous fungi. Fungal genome sequences from the many ongoing[49] and planned[50] projects will expand this view as well as provide extraordinary opportunities for comparative analyses. This new era in fungal biology promises to yield insight into this important group of organisms, as well as to provide a deeper understanding of the fundamental cellular processes common to all eukaryotes. □

Methods

Strain and growth conditions

Twenty 5-ml cultures of *N. crassa* wild-type strain 74-OR23-1VA (Fungal Genetics Stock Center 2489) were grown on a shaker in Vogel's minimal medium[51] for 3 days at 32 °C. Tissues were collected, frozen dried overnight and DNA was extracted as previously described[52]. DNA from the 20 samples was mixed and used for library construction.

Sequencing and assembly

The genome was sequenced by the WGS method. Plasmid (4-kb inserts) and fosmid (40-kb inserts) libraries were generated as described at http://www.genome.wi.mit.edu/. Jumping clone (cosmid) libraries with 30-kb inserts were generated as described

Annotation and analysis

59. Yuan, W., Gentil, G., Budde, A. & Leong, S. Characterization of the *Ustilago maydis sid2* gene encoding a multidomain peptide synthetase in the ferrichrome biosynthetic gene cluster. *J. Bacteriol.* 183, 4040–4051 (2001).
60. Lu, S.-W., Yoder, O. & Turgeon, B. G. Highly conserved virulence-related CPS1 homologs from plant and human pathogenic fungi. *Fungal Genet. News* 48, 3246 (2001).
61. Feng, B. *et al.* Molecular cloning and characterization of *WdPKS1*, a gene involved in dihydroxynaphthalene melanin biosynthesis and virulence in *Wangiella (Exophiala) dermatitidis*. *Infect. Immun.* 69, 1781–1794 (2001).
62. Takano, Y. *et al.* Structural analysis of PKS1, a polyketide synthase gene involved in melanin biosynthesis in *Colletotrichum lagenarium*. *Mol. Gen. Genet.* 249, 162–167 (1995).
63. Takano, Y., Kubo, Y., Kawamura, C., Tsuge, T. & Furusawa, I. The *Alternaria alternata* melanin biosynthesis gene restores appressorial melanization and penetration of cellulose membranes in the melanin-deficient albino mutant of *Colletotrichum lagenarium*. *Fungal Genet. Biol.* 21, 131–140 (1997).
64. Nelson, M. A. *et al.* Expressed sequences from conidial, mycelial, and sexual stages of *Neurospora crassa*. *Fungal Genet. Biol.* 21, 348–363 (1997).
65. Kurosawa, E. Experimental studies on the nature of the substance secreted by the 'bakanae' fungus. *Trans. Nat. Hist. Soc. Formosa* 16, 213–227 (1926) (in Japanese).
66. Vigfusson, N. & Cano, R. Artificial induction of the sexual cycle of *Neurospora crassa*. *Nature* 249, 383–385 (1974).
67. Graia, F. *et al.* Genome quality control: RIP (repeat-induced point mutation) comes to Podospora. *Mol. Microbiol.* 40, 586–595 (2001).
68. Ikeda, K. *et al.* Repeat-induced point mutation (RIP) in *Magnaporthe grisea*: implications for its sexual cycle in the natural field context. *Mol. Microbiol.* 45, 1355–1364 (2002).
69. TIGR Microbial Database (http://www.tigr.org/tdb/mdb/mdbinprogress.html) (2003).
70. Fungal Genome Initiative (http://www-genome.wi.mit.edu/seq/fgi/) (2002).
71. Luo, Z., Freitag, M. & Sachs, M. S. Translational regulation in response to changes in amino acid availability in *Neurospora crassa*. *Mol. Cell. Biol.* 15, 5235–5245 (1995).
72. Venter, J. C. *et al.* The sequence of the human genome. *Science* 291, 1304–1351 (2001).
73. Pickford, A., Braccini, L., Macino, G. & Cogoni, C. The QDE-3 homologue RecQ-2 co-operates with QDE-3 in DNA repair in *Neurospora crassa*. *Curr. Genet.* 42, 220–227 (2003).

Supplementary Information accompanies the paper on *Nature*'s website (http://www.nature.com/nature).

Acknowledgements The authors would like to thank J. Arnold, H. Inoue, G. Turner, B. Bowman, P. Harrison and P. Youderian for their support. We also thank Lisa Bianchina, V. Alga and J. Hoheisel for making available the BAC libraries used during sequencing; M. Kumar for developing the web pages hosting the *Neurospora* Intron analysis at MIPS; the Torrey Mesa Research Institute/Syngenta for providing genome data for *C. heterostrophus*, *B. fuckeliana*, *G. verticillioides* and *G. zeae*; and all members of the Whitehead Institute/MIT Center for Genome Research sequencing group. Funding for the *Neurospora* genome project was provided by the National Science Foundation. Additional funding was provided by the Deutsche Forschungsgemeinschaft, The Israel Science Foundation and the National Institutes of Health.

Competing interests statement The authors declare that they have no competing financial interests.

Correspondence and requests for materials should be addressed to J.E.G (e-mail: jgalag@mit.edu) or B.B. (e-mail: bwb@genome.wi.mit.edu). The whole-genome shotgun project has been deposited at DDBJ/EMBL/GenBank under the project accession AABX00000000. The version described in this paper is the first version, AABX01000000.

Affiliations for authors: 1, Whitehead Institute Center for Genome Research, 320 Charles Street, Cambridge, Massachusetts 02141, USA; 2, Department of Plant Pathology, University of California, Riverside, California 92521, USA; 3, Institute of Molecular Biology, University of Oregon, Eugene, Oregon 97403, USA; 4, Institute of Cell and Molecular Biology, University of Edinburgh, Edinburgh EH9 3JH, UK; 5, Celera Genomics, Rockville, Maryland 20850, USA; 6, Department of Biology, Texas A & M University, College Station, Texas 77843, USA; 7, Department of Biology, University of New Mexico, Albuquerque, New Mexico 87131, USA; 8, Department of Cellular and Structural Biology, University of Colorado Health Sciences Center, Denver, Colorado 80262, USA; 9, Department of Microbiology, University of Kansas Medical School, Kansas City, Kansas 66160, USA; 10, Department of Zoology, University of Florida, Gainesville, Florida 32611-8525, USA; 11, Department of Plant Pathology and Microbiology, Faculty of Agricultural, Food and Environmental Quality Sciences, The Hebrew University of Jerusalem, Rehovot 76100, Israel; 12, Institute of Biochemistry, Heinrich Heine University, 40225 Düsseldorf, Germany; 13, Laboratory of Plant Molecular Biology, Rockefeller University, New York, New York 10021, USA; 14, Department of Genome Oriented Bioinformatics, Technical University of Munich, Wissenschaftszentrum Weihenstephan, 85350 Freising-Weihenstephan, Germany; 15, Institute for Bioinformatics (MIPS), GSF-National Research Center for Environment and Health, Ingolstaedter Landstrasse 1, 85764 Neuherberg, Germany; 16, T.H. Morgan School of Biological Sciences, University of Kentucky, Lexington, Kentucky 40506, USA; 17, The Institute for Cellular and Molecular Biology, The University of Texas at Austin, Austin, Texas 78712, USA; 18, The Institute for Genomic Research, 9712 Medical Center Drive, Rockville, Maryland 20878, USA; 19, Department of Plant and Microbial Biology, University of California, Berkeley, California 94720, USA; 20, Department of Chemistry and Biochemistry, University of California, Los Angeles, California 90095, USA; 21, Dipartimento Biotecnologie Cellulari ed Ematologia, Universita' di Roma La Sapienza, Rome, Italy; 22, School of Biological Sciences, Flinders University, P.O. Box 2100, Adelaide, South Australia 5001; 23, Department of Molecular Genetics, The Ohio State University, Columbus, Ohio 43210, USA; 24, Department of Molecular Genetics, The Ohio State University, Columbus, Ohio 43211, USA; 25, Department of Plant Pathology, University of Arizona, Tucson, Arizona 85721, USA; 26, School of Biological Sciences, University of Missouri-Kansas City, Kansas City, Missouri 64110, USA; 27, Department of Genetics, Dartmouth Medical School, Hanover, New Hampshire 03755, USA; 28, School of Biology, Leeds University, Leeds LS2 9JT, UK; 29, Department of Chemistry, California State Polytechnic University Pomona, Pomona, California 91768, USA; 30, Department of Plant Pathology and Microbiology, Texas A & M University, College Station, Texas 77843, USA; 31, Department of Environmental and Biomolecular Systems, OGI School of Science and Engineering, Oregon Health and Science University, Beaverton, Oregon 97006, USA; 32, Department of Biology, MIT, Cambridge, Massachusetts 02139, USA

Bibliography

D. G. Allen, J. R. Blinks, and F. G. Prendergast. Aequorin luminescence: relation of light emission to calcium concentration - A calcium-independent component. *Science*, 195:996–998, 1977.

E. D. Allen, R. Aiuto, and A. S. Sussman. Effects of cytochalasins on *Neurospora crassa*. I. growth and ultrastructure. *Protoplasma*, 102:63–75, 1980.

G. J. Allen, S. R. Muir, and D. Sanders. Release of Ca^{2+} from individual plant vacuoles by both $InsP_3$ and cyclic ADP-Ribose. *Science*, 268:735–737, 1995.

A. Alsina and N. Rodriguez-Del Valle. Effects of divalent cations and functionally related substances on the yeast to mycelium transition of *Sporothrix schenckii*. *Sabouraudia*, 22:1–5, 1984.

J. B. Ames, K. B. Hendricks, T. Strahl, I. G. Huttner, and N. Hamasakiand J. Thorner. Structure and calcium-binding properties of Frq1, a novel calcium sensor in the yeast *Saccharomyces cerevisiae*. *Biochemistry*, 39:12149–12161, 2000.

T. Andoh, T. Yoko, Y. Matsui, and A. Toh. Molecular cloning of the *plc1*$^+$ gene of *Schizosaccharomyces pombe*, which encodes a putative phosphoinositide-specific phospholipase C. *Yeast*, 11:179–185, 1995.

A. Antebi and G. R. Fink. The yeast Ca^{2+}-ATPase homologue, *PMR1*, is required for normal Golgi function and localizes in a novel Golgi-like distribution. *Molecular Biology of the Cell*, 3:633–654, 1992.

D. S. Arora and D. Ohlan. *In vitro* studies on antifungal activity of tea (*Camellia sinensis*) and coffee (*Coffea arabica*) against wood-rotting fungi. *Journal of Basic Microbiology*, 37:159–165, 1997.

K. B. Axelsen and M. G. Palmgren. Evolution of substrate specificities in the P-type ATPase superfamily. *Journal of Molecular Evolution*, 46:84–101, 1998.

K. B. Axelsen and M. G. Palmgren. Inventory of the superfamily of p-type ion pumps in *Arabidopsis*. *Plant Physiology*, 126:696–706, 2001.

M. N. Badminton, J. M. Kendall, G. Sala-Newby, and A. K. Campbell. Nucleoplasmin-targeted aequorin provides evidence for a nuclear calcium barrier. *Experimental Cell Research*, 216:236–243, 1995.

C. D. Bauer, W. Simonis, and G. Schonknecht. Different xanthines cause membrane potential oscillations in a unicellular green alga pointing to a ryanodine/cADPR receptor Ca^{2+} channel. *Plant and Cell Physiology*, 20:453–456, 1999.

P. J. Belde, J. H. Vossen, G. W. Borst-Pauwels, and A. P. Theuvent. Inositol 1,4,5-trisphosphate releases Ca^{2+} from vacuolar membrane vesicles of *Saccharomyces cerevisiae*. *FEBS Letters*, 323:113–118, 1993.

B. Benito, B. Garciadeblás, and A. Rodríguex-Navarro. Molecular cloning of the calcium and sodium ATPases in *Neurospora crassa*. *Molecular Microbiology*, 35:1079–1088, 2000.

M. J. Berridge. Inositol trisphosphate and calcium signalling. *Nature*, 361:315–325, 1993.

M. J. Berridge. Capacitative calcium entry. *Biochemical Journal*, 312:1–11, 1995.

M. J. Berridge, M. D. Bootman, and P. Lipp. Calcium - a life and death signal. *Nature*, 395:645–648, 1998.

M. J. Berridge and G. Dupont. Spatial and temporal signalling by calcium. *Current Opinions in Cell Biology*, 6:267–274, 1994.

M. J. Berridge, P. Lipp, and M. D. Bootman. The versatility and universality of calcium signalling. *Nature Reviews in Molecular Cell Biology*, 1:11–21, 2000.

V. Betina, D. Mičeková, and P. Nemec. Antimicrobial properties of cytochalasins and their alteration of fungal morphology. *Journal of General Microbiology*, 71: 343–349, 1971.

D. Bhattacharya, L. Medlin, P. Wainwright, E. Ariztia, C. Bibeau, S. Stickel, and M. Sogin. Algae containing chlorphylls a + c are paraphyletic: molecular evolutionary analysis of the Chromophyta. *Evolution*, 46:1801–1817, 1992.

T. N. Bibikova, E. B. Blancaflor, and S. Gilroy. Microtubules regulate tip growth and orientation in root hairs of *Arabidopsis thaliana*. *Plant Journal*, 17:657–665, 1999.

P. R. Binks, G. D. Robson, M. W. Goosey, and A. P. Trinci. Relationships between phosphatidylcholine content, chitin synthesis, growth, and morphology of *Aspergillus nidulans choC*3. *FEMS Microbiology Letters*, 83:159–164, 1992.

C. J. Birchwood, J. D. Saba, R. C. Dickson, and K. W. Cunningham. Calcium influx and signaling in yeast stimulated by intracellular sphingosine 1-phosphate accumulation. *Journal of Biological Chemistry*, 276:11712–11718, 2001.

S. Blackford, P. A. Rea, and D. Sanders. Voltage sensitivity of H^+/Ca^{2+} antiport in higher plant tonoplast suggests a role in vacuolar calcium accumulation. *Journal of Biological Chemistry*, 265:9617–9620, 1990.

J-W. Bok, T. Sone, L. B. Silverman-Gavrila, R. R. Lew, F. J. Bowring, D. E. Catcheside, and A. J. Griffiths. Structure and function analysis of the calcium-related gene *spray* in *Neurospora crassa*. *Fungal Genetics and Biology*, 32: 145–158, 2001.

M. Bonilla, K. K. Nastase, and K. W. Cunningham. Essential role of calcineurin in response to endoplasmic reticulum stress. *The EMBO Journal*, 21:2343–2353, 2002.

M. D. Bootman, T. J Collins, C. M. Pappiatt, L. S. Prothero, L. MacKenzie, P. De Smet, M. Travers, S. C. Tovey, J. T. Seo, M. J. Berridge, F. Ciccolini, and P. Lipp. Calcium signalling - an overview. *Seminars in Cell and Developmental Biology*, 12:3–10, 2001.

E. J. Bowman and B. J. Bowman. Cellular role of the V-ATPase in *Neurospora crassa*: analysis of mutants resistant to concanamycin or lacking the catalytic subunit A. *Journal of Experimental Biology*, 203:97–106, 2000.

E. J. Bowman, R. Kendle, and B. J. Bowman. Disruption of *vma-1*, the gene encoding the catalytic subunit of the vacuolar H^+-ATPase, causes severe morphological changes in *Neurospora crassa*. *Journal of Biological Chemistry*, 275:167–176, 2000.

D. Bray. Cytochalasin action. *Nature*, 282:671, 1979.

S. S. Brown and J. A. Spudich. Mechanism of action of cytochalasin: evidence that it binds to actin filament ends. *Journal of Cell Biology*, 88:487–491, 1981.

C. Brownlee. Intracellular signalling: Sphingosine-1-phosphate branches out. *Current Biology*, 11:R535–R538, 2001.

H. Brunswick. Untersuchungen über die Geschlechts- und Kernver-hältnisse bei der Hymenomyzetengattung. *Coprinus. Bot. Abh.*, 5:1–152, 1924.

D. S. Bush. Calcium regulation in plant cells and its role in signalling. *Annual Review of Plant Physiology and Plant Molecular Biology*, 46:95–122, 1995.

C. M. Calvert and D. Sanders. Inositol trisphosphate-dependent and -independent Ca^{2+} mobilization pathways at the vacuolar membrane of *Candida albicans*. *Journal of Biological Chemistry*, 270:7272–7280, 1995.

N. Capelli, D. van Tuinen, R. Ortega Perez, J. F. Arrighi, and G. Turian. Molecular cloning of a cDNA encoding calmodulin from *Neurospora crassa*. *FEBS Letters*, 321:63–68, 1993.

E. Carafoli. Calcium signaling: a tale for all seasons. *Proceedings of the National Academy of Sciences of the USA*, 99:1115–1122, 2002.

E. Carnero, J. C. Ribas, B. Garcia, A. Duran, and Y. Sanchez. *Schizosaccharomyces pombe* Ehs1p is involved in maintaining cell wall integrity and in calcium uptake. *Molecular and General Genetics*, 264:173–183, 2000.

P. Catty, A. de Kerchove d'Exaerde, and A. Goffeau. The complete inventory of the yeast *Saccharomyces cerevisiae* P-type transport ATPases. *FEBS Letters*, 409:325–332, 1997.

P. Catty and A. Goffeau. Identification and phylogenetic classification of eleven putative P-type calcium transport ATPase genes in the yeasts *Saccharomyces cerevisiae* and *Schizosaccharomyces pombe*. *Bioscience Reports*, 16:75–85, 1996.

T. H. Chen, C. S. Hsu, P. J. Tsai, Y. F. Ho, and N. S. Lin. Heterotrimeric G-protein and signal transduction in the nematode-trapping fungus *Arthrobotrys dactyloides*. *Planta*, 212:858–863, 2001.

H. A. Colbert, T. L. Smith, and C. I. Bargmann. OSM-9, a novel protein with structural similarity to channels, is required for olfaction, mechanosensation, and olfactory adaptation in *Caenorhabditis elegans*. *Journal of Neuroscience*, 17:8259–8269, 1997.

A. J. Collinge, M. H. Fletcher, and A. P. J. Trinci. Physiology and cytology of septation and branching in a temperature-sensitive colonial mutant (*cot-1*) of *Neurospora crassa*. *Transactions of the British Mycolological Society*, 71: 107–120, 1978.

A. J. Collinge and A. P. J. Trinci. Hyphal tips of wild-type and spreading colonial mutants of *Neurospora crassa*. *Archives für Microbiologie*, 99:353–368, 1974.

A. J. Collis. *The development of transgenic aequorin as an indicator for cytosolic free calcium in* Neurospora crassa. PhD thesis, University of Edinburgh, 1996.

G. Cornelius, G. Gebauer, and D. Techel. Inositol trisphosphate induces calcium release from *Neurospora crassa* vacuoles. *Biochemical and Biophysical Research Communications*, 162:852–856, 1989.

G. Cornelius and H. Nakashima. Vacuoles play a decisive role in calcium homeostasis in *Neurospora crassa*. *Journal of General Microbiology*, 133:2341–2347, 1987.

B. Crocken and E. L. Tatum. The effect of sorbose on metabolism and morphology of *Neurospora*. *Biochimica et Biophysica Acta*, 156:1–8, 1968.

S. R. Cronin, A. Khoury, D.K. Ferry, and R.Y. Hampton. Regulation of HMG-CoA reductase degradation requires the P-type ATPase Cod1p/ Spf1p. *Journal of Cell Biology*, 148:915–924, 2000.

S. R. Cronin, R. Rao, and R. Y. Hampton. Cod1p/Spf1p is a P-type ATPase involved in ER function and Ca^{2+} homeostasis. *Journal of Cell Biology*, 157: 1071–1028, 2002.

M. C. Cruz, A. L. Goldstein, J. R. Blankenship, M. Del Poeta, D. Davis, M. E. Cardenas, J. Perfect, J. H. McCusker, and J. Heitman. Calcineurin is essential for survival during membrane stress in *Candida albicans*. *The EMBO Journal*, 21:546–559, 2002.

K. W. Cunningham and G. R. Fink. Ca^{2+} transport in *Saccharomyces cerevisiae*. *Journal of Experimental Biology*, 196:157–166, 1994a.

K. W. Cunningham and G. R. Fink. Calcineurin-dependent growth control in *Saccharomyces cerevisiae* mutants lacking *PMC1*, a homolog of plasma membrane Ca^{2+} ATPases. *Journal of Cell Biology*, 124:351–363, 1994b.

K. W. Cunningham and G. R. Fink. Calcineurin inhibits *VCX1*-dependent H^+/Ca^{2+} exchange and induces Ca^{2+} ATPases in *Saccharomyces cerevisiae*. *Molecular and Cellular Biology*, 16:2226–2237, 1996.

M. S. Cyert. Genetic analysis of calmodulin and its targets in *Saccharomyces cerevisiae*. *Annual Review of Genetics*, 35:647–672, 2001.

M. S. Cyert, R. Kunisawa, D. Kaim, and J. Thorner. Yeast has homologs (*CNA1* and *CNA2* gene products) of mammalian calcineurin, a calmodulin-regulated phosphoprotein phosphatase. *Proceedings of the National Academy of Sciences of the USA*, 88:7376–7380, 1991.

M. S. Cyert and J. Thorner. Regulatory subunit (*CNB1* gene product) of yeast Ca^{2+}/calmodulin-dependent phosphosphoprotein phosphatases is required for adaption to pheromone. *Molecular Cell Biology*, 269:3460–3469, 1992.

T. N. Davis. Mutational analysis of calmodulin in *Saccharomyces cerevisiae*. *Cell Calcium*, 13:435–444, 1992.

T. N. Davis, M. S. Urdea, F. R. Masiarz, and J. Thorner. Isolation of the yeast calmodulin gene: calmodulin is an essential protein. *Cell*, 47:423–431, 1986.

C. de Virgilio, N. Burckert, J. M. Neuhaus, T. Boller, and A. Wiemken. *CNE1*, a *Saccharomyces cerevisiae* homologue of the genes encoding mammalian calnexin and calreticulin. *Yeast*, 9:185–188, 1993.

J. W. Deacon. *Modern Mycology*, chapter 1. Blackwell Science, 3rd edition, 1997.

I. Degand, P. Catty, E. Talla, D. Thines-Sempoux, A de Kerchove d'Exaerde,

A. Goffeau, and M. Ghislain. Rabbit sarcoplasmic reticulum Ca^{2+}-ATPase replaces yeast *PMC1* and *PMR1* cCa^{2+}-ATPases for cell viability and calcineurin-dependent regulation of calcium tolerance. *Molecular Microbiology*, 31:545–556, 1999.

L. del Pozo, L. Osaba, J. Corchero, and A. Jimenez. A single nucleotide change in the *MNR1* (*VCX1/HUM1*) gene determines resistance to manganese in *Saccharomyces cerevisiae*. *Yeast*, 15:371–375, 1999.

V. Denis and M. S. Cyert. Internal Ca^{2+} release in yeast is triggered by hypertonic shock and mediated by a TRP channel homologue. *Journal of Cell Biology*, 156: 29–34, 2002.

J. W. Dicker and G. Turian. Calcium deficiencies and apical hyperbranching in the wild-type and the '*frost*' and '*spray*' morphological mutants of *Neurospora crassa*. *Journal of General Microbiology*, 136:1413–1420, 1990.

P. DuBois. *Using csh & tcsh*. O'Reilly, 1st edition, 1995.

T. Dunn, K. Gable, and T. Beeler. Regulation of cellular Ca^{2+} by yeast vacuoles. *Journal of Biological Chemistry*, 269:7273–7278, 1994.

G. Durr, J. Strayle, R. Plemper, S. Elbs, S. K. Klee, P Catty, D. H. Wolf, and H. K. Rudolph. The medial-Golgi ion pump Pmr1 supplies the yeast secretory pathway with Ca^{2+} and Mn^{2+} required for glycosylation, sorting, and endoplasmic reticulum-associated protein degradation. *Molecular Biology of the Cell*, 9:1149–1162, 1998.

Y. Elad and B. Kirshner. Calcium reduces *Botrytis cinerea* damage to plants *Ruscus hypoglossum*. *Phytoparasitica*, 20:285–291, 1992.

A. L. Facanha, H. Appelgren, M. Tabish, L. Okorokov, and K. Ekwall. The endoplasmic reticulum cation P-type ATPase Cta4p is required for control of

cell shape and microtubule dynamics. *Journal of Cell Biology*, 157:1029–1039, 2002.

B. Favre, G. Mauco, G. Turian, and H. Chap. An uncommon multiphosphorylated lipid in *Neurospora crassa* whose formation is catalysed *in vitro* by a calcium- and phospholipid-dependent kinase. *Plant Science*, 77:67–80, 1991.

N. Ferrol and A. B. Bennett. A single gene may encode differentially localized Ca^{2+}-ATPases in tomato. *Plant Cell*, 8:1159–1169, 1996.

M. Fischer, N. Schnell, J. Chattaway, P. Davies, G. Dixon, and D. Sanders. The *Saccharomyces cerevisiae CCH1* gene is involved in calcium influx and mating. *FEBS Letters*, 419:259–262, 1997.

J. S. Flick and J. W. Thorner. Genetic and biochemical characterization of a phosphatidylinositol-specific phospholipase C in *Saccharomyces cerevisiae*. *Methods in Cell biology*, 13:5861–5876, 1993.

M. R. Flory, M. Morphew, J. D. Joseph, A. R. Means, and T. N. Davis. Pcp1p, an Spc110p-related calmodulin target at the centrosome of the fission yeast *Schizosaccharomyces pombe*. *Cell Growth and Differentiation*, 13:47–58, 2002.

C. Forster and P. M. Kane. Cytosolic Ca^{2+} homeostasis is a constitutive function of the V-ATPase in *Saccharomyces cerevisiae*. *Journal of Biological Chemistry*, 275:38245–38253, 2000.

D. S. Fox, M. C. Cruz, R. A. Sia, H. Ke, G. M. Cox, M. E. Cardenas, and J. Heitman. Calcineurin regulatory subunit is essential for virulence and mediates interactions with FKBP12-FK506 in *Cryptococcus neoformans*. *Molecular Microbiology*, 39:835–849, 2001.

D. S. Fox and J. Heitman. Good fungi gone bad: the corruption of calcineurin. *Bioessays*, 24:894–903, 2002.

L. N. Frazer and D. Moore. Antagonists and inhibitors of calcium accumulation do not impair gravity perception though they adversely affect the gravity responces of *Coprinus cinereus* stipes. *Mycological Research*, 97:1113–1118, 1993.

M. D. Fricker, C. Plieth, H. Knight, E. Blancaflor, M. R. Knight, N. S. White, and S. Gilroy. Fluorescence and luminescence techniques to probe ion activities in living plant cells. In W. T. Mason, editor, *Fluorescent and Luminescent Probes for Biological Activity*, pages 569–596. Academic Press, 2^{nd} edition, 1999.

G. M. Gadd. *The Growing Fungus*, chapter Signal Transduction in Fungi, pages 183–210. Chapman and Hall, 1994.

G. M. Gadd and A. H. Brunton. Calcium involvement in dimorphism of *Ophiostomac ulmi*, the dutch elm disease fungus, and characterization of calcium uptake in yeast cells and germ tubes. *Journal of General Microbiology*, 138:1561–1571, 1992.

J. E. Galagan, S. E. Calvo, K. A. Borkovich, E. U. Selker, N. D. Read, D. Jaffe, W. FitzHugh, L. J. Ma, S. Smirnov, S. Purcell, B. Rehman, T. Elkins, R. Engels, S. Wang, C. B. Nielsen, J. Butler, M. Endrizzi, D. Qui, P. Ianakiev, D. Pedersen, M. Nelson, M. Washburne, C. P. Selitrennikoff, J. A. Kinsey, E. L. Braun, A. Zelter, U. Schulte, G. O. Kothe, G. Jedd, W. Mewes, C. Staben, E. Marcotte, D. Greenberg, A. Roy, K. Foley, J. Naylor, N. Thomann, R. Barrett, S. Gnerre, M. Kamal, M. Kamvysselis, E. Mauceli, C. Bielke, S. Rudd, D. Frishman, S. Krystofova, C. Rasmussen, R. L. Metzenberg, D. D. Perkins, S. Kroken, C. Cogoni, G. Macino, D. Catcheside, W. Li, R. J. Pratt, S. A. Osmani, C. C. DeSouza, L. Glass, M. J. Orbach, J. Berglund, R. Voelker, O. Yarden, M. Plamann, S. Seiler, J. Dunlap, A. Radford, R. Aramayo, D. D. Natvig, L. A. Alex, G. Mannhaupt, D. J. Ebbole, M. Freitag, I. Paulsen, M. S. Sachs, E. S. Lander, C. Nusbaum, and B. Birren. The genome sequence of the filamentous fungus *Neurospora crassa*. *Nature*, 422:859–868, 2003.

A. Garrill, R. R. Lew, and I. B. Heath. Stretch-activated Ca^{2+} and Ca^{2+}-activated K^+ channels in the hyphal tip plasma membrane of the oomycete *Saprolegnia ferax*. *Journal of Cell Science*, 101:721–730, 1992.

M. Ghislain, A. Goffeau, D. Halachmi, and Y. Eilam. Calcium homeostasis and transport are affected by disruption of *cta3*, a novel gene encoding Ca^{2+}-ATPase in *Schizosaccharomyces pombe*. *Journal of Biological Chemistry*, 265:18400–18407, 1990.

J. S. C. Gilchrist, M. P. Czubryt, and G. N. Pierce. Calcium and calcium-binding proteins in the nucleus. *Molecular and Cellular Biochemistry*, 135:79–88, 1994.

M. Girbardt. Die Ultrastruktur der Apikalregion von Pilzhyphen. *Protoplasma*, 67:413–441, 1969.

S. Giri and G. K. Khuller. Possible involvement of Ca^{2+}/calmodulin-dependent protein kinase in the regulation of phospholipid biosynthesis in *Microsporum gypseum*. *Molecular and Cellular Biochemistry*, 194:265–270, 1999.

S. Giri, N. Mago, A. Bindra, and G. K. Khuller. Possible role of calcium in phospholipid synthesis of *Microsporum gypseum*. *Biochimica et Biophysica Acta*, 1215:337–340, 1994.

A. Goffeau, B. G. Barrell, H. Bussey, R. W. Davis, B. Dujon, H. Feldmann, F. Galibert, J. D. Hoheisel, C. Jacq, M .Johnston, E. J. Louis, H. W. Mewes, Y. Murakami, P. Philippsen, H. Tettelin, and S. G. Oliver. Life with 6000 genes. *Science*, 274:546–567, 1996.

A. Goffeau et al. The yeast genome directory. *Nature*, 387(Suppl.):1–105, 1997.

M. Gong, A. H. van der Luit, M. R. Knight, and A. J. Trewavas. Heat-shock-induced changes in intracellular Ca^{2+} level in tobacco seedlings in relation to thermotolerance. *Plant Physiology*, 116:429–437, 1998.

G. W. Gooday. Inhibition of chitin metabolism. In P. J. Kuhn, A. P. Trinci, M. J. Jung, M. W. Goosey, and L. G. Copping, editors, *Biochemistry of Cell Walls and Membranes in Fungi*, pages 61–74. Springer Verlag, 1990.

R. Gorovits, O. Propheta, M. Kolot, V. Dombradi, and O. Yarden. A mutation within the catalytic domain of COT1 kinase confers changes in the presence of two COT1 isoforms and in Ser/Thr protein kinase and phosphatase activities in *Neurospora crassa*. *Fungal Genetics and Biology*, 27:264–274, 1999.

N. A. R. Gow, P. F. P. Miller, and G. W. Gooday. Life at the apex: growth of the hyphal tip. *Journal of Chemical Technology and Biotechnology*, 56:217–219, 1992.

V. Greene, H. Cao, F. A. X. Schanna, and D. C. Bartelt. Oxidative stress-induced calcium signalling in *Aspergillus nidulans*. *Cellular Signalling*, 14:437–443, 2002.

M. C. Gustin, X. L. Zhou, L. Martinac, and C Kung. A mechanosensitive ion channel in the yeast plasma membrane. *Science*, 242:762–765, 1988.

D. Halachmi, M. Ghislain, and Y. Eilam. An intracellular ATP-dependent calcium pump within the yeast *Schizosaccharomyces pombe* encoded by the gene cta3. *European Journal of Biochemistry*, 207:1003–1008, 1992.

J. T. Hancock. *Cell Signalling*, chapter Intracellular Calcium: its Control and Role as an Intracellular Signal, pages 144–166. Addison Wesley Longman Ltd, 1997.

R. C. Hardie and B. Minke. The trp gene is essential for a light-activated Ca^{2+} channel in *Drosophila* photoreceptors. *Neuron*, 8:643–651, 1992.

G. E. Hardingham, S. Chawla, C. M. Johnson, and H. Bading. Distinct functions of nuclear and cytoplasmic calcium in the control of gene expression. *Nature*, 385:260–265, 1997.

R. L. Harold and F. M. Harold. Ionophores and cytochalasins modulate branching in *Achlya bisexualis*. *Journal of General Microbiology*, 132:213–219, 1986.

I. B. Heath and G. Steinberg. Mechanisms of hyphal tip growth: tube dwelling amebae revisited. *Fungal Genetics and Biology*, 28:79–93, 1999.

P. K. Hepler and R. O. Wayne. Calcium and plant development. *Annual Review of Plant Physiology*, 36:397–439, 1985.

A. Hernandez, D. T. Cooke, and D. T. Clarkson. Ca^{2+} ATPase-driven calcium accumulation in *Ustilago maydis* plasma membrane vesicles. *Microbiology*, 140: 3047–3051, 1994.

S. Higuchi, J. Tamura, P. Ratana Giri, J. W. Polli, and R. L. Kincaid. Calmodulin-dependent protein phosphatase from *Neurospora crassa*. molecular cloning and expression of recombinant catalytic subunit.

T. Hoshino, A. Mizutani, H. Hidaka, and T. Yamane. Identification of calcium-calmodulin-dependent protein kinase and endogenous substrate of *Fusarium oxysporum*. *FEMS Microbiology Letters*, 94:27–30, 1992.

S. L. Hosking, G. D. Robson, and A. P. J. Trinci. Phosphoinositides play a role in hyphal extension and branching in *Neurospora crassa*. *Experimental Mycology*, 19:71–80, 1995.

D. Hudecoca, L. Varecka, V. Vollek, and V. Betina. Growth and morphogenesis of *Botrytis cinerea*. Effects of exogenous calcium ions, calcium channel blockers and cyclosporin A. *Folia Microbiologica*, 39:269–275, 1994.

G. Hyde. Calcium imaging: a primer for mycologists. *Fungal Genetics and Biology*, 24:14–23, 1998.

H. Iida, H. Nakamura, T. Ono, M. S. Okumura, and Y. Anraku. MID1, a novel saccharomyces cerevisiae gene encoding a plasma membrane protein, is required

for Ca^{2+} influx and mating. *Molecular and Cellular Biology*, 14:8259–8271, 1994.

S. Inouye, M. Noguchi, Y. Sakaki, Y. Takagi, T. Miyata, S. Iwanaga, T. Miyata, F. I., and Tsuji. Cloning and sequence analysis of cDNA for the luminescent protein aequorin. *Proceedings of the National Academy of Sciences of the USA*, 82:3154–3158, 1985.

M. T. Islam and S. Tahara. Chemotaxis of fungal zoospores, with special reference to *Aphanomyces cochlioides*. *Bioscience Biotechnology and Biochemistry*, 65: 1933–1948, 2001.

S. L. Jackson and I. B. Heath. Roles of calcium ions in hyphal tip growth. *Microbiological Reviews*, 57:367–382, 1993.

T. Jayashree, J. Praveen Rao, and C. Subramanyam. Regulation of aflatoxin production by Ca^{2+}/calmodulin-dependent protein phosphorylation and dephosphorylation. *FEMS Microbiology Letters*, 183:215–219, 2000.

J. D. Joseph and A. R. Means. Identification and characterization of two Ca^{2+}/CaM-dependent protein kinases required for normal nuclear division in *Aspergillus nidulans*. *Journal of Biological Chemistry*, 275:38230–38238, 2000.

J. D. Joseph and A. R. Means. Calcium binding is required for calmodulin function in *Aspergillus nidulans*. *Eukaryotic Cell*, 1:119–125, 2002.

O. J. Jung, E. J. Lee, J. W. Kim, Y. R. Chung, and C. W. Lee. Identification of putative phosphoinositide-specific phospholipase C genes in filamentous fungi. *Molecules and Cells*, 7:192–199, 1997.

P. R. Juvvadi, M. Arioka, H. Nakajima, and K. Kitamoto. Cloning and sequence analysis of cnaA gene encoding the catalytic subunit of calcineurin from *Aspergillus oryzae*. *FEMS Microbiology Letters*, 204:169–174, 2001.

A. Kallies, G. Gebauer, and L. Rensing. Heat shock effects on second messenger systems of *Neurospora crassa*. *Archives für Microbiologie*, 170:191–200, 1998.

J. M. Kendall and M. N. Badminton. *Aequorea victoria* bioluminescence moves into an exciting new era. *Trends in Biotechnology*, 16:216–224, 1998.

J. M. Kendall, R. L. Dormer, and A. K. Campbell. Targeting aequorin to the endoplasmic reticulum of living cells. *Biochemical and Biophysical Research Communications*, 189:1008–1016, 1992.

Y. K. Kim, D. Li, and P. E. Kolattukudy. Induction of Ca^{2+}-calmodulin signaling by hard-surface contact primes *Colletotrichum gloeosporoides* conidia to germinate and form appressoria. *Journal of Bacteriology*, 180:5144–5150, 1998.

F. Kippert. Cellular signalling and the complexity of biological timing: insights from the ultradian clock of *Schizosaccharomyces pombe*. *Philosophical Transactions of the Royal Society Of London Series B - Biological Sciences*, 356: 1725–1733, 2001.

H. Knight and M. R. Knight. Recombinant aequorin methods for intracellular calcium measurement in plants. *Methods in Cell Biology*, 49:199–214, 1995.

M. R. Knight, A. K. Campbell, S. M. Smith, and A. J. Trewavas. Recombinant aequorin as a probe for cytosolic free Ca^{2+} in *Escherichia coli*. *FEBS Letters*, 282:405–408, 1991a.

M. R. Knight, A. K. Campbell, S. M. Smith, and Anthony J Trewavas. Transgenic plant aequorin reports the effects of cold-shock and elicitors on cytoplasmic calcium. *Nature*, 352:524–526, 1991b.

M. R. Knight, N. D. Read, A. K. Campbell, and A. J. Trewavas. Imaging calcium dynamics in living plants using semi-synthetic recombinant aequorins. *Journal of Cell Biology*, 121:83–90, 1993.

S. Komori, M. Itagaki, T. Unno, and H. Ohashi. Caffeine and carbachol act on common Ca^{2+} stores to release Ca^{2+} in guinea-pig ileal smooth muscle. *European Journal of Pharmacology*, 277:173–180, 1995.

L. B. Kornstein, M. L. Gaiso, R. L. Hammell, and D. C. Bartelt. Cloning and sequence determination of a cDNA encoding *Aspergillus nidulans* calmodulin-dependent multifunctional protein kinase. *Gene*, 113:75–82, 1992.

G. O. Kothe and S. J. Free. Calcineurin subunit B is required for normal vegetative growth in *Neurospora crassa*. *Fungal Genetics and Biology*, 23:248–258, 1998.

O. Kozlova-Zwinderman. *Calcium Measurement in Living Filamentous Fungi Expressing Codon-Optimised Aequorin*. PhD thesis, University of Edinburgh, 2002.

A. Kreusch, P. J. Pfaffinger, C. F. Stevens, and S. Choe. Crystal structure of the tetramerization domain of the shaker potassium channel. *Nature*, 392:945–948, 1998.

S. Krystova, L. Varecka, and V. Betina. The $^{45}Ca^{2+}$ uptake by *Trichoderma viride* mycelium. correlation with growth and conidiation. *General Physiology and Biophysics*, 14:323–337, 1995.

T. Kuno, H. Tanaka, H. Mukai, C.D. Chang, K. Hiraga, T. Miyakawa, and C. Tanaka. cDNA cloning of calcineurin B homolog in *Saccharomyces cerevisiae*. *Biochemical and Biophysical Research Communications*, 180:1159–1163, 1991.

S. I. Kwon, C. D. van Dohlon, and A. J. Anderson. Gene sequence analysis of an opportunistic wheat pathogen, an isolate of *Fusarium proliferatum*. *Canadian Journal of Botany*, 79:1115–1121, 2001.

P. L. Lakin-Thomas. Effects of inositol starvation on the levels of inositol phosphates and inositol lipids in *Neurospora crassa*. *Biochemical Journal*, 292: 805–811, 1993.

P. J. Lapinskas, S. J. Lin, and V. C. Culotta. The role of the *Saccharomyces* cerevisiae *CCC1* gene in the homeostasis of manganese ions. *Molecular Microbiology*, 21:519–528, 1996.

F. R. Lauter, U. Marchfelder, V. E. A. Russo, C. T. Yamashiro, E. Yatzkan, and O. Yarden. Photoregulation of *cot-1*, a kinase-encoding gene involved in hyphal growth in *Neurospora crassa*. *Fungal Genetics and Biology*, 23:300–310, 1998.

S. Y. Lee and R. E. Klevit. The whole is not the simple sum of its parts in calmodulin from *S. cerevisiae*. *Biochemistry*, 39:4225–4230, 2000.

N. N. Levina, R. R. Lew, G. J. Hyde, and I. B. Heath. The roles of Ca^{2+} and plasma membrane ion channels in hyphal tip growth of *Neurospora crassa*. *Journal of Cell Science*, 108:3405–3417, 1995.

F. Liang and H. Sze. A high-affinity Ca^{2+} pump, ECA1, from the endoplasmic reticulum is inhibited by cyclopiazonic acid but not by thapsigargin. *Plant Physiology*, 118:817–825, 1998.

D. C. Lin, K. D. Tobin, M. Grumet, and S. Lin. Cytochalasins inhibit nuclei-induced actin polymerization by blocking filament elongation. *Journal of Cell Biology*, 84:455–460, 1980.

Y. Liu, S. Ishii, M. Tokai, H. Tsutsumi, O. Ohki, R. Akada, K. Tanaka, E. Tsuchiya, S. Fukui, and T. Miyakawa. The *Saccharomyces cerevisiae* genes (*CMP1* and *CMP2*) encoding calmodulin-binding proteins homologus to the catalytic subunit of mammalian protein phosphatase 2B. *General Genetics*, 227:52–59, 1991.

E. G. Locke, M. Bonilla, L. Liang, Y. Takita, and K. W. Cunningham. A homolog of voltage-gated Ca^{2+} channels stimulated by depletion of secretory Ca^{2+} in yeast. *Molecular Cell Biology*, 20:6686–6694, 2000.

R. López-Franco, S. Bartnicki-Garcia, and C. E. Bracker. Pulsed growth of fungal hyphal tips. *Proceedings of the National Academy of Sciences of the USA*, 91: 12228–12232, 1994.

R. López-Franco and C. E. Bracker. Diversity and dynamics of the Spitzenkörper in growing hyphal tips of higher fungi. *Protoplasma*, 195:90–111, 1996.

K. P. Lu, S. A. Osmani, A. H. Osmani, and A. R. Means. Cooperative regulation of cell proliferation by calcium and calmodulin in *Aspergillus nidulans*. *Molecular Endocrinology*, 6:365–374, 1992.

K. P. Lu, S. A. Osmani, A. H. Osmani, and A. R. Means. Essential roles for calcium and calmodulin in G2/M progression in *Aspergillus nidulans*. *Journal of Cell Biology*, 121:621–630, 1993.

R. L. Mach, S. Zeilinger, D. Kristufek, and C. P. Kubicek. Ca^{2+}-calmodulin antagonists interfere with xylanase formation and secretion in *Trichoderma reesei*. *Biochimica et Biophysica Acta*, 1403:281–289, 1998.

R. Malhó, A. Moutinho, A. van der Luit, and A. J. Trewavas. Spatial characteristics of calcium cignalling: the calcium wave as a basic unit in plant cell calcium signalling. *Philosophical Transactions of the Royal Society of London Series B - Biological Sciences*, 353:1463–1473, 1998.

S. Malmström, P. Askerlund, and M. G. Palmgren. A calmodulin-stimulated Ca^{2+}-ATPase from plant vacuolar membranes with aputative regulatory domain at its N-terminus. *FEBS Letters*, 400:324–328, 1997.

C. Mao, S. H. Kim, J. S. Almenoff, X. L. Rudner, D. M. Kearney, and L. A. Kindman. Molecular cloning and characterization of SCaMPER, a sphingolipid ca^{2+} release-mediating protein from endoplasmic reticulum. *Proceedings of the National Academy of Sciences of the USA*, 93:1993–1996, 1996.

E. E. Margolles-Clark, S. Abreu, and B. J. Bowman. Characterization of a vacuolar Ca^{2+}/H^{+} exchanger (CAX) of *Neurospora crassa*. *Fungal Genetics Newsletters*, 46(Suppl.):37, 1999.

P. Markham. Stress management: filamentous fungi as exemplary survivors. *FEMS Microbiology Letters*, 100:379–386, 1992.

P. Markham and B. W. Bainbridge. Effect of choline deprivation on the growth, morphology and ultrastructure of a choline-requiring mutant of *Aspergillius nidulans*. *FEMS Microbiology Letters*, 90:217–222, 1992.

P. Markham, G. D. Robson, B. W. Bainbridge, and A. P. Trinci. Choline: Its role in the growth of filamentous fungi and the regulation of mycelial morphology. *FEMS Microbiology Reviews*, 104:287–300, 1993.

T. Maruoka, Y. Nagasoe, S. Inoue, Y. Mori, J. Goto, M. Ikeda, and H. Iida. Essential hydrophilic carboxyl-terminal regions including cysteine residues of the yeast stretch-activated calcium-permeable channel Mid1. *Journal of Biological Chemistry*, 277:11645–11652, 2002.

T. Maruyama, T. Kanaji, S. Nakade, T. Kanno, and K. Mikoshiba. 2APB, 2-aminoethoxydiphenyl borate, a membrane-penetrable modulator of Ins(1,4,5)P3-induced Ca^{2+} release. *Journal of Biological Chemistry*, 122:498–505, 1997.

P. Mäser, S. Thomine, J. I. Schroeder, J. M. Ward, K. Hirschi, H. Sze, I. N. Talke, A. Amtmann, F. J. Maathuis, D. Sanders, J. F. Harper, J. Tchieu, M. Gribskov, M. W. Persans, D. E. Salt, S. A. Kim, and M. L. Guerinot. Phylogenetic relationships within cation transporter families of *Arabidopsis*. *Plant Physiology*, 126:1646–1667, 2001.

D. P. Matheos, T. J. Kingsbury, U. S. Ahsan, and K. W. Cunningham. Tcn1p/Crz1p, a calcineurin-dependent transcription factor that differentially

regulates gene expression in *Saccharomyces cerevisiae*. *Genes and Development*, 11:3445–3458, 1997.

T. K. Matsumoto, A. J. Ellsmore, S. G. Cessna, P. S. Low, J. M. Pardo, R. A. Bressan, and P. M. Hasegawa. An osmotically induced cytosolic Ca^{2+} transient activates calcineurin signaling to mediate ion homeostasis and salt tolerance of *Saccharomyces cerevisiae*. *Journal of Biological Chemistry*, 277:33075–33080, 2002.

R. R. McKay, C. L. Szymeczek-Seay, J. P. Lievremont, G. S. Bird, C. Zitt, E. Jungling, A. Luckhoff, and J. W. Putney Jr. Cloning and expression of the human transient receptor potential 4 (TRP4) gene: localization and functional expression of human TRP4 and TRP3. *Biochemical Journal*, 351:735746, 2000.

M. T. McNally and S. J. Free. Isolation and characterisation of a *Neurospora* glucose-repressible gene. *Current Genetics*, 14:545–551, 1988.

M. B. Melnick, C. Melnick, M. Lee, and D. O. Woodward. Structure and sequence of the calmodulin gene from *Neurospora crassa*. *Biochimica et Biophysica Acta*, 1171:334–336, 1993.

J. Michiels, C. Xi, J. Verhaert, and J. Vanderleyden. The functions of Ca^{2+} in bacteria: a role for EF-hand proteins? *Trends in Microbiology*, 10:87–93, 2002.

A. J. Miller. *Ion-selective microelectrodes. In Plant Cell Biology: a Practical Approach*, pages 283–296. Oxford: IRL Press, 1994.

A. J. Miller, G. Vogg, and D. Sanders. Cytosolic calcium homeostasis in fungi: roles of plasma membrane transport and intracellular sequestration of calcium. *Proceedings of the National Academy of Sciences of the USA*, 87:9348–9352, 1990.

A. Miseta, L. Fu, R. Kellermayer, J. Buckley, and D. M. Bedwell. The Golgi apparatus plays a significant role in the maintenance of Ca^{2+} homeostasis in the

vps33DELTA vacuolar biogenesis mutant of *Saccharomyces cerevisiae*. *Journal of Biological Chemistry*, 274:5939–5947, 1999a.

A. Miseta, R. Kellermayer, D. P. Aiello, L. Fu, and D. M. Bedwell. The vacuolar Ca^{2+}/H^{+} exchanger Vcx1p/Hum1p tightly controls cytosolic Ca^{2+} levels in *S. cerevisiae*. *FEBS Letters*, 451:132–136, 1999b.

N. C. Mishra and E. L. Tatum. Effect of L-sorbose on polysaccharide synthetases of *Neurospora crassa* (glycogen- -1,3-glucan-morphology-cell wall-digitonin-particulate enzymes). *Proceedings of the National Academy of Sciences of the USA*, 69:313–317, 1972.

A. Miyawaki, J. Llopis, R. Heim, J. M. McCaffery, J. A. Adams, M. Ikura, and R. Y. Tsien. Fluorescent indicators for ca^{2+} based on green fluorescent proteins and calmodulin. *Nature*, 388:882–887, 1997.

M. Mizunuma, D. Hirata, K. Miyahara, E. Tsuchiya, and T. Miyakawa. Role of calcineurin and Mpk1 in regulating the onset of mitosis in budding yeast. *Nature*, 392:303–306, 1998.

M. Mizunuma, D. Hirata, R. Miyaoka, and T. Miyakawa. GSK-3 kinase Mck1 and calcineurin coordinately mediate Hsl1 down-regulation by Ca^{2+} in budding yeast. *The EMBO Journal*, 20:1074–1085, 2001.

J. Moniakis, M. B. Coukell, and A. Forer. Molecular cloning of an intracellular P-type ATPase from *Dictyostelium* that is up-regulated in calcium-adapted cells. *Journal of Biological Chemistry*, 270:28276–28281, 1995.

M. J. Moser, S. Y. Lee, R. E. Klevit, and T. N. Davis. Ca^{2+} binding to calmodulin and its role in *Schizosaccharomyces pombe* as revealed by mutagenesis and NMR spectroscopy. *Journal of Biological Chemistry*, 270:20643–20652, 1995.

E. M. Muller, E. G. Locke, and K. W. Cunningham. Differential regulation of

two Ca^{2+} influx systems by pheromone signaling in *Saccharomyces cerevisiae*. *Genetics*, 159:1527–1538, 2001.

G. Muthukumar, A. W. Nickerson, and K. W. Nickerson. Calmodulin levels in yeasts and filamentous fungi. *FEMS Microbiology Letters*, 41:253–255, 1987.

G. Muthukumar and K. W. Nickerson. Ca(ii)-calmodulin regulation of fungal dimorphism in *Ceratocystis ulmi*. *Journal of Bacteriology*, 159:390–392, 1984.

J. Nakajima-Shimada, H. Iida, F. I. Tsuji, and Y. Anraku. Galactose-dependent expression of the recombinant Ca^{2+} binding protoprotein aequorin in yeast. *Biochemical and Biophysical Research Communications*, 174:115–122, 1991a.

J. Nakajima-Shimada, H. Iida, F. I. Tsuji, and Y. Anraku. Monitoring of intracellular calcium in *Saccharomyces cerevisiae* with an apoaequorin cDNA expression system. *Proceedings of the National Academy of Sciences of the USA*, 88:6870–6882, 1991b.

T. Nakamura, Y. Liu, D. Hirata, H. Namba, S. Harada, T. Hirokawa, and T. Miyakawa. Protein phosphatase type 2B (calcineurin)-mediated, FK506-sensitive regulation of intracellular ions in yeast is an important determinant for adaption to high salt stress conditions. *The EMBO Journal*, 12:4063–4071, 1993.

C. Navarre and A. Goffeau. Membrane hyperpolarization and salt sensitivity induced by deletion of PMP3, a highly conserved small protein of yeast plasma membrane. *The EMBO Journal*, 19:2515–2524, 2000.

G. Nelson. *Development of the Recombiant Aequorin Method and its Evaluation for Calcium Measurement in Filamentous Fungi.* PhD thesis, University of Edinburgh, 1999.

G. Nelson, O. Kozlova-Zwinderman, A. J. Collis, M. R. Knight, J. R. S. Fincham, C. P. Stanger, A. Renwick, J. G. M. Hessing, P. J. Punt, C. A. M. J. J. van den

Hondel, and N. D. Read. Calcium measurement in living filamentous fungi expressing codon-optimised aequorin. *Molecular Microbiology*, 2003. In press.

M. A. Nelson. The *Neurospora* - fungal genome initiative: White paper. http://biology.unm.edu/biology/ngp/WhitePaper.html, 2000.

A. Odom, S. Muir, E. Lim, D. L. Toffaletti, J. Perfect, and J. Heitman. Calcineurin is required for virulence of *Cryptococcus neoformans*. *The EMBO Journal*, 16:2576–2589, 1997.

Y. Ohsumi and Y. Anraku. Calcium transport driven by a proton motive foarce in vacuolar membrans vesicles of *Saccharomyces cerevisiae*. *Journal of Biological Chemistry*, 258:5614–5617, 1983.

Y. Ohya and Y. Anraku. A galactose-dependent cmd1 mutant of *Saccharomyces cerevisiae*: involvement of calmodulin in nuclear division. *Current Genetics*, 15:113–120, 1989.

Y. Ohya and Y. Anraku. Yeast calmodulin: structural and functional elements essential for the cell cycle. *Cell Calcium*, 13:445–455, 1992.

Y. Ohya, H. Kawasaki, K. Suzuki, J. Londesborough, and Y. Anraku. Two yeast genes encoding calmodulin-dependent protein kinases. isolation, sequencing and bacterial expressions of *CMK1* and *CMK2*. *Journal of Biological Chemistry*, 266:12784–12794, 1991a.

Y. Ohya, N. Umemoto, I. Tanida, A. Ohta, H. Iida, and Y. Anraku. Calcium-sensative *cls* mutants of *Saccharomyces cerevisiae* showing a Pet- phenotype are ascribable to defects of vacuolar membrane H^+-ATPase activity. *Journal of Biological Chemistry*, 266:13971–13977, 1991b.

Y. Ohya, I. Uno, T. Ishikawa, and Y. Anraku. Purification and biochemical properties of calmodulin from *Saccharomyces cerevisiae*. *European Journal of Biochemistry*, 168:13–19, 1987.

L. A. Okorokov, A. J. Kuranov, E. V. Kuranova, and R. D. Silva. Ca^{2+}-transporting ATPase(s) of the reticulum type in intracellular membranes of *Saccharomyces cerevisiae*. Biochemical identification. *FEMS Microbiology Letters*, 146:39–46, 1997.

M. J. Orbach. A cosmid with a HyR marker for fungal library construction and screening. *Gene*, 150:159–162, 1994.

M. Paidhungat and S. Garrett. A homolog of mammalian, voltage-gated calcium channels mediates yeast pheromone-stimulated Ca^{2+} uptake and exacerbates the *cdc1* (ts) growth defect. *Molecular and Cellular Biology*, 17:6339–6347, 1997.

C. P. Palmer, X. L. Zhou, J. Lin, S. H. Loukin, C. Kung, and Y. Saimi. A TRP homolog in *Saccharomyces cerevisiae* forms an intracellular Ca^{2+}-permeable channel in the yeast vacuolar membrane. *Proceedings of the National Academy of Sciences of the USA*, 98:7801–7805, 2001.

J. L. Paluh, M. J. Orbach, T. L. Legerton, and C. Yanofsky. The cross-pathway control gene of *Neurospora crassa*, *cpc-1*, encodes a protein similar to *GCN4* of yeast and the DNA-binding domain of the oncogene v-*jun*-encoded protein. *Proceedings of the National Academy of Sciences of the USA*, 85:3728–3732, 1988.

C. S. Park, J. Y. Kim, C. Crispino, C. C. Chang, and D. D. Ryu. Molecular cloning of *YlPMR1*, a *S. cerevisiae PMR1* homologue encoding a novel P-type secretory pathway Ca^{2+}-ATPase, in the yeast *Yarrowia lipolytica*. *Gene*, 206: 107–116, 1998.

S. Y. Park, S. B. Seo, S. J. Lee, J. G. Na, and Y. J. Kim. Mutation in *PMR1*, a Ca^{2+}-ATPase in Golgi, confers salt tolerance in *Saccharomyces cerevisiae* by inducing expression of *PMR2*, an Na^{+}-ATPase in plasma membrane. *Journal of Biological Chemistry*, 276:28694–28699, 2001.

D. D. Perkins. *Neurospora*: the organism behind the molecular revolution. *Genetics*, 130:687–701, 1992.

D. D. Perkins, A. Radford, D. Newmeyer, and M. Bjorkman. Chromosomal loci of *Neurospora crassa*. *Microbiological Reviews*, 46:426–570, 1982.

D. Pietrobon, F. D. Di Virgilio, and T. Pozzan. Structural and functional aspects of calcium homeostasis in eukaryotic cells. *European Journal of Biochemistry*, 193:599–562, 1990.

D. Pitt and J. C. Barners. Calcium-induced conidiation in *Penicillium notatum*. *Journal of General Microbiology*, 139:3053–3063, 1999.

D. Pitt and J. C. Barnes. Calcium homeostasis, signaling and protein-phosphorylation during calcium-induced conidiation in *Penicillium notamun*. *Journal of General Microbiology*, 139:3053–3063, 1993.

J. K. Pittman and K. D. Hirschi. Regulation of CAX1, an *Arabidopsis* Ca^{2+}/H^{+} antiporter. identification of an N-terminal autoinhibitory domain. *Plant Physiology*, 127:1020–1029, 2001.

J. K. Pittman, T. Shigaki, N. H. Cheng, and K. D. Hirschi. Mechanism of N-terminal autoinhibition in the *Arabidopsis* Ca^{2+}/H^{+} antiporter CAX1. *Journal of Biological Chemistry*, 277:26452–26459, 2002a.

J. K. Pittman, C. S. Sreevidya, T. Shigaki, H. Ueoka-Nakanishi, and K. D. Hirschi. Distinct N-terminal regulatory domains of Ca^{2+}/H^{+} antiporters. *Plant Physiology*, 130:1054–1062, 2002b.

T. C. Pozos, I. Sekler, and M. S. Cyert. The product of *HUM1*, a novel yeast gene, is required for vacuolar Ca^{2+}/H^{+} exchange and is related to mammalian Na^{2+}/Ca^{2+} exchangers. *Molecular and Cellular Biology*, 16:3730–3741, 1996.

D. Prasher, R. O. McCann, and M. J. Cormier. Cloning and expression of the cDNA coding for aequorin, a bioluminescent calcium-binding protein. *Biochemical and Biophysical Research Communications*, 126:1259–1268, 1985.

T. R. Prezant, W. E. Jr Chaltraw, and N. Fischel-Ghodsian. Identification of an overexpressed yeast gene which prevents aminoglycoside toxicity. *Microbiology*, 142:3407–3414, 1996.

H. Prokisch, O. Yarden, M. Dieminger, M. Tropschug, and I. B. Barthelmess. Impairment of calcineurin function in *Neurospora crassa* reveals its essential role in hyphal growth, morphology and maintenance of the apical Ca^{2+} gradient. *Molecular and General Genetics*, 256:104–114, 1997.

O. Propheta, J. Vierula, P. Toporowski, R. Gorovits, and O. Yarden. The *Neurospora crassa* colonial temperature-sensitive 3 (*cot-3*) gene encodes protein elongation factor 2. *Molecular and General Genetics*, 264:894–901, 2001.

J. P. Rao, G. Reena, and C. Subramanyam. Calmodulin-dependent protein phosphorylation during conidial germination and growth of *Neurospora crassa*. *Mycological Research*, 101:1484–1488, 1997.

J. Praveen Rao and C. Subramanyam. Requirement of Ca^{2+} for aflatoxin production: Inhibitory effect of Ca^{2+} channel blockers on aflatoxin production by *Aspergillus parasiticus* NRRL 2999. *Letters in Applied Microbiology*, 28: 85–88, 1999.

C. Rasmussen, C. Garen, S. Brining, R. L. Kincaid, R. L. Means, and A. R. Means. The calmodulin-dependent protein phosphatase catalytic subunit (calcineurin A) is an essential gene in *Aspergillus nidulans*. *The EMBO Journal*, 13:3917–3924, 1994.

C. Rasmussen and G. Rasmussen. Inhibition of G2/M progression in *Schizosaccharomyces pombe* by a mutant calmodulin kinase II with constitutive activity. *Molecular Biology of the Cell*, 5:785–795, 1994.

C. D. Rasmussen, R. L. Means, K. P. Lu, G. S. May, and A. R. Means. Characterization and expression of the unique calmodulin gene of *Aspergillus nidulans*. *Journal of Biological Chemistry*, 265:13767–13775, 1990.

N. D. Read, W. T. G. Allan, H. Knight, M. R. Knight, R. Malhó, A. Russell, P. S. Shacklock, and A. J. Trewavas. Imaging and measurement of cytosolic free calcium in plant and fungal cells. *Journal of Microscopy*, 166:57–86, 1992.

J. L. Reissig and S. G. Kinney. Calcium as a branching signal in *Neurospora crassa*. *Journal of Bacteriology*, 154:1397–1402, 1983.

Z. Resheat-Eini, R. Gorovits, and O. Yarden. The phenotype of the *Neurospora crassa cot-5* mutant, defective in a mannosyltransferase, can be suppressed by increased medium osmoticum. 22nd Fungal Genetics Conference, Pacific Grove, California, 2003.

G. C. Reynaga-Penüia, G. Gierz, and S. Bartnicki-Garcia. Analysis of the role of the spitzenkörper in fungal morphogenesis by computer simulation of apical branching in *Aspergillus niger*. *Proceedings of the National Academy of Sciences of the USA*, 94:9096–9101, 1997.

M. Riquelme, C. G. Reynaga-Peña, G. Gierz, and S. Bartnicki-García. What determines growth direction in fungal hyphae? *Fungal Genetics and Biology*, 24:101–109, 1998.

N. Rivera-Rodriguez and N. Rodriguez-Del Valle. Effects of calcium ions on the germination of *Sporothrix schenckii* conidia. *Journal of Medical and Veterinary Mycology*, 30:185–195, 1992.

R. Rizzuto, M. Brini, and T. Pozzan. Targeting recombinant aequorin to specific intracellular organelles. *Methods in Cell Biology*, 40:339–358, 1994.

R. Rizzuto, A. W. M. Simpson, M. Brini, and T. Pozzan. Rapid changes of

mitochondrial Ca^{2+} revealed by specifically targeted recombinant aequorin. *Nature*, 358:325–327, 1992.

G. D. Robson, M. G. Wiebe, and A. P. Trinci. Exogenious cAMP and cGMP modulate branching in *Fusarium graminearum*. *Journal of General Microbiology*, 137:963–969, 1991a.

G. D. Robson, M. G. Wiebe, and A. P. Trinci. Involvement of Ca^{2+} in the regulation of hyphal extension and branching in *Fusarium graminearum* A-3/5. *Experimental Mycology*, 15:263–272, 1991b.

G. D. Robson, M. G. Wiebe, and A. P. Trinci. Low calcium concentrations induce increased branching in *Fusarium graminearum*. *Mycological Research*, 95:561–565, 1991c.

A. A. Rodrigues, C. Pina-Vaz, P. A. Mardh, J. Martinez de Oliveira, and A. Freitas da Fonseca. Inhibition of germ tube formation by *Candida albicans* by local anesthetics: an effect related to ionic channel blockade. *Current Microbiology*, 40:145–148, 2000.

P. Rosay, S. A. Davies, Y. Yu, M. Ali-Sozen, K. Kaiser, and J. A. T. Dow. Cell-type specifica calcium signalling in a *Drosophila epithelium*. *Journal of Cell Science*, 110:1683–1692, 1997.

F. T. Sabie and G. M. Gadd. Involvement of a Ca^{2+}-calmodulin interaction in the yeast-mycelial transition of *Candida albicans*. *Mycopathologia*, 108:47–54, 1989.

Y. Sadakane and H. Nakashima. Light-induced phase shifting of the circadian conidiation rhythm is inhibited by calmodulin antagonists in *Neurospora crassa*. *Journal of Biological Rhythms*, 11:234–240, 1996.

F. B. Sailsbury and C. W. Ross. *Plant Physiology*, chapter 17, pages 357–360. Wadsworth Inc., 4^{th} edition, 1992.

J. Sambrook, E. F. Fritsch, and T. Maniatis. *Molecular Cloning - A Laboratory Manual.* Cold Spring Harbor Laboratory Press, 2nd edition, 1989.

D. Sanders, C. Brownlee, and J. F. Harper. Communicating with calcium. *Plant Cell*, 11:691–706, 1999.

D. Sanders, J. Pelloux, C. Brownlee, and J. F. Harper. Calcium at the crossroads of signaling. *Plant Cell*, pages S401–S417, 2002.

S. Saran, H. Nakao, M. Tasaka, H. Iida, F. I. Tsuji, V. Nanjundiah, and I. Takeuchi. Intracellular free calcium level and its response to cAMP stimulation in developing *Dictyostelium* cells transformed with jellyfish apoaequorin cDNA. *FEBBS Letters*, 337:43–47, 1994.

M. Schliwa. Action of cytochalasin D on cytoskeletal networks. *Journal of Cell Biology*, 92:79–91, 1982.

J. Schmid and F. M. Harold. Dual roles for calcium ions in apical growth of *Neurospora crassa*. *Journal of General Microbiology*, 134:2623–2631, 1988.

M. Schreiber and L. Salkoff. A novel calcium-sensing domain in the BK channel. *Biophysical Journal*, 73:1355–1363, 1997.

C Schultz, G Gebauer, T Metschies, L Rensing, and B Jastorff. cis, cis-cyclohexane 1,3,5-triol polyphosphates release calcium from *Neurospora crassa* via an unspecific Ins 1,4,5-P3 receptor. *Biochemical and Biophysical Research Communications*, 166:1319–1327, 1990.

N. W. Seidler, I. Jona, M. Vegh, and A. Martonosi. Cyclopiazonic acid is a specific inhibitor of the Ca^{2+}-ATPase of sarcoplasmic reticulum. *Journal of Biological Chemistry*, 264:17816–17823, 1989.

E. U. Selker. Repeat-induced point mutation and DNA methylation. In J. W. Bennett and L. L. Lasure, editors, *More Gene Manipulations in Fungi*, pages 258–265. Academic Press Inc., 1991.

B. D. Shaw and H. C. Hoch. Ca^{2+} regulation of *Phyllosticta ampelicida* pycnidiospore germination and appressorium formation. *Fungal Genetics and Biology*, 31:43–53, 2000.

B. S. Shaw, O. Koslova, N. D. Read, G. Turgeon, and H. C. Hoch. Expression of recombinant aequorin as an intracellular calcium reporter in the phytopathogenic fungus *Phyllosticta ampelicida*. *Fungal Genetics and Biology*, 34:207–215, 2001.

A. Sievers and M. B. Busch. An inhibitor of the Ca^{2+}-ATPases in the sarcoplasmic and endoplasmic reticula inhibits transduction of the gravity stimulus in cress roots. *Planta*, 188:619–622, 1992.

L. B. Silverman-Gavrila and R. R. Lew. Calcium and tip growth in *Neurospora crassa*. *Protoplasma*, 213:203–217, 2000.

L. B. Silverman-Gavrila and R. R. Lew. Regulation of the tip-high $[Ca^{2+}]$ gradient in growing hyphae of the fungus *Neurospora crassa*. *European Journal of Cell Biology*, 80:379–390, 2001.

L. B. Silverman-Gavrila and R. R. Lew. An IP_3-activated Ca^{2+} channel regulates fungal tip growth. *Journal of Cell Science*, 115:5013–5025, 2002.

U. P. Singh and B. Prithiviraj ad B. K. Sarma. Effect of calcium and calmodulin modulators on the development of *Erysiphe pisi* on pea leaves. *Microbiological Research*, 156:65–69, 2001.

T. P. Snutch, W. J. Tomlinson, J. P. Leonard, and M. M. Gilbert. Distinct calcium channels are generated by alternative splicing and are differentially expressed in the mammalian CNS. *Neuron*, 7:4557, 1991.

Y. S. Sohn, C. S. Park, S. B. Lee, and D. D. Ryu. Disruption of *PMR1*, encoding a Ca^{2+}-ATPase homolog in *Yarrowia lipolytica*, affects secretion and processing of homologous and heterologous proteins. *Journal of Bacteriology*, 180:6736–6742, 1998.

T. Sone and A. J. F. Griffiths. The *frost* gene of *Neurospora crassa* is a homolog of yeast *cdc1* and affects hyphal branching via manganese homeostasis. *Fungal Genetics and Biology*, 28:227–237, 1999.

S. Spiegel and S. Milstien. Sphingosine 1-phosphate, a key cell signaling molecule. *Journal of Biological Chemistry*, 277:25851–25854, 2002.

C. Staben, B. Jensen, M. Singer, J. Pollock, M Schectman, J. Kinsey, and E. Selker. Use of a bacterial hygromycin B resistance gene as a dominant selectable marker in *Neurospora crassa* transformation. *Fungal Genetics Newsletter*, 36:79–81, 1989.

A. Stathopoulos-Gerontides, J. J. Guo, and M. S. Cyert. Yeast calcineurin regulates nuclear localization of the Crz1p transcription factor through dephosphorylation. *Genes and Development*, 13:798–803, 1999.

D. A. Stirling and M. J. Stark. Mutations in SPC110, encoding the yeast spindle pole body calmodulin-binding protein, cause defects in cell integrity as well as spindle formation. *Biochimica et Biophysica Acta*, 1499:85–100, 2000.

J. Strayle, T. Pozzan, and H. Rudolph. Steady-state free Ca^{2+} in the yeast endoplamic reticulum reaches only 10 mM and is mainly controlled by the secretory pathway pump Pmr1. *The EMBO Journal*, 18:4733–4743, 1999.

P. Stroobant, J. B. Dame, and G. A. Scarborough. The *Neurospora* plasma membrane Ca^{2+} pump. *Federal Proceedings*, 39:2437–2441, 1980.

P. Stroobant and G. A. Scarborough. Active transport of calcium in *Neurospora* plasma membrane vesicles. *Proceedings of the National Academy of Sciences of the USA*, 76:3102–3106, 1979.

R. Sugiura, S. O. Sio, H. Shuntoh, and T. Kuno. Calcineurin phosphatase in signal transduction: lessons from fission yeast. *Genes Cells*, 7:619–627, 2002.

G. H. Sun, A. Hirata, Y. Ohya, and Y. Anraku. Mutations in yeast calmodulin cause defects in spindle pole body functions and nuclear integrity. *Journal of Cell Biology*, 119:1625–1639, 1992.

H. A. Sundberg, L. Goetsch, B. Byers, and T. N. Davis. Role of calmodulin and Spc110p interaction in the proper assembly of spindle pole body compenents. *Journal of Cell Biology*, 133:111–124, 1996.

C. Suzuki. Immunochemical and mutational analyses of P-type ATPase Spf1p involved in the yeast secretory pathway. *Bioscience, Biotechnology, and Biochemistry*, 65:2405–2411, 2001.

T. Tada, M. Ohmori, and H. Iida. Molecular dissection of the hydrophobic segments H3 and H4 of the yeast Ca^{2+} channel component Mid1. *Journal of Biological Chemistry*, 278:9647–9654, 2003.

T. Tanabe, H. Takeshima, A. Mikami, V. Flockerzi, H. Takahashi, K. Kangawa, M. Kojima, H. Matsuo, T. Hirose, and S. Numa. Primary structure of the receptor for the calcium channel blockers from skeletal muscle. *Nature*, 328: 313318, 1987.

Y. Tasaka, Y. Nakagawa, C. Sato, M. Mino, N. Uozumi, N. Murata, S.Muto, and H. Iida. yam8^{+}, a *Schizosaccharomyces pombe* gene, is a potential homologue of the *Saccharomyces cerevisiae* MID1 gene encoding a stretch-activated Ca^{2+}-permeable channel. *Biochemical and Biophysical Research Communications*, 269:265–269, 2000.

D. Techel, G. Gebauer, W. Kohler, T. Braumann, B. Jastorff, and L. Rensing. On the role of Ca^{2+}-calmodulin-dependent and cAMP-dependent protein phosphorylation in the circadian rhythm of *Neurospora crassa*. *Journal of Comparative Physiology. B, Biochemical, Systemic, and Environmental Physiology*, 159:695–706, 1990.

J. D. Thompson. The CLUSTAL_X windows interface: flexible strategies for multiple sequence alignment aided by quality analysis tools. *Nucleic Acids Research*, 25:4876–4882, 1997.

R. Tisi, S. Baldassa, F. Belotti, and E. Martegani. Phospholipase C is required for glucose-induced calcium influx in budding yeast. *FEBS Letters*, 520:133–138, 2002.

S. Torralba, I. B. Heath, and F. P. Ottensmeyer. Ca^{2+} shuttling in vesicles during tip growth in *Neurospora crassa*. *Fungal Genetics and Biology*, 33:181–193, 2001.

C. Toyoshima, M. Nakasako, H. Nomura, and H. Ogawa. Crystal structure of the calcium pump of sarcoplasmic reticulum at 2.6 Å resolution. *Nature*, 405: 647–655, 2000.

F. Trail, X. Haixin, R. Lorabger, and D. Gadoury. Physiological and environmental aspects of ascospore discharge in *Gibberella zeae* (anamorph *Fusarium graminearum*). *Mycologia*, 94:181–189, 2002.

A. J. Trewavas and R. Malhó. Signal perception and transduction: the origin of the phenotype. *Plant Cell*, 9:1181–1195, 1997.

A. P. Trinci. Growth of wild type and spreading colonial mutants of *Neurospora crassa* in batch culture and on agar medium. *Archives für Microbiologie*, 91: 113–126, 1973a.

A. P. Trinci. The hyphal growth unit of wild type and spreading colonial mutants of *Neurospora crassa*. *Archives für Microbiologie*, 91:127–136, 1973b.

A. P. Trinci and A. Collinge. Influence of L-sorbose on the growth and morphology of *Neurospora crassa*. *Journal of General Microbiology*, 78:179–192, 1973.

A. P. J. Trinci. A study of the kinetics of hyphal extension and branch initiation of fungal mycelia. *Journal of General Microbiology*, 81:225–236, 1974.

P. J. Tsai, J. Tu, and T. H. Chen. Cloning of a Ca^{2+}/calmodulin-dependent protein kinase gene from the filamentous fungus *Arthrobotrys dactyloides*. *FEMS Microbiology Letters*, 212:7–13, 2002.

D. Uccelletti, F. Farina, and C. Palleschi. The *KlPMR1* gene of *Kluyveromyces lactis* encodes for a P-type Ca^{2+}-ATPase. *Yeast*, 15:593–599, 1999.

A. H. van der Luit. *The Regulation of Calmodulin Gene Expression by Nuclear Calcium in Plants*. PhD thesis, University of Edinburgh, 1998.

B. Vannier, M. Peyton, G. Boulay, D. Brown, N. Qin, M. Jiang, X. Zhu, and L. Birnbaumer. Mouse trp2, the homologue of the human trpc2 pseudogene, encodes mTrp2, a store depletion-activated capacitative Ca^{2+} entry channel. *Proceedings of the National Academy of Sciences of the USA*, 96:2060–2064, 1999.

H. J. A. Vougel. Convenient growth medium for *Neurospora* (Medium N). *Microbiological Genetics Bulletin*, 13:42–43, 1956.

H. Wang, J. Entwistle, E. Morlon, D. B. Archer, J. F. Peberdy, M. Ward, and D. J. Jeenes. Isolation and characterisation of a calnexin homologue, clxA, from *Aspergillus niger*. *Molecular Genetics and Genomics*, 268:684–691, 2003.

Z. Wang, M. Deak, and S. J. Free. A cis-acting region required for the regulated expression of *grg-1*, a *Neurospora* glucose-repressible gene. Two regulatory sites (CRE and NRSS) are required to repress *grg-1* expression. *Journal of Molecular Biology*, 237:65–74, 1994.

M. K. Watters, A. Virag, J. Haynes, and A. J. F. Griffiths. Branch initiation in *Neurospora* is influenced by the events at the previous branch. *Mycological Research*, 104:805–809, 2000.

H. J. Watts, A. A. Very, T. H. Perera, J. M. Davies, and N. A. Gow. Thigmotropism and stretch-activated channels in the pathogenic fungus *Candida albicans*. *Microbiology*, 144:689–695, 1998.

Y. Wei, V. Marchi, R. Wang, and R. Rao. An N-terminal EF hand-like motif modulates ion transport by Pmr1, the yeast Golgi Ca^{2+}/Mn^{2+}-ATPase. *Biochemistry*, 38:14534–14541, 1999.

M. G. Wiebe, G. D. Robson, and A. P. Trinci. Edifenphos (hinosan) reduces hyphal extension, hyphal growth unit length and phosphatidylcholine content of *Fusarium graminearum* A 3/5, but has no effect on specific growth rate. *Journal of General Microbiology*, 136:979–984, 1990.

M. G. Wiebe, G. D. Robson, and A. P. Trinci. Evidence for the independent regulation of hyphal extension and branch initiation in *Fusarium graminearum* A 3/5. *FEMS Microbiology Letters*, 90:179–184, 1992.

V. Wood et al. The genome sequence of *Schizosaccharomyces pombe*. *Nature*, 414: 871–880, 2002.

C. T. Yamashiro, O. Yarden, and C. Yanofsky. A dominant selectable marker that is meiotically stable in *Neurospora crassa*: the *amdS* gene of *Aspergillus nidulans*. *Molecular and General Genetics*, 236:121–124, 1992.

J. Yang, H. A. Kang, S. M. Ko, S. K. Chae, D. D. Ryu, and J. Y. Kim. Cloning of the *Aspergillus niger* pmrA gene, a homologue of yeast *PMR1*, and characterization of a pmrA null mutant. *FEMS Microbiology Letters*, 199:97–102, 2001a.

Y. Yang, P. Cheng, G. Zhi, and Y. Liu. Identification of a calcium/calmodulin-dependent protein kinase that phosphorylates the *Neurospora* circadian clock protein FREQUENCY. *Journal of Biological Chemistry*, 276:41064–41072, 2001b.

O. Yarden, M. Plamann, D. J. Ebbole, and C. Yanofsky. *cot-1*, a gene required for hyphal elongation in *Neurospora crassa*, encodes a protein kinase. *The EMBO Journal*, 11:2159–2166, 1992.

E. Yatzkan, B. Szöör, Z. Fehér, V. Dombrádi, and O. Yarden. Protein phosphatase 2A is involved in hyphal growth of *Neurospora crassa*. *Molecular and General Genetics*, 259:523–531, 1998.

R. R. Ye and A. Bretscher. Identification and molecular characterization of the calmodulin-binding subunit gene (*CMP1*) of protein phosphotase 2B from *Saccharomyces cerevisiae*. an alpha-factor inducible gene. *European Journal of Biochemistry*, 204:713–723, 1992.

T. Yoshida, T. Toda, and M. Yanagida. A calcineurin-like gene ppb1$^+$ in fission yeast: mutant defects in cytokinesis, cell polarity, mating and spindle pole body positioning. *Journal of Cell Science*, 107:1725–1735, 1994.

H. Yoshimoto, K. Saltsman, A. P. Gasch, X. H. Li, N. Ogawa, D. Botstein, P. O. Brown, and M. S. Cyert. Genome-wide analysis of gene expression regulated by the calcineurin/Crz1p signaling pathway in *Saccharomyces cerevisiae*. *Journal of Biological Chemistry*, 277:31079–31088, 2002.

X. L. Zhou, , and C. Kung. A mechanosensitive ion channel in *Schizosaccharomyces pombe*. *The EMBO Journal*, 11:2869–2875, 1992.

X. L. Zhou, M. A. Stumpf, H. C. Hoch, and C. Kung. A mechanosensitive channel in whole cells and membrane patches of the fungus *Uromyces*. *Science*, 253: 1415–1417, 1991.